Habilitation a Diriger des Recherches

de l'Université Paris XI Orsay

présentée et soutenue publiquement le 19 Février 2016

par

Andrea Zoia

Laboratoire de Transport Stochastique et Déterministe
CEA/Saclay, DEN/DANS/DM2S/SERMA/LTSD

Composition du jury :

Président :	Henk HILHORST
Rapporteurs :	Imre PAZSIT
	Claude LE BRIS
	Olivier BÉNICHOU
Examinateurs :	Richard SANCHEZ
	Cheikh M. DIOP
	Alberto ROSSO

Author
Andrea Zoia

Stochastic particle transport: from the Boltzmann equation to the Feynman-Kac approach

Abstract

A prominent and distinct advantage of Monte Carlo methods as applied to the study of stochastic transport processes is that they do not require the knowledge of the deterministic equations for the evolution of the desired physical observables. In particular, *Monte Carlo simulation can be conceived directly from the abstracted physical process without ever even considering a transport equation. Average particle behaviour in the Monte Carlo process certainly is described by the transport equation, just as a ball's motion is described by Newton's equation. But as a philosophical matter, saying that Monte Carlo is 'solving' the transport equation seems a bit like saying that a ball is 'solving' Newton's equation* [1]. Nonetheless, knowledge of the Boltzmann transport equation has largely inspired the Monte Carlo methods used for computing the particle densities in phase space, and turns out to be highly fruitful during both their conception and their subsequent analysis.

While phase space densities in most cases provide a satisfactory description of the average behaviour of the random paths of the transported particles, a number of interesting questions can not be simply answered in terms of these sole quantities: examples are widespread and concern for instance the occupation statistics of the particles within a volume, the distribution of the number of descendant particles at a given time, and the survival probabilities. In all such cases, the description of the transport process must be achieved in a framework that is necessarily broader than that of the Boltzmann equation, which by its very nature only concerns the average behaviour.

Monte Carlo simulation, on the other hand, is ideally suited to extract the full distribution of any observable, even those that are usually not accessible by means of experimental measurements. In this respect, Monte Carlo goes much further than just solving the Boltzmann equation. By analogy with the case of average particle densities, where Monte Carlo methods and the Boltzmann equation are mutually profitable, in the case of arbitrary observables it would therefore be highly desirable to also guide the Monte Carlo simulation by means of the corresponding evolution equations.

This document provides a synthesis of my research work on stochastic transport processes and Monte Carlo methods, in preparation of the *Habilitation* degree at the Université Paris XI Orsay. We will first formally derive a family of evolution equations for a very broad class of physical observables by resorting to the Feynman-Kac formalism. Subsequently, we will apply such Feynman-Kac evolution equations to the analysis of some relevant problems emerging in the field of radiation transport in nuclear reactor physics, and compare the obtained results to Monte Carlo simulations.

[1] T. E. Booth, *Common misconceptions in Monte Carlo particle transport*, Appl. Radiat. Isot. **70**, 1042 (2012).

Contents

Acknowledgments

Ce que nous connaissons est peu de chose,
ce que nous ignorons est immense.

Pierre-Simon, marquis de Laplace

To the memory of my mum.

I would like to express my gratitude to Professor Imre Pazsit (Chalmers University), and to Drs. Claude Le Bris (Ecole Nationale des Ponts et Chaussées) and Olivier Bénichou (CNRS / Université Pierre et Marie Curie) for doing me the honour of accepting to review this manuscript. I also wish to thank Professor Henk Hilhorst (Université Paris Sud - Orsay), and Drs. R. Sanchez (CEA), C. M. Diop (CEA) and Alberto Rosso (CNRS / Université Paris Sud - Orsay) for taking part in the HDR jury.

The achievements discussed in this manuscript would not have been possible without the stimulating scientific environment provided by the DM2S department of the Commissariat à l'Energie Atomique, first during my post-doctoral appointment at the LSET laboratory (2008-2009) and then at the LTSD laboratory (2009 -). For this I would like to warmly thank Christian Cavata, Richard Lenain, Patrick Blanc-Tranchant, Sylvie Naury, Franck Gabriel and Philippe Montarnal at the DM2S department.

My deepest gratitude goes to my colleagues at LTSD, and to the TRIPOLI-4 team in particular, for having introduced me to (almost) all of the secrets of a real-world Monte Carlo code, and for having patiently and friendly answered my countless questions on every possible aspect of stochastic transport, from computer science to transport theory. And, most importantly, for having made me feel at home in the laboratory. I gratefully acknowledge also the contributions of the students I had the privilege to advise, and I wish to thank them for always asking the right questions.

Many thanks go to FX and Odile for their invaluable help with the mysteries of C++ classes and with the subtleties of computer programming, and to Cédric for sharing his deep knowledge of nuclear physics and kinematics. I am greatly indebted to Cheikh, Richard, Mireille and Fausto for the numberless scientific discussions at the LTSD, for their wisdom and for their constant encouragement. Finally, let me conclude by specially thanking Emeric, Alain, Eric and Alberto for their long-standing friendship, their guidance, their advice, and their unwavering support during these years.

Part I

An introduction to stochastic transport

Chapter 1

A survey of transport phenomena

Je présente ici, sans le secours de l'Analyse, les principes et les résultats généraux de cette théorie, en les appliquant aux questions les plus importantes de la vie, qui ne sont en effet, pour la plupart, que des problèmes de probabilités. On peut même dire, à parler en rigueur, que presque toutes nos connaissances ne sont que probables.

Pierre-Simon, marquis de Laplace, *Essai philosophique sur les probabilités* (1814).

1.1 Introduction

A number of systems emerging in physics, life and social sciences, and engineering can be modelled in terms of 'particles' travelling in a host medium and changing at random their state (position, direction, energy, and so on) upon encountering other particles (of the same or other kind) or the medium itself. The nature of these random travels depends on the system under consideration, and may strongly vary from one system to another. In particular, the randomness of these paths may result either from the intrinsic stochastic nature of the underlying process, or from uncertainty [1–12]. Following [3–5], we shall accept that some transport phenomena, while possibly originating from deterministic and reversible events, can in practice be described only by resorting to the laws of probability. Examples are numberless and the literature on the subject is consequently overwhelmingly rich. Here we simply illustrate some of these mechanisms, so as to provide a general picture.

The recognition that the motion of a gas (the molecular chaos) can be addressed in terms of the underlying stochastic process is due to the pioneering work by Boltzmann in 1872 [13, 14]. These results were further explored by Einstein (1905) and Smoluchowski (1906) in order to explain the thermal agitation of water molecules by means of the random motion of suspended pollen (the so-called Brownian motion) [15–19]. This probabilistic approach based on random walks was key to the interpretation of the Nobel-winning experimental determination of the Avogadro number by Perrin [20]. The physical theory of Brownian motion was then developed on solid mathematical grounds by Langevin (1908), whose general technique could be extended to the study of other systems involving the response to an external random disturbance [18, 19, 21].

These ideas have been progressively refined and applied to other fields by many researchers. Neutron diffusion and multiplication in fissile media is one of such subjects, thanks to the outstanding contributions of Kolmogorov, Pál and Bell in the investigation of random displacements coupled

with birth and death events, leading to the so-called theory of branching processes [3, 22–33] and neutron noise [4, 25, 26, 34–36]. The same phenomena appear also in nuclear cascades induced by cosmic rays [1, 3, 29, 32, 37]. The study of neutron ramification is intimately related to (and borrows most of the terminology and related mathematical techniques from) the modelling of life sciences [3, 6, 28, 29, 32], encompassing the analysis of population growth [38–42], transmission of genes over generations via mutation and selection [24, 43–48], bacterial colonies [49–53], animals looking for food (chemotaxis) [54–60] and the spread of epidemics [39, 61–65]. In all such cases, a purely deterministic approach based on the knowledge of the average (expected) behaviour alone may be misleading, and a stochastic approach is essential in capturing the possibly large fluctuations of the population around the average.

In the early developments of transport theory, radiative transfer has been thoroughly explored in connection with astronomy and astrophysics [66]. More recently, the same formalism has been applied to photon propagation through the atmosphere [10, 11, 67–69] and more generally through engineered optical materials [70–72], turbid and holey media [73–76], biological tissues [77, 78], or atomic vapours [79]. Charge transport in semiconductors has been also dealt with within this framework, by means of models based on randomly hopping particles [80–88].

Stochastic transport emerges in the field of tracer migration [12], such as in chemical reaction kinetics [89, 90], molecular dynamics [91, 92], diffusion through membranes as in the case of DNA translocation [93–96], propagation of active molecules in living bodies [97–99], multi-scale modelling of complex fluids [100], or fluid propagation through porous media and scale-free structures [18, 19, 101, 102].

Models based on random walks are widely used in social sciences [103], so as to assess insurance risks [1], analyse the variation of prices in the stock market and the collective dynamics of sellers and buyers (the so-called herding and crowding mechanisms) [9], explain search strategies [104–109], queues [1] and traffic flow [110, 111].

While a rigorous classification can not be established, transport phenomena roughly belong to two basic categories [5]: *i*) in some of them, the walker streams freely between random interactions with the host medium and moves independently of the other tracer particles; *ii*) in some others the trajectory of a single walker actually depends on the complex correlations resulting from the interactions of the walker with the other walkers (and possibly also with the medium). In the former case, the random motion undergoes a *self-diffusion* and is basically linear, whereas in the latter the random motion obeys non-linear *collective phenomena*. The study of such phenomena and the development of the mathematical tools aimed at capturing their common features and providing a unified description goes under the name of *transport theory* [3, 5, 112–115].

1.2 Particle densities in phase space

What all the examples of the previous Section have in common is that the quantity of interest is a walker that moves at random in a medium (more generally, in the phase space), which immediately calls for a *probabilistic approach* at the particle level. Indeed, we expect the motion of such a particle to be described by a probability field, whose evolution equation we would like to eventually determine [5]. In other words, due to the random nature of these walkers, the exact number of particles at a given phase space position fluctuates and can not be deterministically predicted. In most cases, it is not possible to directly observe the motion of a single tracer, so that the properties of the system are characterized by analysing some physical observable, typically averaged over multiple realizations of the walker trajectories in the phase space. This means that one is generally interested in knowing the probability density of finding the walker in a given region of the phase space, or rather the first moments of such density: for instance, the average particle

position or the average particle number, and their fluctuations.

To simplify the matter, we will assume that the phase space is entirely defined in terms of two variables, namely the vector position $\mathbf{r}$ and the vector velocity $\mathbf{v}$ of the walker at a given time t. In other words, a classical approach is proposed here, and quantum variables (such as spin, for instance) will be neglected. This is done for two reasons: first, this approach provides a fairly general framework for dealing with the vast majority of the random walk processes described above. Second, should other phase space variables be indispensable to fully characterize the system evolution, it would not be complicated to accommodate for them by following the same strategy [3,5,112,116,117].

One of the most useful physical quantities associated to the underlying random walk is possibly the *phase-space density function* $N_t(\mathbf{r},\mathbf{r})$, which is such that

$$N_t(\mathbf{r},\mathbf{v})d\mathbf{r}d\mathbf{v} \tag{1.1}$$

represents the average number of particles in the infinitesimal phase space volume $d\mathbf{r}d\mathbf{v}$ located around $\mathbf{r},\mathbf{v}$ at time t [3,5]. The phase space density $N_t(\mathbf{r},\mathbf{v})$ is actually a one-particle density, and contains information *only on the average behaviour* of the walkers. In other words, particle-particle correlations are neglected, and information about the fluctuations of the particle number (or about higher moments) can not be extracted based on this quantity [3,5]. In principle, this would require knowledge of the doublet distribution $N_t(\mathbf{r}_1,\mathbf{v}_1,\mathbf{r}_2,\mathbf{v}_2)$, giving the average number of particle pairs found simultaneously at $d\mathbf{r}_1d\mathbf{v}_1d\mathbf{r}_2d\mathbf{v}_2$ around $\mathbf{r}_1,\mathbf{v}_1,\mathbf{r}_2,\mathbf{v}_2$ at time t [3,5], and more generally s-body partition functions (see the discussion in Sec. 2.3). In some cases, one is interested in knowing the average number $N_t(A)$ of walkers being present in a given portion A of the phase space at time t: in this case, it suffices to integrate

$$N_t(A)=\int_A d\mathbf{r}d\mathbf{v}N_t(\mathbf{r},\mathbf{v}) \tag{1.2}$$

over the position-velocity sub-space A. This quantity plays a fundamental role in almost every single application described above: just to provide some examples, in nuclear reactor physics and more generally radiative transport $N_t(A)$ is the average neutron or photon number, and is thus proportional to the deposited energy; in the study of epidemics, $N_t(A)$ may represent the average number of infected individuals in a given region; in genetics, $N_t(A)$ would be the average number of genes between given types; and so on. Another useful physical quantity is the phase space current density $\mathbf{J}_t(\mathbf{r},\mathbf{v})=\mathbf{v}N_t(\mathbf{r},\mathbf{v})$, which is such that

$$\mathbf{J}_t(\mathbf{r},\mathbf{v})\cdot d\mathbf{S}d\mathbf{v} \tag{1.3}$$

represents the average number of particles that cross the infinitesimal surface $d\mathbf{S}$ per unit time having velocity $d\mathbf{v}$ around $\mathbf{v}$ at time t [5].

1.2.1 General form of the transport equation

A formal equation for the evolution of the phase space density function $N_t(\mathbf{r},\mathbf{v})$ can be derived from a simple argument, following a balance principle [3,5,14]. Consider an arbitrary volume V: if we ignore the effects of macroscopic forces, the rate at which the particle number in V may evolve can only depend on leakages through the surface $S=\partial V$ of V, on collisions (in which case the particles change their speeds and directions), or on external sources $\mathcal{Q}_t(\mathbf{r},\mathbf{v})$. In mathematical terms, we have then

$$\frac{\partial}{\partial t}\int_V N_t(\mathbf{r},\mathbf{v})d\mathbf{r}d\mathbf{v}=-\int_S d\mathbf{S}\cdot\mathbf{J}_t(\mathbf{r},\mathbf{v})d\mathbf{v}+\int_V\left(\frac{\partial N_t}{\partial t}\right)_{coll}d\mathbf{r}d\mathbf{v}+\int_V\mathcal{Q}_t(\mathbf{r},\mathbf{v})d\mathbf{r}d\mathbf{v}, \tag{1.4}$$

where we have denoted by $\left(\frac{\partial N_t}{\partial t}\right)_{coll}$ the rate of change of N_t due to collisions of the walker with the host medium and/or with the other particles. Now, the volume V being arbitrary and not depending on time, the partial derivative with respect to time in the first term of Eq. (1.4) can be brought inside the integral. Then, Gauss theorem may be used to manipulate the leakage terms as follows:

$$\int_S d\mathbf{S}\cdot\mathbf{J}_t(\mathbf{r},\mathbf{v}) = \int_V \nabla_{\mathbf{r}}\cdot\mathbf{J}_t(\mathbf{r},\mathbf{v})d\mathbf{r} = \int_V \mathbf{v}\cdot\nabla_{\mathbf{r}}N_t(\mathbf{r},\mathbf{v})d\mathbf{r}, \tag{1.5}$$

where we have used $\nabla_{\mathbf{r}}\cdot\mathbf{v}N_t = \mathbf{v}\cdot\nabla_{\mathbf{r}}N_t$, since $\mathbf{r}$ and $\mathbf{v}$ are independent variables [3, 5]. Now, from the arbitrariness of the volume V, Eq. (1.4) can be satisfied only if the integrand is identically zero, which therefore leads to

$$\boxed{\frac{\partial}{\partial t}N_t(\mathbf{r},\mathbf{v}) + \mathbf{v}\cdot\nabla_{\mathbf{r}}N_t(\mathbf{r},\mathbf{v}) = \left(\frac{\partial N_t}{\partial t}\right)_{coll} + \mathcal{Q}_t(\mathbf{r},\mathbf{v}),} \tag{1.6}$$

which is the *general form of the transport equation* for the phase space density $N_t(\mathbf{r},\mathbf{v})$, in the absence of external forces [3, 5, 14].

A simpler derivation of the same balance equation can be achieved by equating the rate of change of N_t along a trajectory (i.e., the total derivative) to the collision rate [5], which yields

$$\frac{d}{dt}N_t(\mathbf{r},\mathbf{v}) = \left(\frac{\partial N_t}{\partial t}\right)_{coll} + \mathcal{Q}_t(\mathbf{r},\mathbf{v}). \tag{1.7}$$

This equation has the advantage of easily including the effects of an external force field $\mathbf{F}$ (divided by the mass of the particle). Indeed, the total derivative can be developed as

$$\frac{d}{dt} = \frac{\partial}{\partial t} + \mathbf{v}\cdot\nabla_{\mathbf{r}} + \mathbf{F}\cdot\frac{\partial}{\partial\mathbf{v}}. \tag{1.8}$$

This immediately leads to

$$\frac{\partial}{\partial t}N_t(\mathbf{r},\mathbf{v}) + \mathbf{v}\cdot\nabla_{\mathbf{r}}N_t(\mathbf{r},\mathbf{v}) + \mathbf{F}\cdot\frac{\partial}{\partial\mathbf{v}}N_t(\mathbf{r},\mathbf{v}) = \left(\frac{\partial N_t}{\partial t}\right)_{coll} + \mathcal{Q}_t(\mathbf{r},\mathbf{v}). \tag{1.9}$$

In most cases, we will neglect the effects of external forces, so that Eq. (1.9) reduces to Eq. (1.6). Equation (1.9) is exact, but formal: to proceed further, the collision rate must now be specified.

1.2.2 Collision phenomena

The specific form of the collision term $\left(\frac{\partial N_t}{\partial t}\right)_{coll}$ clearly depends on the physical process under investigation and on the type of particle being transported. We will assume that the random walker can be described as a distinct point particle without wave properties [5]. As mentioned above, the typical transport processes can be regrouped into self-diffusions through the host medium, and collective phenomena.

In the former case, the walker streams freely through the traversed medium and interacts at random with the background [5, 113]. Examples are widespread and include the propagation of neutrons and photons in matter (because of their weak density as compared to that of the nuclei of the host medium) [3,30,31], the flight of light in atmosphere [10,11,67–69], and the motion of a tagged particle (a tracer) in a medium composed of identical particles [12, 18, 19]. For self-diffusions, it is sufficient to follow the tracer particle, and the medium is only considered as the source of randomness for the motion of the walker: the effects of the walker on the medium can be typically neglected. In all

these cases, the collision term is *linear*, in that the probability that the walker collides at a given point in phase space does not depend on the probability of finding one or more other walkers at the same point [5,113]. This linearity might nonetheless break down whenever the walker concentration in the host medium is so high that the medium properties change because of the presence of the walkers. These phenomena, which go under the name of *depletion*, play an important role in neutron transport in nuclear fuel at high burn-up level (after a long permanence in the reactor, the compositions of the fuel elements have changed because of the continued neutron reactions) [3,30,31]. Similar effects emerge in the transport of high density tracers in porous media [118, 119], or in the erosion of the susceptible population in the propagation of virulent epidemics [38, 61, 62]. In the latter case, the motion of the walker is correlated to those of the other walkers in the traversed medium, so that the resulting displacements are due to collective phenomena, and the collision term becomes *non-linear*, i.e., $\left(\frac{\partial N_t}{\partial t}\right)_{coll}$ explicitly depends on the phase space density $N_t(\mathbf{r}, \mathbf{v})$. Examples emerge for instance in gas and plasma dynamics [14, 120] or in traffic flows [3, 5, 14, 110, 111].

1.3 The linear Boltzmann equation

In the following, we will restrict our attention to *self-diffusion phenomena in a background medium*. We will furthermore make a simplifying hypothesis: interactions with the host medium occur instantaneously at a given point in space, which means that the particle streams until it undergoes a collision event, whereupon its state changes at random [3, 5, 14, 113]. The particle can be then absorbed, change its velocity and direction, or give rise to a random number of descendants of the same or other kinds. The assumption of instantaneous collisions is justified when the interaction forces act at short range, and when particle re-emission after the collision takes a time interval much shorter than the typical flight time between successive collisions: this is the case when the transported particle is a diluted species with respect to the host medium, so that mean free paths are many times larger than the characteristic space scale over which a collision event occurs. For the case of neutrons, e.g., the typical time scale of a neutron-nucleus collision is about 10^{-14} s, with a correlation length of about 10^{-13} cm, which are to be compared, respectively, with the typical lifetime of a neutron in a nuclear system ($10^{-6} - 10^{-4}$ s) and the typical inter-collision distance (some cm). The hypotheses leading to linear transport apply more broadly to the propagation of photons, electrons and charge carriers, phonons, and living organisms [3, 5, 6, 14, 82, 113].

Within this context, it is possible to explicitly derive an expression for the collision term [5, 14, 113]. The starting point is the concept of macroscopic *cross section* $\Sigma(\mathbf{r}, \mathbf{v})$, which defines the probability of interaction per unit length travelled by a particle having velocity $\mathbf{v}$ at point $\mathbf{r}$ [3,5,113]. The cross section carries the units of the inverse of a length. Conventionally, the macroscopic cross section can be decomposed in the product of a number density of the medium (which carries the dependence on $\mathbf{r}$) times a microscopic cross section carrying the dependence on the velocity $\mathbf{v}$. The inverse of the cross section is called the *mean free path* $\lambda = 1/\Sigma$, and represents the average distance travelled by the particle between any two interactions with the medium [3, 5, 113]. The previous requirement on collision events being well localized in space implies that the mean free paths are much larger than both the particle wavelength and the range of the interaction forces involved in the collisions [3, 5].

Following an interaction at a site $\mathbf{r}$, the features of the particle after the collision can be characterized in terms of the *scattering probability density function* $f_C(\mathbf{v}' \to \mathbf{v})$, which is such that

$$f_C(\mathbf{v}' \to \mathbf{v}) d\mathbf{v} \tag{1.10}$$

gives the probability that any secondary particle induced by an incident particle with velocity $\mathbf{v}'$ will be emitted with velocity $d\mathbf{v}$ around $\mathbf{v}$. If we want to take into account the fact that the walker can

be possibly absorbed at the interaction, or give rise to multiple particles, it is necessary to introduce the average number $\nu(\mathbf{v}')$ of emitted particles induced by an incident particle having velocity $\mathbf{v}'$. The *multiplicity* term $\nu(\mathbf{v}')$ depends on the event (it can be zero for absorption, one for scattering, or larger for other reactions such as fission). The entire collision process can be then condensed into a *scattering kernel*

$$\Sigma(\mathbf{v}' \to \mathbf{v}|\mathbf{r}) = \sum_i^I \Sigma_i(\mathbf{r}, \mathbf{v}')\nu_i(\mathbf{v}')f_{C_i}(\mathbf{v}' \to \mathbf{v}), \tag{1.11}$$

which gives the average number of particles (per unit travelled length) created at $\mathbf{r}$ with velocity in $d\mathbf{v}$ around $\mathbf{v}$, for an incoming particle with velocity $\mathbf{v}'$ [3, 5]. Reactions of kind i are summed out of a set of I possible events (with associated cross section $\Sigma_i(\mathbf{r}, \mathbf{v}')$), each giving rise on average to $\nu_i(\mathbf{v}')$ particles distributed according to the density $f_{C_i}(\mathbf{v}' \to \mathbf{v})$. By definition,

$$\sum_i^I \Sigma_i(\mathbf{r}, \mathbf{v})\nu_i(\mathbf{v}) = \int \Sigma(\mathbf{v} \to \mathbf{v}'|\mathbf{r})d\mathbf{v}'. \tag{1.12}$$

We will assume that the physical properties of the medium, hence the cross sections, are stationary with respect to time. Now, according to the previous definitions, the collision rate is $v\Sigma(\mathbf{r}, \mathbf{v})$, where we have defined the particle speed $v = |\mathbf{v}|$. Then, the global rate at which interactions (of any kind) occur per unit volume is $v\Sigma(\mathbf{r}, \mathbf{v})N_t(\mathbf{r}, \mathbf{v})$, which takes the name of collision rate density. Similarly, the collision rate density at which particles having velocity $\mathbf{v}'$ induce the production of secondary particles having velocities $\mathbf{v}$ is $v'\Sigma(\mathbf{v}' \to \mathbf{v}|\mathbf{r})N_t(\mathbf{r}, \mathbf{v}')$.

Hence, the collision term $\left(\frac{\partial N_t}{\partial t}\right)_{coll}$ can be expressed as

$$\left(\frac{\partial N_t}{\partial t}\right)_{coll} = \int v'\Sigma(\mathbf{v}' \to \mathbf{v}|\mathbf{r})N_t(\mathbf{r}, \mathbf{v}')d\mathbf{v}' - v\Sigma(\mathbf{r}, \mathbf{v})N_t(\mathbf{r}, \mathbf{v}). \tag{1.13}$$

Equation (1.13), coupled with the balance equation (1.6), finally gives the linear transport equation for $N_t(\mathbf{r}, \mathbf{v})$, namely,

$$\boxed{\frac{\partial}{\partial t}N_t + \mathbf{v} \cdot \nabla_{\mathbf{r}} N_t = \int v'\Sigma(\mathbf{v}' \to \mathbf{v}|\mathbf{r})N_t(\mathbf{r}, \mathbf{v}')d\mathbf{v}' - v\Sigma(\mathbf{r}, \mathbf{v})N_t + \mathcal{Q}_t(\mathbf{r}, \mathbf{v}),} \tag{1.14}$$

which is a *linear Boltzmann equation* in the absence of external forces [5, 14, 113]. Equation (1.14) is a linear integral-differential equation for the phase space density N_t, where linearity stems from assuming that cross sections are known. This hypothesis can be actually relaxed so to accommodate for cross sections that depend on N_t (the resulting Boltzmann equation would be then non-linear). This is typically the case of gases of interacting particles and/or walkers modifying the traversed medium [3, 5, 14, 113].

The product $\varphi_t(\mathbf{r}, \mathbf{v}) = vN_t(\mathbf{r}, \mathbf{v})$ appears frequently in transport theory, and carries the name of *phase space flux* [3, 5]. This quantity is simply related to the phase space current by $\mathbf{J}_t(\mathbf{r}, \mathbf{v}) = \boldsymbol{\omega}\varphi_t(\mathbf{r}, \mathbf{v})$, where $\boldsymbol{\omega} = \mathbf{v}/v$ is the particle direction. The linear Boltzmann equation (1.14) can be then rewritten in terms of the flux $\varphi_t(\mathbf{r}, \mathbf{v})$ as

$$\boxed{\frac{1}{v}\frac{\partial}{\partial t}\varphi_t + \boldsymbol{\omega} \cdot \nabla_{\mathbf{r}}\varphi_t = \int \Sigma(\mathbf{v}' \to \mathbf{v}|\mathbf{r})\varphi_t(\mathbf{r}, \mathbf{v}')d\mathbf{v}' - \Sigma(\mathbf{r}, \mathbf{v})\varphi_t + \mathcal{Q}_t(\mathbf{r}, \mathbf{v}).} \tag{1.15}$$

1.3.1 Prompt and delayed particles

The case of neutrons in nuclear reactor physics deserves a distinct treatment. Upon collision with a fissile nucleus, the neutron is absorbed, and the collided nucleus becomes unstable. After

a negligible time lapse, the unstable nucleus splits into several fragments (typically two), and sets free a variable number of other neutrons. These neutrons, which are labelled as *prompt*, behave exactly as the original neutron, and start to diffuse into the medium. The fission fragments usually undergo β^- nuclear reactions, which leave them on an excited state with an excess of neutrons. The fragments then decay to their fundamental state by emitting supplementary neutrons into the system. Each fissile isotope leads to a number of possible fission fragments, which are customarily grouped in so-called families [30]. The extra neutrons emitted after the decay time of the β^- nuclear reactions are labelled as *delayed* (as opposed to prompt neutrons, which are emitted instantaneously at fission events) [30]. Between the fission event and the actual emission from the fission fragments by β^- decay, the delayed neutrons are named *precursors*. The emitted delayed neutrons hold the same position as the associated precursors. In stochastic biological models of epidemics, similar prompt-delayed particle systems exist. For instance, the delayed particles would represent patients during incubation, whereas prompt particles would represent patients with apparent symptoms [4].

The coupled equations for the evolution of the neutron density $N_t(\mathbf{r}, \mathbf{v})$ and the precursor concentrations $c_t^{i,j}(\mathbf{r})$ are as follows:

$$\frac{\partial}{\partial t} N_t(\mathbf{r}, \mathbf{v}) + L\, N_t(\mathbf{r}, \mathbf{v}) = F_p\, N_t(\mathbf{r}, \mathbf{v}) + \sum_{i,j} \chi_d^{i,j}(\mathbf{r}, v) \lambda_{i,j} c_t^{i,j}(\mathbf{r}) \tag{1.16}$$

and

$$\frac{\partial}{\partial t} c_t^{i,j}(\mathbf{r}) = \int \nu_d^{i,j}(v') \Sigma_f^i(\mathbf{r}, v') v' N_t(\mathbf{r}, \mathbf{v}')\, \mathrm{d}\mathbf{v}' - \lambda_{i,j} c_t^{i,j}(\mathbf{r}). \tag{1.17}$$

We have here defined the *net disappearance* operator

$$L\, f = \mathbf{v} \cdot \nabla f + \Sigma_t v f - \int \Sigma_s(\mathbf{r}, \mathbf{v}' \to \mathbf{v}) v' f(\mathbf{r}, \mathbf{v}')\, \mathrm{d}\mathbf{v}', \tag{1.18}$$

and the prompt fission operator

$$F_p\, f = \chi_p(\mathbf{r}, v) \int \nu_p(v') \Sigma_f(\mathbf{r}, v') v' f(\mathbf{r}, \mathbf{v}')\, \mathrm{d}\mathbf{v}'. \tag{1.19}$$

Here Σ_t is the total cross-section, Σ_s is the differential scattering cross-section, χ_p is the normalized spectrum for prompt fission neutrons, ν_p is the average number of prompt fission neutrons, Σ_f is the fission cross-section, $\chi_d^{i,j}$ is the normalized spectrum of delayed neutrons emitted from precursor family j of isotope i, $\lambda_{i,j}$ is the decay constant of precursor family j of isotope i, $\nu_d^{i,j}$ is the average number of precursors of family j induced on the fissile isotope i, and the double sum is extended over all fissile isotopes i and over all precursor families j for each fissile isotope. The equations above are completed by assigning the proper initial and boundary conditions for φ and $c^{i,j}$. We have assumed here that all physical parameters (such as cross-sections, velocity spectra, and so on) are time-independent [30]. If n fissile isotopes are present, each associated to m precursors families, Eqs. (1.16) and (1.17) form a system of $1 + n \times m$ equations to be solved simultaneously.

1.3.2 Boundary conditions, stationary solutions and existence

The mathematical description of the phase space density $N_t(\mathbf{r}, \mathbf{v})$ must be completed by assigning proper initial and boundary conditions [3,5]. As for the initial condition, given the local-in-time character of the transport Eq. (1.14) (denoted by the presence of a single first order derivative with respect to time), a single condition of the kind

$$N_0(\mathbf{r}, \mathbf{v}) = h(\mathbf{r}, \mathbf{v}) \tag{1.20}$$

must be specified, where h is some known function of the phase space coordinates. The boundary conditions depend on the distinct problem under analysis. An exhaustive list can hardly be achieved: here we suggest some of the most common in the applications of interest.

- *Leakage conditions (free surface).* The particles are considered to be lost upon crossing the outer boundary S of the domain V, and no re-entering is allowed. In this case, the natural condition on $N_t(\mathbf{r}, \mathbf{v})$ is to impose a vanishing concentration on the boundary, when the direction is aimed inward (there are no particles that can cross the boundary from the exterior). This leads to $N_t(\mathbf{r} \in S, \mathbf{v}) = 0$ when $\mathbf{v} \cdot \mathbf{n}_S < 0$, $\mathbf{n}_S$ being the unit vector normal to the surface S. In the jargon of statistical physics, these boundary conditions are also called absorbing boundaries, as they correspond to a perfect absorber for the particles, located at S.

- *Reflecting conditions.* In this case, particles are reflected at S, which imposes that the incidence and reflection angles are equal. In terms of the phase space density, this means that $N_t(\mathbf{r} \in S, \mathbf{v}) = N_t(\mathbf{r} \in S, \mathbf{v}_r)$ when $\mathbf{v} \cdot \mathbf{n}_S < 0$, where the velocity vector $\mathbf{v}_r$ is such $\mathbf{v}_r \cdot \mathbf{n}_S = \mathbf{v} \cdot \mathbf{n}_S$ and $\mathbf{v} \times \mathbf{v}_r \cdot \mathbf{n}_S = 0$. Reflecting and leakage conditions can be combined on different portions of the boundary S.

- *Periodic conditions.* If particular symmetries for the particle walks can be exploited, periodic boundary conditions might be imposed, and the outgoing density on a given boundary is then equated to the ingoing density on another boundary.

- *Interfaces.* In the absence of localized sources, continuity in the phase space densities is required across an interface between two regions V_1 and V_2 with different physical properties, which implies $N_t(\mathbf{r} \in S, \mathbf{v}) = N_t(\mathbf{r} \in S, \mathbf{v})$, S being the frontier between the two media.

- *Infinity.* For unbounded media, some regular behaviour is to be imposed at infinity, for instance in the form $N_t(\mathbf{r}, \mathbf{v}) < +\infty$ when $r = |\mathbf{r}| \to \infty$. In most cases, we will however impose a stronger condition of the kind $N_t(\mathbf{r}, \mathbf{v}) \to 0$ at infinity.

For reasonable initial and boundary conditions, existence, uniqueness and continuous dependence on initial data for the Boltzmann equation (1.14) have been extensively studied and rigorously demonstrated for a variety of collision kernels [3,5,14]. Attention should be paid to a subtle issue: when particles can be multiplied in the traversed medium (as in the case of neutrons, bacterial growth or epidemics), the asymptotic solution for large t may well not exist. Intuitively, this happens whenever the mass growth due to multiplication is not sufficiently compensated by leakage from the boundaries. It can be shown that the key role in determining the existence of an asymptotic solution for $N_t(\mathbf{r}, \mathbf{v})$ rests on the average number of secondary particles per collision. For $\nu < 1$, asymptotic solutions are bounded. When on the contrary $\nu > 1$ the phase space density might diverge or converge, depending on the non-trivial interplay among geometry, cross sections, ν, and boundary conditions [3,5]. We will come back to this issue later.

1.4 Green's functions and the adjoint Boltzmann equation

Let us denote by $\mathcal{G}(\mathbf{r}, \mathbf{v}, t|\mathbf{r}_0, \mathbf{v}_0, t_0)$ the particle density in $\mathbf{r}, \mathbf{v}$ at time t for a single source particle started from $\mathbf{r}_0, \mathbf{v}_0$ at time t_0 (in the absence of external sources). The function $\mathcal{G}(\mathbf{r}, \mathbf{v}, t|\mathbf{r}_0, \mathbf{v}_0, t_0)$ takes the name of *Green's function* associated to the Boltzmann equation (1.14). Based on the linearity of the Boltzmann equation and on the fact that Eq. (1.14) is local in time (the time derivative is of order one), it can be shown that the Green's function satisfies

$$\mathcal{G}(\mathbf{r}, \mathbf{v}, t|\mathbf{r}_0, \mathbf{v}_0, t_0) = \int d\mathbf{r}' \int d\mathbf{v}' \mathcal{G}(\mathbf{r}, \mathbf{v}, t|\mathbf{r}', \mathbf{v}', t') \mathcal{G}(\mathbf{r}', \mathbf{v}', t'|\mathbf{r}_0, \mathbf{v}_0, t_0) \tag{1.21}$$

for any $t_0 < t' < t$ [121]. When the physical parameters of the system are constant in time, $\mathcal{G}(\mathbf{r}, \mathbf{v}, t|\mathbf{r}_0, \mathbf{v}_0, t_0)$ depends only on the difference $t - t_0$, and without loss of generality we can assume $t_0 = 0$. We will thus write

$$\mathcal{G}_t(\mathbf{r}, \mathbf{v}|\mathbf{r}_0, \mathbf{v}_0) = \mathcal{G}(\mathbf{r}, \mathbf{v}, t|\mathbf{r}_0, \mathbf{v}_0, t_0 = 0). \tag{1.22}$$

The Green's function satisfies also the initial condition

$$\mathcal{G}_0(\mathbf{r}, \mathbf{v}|\mathbf{r}_0, \mathbf{v}_0) = \delta(\mathbf{r} - \mathbf{r}_0)\delta(\mathbf{v} - \mathbf{v}_0). \tag{1.23}$$

Now, by taking $t' = t - dt$ in Eq. (1.21), expanding in small powers of dt and then letting $dt \to 0$ [121], the Green's function can be shown to satisfy the *forward* Boltzmann equation

$$\boxed{\frac{\partial}{\partial t}\mathcal{G}_t + \mathbf{v} \cdot \nabla_{\mathbf{r}}\mathcal{G}_t = \int v'\Sigma(\mathbf{v}' \to \mathbf{v}|\mathbf{r})\mathcal{G}_t(\mathbf{r}, \mathbf{v}'|\mathbf{r}_0, \mathbf{v}_0)d\mathbf{v}' - v\Sigma(\mathbf{r}, \mathbf{v})\mathcal{G}_t.} \tag{1.24}$$

Similarly, by taking $t' = t_0 + dt$ in Eq. (1.21), expanding in small powers of dt and then letting again $dt \to 0$ [121], the Green's function can be shown to satisfy the *backward* Boltzmann equation

$$\boxed{\frac{\partial}{\partial t}\mathcal{G}_t - \mathbf{v}_0 \cdot \nabla_{\mathbf{r}_0}\mathcal{G}_t = \int v_0\Sigma(\mathbf{v}_0 \to \mathbf{v}_0'|\mathbf{r}_0)\mathcal{G}_t(\mathbf{r}, \mathbf{v}|\mathbf{r}_0, \mathbf{v}_0')d\mathbf{v}_0' - v_0\Sigma(\mathbf{r}_0, \mathbf{v}_0)\mathcal{G}_t,} \tag{1.25}$$

which is the *adjoint* equation with respect to Eq. (1.24), the operators acting on the initial coordinates $\mathbf{r}_0, \mathbf{v}_0$. While the forward and backward equations for the Green's function share the same initial condition (Eq. (1.23)), care must be taken concerning the boundary conditions: those of the backward equation are adjoint to those of the forward equation [4, 30, 121]. The forward and backward equations represent a dual alternative for the calculation of the same quantity (a rigorous proof of the complete equivalence of the two forms can be given based on a theorem of Lánczos on linear operator theory [4, 121]).

In the forward interpretation of the Green's function, the variables are $\mathbf{r}, \mathbf{v}$ and $\mathbf{r}_0, \mathbf{v}_0$ are considered as given parameters: in this case, $\mathcal{G}(\mathbf{r}, \mathbf{v}|\mathbf{r}_0, \mathbf{v}_0)$ represents the average number of particles at $\mathbf{r}, \mathbf{v}$ (for a source particle at $\mathbf{r}_0, \mathbf{v}_0$). Conversely, in the backward interpretation the variables are $\mathbf{r}_0, \mathbf{v}_0$ and $\mathbf{r}, \mathbf{v}$ take the role of given parameters: in this case, $\mathcal{G}(\mathbf{r}, \mathbf{v}|\mathbf{r}_0, \mathbf{v}_0)$ represents the *importance* of a neutron injected into the system at $\mathbf{r}_0, \mathbf{v}_0$ (with respect to a point-like detector located at $\mathbf{r}, \mathbf{v}$) [4, 30, 121].

Observe that the density $N_t(\mathbf{r}, \mathbf{v})$ for a given distributed source $\mathcal{Q}$ is related to the Green's function by

$$N_t(\mathbf{r}, \mathbf{v}) = \int_0^t dt' \int d\mathbf{r}_0 \int d\mathbf{v}_0 \mathcal{G}_{t-t'}(\mathbf{r}, \mathbf{v}|\mathbf{r}_0, \mathbf{v}_0)\mathcal{Q}_{t'}(\mathbf{r}_0, \mathbf{v}_0) \tag{1.26}$$

By analogy, we can define the importance of a particle with respect to a distributed detector region V in the phase space by introducing the adjoint particle density $N^\dagger$

$$N_t^\dagger(\mathbf{r}_0, \mathbf{v}_0) = \int d\mathbf{r} \int d\mathbf{v} \mathcal{G}_t(\mathbf{r}, \mathbf{v}|\mathbf{r}_0, \mathbf{v}_0)\mathcal{Q}^\dagger(\mathbf{r}, \mathbf{v}), \tag{1.27}$$

where the adjoint source $\mathcal{Q}^\dagger(\mathbf{r}, \mathbf{v})$ satisfies $\mathcal{Q}^\dagger = 1$ if $\mathbf{r}, \mathbf{v} \in V$ and $\mathcal{Q}^\dagger = 0$ elsewhere. From these definitions stems the *reciprocity* relation between the forward and adjoint densities, namely,

$$\int d\mathbf{r} \int d\mathbf{v} N_t(\mathbf{r}, \mathbf{v})\mathcal{Q}^\dagger(\mathbf{r}, \mathbf{v}) = \int_0^t dt' \int d\mathbf{r}_0 \int d\mathbf{v}_0 N_{t-t'}^\dagger(\mathbf{r}_0, \mathbf{v}_0)\mathcal{Q}_{t'}(\mathbf{r}_0, \mathbf{v}_0). \tag{1.28}$$

1.5 The spectrum of the Boltzmann operator

Equation (1.14) can be recast in the compact formula

$$\frac{\partial}{\partial t} N_t(\mathbf{r}, \mathbf{v}, t) = \mathcal{L} N_t(\mathbf{r}, \mathbf{v}, t), \tag{1.29}$$

where we have introduced the Boltzmann operator $\mathcal{L}$ acting on the particle density N, namely,

$$\mathcal{L} = -\mathbf{v} \cdot \nabla_{\mathbf{r}} - v\Sigma(\mathbf{r}, \mathbf{v}) + \int v' \Sigma(\mathbf{v}' \to \mathbf{v}|\mathbf{r}). \tag{1.30}$$

Determining the spectrum $\sigma[\mathcal{L}]$ of the Boltzmann operator $\mathcal{L}$ is an essential prerequisite for the analysis of time-dependent transport problems. Moreover, knowing the whole spectrum $\sigma[\mathcal{L}]$ (i.e., the set of eigenvalues α and associated eigenfunctions N_α) amounts to characterizing the operator $\mathcal{L}$ itself, and this in turn allows for eigenfunction expansions of the full time-dependent solution, starting from an assigned initial distribution $N_0(\mathbf{r}, \mathbf{v})$ [5]. These issues are crucial in many technological problems associated, e.g., with neutron transport [122], such as start-up of commercial reactors [123], analysis of accelerator-driven systems [124], material control and accountability in critical assemblies [125], and pulsed neutron reactivity measurements [126], just to name a few.

Unfortunately, the operator $\mathcal{L}$ is in general not self-adjoint, not compact, and possibly unbounded, which makes its analysis highly non trivial [5, 127]. Only a few general properties of the spectrum of $\mathcal{L}$ are known so far, since the pioneering works on one-speed isotropic transport in slab geometries [128–130]. Some surprising features have emerged, such as for instance the possible presence of a *continuous spectrum* in addition to a point (discrete) spectrum, which do not always have a counterpart in diffusion theory [131, 132]. In most applications, one is naturally led to consider bodies of finite size, convex, and with vacuum boundary conditions (particles cannot re-enter once they have left the system): even with this restriction, the properties of the spectrum depend on the specific details of the operator. For instance, in the case of isotropic scattering the spectrum is purely discrete when the minimum neutron velocity, say v_0, is bounded away from zero, whereas a continuous spectrum can arise in the region $\Re\{\alpha\} < -\min[v\Sigma(\mathbf{r}, v)]$ when v_0 is allowed to vanish [133, 134]. For an overview of the properties of $\sigma[\mathcal{L}]$ as a function of geometry, collision kernels, and boundary conditions, see for instance [5, 127, 135, 136] and references therein.

In general, one is interested in using the knowledge on $\sigma[\mathcal{L}]$ in order to derive the eigenfunction expansion of the initial value problem in Eq. 1.29. In view of the functional form of Eq. 1.29, it is natural to postulate for N_t a time dependence of exponential kind, namely $N_t(\mathbf{r}, \mathbf{v}) = N_\alpha(\mathbf{r}, \mathbf{v}) e^{\alpha t}$, which leads to

$$-\mathbf{v} \cdot \nabla_{\mathbf{r}} N_\alpha - v\Sigma(\mathbf{r}, \mathbf{v}) N_\alpha + \int v' \Sigma(\mathbf{v}' \to \mathbf{v}|\mathbf{r}) N_\alpha(\mathbf{r}, \mathbf{v}') dv' = \alpha N_\alpha. \tag{1.31}$$

Due to the possible presence of a continuous spectrum, the general form of the eigenvalue expansion will be

$$N_t(\mathbf{r}, \mathbf{v}) = \sum_i a_i N_{\alpha_i} e^{\alpha_i t} + \int g(\alpha) N_\alpha e^{\alpha t} d\alpha, \tag{1.32}$$

where the former term on the right hand side is the eigenfunction expansion pertaining to the discrete component of $\sigma[\mathcal{L}]$, with (generally complex) discrete eigenvalues α_i and weight coefficients a_i depending on the initial conditions, and the latter is the contribution due to the continuous portion of the spectrum, with density $g(\alpha)$ [5, 134, 137]. A more rigorous proof can be given by taking the Laplace transform of Eq. 1.29. Then, seeking the formal inverse transform (the Bromwich integral) and applying Cauchy's residual theorem precisely yields Eq. 1.32 [5].

Very broad conditions for the well-posedness of the eigenvalue equation 1.31 for reasonable collision kernels and bounded domains have been thoroughly discussed [5, 138, 139]. In particular, it has been shown that under mild assumptions a dominant discrete eigenvalue α_0 exists, which is simple, real, larger than the real parts of all the other α, and whose associated eigenfunction $N_{\alpha_0}(\mathbf{r}, \mathbf{v})$ is non-negative [138, 139]. This ensures that, after a transient, the particle population will grow in time as $N_t \propto e^{\alpha_0 t}$: when $\alpha_0 > 0$, the system is *super-critical* and the population diverges exponentially fast; when $\alpha_0 < 0$, the system is *sub-critical* and the population dies out exponentially fast; finally, when $\alpha_0 = 0$ the system is exactly *critical* and the population is constant in time. However, it has been argued that the discrete spectrum *may not exist*, for instance when the size of the system is below some critical threshold: in this case, the time behaviour would be imposed by the continuous portion of $\sigma[\mathcal{L}]$, and the asymptotic decay of N_t would be non-exponential [5, 131, 132, 138, 139].

When delayed particles are also present, spectral analysis is slightly more complicated. To characterize the asymptotic evolution of neutrons in the presence of precursors, an exponential relaxation of the kind

$$N_t(\mathbf{r}, \mathbf{v}) = \sum_{\alpha} N_\alpha(\mathbf{r}, \mathbf{v}) e^{\alpha t} \tag{1.33}$$

and

$$c_t^{i,j}(\mathbf{r}) = \sum_{\alpha} c_\alpha^{i,j}(\mathbf{r}) e^{\alpha t} \tag{1.34}$$

is simultaneously postulated for both the neutron density and the precursors concentrations, where the values α represent the relaxation frequencies of the system [5, 30]. Equations (1.33) and (1.34) stem again from imposing the separation of variables in Eqs. (1.16) and (1.17). Yet, proving the feasibility of such an expansion is highly non-trivial in general, and precise (although not very restrictive) conditions are required on the geometry of the domain and on the material cross-sections [5, 30, 138]. Here, for the sake of simplicity, we will assume that such conditions are met (which is typically the case for almost all systems of practical interest) and that there exists a set of values α such that separation of variables is allowed. Then, substituting Eqs. (1.33) and (1.34) into Eqs. (1.16) and (1.17), respectively, yields

$$\alpha N_\alpha(\mathbf{r}, \mathbf{v}) + L\, N_\alpha(\mathbf{r}, \mathbf{v}) = F_p\, N_\alpha(\mathbf{r}, \mathbf{v}) + \sum_{i,j} \chi_d^{i,j}(\mathbf{r}, v) \lambda_{i,j} c_\alpha^{i,j}(\mathbf{r}) \tag{1.35}$$

and

$$\alpha c_\alpha^{i,j}(\mathbf{r}) = \int \nu_d^{i,j}(v') \Sigma_f^i(\mathbf{r}, v') v' N_\alpha(\mathbf{r}, \mathbf{v}')\, \mathrm{d}\mathbf{v}' - \lambda_{i,j} c_\alpha^{i,j}(\mathbf{r}), \tag{1.36}$$

which formally represent a system of *coupled eigenvalue equations* for the neutron density N_α and the precursors $c_\alpha^{i,j}$, the eigenvalues being α. In principle, Eqs. (1.35) and (1.36) have $1 + n \times m$ sets of eigenvalues associated to the prompt and delayed components [30, 140, 141].

Chapter 2

From macroscopic to microscopic

Can any of your readers refer me to a work wherein I should find a solution of the following problem, or failing the knowledge of any existing solution provide me with an original one? I should be extremely grateful for aid in the matter.
A man starts from a point O and walks l yards in a straight line; he then turns through any angle whatever and walks another l yards in a second straight line. He repeats this process n times.
I require the probability that after these n stretches he is at a distance between r and r + dr from his starting point, O.

K. Pearson, Nature **27**, 294 (1905).

2.1 Introduction

A natural question arises about the probabilistic laws describing the evolution of the microscopic trajectories whose average properties obey Eq. (1.14). We already know from the previous description that the picture leading to the Boltzmann equation rests upon particles freely streaming between collisions occurring at random, whereupon the particle velocity is instantaneously redistributed according to the scattering kernel. Therefore, we must now address the statistical distribution of flight lengths between collisions. Let us assume that the medium properties are stationary, which we have implicitly done in the previous derivation. We begin by observing that

$$-\frac{d}{ds}N_{t-s}(\mathbf{r}-s\mathbf{v},\mathbf{v}) = \frac{\partial}{\partial t}N_{t-s}(\mathbf{r}-s\mathbf{v},\mathbf{v}) + \mathbf{v}\cdot\nabla_{\mathbf{r}}N_{t-s}(\mathbf{r}-s\mathbf{v},\mathbf{v}) \tag{2.1}$$

for any $s \geq 0$. Then, from Eq. (1.14) it follows

$$-\frac{d}{ds}N_{t-s}(\mathbf{r}',\mathbf{v}) = \int v'\Sigma(\mathbf{v}'\to\mathbf{v}|\mathbf{r}')N_{t-s}(\mathbf{r}',\mathbf{v}')d\mathbf{v}' - v\Sigma(\mathbf{r}',\mathbf{v})N_{t-s}(\mathbf{r}',\mathbf{v}) + \mathcal{Q}_{t-s}(\mathbf{r}',\mathbf{v}), \tag{2.2}$$

where we have set $\mathbf{r}' = \mathbf{r} - s\mathbf{v}$. We multiply now both sides of Eq. (2.2) by the factor

$$\Pi_s(\mathbf{r},\mathbf{v}) = e^{-\int_0^s \Sigma(\mathbf{r}-s'\mathbf{v},\mathbf{v})vds'}. \tag{2.3}$$

By using

$$-\Pi_s\frac{d}{ds}N_{t-s}(\mathbf{r}',\mathbf{v}) + \Pi_s v\Sigma(\mathbf{r}',\mathbf{v})N_{t-s}(\mathbf{r}',\mathbf{v}) = -\frac{d}{ds}\left[\Pi_s N_{t-s}(\mathbf{r}',\mathbf{v})\right], \tag{2.4}$$

we obtain

$$-\frac{d}{ds}\left[\Pi_s N_{t-s}(\mathbf{r}',\mathbf{v})\right] = \Pi_s\left[\int v'\Sigma(\mathbf{v}'\to\mathbf{v}|\mathbf{r}')N_{t-s}(\mathbf{r}',\mathbf{v}')d\mathbf{v}' + \mathcal{Q}_{t-s}(\mathbf{r}',\mathbf{v})\right]. \tag{2.5}$$

Integrating Eq. (2.5) over s between $s=0$ and $s\to\infty$ yields an integral form of the Boltzmann equation, namely,

$$N_t(\mathbf{r},\mathbf{v}) = \int_0^\infty \Pi_s(\mathbf{r},\mathbf{v})\chi_{t-s}(\mathbf{r}-s\mathbf{v},\mathbf{v})ds, \tag{2.6}$$

with

$$\chi_s(\mathbf{r},\mathbf{v}) = \int v'\Sigma(\mathbf{v}'\to\mathbf{v}|\mathbf{r})N_s(\mathbf{r},\mathbf{v}')d\mathbf{v}' + \mathcal{Q}_s(\mathbf{r},\mathbf{v}). \tag{2.7}$$

The physical meaning of Eq. (2.6) is the following: the quantity χ_s represents the average number of particles appearing at coordinates $\mathbf{r},\mathbf{v}$ in the phase space at time s (i.e., those having had a collision at some previous time and having being scattered to the chosen velocity, plus those coming directly from the source $\mathcal{Q}_s$), whereas Π_s represents the (Poissonian) probability that the particles do not undergo any collision up to time s [3,5].

Given the peculiar nature of the probability Π_s in Eq. (2.3), it follows that the displacements of the trajectories underlying the Boltzmann equation (1.14) obey a *non-homogeneous Poisson process* with parameter $\Sigma(\mathbf{r},\mathbf{v})$ [2,3,5,113,142–146]. In other words, a particle travelling along a direction $\boldsymbol{\omega}$ with speed v performs a *Markovian random walk* having exponentially distributed flight times with average $1/(v\Sigma)$ [1]. Observe that time and space increments are directly correlated via the speed of the flight. Because of the exponential distribution of the time and space increments, such random walks are often called *exponential flights* [2].

While much attention has been given to random walks on regular Euclidean lattices, and to the corresponding scaling limits [2,7,8], less has been comparatively devoted to the case where the direction of propagation can change continuously at each collision [142,143,147–150]. Exponential flights are intimately connected to the Boltzmann equation (1.14) and describe, among others, neutron or photon propagation through matter [14,30,31,67,77,142,143,145], or electron motion in semiconductors [80–82], when the host medium is homogeneous at the scale of a mean free path [3,5,73–75]. The Markovian property of exponential flights is such that the random walk describing the evolution of position and velocity $\mathbf{r},\mathbf{v}$ in the phase space is memoryless: knowledge of both $\mathbf{r}$ and $\mathbf{v}$ at any time t is sufficient to characterize the future evolution of the walk [2,5,14,113].

2.2 From exponential flights to random flights

So far, we have attempted a description of the underlying stochastic process by determining the evolution of the phase space coordinates as a function of time. Alternatively, it is possible to examine the behaviour of exponential flights at the *collision points* alone, which correspond to the *renewal* points of the Markovian process. Loosely speaking, we will denote each successive collision undergone by a particle by the term *generation*. Let us introduce the quantity

$$\psi_g(\mathbf{r},\mathbf{v}), \tag{2.8}$$

[1] This is coherent with our previous assumption about the role of the cross sections Σ in the characterization of the travelling particles. A Poisson distribution implies in particular that the probability of interaction must be constant per unit of elementary length ds aligned along a specified direction, and proportional to ds via the cross section Σ: Prob[interaction] $\propto \Sigma ds$ [3,5].

[2] Exponential flights are preferentially called *free flights* in the semiconductors community [80–82].

representing the *average density* of particles entering a collision at $\mathbf{r}$, having velocity $\mathbf{v}$, at the g-th generation. We will call $\psi_g(\mathbf{r},\mathbf{v})$ the *incident particle density* in phase space [30, 31, 113]. At each generation, particles undergo a collision at $\mathbf{r}'$ with velocity $\mathbf{v}'$, with an average number ν being scattered to a velocity $\mathbf{v}$ by a *collision kernel* $C(\mathbf{v}' \to \mathbf{v}|\mathbf{r}')$. The collision kernel can be represented as

$$C(\mathbf{v}' \to \mathbf{v}|\mathbf{r}) = \sum_i^I p_i(\mathbf{r},\mathbf{v}')\nu_i(\mathbf{v}')f_{C_i}(\mathbf{v}' \to \mathbf{v}). \tag{2.9}$$

where $p_i(\mathbf{r},\mathbf{v}')$ is the probability of undergoing event i at collision, out of a set of I possible events. This probability can be expressed as

$$p_i(\mathbf{r},\mathbf{v}') = \frac{\Sigma_i(\mathbf{r},\mathbf{v}')}{\Sigma(\mathbf{r},\mathbf{v}')}, \tag{2.10}$$

i.e., the ratio between the i event cross section Σ_i and the total cross section Σ. The quantity $\nu_i(\mathbf{v}')$ is the multiplicity of secondary particles leaving reaction i, and $f_{C_i}(\mathbf{v}' \to \mathbf{v})$ is the corresponding normalized distribution in the velocity space of the secondary particles. The sum of p_i and the integral of the distribution function over the whole energy space are normalized to one. Then, the secondary particles emitted at collision are transported to the next collision by a *displacement kernel* $T(\mathbf{r}' \to \mathbf{r}|\mathbf{v})$. Thus, the following recursive Chapman-Kolmogorov equation [30, 31, 113] can be established for ψ_g, namely,

$$\psi_{g+1}(\mathbf{r},\mathbf{v}) = \int d\mathbf{r}' \int d\mathbf{v}' T(\mathbf{r}' \to \mathbf{r}|\mathbf{v})C(\mathbf{v}' \to \mathbf{v}|\mathbf{r}')\psi_g(\mathbf{r}',\mathbf{v}'). \tag{2.11}$$

The initial condition $\psi_1(\mathbf{r},\mathbf{v})$ represents the average particle density entering a collision at the first generation, coming directly from the source (the so-called *uncollided density* [30, 113]):

$$\psi_1(\mathbf{r},\mathbf{v}) = \int d\mathbf{r}' T(\mathbf{r}' \to \mathbf{r}|\mathbf{v})\mathcal{Q}(\mathbf{r}',\mathbf{v}), \tag{2.12}$$

$\mathcal{Q}$ being the particle source.

Equation (2.11) is a Boltzmann-like integral balance equation for the incident particle density $\psi_g(\mathbf{r},\mathbf{v})$ [30, 113]. As such, it has a close relationship with respect to the integral-differential Boltzmann equation (1.14) describing the evolution of exponential flights with respect to time [30, 113]. On the basis of the previous considerations concerning the nature of the Boltzmann equation, it is apparent that the displacement kernel $T(\mathbf{r}' \to \mathbf{r}|\mathbf{v})$ should have an *exponential* behaviour, which would impose

$$T(\mathbf{r}' \to \mathbf{r}|\mathbf{v}) = \Sigma(\mathbf{r},\mathbf{v})e^{-\int_0^{\boldsymbol{\omega}\cdot(\mathbf{r}-\mathbf{r}')} \Sigma(\mathbf{r}'+s\boldsymbol{\omega},\mathbf{v})ds}. \tag{2.13}$$

In this case, Eq. (2.11) represents the integral form of the time-dependent Bolzmann equation (1.14), when the particle displacements are measured only at discrete generations [30, 31, 113].

However, observe that in the derivation of Eq. (2.11) we did not explicitly use the functional form of the kernel T. Actually, Eq. (2.11) holds true for *any* reasonable collision kernel C and displacement kernel T. In this respect, equation (2.11) describes the dynamical evolution of the particle density of a discrete random walk composed of random displacements ('flights' along straight lines) obeying the kernel T and random velocity redistributions ('collisions' with the surrounding medium) obeying the collision kernel C [2, 7, 8, 147, 147, 148]. The simplest formulation of these processes, which take the name of *random flights*, was originally proposed by Pearson (1905) for jumps of constant length [151] and later extended by Kluyver (1906) [152] and Rayleigh (1919) [153]. Random flights play a prominent role in the description of many physical or biological systems,

including neutron or photon propagation through disordered matter or turbid media (when the scale of heterogeneity is comparable to that of a mean free path) [70–76, 79], or chemical and biological species migration [50, 54–58]. Random flights are Markovian at collision events, i.e., they are semi-Markovian, and formally define a *renewal process*: knowledge of the coordinates $\mathbf{r}, \mathbf{v}$ at a given generation (i.e., entering a collision point) is sufficient to characterize the subsequent evolution of the process; in general, nonetheless, random flights are not Markovian at arbitrary times in between collisions [2, 7, 8].

The class of exponential flights is included in that of random flights: when T obeys Eq. (2.13), we recover exponential flights, and Markovianity is thus preserved all along the trajectory, because of the memoryless nature of the exponential distribution. In this case, Eq. (2.11) describes the evolution of exponential flights with respect to discrete generations, whereas the Boltzmann equation (1.14) describes the evolution of the same process with respect to time [2].

2.3 The Boltzmann equation and the kinetic equations

The approach pursued here in order to set up the linear Boltzmann equation (1.14) has been purely heuristic, via the definition of cross sections and the subsequent derivation of an explicit form of the collision term. The Boltzmann equation has been originally established in the context of the kinetic theory of gas in 1860 [3,5,13,14]. A rigorous approach to the derivation of Eq. (1.14) from first principles has been the subject of intense research activities since 1940, and several strategies have been so far proposed in literature, which go under the name of *non-equilibrium statistical mechanics* [3,5,115]. The underlying idea is to build upon the exact microscopic equations of motion (Hamiltonian mechanics in phase space for classical systems such as gases, or quantum mechanical equations if needed) for the ensemble of particles composing the system under consideration. This system is typically huge, and can be meaningfully described only in a probabilistic way. Then, the precise aim of non-equilibrium statistical mechanics is to show under which approximations equations of the Boltzmann type (linear or nonlinear) can be derived for some observables of the system.

Illustrating the precise details of this derivation is far beyond the scope of the present work; however, for the sake of completeness, we sketch here an argument of plausibility. As a case study, we will consider a gas of identical classical particles in a box. A detailed study of the quantum-mechanical analogue, which would be more appropriate for neutrons, has been derived in [112,116,117]. A macroscopic volume of such a gas will contain an enormous amount of particles, of the order of, say, $M \simeq 10^{19}$ per cubic centimeter. In principle, the evolution of such a system can be exactly computed starting from the M-body kinetic equations

$$\begin{cases} \dot{\mathbf{r}}_i = \mathbf{v}_i \\ \dot{\mathbf{v}}_i = \mathbf{F}(\mathbf{r}_i), \end{cases} \tag{2.14}$$

for the position $\mathbf{r}_i(t)$ and the velocity $\mathbf{v}_i(t)$, where $i = 1, \cdots, M$ and $\mathbf{F}(\mathbf{r}_i) = \sum_{j \neq i} \mathbf{F}_{i,j}(\mathbf{r}_i, \mathbf{r}_j)$ are the internal forces exerted by every particle j on particle i divided by the mass of the particle [3,5,115]. We will assume for the sake of simplicity that there are no external forces acting on the particles, and that $\mathbf{F}_{i,j}$ is conservative and derivable from velocity-independent scalar functions. In order to describe the dynamical evolution of the system, it is convenient to condense Eqs. (2.14) in the form

$$\frac{d\mathbf{z}}{dt} = \mathbf{Z}, \tag{2.15}$$

where $\mathbf{z} = \{\mathbf{r}_1, \mathbf{v}_1, \cdots, \mathbf{r}_M, \mathbf{v}_M\}$ is a point in the $6M$-dimensional phase space, and $\mathbf{Z} = \{\mathbf{v}_1, \mathbf{F}_1, \cdots, \mathbf{v}_M, \mathbf{F}_M\}$ is the (known) forcing term, with the initial condition $\mathbf{z}_{t=0} = \mathbf{z}_0$.

The system (2.14) is composed of $6M$ equations (3 position coordinates plus 3 velocity coordinates per particle) and can in principle be solved once the $6M$ initial conditions are provided. Given that M is huge, however, simple practical considerations clearly show that this approach is hopeless: the equations can not be formally written down in a reasonable amount of time, nor can they be handled by a computer because of the computational cost and the memory occupation that would be required. Moreover, even though a remedy were to be found to theses problems, the system would still strongly depend on the least precision or truncation error on the initial condition, so that after an infinitesimal time the integration will become useless. Thus, one is naturally led to approach this problem from the probabilistic point of view [3, 5, 115].

2.3.1 The Gibbs ensembles

The idea first proposed by Gibbs in 1902 is to condense our ignorance on the initial data $\mathbf{z}_0$ by assigning a probability density $\rho_0(\mathbf{z}) = \rho(\mathbf{z}, t = 0)$ [3, 115, 154]. In other words, the initial state is allowed to assume different values with a given distribution: the collection of the allowed states is called the *ensemble*. The goal is then to derive an equation for the evolution of the density $\rho(\mathbf{z}, t)$ at subsequent times $t > 0$. The quantity $\rho(\mathbf{z}, t)$ is called the *ensemble density function* and physically represents (up to a normalization factor) the probability density that an unspecified state is occupied in a phase space volume [3, 115, 154]. We may write

$$\rho(\mathbf{z}, t) \propto f_M(\mathbf{r}_1, \mathbf{v}_1, \cdots, \mathbf{r}_M, \mathbf{v}_M, t), \tag{2.16}$$

where f_M is the M-body joint probability density of finding the first particle at $\mathbf{r}_1$ with velocity $\mathbf{v}_1$, the second particle at $\mathbf{r}_2$ with velocity $\mathbf{v}_2$, $\cdots$, and the M-th particle at $\mathbf{r}_M$ with velocity $\mathbf{v}_M$. The quantity f_M is often called the *master function* [3, 115, 154]. By observing that Eq. (2.15) defines the dynamics of a point with velocity $\mathbf{Z}$, and that giving an initial distribution of $\mathbf{z}_0$ means that the single point $\mathbf{z}$ is replaced with a sort of fluid having density ρ, applying mass conservation yields

$$\frac{\partial}{\partial t}\rho(\mathbf{z}, t) + \nabla_{\mathbf{z}} \cdot \rho(\mathbf{z}, t)\mathbf{Z} = 0, \tag{2.17}$$

which takes the name of *Liouville equation*, with initial condition $\rho(\mathbf{z}, 0) = \rho_0(\mathbf{z})$ [3, 14, 115]. Now, since $\mathbf{r}$ and $\mathbf{v}$ are independent variables in the phase space, then $\nabla \cdot \mathbf{Z} = 0$ (this requires that the forces $\mathbf{F}$ do not depend on velocity, which is the case for the system considered here). Then, Eq. (2.17) can be rewritten as

$$\frac{\partial}{\partial t}\rho(\mathbf{z}, t) + \mathbf{Z} \cdot \nabla_{\mathbf{z}}\rho(\mathbf{z}, t) = 0, \tag{2.18}$$

which, by making the variables explicit, yields

$$\frac{\partial}{\partial t}\rho(\mathbf{z}, t) + \sum_{i=1}^{M} \left(\mathbf{v}_i \cdot \nabla_{\mathbf{r}_i} + \mathbf{F}_i \cdot \frac{\partial}{\partial \mathbf{v}_i} \right) \rho(\mathbf{z}, t) = \frac{\partial}{\partial t}\rho(\mathbf{z}, t) + \{\mathcal{H}, \rho\} = 0, \tag{2.19}$$

where $\mathcal{H}$ is the Hamiltonian of the system and $\{\cdot, \cdot\}$ are the Poisson brackets [3, 14, 115]. By using the total derivative notation, Eq. (2.19) can be equivalently formulated as

$$\frac{d}{dt}\rho(\mathbf{z}, t) = 0, \tag{2.20}$$

which takes the name of *Liouville theorem* [3, 14, 115]. This shows that the probability density $\rho(\mathbf{z}, t)$ is constant (and equal to the initial condition) along the trajectories in the $6M$-dimensional phase space. This consideration has an important consequence, namely that the flow of $\rho(\mathbf{z}, t)$ in the phase

space is volume-preserving. Actually, each point $\mathbf{z} = \mathbf{z}(\mathbf{z}_0, t)$ can be seen as a mapping of the initial conditions onto the positions occupied at a later time t. Then, by the uniqueness of the solution of Eq. (2.15) in the phase space, it follows that the probability of finding the point $\mathbf{z}$ at time t in a given region A must equal the probability that the point $\mathbf{z}_0$ lies within the region A_0 of the points whose image at time t is A. In other words,

$$\int_A \rho(\mathbf{z}, t) d\mathbf{z} = \int_{A_0} \rho_0(\mathbf{z}_0) d\mathbf{z}_0, \tag{2.21}$$

which shows that the volume in the phase space is preserved [3, 115]. When the initial condition is known exactly, we have $\rho_0(\mathbf{z}) = \delta(\mathbf{z} - \mathbf{z}_0)$: in this case the solution of the Liouville equation will be a delta function for all subsequent times, which implies that the system trajectory will deterministically evolve in the phase space without any uncertainty.

To proceed further on, we assume that the gas particles have a diameter ϵ and that particles can interact with the walls of the box via elastic collisions, or with each other via hard-sphere collisions. The hard-sphere collision means that particles do not interact until their mutual distance is smaller than ϵ, whereupon an infinite repulsive central force is applied: this is an adequate model for a gas of classical neutral particles interacting only at short distance (billiard balls). It can be shown that the Liouville theorem (2.21) for the conservation of the phase space volume remains valid also when the forces $\mathbf{F}$ are instantaneous such those of the hard-sphere gas [3, 14, 115]. What is the effect of the particle interactions with the walls and with each other on the initial uncertainty $\rho_0(\mathbf{z}_0)$? Let us assume for the sake of simplicity that the initial condition for a given particle is a uniform distribution of size $\Delta\mathbf{r}\Delta\mathbf{v}$ centered on some $\mathbf{r}_0, \mathbf{v}_0$. It can be shown then the rectangular area $\Delta\mathbf{r}\Delta\mathbf{v}$ of the accessible positions and velocities in the phase space is progressively stretched and subdivided in thin foils (the volume being preserved by the Liouville theorem) whose thickness is roughly proportional to $(\epsilon/\lambda)^q$, where λ is the mean free path of a particle and q is the number of collisions undergone by the particle. For a typical diluted gas, $\lambda/\epsilon \geq 10$, which means that after a thousand collisions the thickness of this foliated structure in the phase space is of the order of 10^{-1000}. This means that even infinitesimal external perturbations will affect the structure of the phase space characterizing the particle evolution. In other words, not only the initial conditions are uncertain, but even the collision mechanism that ultimately determines the fate of the particles must be practically dealt with in probabilistic terms [14].

2.3.2 The s-particle distributions

Usually, we are not interested in determining precisely the position and velocity of each particle of the gas. Rather, one typically wants to assess the macroscopic properties of the system (a physical observable such as pressure or temperature), which can be expressed as averages of some functional $\mathcal{O}$ over the particle distribution f_M in phase space, namely,

$$\langle \mathcal{O} \rangle = \int \mathcal{O}(\mathbf{z}) f_M d\mathbf{z}, \tag{2.22}$$

which takes the name of ensemble average over all possible configurations of the system compatible with the underlying dynamics. The central postulate of statistical mechanics is the so-called *hypothesis of ergodicity* [3, 115], which yields

$$\int \mathcal{O}(\mathbf{z}) f_M d\mathbf{z} = \lim_{N\to\infty} \frac{1}{N} \sum_{j=1}^{N} \mathcal{O}_j, \tag{2.23}$$

where $\mathcal{O}_j$ is the observed value of the functional $\mathcal{O}$ at the j-th experimental measurement under identical circumstances.

It is reasonable to assume that the average observable $\langle\mathcal{O}\rangle$ will remain unchanged under an arbitrary permutation of any two gas particles chosen at will. From the symmetry argument, the average observable will most often depend on *symmetrical sums* of terms, each based on the coordinates of a few particles (typically, one or two) [3,14,115]: in other words, instead of computing the M-body probability density function f_M (whose evolution is governed by the Liouville equation) one is frequently called to handle s-particle distributions of the kind

$$f_s(\mathbf{r}_1, \mathbf{v}_1, \cdots, \mathbf{r}_s, \mathbf{v}_s, t) = \frac{M!}{(M-s)!} \int f_M \prod_{i=s+1}^{M} d\mathbf{r}_i d\mathbf{v}_i, \tag{2.24}$$

$s \ll M$, obtained by integrating the M-body probability density function f_M over the position and velocity coordinates of the other $M-s$ particles [3,14,115]. As defined, the s-tuple distributions are independent of the order with which the particles occupy a given state. In particular, the one-particle distribution reads

$$f_1(\mathbf{r}_1, \mathbf{v}_1, t) = \frac{M!}{(M-1)!} \int f_M \prod_{i=2}^{M} d\mathbf{r}_i d\mathbf{v}_i = M \int f_M \prod_{i=2}^{M} d\mathbf{r}_i d\mathbf{v}_i. \tag{2.25}$$

The quantity f_1/M represents the reduced one-particle probability density that particle number one is at $\mathbf{r}_1$ with velocity $\mathbf{r}_1$. Similarly, the two-particle distribution reads

$$f_2(\mathbf{r}_1, \mathbf{v}_1, \mathbf{r}_2, \mathbf{v}_2, t) = \frac{M!}{(M-2)!} \int f_M \prod_{i=3}^{M} d\mathbf{r}_i d\mathbf{v}_i = M(M-1) \int f_M \prod_{i=3}^{M} d\mathbf{r}_i d\mathbf{v}_i. \tag{2.26}$$

The quantity $f_2/M(M-1)$ represents the reduced joint probability density that particle number one is at $\mathbf{r}_1$ with velocity $\mathbf{r}_1$ and particle number two is at $\mathbf{r}_2$ with velocity $\mathbf{r}_2$.

As said, f_M satisfies the Liouville equation, namely,

$$\frac{\partial}{\partial t} f_M + \sum_{i=1}^{M} \Big[\mathbf{v}_i \cdot \nabla_{\mathbf{r}_i} f_M + \mathbf{F}_i \cdot \nabla_{\mathbf{v}_i} f_M \Big] = 0, \tag{2.27}$$

The equations for the s-tuple distributions can be obtained multiplying Eq. (2.27) by $M!/(M-s)!$ and integrating over phase space variables as in Eq. (2.24) [3,14,115]. By various manipulations, we obtain

$$\frac{\partial}{\partial t} f_s + \sum_{i=1}^{s} \mathbf{v}_i \cdot \nabla_{\mathbf{r}_i} f_s + \sum_{i=1}^{s} \sum_{j \neq i} \mathbf{F}_{i,j} \cdot \nabla_{\mathbf{v}_i} f_s + \sum_{i=1}^{s} \nabla_{\mathbf{v}_i} \cdot \int \mathbf{F}_{s+1,i} f_{s+1} d\mathbf{r}_{s+1} d\mathbf{v}_{s+1} = 0, \tag{2.28}$$

Equations (2.28) form the so-called BBGKY hierarchy (from Bogoliubov, Born, Green, Kirkwood and Yvon) relating the s-th order distribution to that of the $(s+1)$-th order [3, 14, 115]. Some closure is therefore needed in order to obtain explicit solutions. Let us consider the special case $s = 1$, corresponding to the one-particle distribution. From Eq. (2.28), f_1 satisfies

$$\frac{\partial}{\partial t} f_1 + \mathbf{v}_1 \cdot \nabla_{\mathbf{r}_1} f_s = -\nabla_{\mathbf{v}_1} \cdot \int \mathbf{F}_{2,1} f_2 d\mathbf{r}_2 d\mathbf{v}_2. \tag{2.29}$$

The only practical means to progress is to introduce some assumptions that allow relating f_2 to f_1 [3]. Four *postulates* are then adopted:

i. in the region of the phase space where the internal forces $\mathbf{F}_{2,1}$ differ appreciably from zero, no other bodies affect the dynamics of the particle pair. This will be true provided that the gas is not too dense, which is coherent with the physical picture provided above: particle freely stream through space at constant velocity, and occasionally collide with another particle. Three-body collisions are assumed to be very rare.

ii. when particles enter a collision,

$$f_2(\mathbf{r}_1, \mathbf{v}_1, \mathbf{r}_2, \mathbf{v}_2, t) \simeq f_1(\mathbf{r}_1, \mathbf{v}_1, t) f_1(\mathbf{r}_2, \mathbf{v}_2, t). \tag{2.30}$$

This is the so-called *chaos hypothesis* introduced by Boltzmann, which implies that correlations between colliding particles can be neglected [3,13,14,115]. This is likely to be true for a diluted gas, when particles arrive at the collision point from some distance: the probability that the particles have originated from a common previous collision is reasonably small [3].

iii. during the collision event, the rates of change of f_1 and f_2 can be neglected. This corresponds to assuming that the time scale of a collision is much shorter than the time between collisions.

iv. over the distance of particle-particle interactions, f_2 depends only on the relative distance $\mathbf{R} = \mathbf{r}_1 - \mathbf{r}_2$, and the gradient of f_1 can be neglected.

By building upon these arguments (see Appendix A.1 for the details), it is possible to derive a closure for the function f_1, namely,

$$\frac{\partial}{\partial t}\bar{f}_1 + \mathbf{v}_1 \cdot \nabla_{\mathbf{r}_1}\bar{f}_1 = \left(\bar{f}_1, \bar{f}_1\right)_{coll}, \tag{2.31}$$

where the bar sign denotes the average over a time that is long compared to the duration of a collision, and short compared to the duration of a free flight [3], and $\left(\bar{f}_1, \bar{f}_1\right)_{coll}$ represents the contributions to the phase space balance due to the scattering collisions (the explicit expression is provided in Appendix A.1).

Equation (2.31) has formally the same structure as the non-linear Boltzmann equation derived on phenomenological basis by Boltzmann for a gas of interacting particles [3,14]. However, in the original derivation, the Boltzmann equation represented a *mass balance* in the phase space for the quantity N_t, defined such that $N_t d\mathbf{r} d\mathbf{v}$ is the average number of particles in the phase space element. In view of the fact that $N_t(\mathbf{r}, \mathbf{v})$ (the average number of particles) and $\bar{f}_1(\mathbf{r}, \mathbf{v}, t)$ (the time-averaged one-particle distribution) both satisfy the same equation, it may be concluded that they are *different physical concepts associated to the same mathematical quantity*, provided that the approximations introduced here hold true [3,14,115].

2.3.3 Mixtures of gases and the linear Boltzmann equation

So far, we have considered a gas of identical particles. The Boltzmann equation can be easily extended to the case of a mixture of different gases of kind i [3,14,115], in which case we obtain a system of coupled equations of the kind

$$\frac{\partial}{\partial t}\bar{f}_1^{(i)} + \mathbf{v}_1 \cdot \nabla_{\mathbf{r}_1}\bar{f}_1^{(i)} = \sum_j \left(\bar{f}_1^{(i)}, \bar{f}_1^{(j)}\right)_{coll} \tag{2.32}$$

[3] This assumption fails for a gas of neutrons in the presence of fission, which introduces correlations over temporal and spatial scales comparable to those of a typical free flight [3–5]. We will come back to this relevant issue in the following Chapters.

for the one-particle distribution $f_1^{(i)}$ of species i, the sum being extended to all species in the system. As a particular case, it is useful to consider the configuration of two species where the former is a foreign population ($i = A$) and the latter represents a host medium ($i = B$) (usually assumed at thermal equilibrium) [3,14,115]. This would be for instance the case of neutrons or photons colliding with the nuclei of a given moderator. Equation (2.32) gives then

$$\frac{\partial}{\partial t}\bar{f}_1^{(A)} + \mathbf{v}_1 \cdot \nabla_{\mathbf{r}_1}\bar{f}_1^{(A)} = \left(\bar{f}_1^{(A)}, \bar{f}_1^{(A)}\right)_{coll} + \left(\bar{f}_1^{(A)}, \bar{f}_1^{(B)}\right)_{coll} \tag{2.33}$$

$$\frac{\partial}{\partial t}\bar{f}_1^{(B)} + \mathbf{V}_1 \cdot \nabla_{\mathbf{R}_1}\bar{f}_1^{(B)} = \left(\bar{f}_1^{(B)}, \bar{f}_1^{(B)}\right)_{coll} + \left(\bar{f}_1^{(A)}, \bar{f}_1^{(B)}\right)_{coll}. \tag{2.34}$$

Now, the density of the foreign population is typically much lower than that of the host medium (for the case of neutrons in a nuclear reactor, e.g., the former is of the order of 0.1 neutrons per cubic centimeter per Watt, whence about 10^8 per cubic centimeter for a commercial reactor at full power, whereas the latter is of the order of 10^{22} nuclei per cubic centimeter) [30, 31]. This means that $|\bar{f}_1^{(A)}| \ll |\bar{f}_1^{(B)}|$. Under this assumption, we arrive at

$$\frac{\partial}{\partial t}\bar{f}_1^{(A)} + \mathbf{v}_1 \cdot \nabla_{\mathbf{r}_1}\bar{f}_1^{(A)} = \left(\bar{f}_1^{(A)}, \bar{f}_1^{(B)}\right)_{coll} \tag{2.35}$$

$$\frac{\partial}{\partial t}\bar{f}_1^{(B)} + \mathbf{V}_1 \cdot \nabla_{\mathbf{R}_1}\bar{f}_1^{(B)} = \left(\bar{f}_1^{(B)}, \bar{f}_1^{(B)}\right)_{coll}. \tag{2.36}$$

When the species (B) is at equilibrium, the distribution function $\bar{f}_1^{(B)}$ is known (typically, a Maxwellian distribution), and we are left with a linear Boltzmann equation for the species (A):

$$\frac{\partial}{\partial t}\bar{f}_1^{(A)} + \mathbf{v}_1 \cdot \nabla_{\mathbf{r}_1}\bar{f}_1^{(A)} = \left(\bar{f}_1^{(A)}, \bar{f}_1^{(B)}\right)_{coll}. \tag{2.37}$$

By virtue of the analysis of the linear scattering term introduced above and the definition of the scattering cross section, we finally recover the linear Boltzmann equation in the form given in Eq. (1.14), provided that we identify $\bar{f}_1^{(A)}(\mathbf{r}, \mathbf{v}, t) = N_t(\mathbf{r}, \mathbf{v})$ [3, 14, 115].

Observe that in this sketch of derivation of the non-linear and linear Boltzmann equation we have focused on scattering collisions, where the number of particles is preserved. A rigorous treatment of other kinds of particle-medium interactions such as absorptions or fissions, where the number of particles is not preserved, would demand a quantum-mechanical approach: this strategy has been pursued by [112, 116, 117] for the one- and two-particle distributions.

2.4 The diffusion equation and Brownian motion

Sometimes, detailed knowledge of the phase space density $N_t(\mathbf{r}, \mathbf{v})$ is not needed, and one tries to derive an equation for the simpler direction-averaged *spatial density* $n_t(\mathbf{r}) = \int d\boldsymbol{\omega} N_t(\mathbf{r}, \mathbf{v})$ by resorting to some approximations [5, 14]. The hypotheses introduced to derive such an equation for $n_t(\mathbf{r})$ are called the continuum or diffusion limit. Our starting point will be the linear Boltzmann equation (1.14) for $N_t(\mathbf{r}, \mathbf{v})$. For the sake of simplicity, we will assume that the speed v is constant ($d\mathbf{v} = v d\boldsymbol{\omega}$), that cross-sections do not depend on particle direction (i.e., $\Sigma = \Sigma(\mathbf{r})$), and that particles can only be scattered at collisions ($\nu = 1$), which leads to

$$\frac{1}{v}\frac{\partial}{\partial t}\varphi_t + \boldsymbol{\omega} \cdot \nabla_{\mathbf{r}}\varphi_t = \int \Sigma(\mathbf{r}) f_C(\boldsymbol{\omega}' \to \boldsymbol{\omega})\varphi_t(\mathbf{r}, \boldsymbol{\omega}')d\boldsymbol{\omega}' - \Sigma(\mathbf{r})\varphi_t, \tag{2.38}$$

where $\varphi_t(\mathbf{r},\boldsymbol{\omega}) = vN_t(\mathbf{r},\boldsymbol{\omega})$ depends only on position $\mathbf{r}$ and direction $\boldsymbol{\omega}$. Observe that integrating over $\boldsymbol{v}$ the collision term (1.13) gives

$$\int \left(\frac{\partial N_t}{\partial t}\right)_{coll} d\mathbf{v} = \int\int v'\Sigma(\mathbf{r},\mathbf{v}')f_C(\mathbf{v}'\to\mathbf{v})N_t(\mathbf{r},\mathbf{v}')d\mathbf{v}'d\mathbf{v} - \int v\Sigma(\mathbf{r},\mathbf{v})N_t d\mathbf{v} = 0, \tag{2.39}$$

from the normalization of f_C [5, 14]. More generally, it could be shown that for arbitrary suitable collision terms $\left(\frac{\partial N_t}{\partial t}\right)_{coll}$ we have

$$\int \chi(\mathbf{v})\left(\frac{\partial N_t}{\partial t}\right)_{coll} d\mathbf{v} = 0 \tag{2.40}$$

for any $\chi(\mathbf{v})$ being a *collisional invariant*, i.e., a physical quantity that is conserved upon collision [5, 14]. Typical invariants in particle transport are energy, momentum and mass. For the simple diffusive random walk in a host medium considered here, the only invariant is $\chi(\mathbf{v}) = 1$ because the number of particles is conserved at scattering collisions.

Assume that there are no external sources at time $t > t_0$, and that the initial condition is an isotropic point source at time $t_0 = 0$. By integrating Eq. (2.38) over the direction $\boldsymbol{\omega}$ and using Eq. (2.39) we therefore get

$$\frac{1}{v}\frac{\partial}{\partial t}\phi_t(\mathbf{r}) + \nabla_{\mathbf{r}}\cdot\mathbf{j}_t(\mathbf{r}) = 0, \tag{2.41}$$

where we have set

$$\phi_t(\mathbf{r}) = vn_t(\mathbf{r}) = \int \varphi_t(\mathbf{r},\boldsymbol{\omega})d\boldsymbol{\omega}, \tag{2.42}$$

and

$$\mathbf{j}_t(\mathbf{r}) = \int \boldsymbol{\omega}\varphi_t(\mathbf{r},\boldsymbol{\omega})d\boldsymbol{\omega}. \tag{2.43}$$

Equation (2.41) is basically a continuity (conservation) equation for the field $n_t(\mathbf{r})$, the direction-averaged density, which can not however be solved directly, since it depends on the higher order term $\mathbf{j}_t(\mathbf{r})$. To proceed further, we multiply Eq. (2.38) by $\boldsymbol{\omega}$ and integrate again over $d\boldsymbol{\omega}$. This yields

$$\frac{1}{v}\frac{\partial}{\partial t}\mathbf{j}_t(\mathbf{r}) + \nabla_{\mathbf{r}}\cdot\int \boldsymbol{\omega}\boldsymbol{\omega}\varphi_t(\mathbf{r},\boldsymbol{\omega})d\boldsymbol{\omega} + \Sigma\mathbf{j}_t(\mathbf{r}) = \mu_0\Sigma\mathbf{j}_t(\mathbf{r}), \tag{2.44}$$

where μ_0 is the *average scattering angle*

$$\mu_0 = \langle\boldsymbol{\omega}'\cdot\boldsymbol{\omega}\rangle = \frac{1}{\Omega_d}\int d\boldsymbol{\omega}\int d\boldsymbol{\omega}'\boldsymbol{\omega}'\cdot\boldsymbol{\omega}f_C(\boldsymbol{\omega}'\to\boldsymbol{\omega}), \tag{2.45}$$

where

$$\Omega_d = \frac{2\pi^{d/2}}{\Gamma\left(\frac{d}{2}\right)} \tag{2.46}$$

is the surface of the unit sphere in dimension d, and we have used

$$\int d\boldsymbol{\omega}\boldsymbol{\omega}\int d\boldsymbol{\omega}'\Sigma(\mathbf{r})f_C(\boldsymbol{\omega}'\to\boldsymbol{\omega})\varphi_t(\mathbf{r},\boldsymbol{\omega}') = \mu_0\Sigma\mathbf{j}_t(\mathbf{r}). \tag{2.47}$$

We could proceed this way, but this would give rise to a hierarchy of equations, each containing a new unknown [5, 14]. It is then necessary to introduce some approximations to allow for an explicit

equation for $n_t(\mathbf{r})$. We begin by assuming that the flux $\varphi_t(\mathbf{r},\boldsymbol{\omega})$ is only weakly dependent on the direction $\boldsymbol{\omega}$, which gives an expansion of the kind

$$\varphi_t(\mathbf{r},\boldsymbol{\omega}) = \frac{1}{\Omega_d}\phi_t(\mathbf{r}) + \frac{d}{\Omega_d}\boldsymbol{\omega}\cdot\mathbf{j}_t(\mathbf{r}) + \cdots \tag{2.48}$$

where terms of higher order in $\boldsymbol{\omega}$ have been neglected. The zero-th and first order coefficients of the expansion in Eq. (2.48) have been identified with $\phi_t(\mathbf{r})$ and $\mathbf{j}_t(\mathbf{r})$, respectively, on the basis of the definitions given above. It follows then that up to the linear order we have

$$\nabla_{\mathbf{r}}\cdot\int\boldsymbol{\omega}\boldsymbol{\omega}\varphi_t(\mathbf{r},\boldsymbol{\omega})d\boldsymbol{\omega} = \frac{1}{d}\nabla_{\mathbf{r}}\phi_t(\mathbf{r}) + \cdots, \tag{2.49}$$

which therefore from Eq. (2.44) yields

$$\frac{1}{v}\frac{\partial}{\partial t}\mathbf{j}_t(\mathbf{r}) + \frac{1}{d}\nabla_{\mathbf{r}}\phi_t(\mathbf{r}) + \mathbf{j}_t(\mathbf{r}) = 0. \tag{2.50}$$

We have denoted by $\Sigma_{tr}(\mathbf{r}) = (1-\mu_0)\Sigma$ the so-called *transport cross section*, which takes into account anisotropic scattering effects via the average scattering angle μ_0 [5, 14]. In principle, the approximate Eq. (2.50) for $\mathbf{j}_t(\mathbf{r})$, coupled with the exact conservation Eq. (2.41), can be now explicitly solved to give the direction-averaged density $n_t(\mathbf{r})$. However, it is customary to introduce a further approximation, namely

$$\frac{1}{v}\frac{\partial}{\partial t}\mathbf{j}_t(\mathbf{r}) \simeq 0, \tag{2.51}$$

which implies

$$\frac{1}{|\mathbf{j}_t|}\frac{\partial}{\partial t}|\mathbf{j}_t| \ll v\Sigma, \tag{2.52}$$

and physically means that the time variation of the current density $\mathbf{j}_t(\mathbf{r})$ is much slower than the *collision frequency* $v\Sigma$ [5, 14]. Under this assumption, we can then rewrite

$$\frac{1}{d}\nabla_{\mathbf{r}}\phi_t(\mathbf{r}) + \Sigma_{tr}\mathbf{j}_t(\mathbf{r}) = 0, \tag{2.53}$$

whence

$$\mathbf{j}_t(\mathbf{r}) = -\frac{1}{d\Sigma_{tr}}\nabla_{\mathbf{r}}\phi_t(\mathbf{r}), \tag{2.54}$$

which yields the current density $\mathbf{j}_t(\mathbf{r})$ in terms of the flux $\phi_t(\mathbf{r})$, in the form of a Fick's law [5, 14, 30, 31, 113]. Introduce now a *diffusion coefficient*

$$D(\mathbf{r}) = \frac{v}{d\Sigma_{tr}}, \tag{2.55}$$

carrying the customary units of a squared length over a time [5]. Then, Eq. (2.54) can be written as

$$\mathbf{j}_t(\mathbf{r}) = -D(\mathbf{r})\nabla_{\mathbf{r}}n_t(\mathbf{r}), \tag{2.56}$$

which basically says that the current is proportional to the opposite of the gradient of the particle concentration (the conserved quantity).

By finally plugging Eq. (2.54) into Eq. (2.41) we obtain the *diffusion equation*

$$\boxed{\frac{\partial}{\partial t}n_t(\mathbf{r}) = \nabla_{\mathbf{r}}\cdot D(\mathbf{r})\nabla_{\mathbf{r}}n_t(\mathbf{r}),} \tag{2.57}$$

together with the isotropic source as an initial condition [5, 14, 30, 31, 113]. The derivation of Eq. (2.57), which is the diffusion (continuum) limit of the transport equation (2.38), has involved a continuity equation for a conserved quantity (here, the particle mass), plus an approximate closure relation for the higher moments (the so-called transport law) and a further approximation on the time variation of such higher order moments: this scheme always appears when deriving hydrodynamical limits from exact transport equations [5].

Now, by virtue of the Einstein-Smoluchowski interpretation [3, 7, 8, 16–18], the diffusion equation (2.57) is formally identical to the evolution equation for the average density $n_t(\mathbf{r})$ of a *Brownian motion* born at $t_0 = 0$ from a given source and observed at time t. It is therefore reasonable to assume that, under the hypotheses above, the underlying exponential flight process converges towards a Brownian motion with diffusion coefficient D. In other words, in the regime where the previous hypotheses above hold true, the diffusion equation is the *scaling limit* of the Boltzmann equation for the average particle number (the macroscopic observable), and the Brownian motion is correspondingly the scaling limit of the exponential flights (the microscopic process) [5,14].

Boundary conditions for Eq. (2.57) are rather tricky to derive, because of the introduced approximations. For instance, while we require the continuity of the phase space density N_t across an interface, the diffusion approximation implies conservation only of the two first moments n_t and $\mathbf{j}_t$. The free surface boundary is even more difficult to handle. Indeed, the exact condition implies that the inward current at the outer surface must vanish. For the diffusion limit, this condition can only be approximated, and commonly one assumes that the concentration $n_t(\mathbf{r})$ (or equivalently the flux $\phi_t(\mathbf{r})$) vanishes at some *extrapolated distance* $\mathbf{r}_e$ from the outer boundary [14, 113, 155, 156]. The calculation of this extrapolated length is dimension- and geometry-dependent and in most cases is highly non-trivial [14, 155, 156]. Practically, the extrapolated distance $\mathbf{r}_e$ is adjusted so that the computed particle concentration $n_t(\mathbf{r})$ inside the medium is a proper representation of the actual values.

2.5 The role of Monte Carlo simulation

As said above, the key goal of (non-equilibrium) statistical mechanics is to assess the statistical properties of some observable associated to a physical system whose evolution is governed by the stochastic motion of a collection of particles. Each observable can be seen as a question that the experimenter asks about the system under analysis. In this respect, statistical mechanics provides a bridge between the microscopic behaviour of the underlying stochastic processes and the macroscopic deterministic behaviour of the physical observables.

Given a collection of particles undergoing a stochastic process $\mathbf{X}(t)$, we define the observable ω as a functional $\omega = f[\mathbf{X}(t)]$ associated to the process. By construction, such observable will be a random object, whose moments $\mathbb{E}_t[\omega^m]$ (or equivalently full distribution $\mathcal{P}_t(\omega)$) we would like to precisely quantify. The Boltzmann equation provides an example of a deterministic evolution equation for the average (first moment) of the observable $\omega = m(\mathbf{r}, \mathbf{v}, t)$, where $m(\mathbf{r}, \mathbf{v}, t)$ is the random number of particles in phase space at a given time.

The general picture of stochastic particle transport given in the previous Sections provides the ideal framework for the application the *Monte Carlo methods*. The basic idea behind Monte Carlo as applied to transport problems is to simulate a (very large but necessarily finite) ensemble of realizations of trajectories in the phase space and to take ensemble averages over these realizations in order to determine the moments (or the whole distribution) of some physical observable [5, 14, 115, 157–160].

2.5.1 Monte Carlo methods and the linear Boltzmann equation

We will exemplify the application of Monte Carlo methods to the analysis of physical observables emerging in transport processes by considering the stationary Boltzmann equation for exponential flights. Let us recall the transport equation for the incident collision density ψ_g, namely,

$$\psi_{g+1}(\mathbf{r},\mathbf{v}) = \int d\mathbf{r}' \int d\mathbf{v}' T(\mathbf{r}' \to \mathbf{r}|\mathbf{v}) C(\mathbf{v}' \to \mathbf{v}|\mathbf{r}') \psi_g(\mathbf{r}',\mathbf{v}'), \tag{2.58}$$

with the uncollided density (or first-collision source)

$$\psi_1(\mathbf{r},\mathbf{v}) = \int d\mathbf{r}' \int d\mathbf{v}' T(\mathbf{r}' \to \mathbf{r}|\mathbf{v}') \mathcal{Q}(\mathbf{r}',\mathbf{v}'), \tag{2.59}$$

$\mathcal{Q}$ being the particle source. Define now the *stationary* particle density $\psi(\mathbf{r},\mathbf{v})$

$$\psi(\mathbf{r},\mathbf{v}) = \sum_{g=1}^{\infty} \psi_g(\mathbf{r},\mathbf{v}). \tag{2.60}$$

By direct substitution, $\psi(\mathbf{r},\mathbf{v})$ satisfies the linear *stationary* Boltzmann equation

$$\psi(\mathbf{r},\mathbf{v}) = \int d\mathbf{r}' \int d\mathbf{v}' K(\mathbf{r}' \to \mathbf{r}, \mathbf{v}' \to \mathbf{v}) \psi(\mathbf{r}',\mathbf{v}') + \psi_1(\mathbf{r},\mathbf{v}), \tag{2.61}$$

where $K(\mathbf{r}' \to \mathbf{r}, \mathbf{v}' \to \mathbf{v}) = T(\mathbf{r}' \to \mathbf{r}|\mathbf{v}) C(\mathbf{v}' \to \mathbf{v}|\mathbf{r}')$. For exponential flights the jump kernel is defined by

$$T(\mathbf{r}' \to \mathbf{r}|\mathbf{v}) = \Sigma(\mathbf{r},\mathbf{v}) e^{-\int_0^{\boldsymbol{\omega}\cdot(\mathbf{r}-\mathbf{r}')} \Sigma(\mathbf{r}'+s\boldsymbol{\omega},\mathbf{v}) ds} \tag{2.62}$$

and represents the Poisson probability density of performing a displacement between $\mathbf{r}'$ and $\mathbf{r}$ when the starting velocity is $\mathbf{v}$.

Now, recall that the Boltzmann equation precisely describes the average flow of particles undergoing exponential flights. The Monte Carlo method for solving Eq. (2.61) consists in generating a large number of *random walks* of the associated particles in the phase space, such that the ensemble average of a given observable defined on the random walk converges to the corresponding physical quantity weighted by ψ [157–159]. Each random walk can be seen as the physical stochastic trajectory of the transported particle, which travels along straight lines according to the transfer kernel T, separated by collisions, described by the collision kernel C. The random walks start from the source $\mathcal{Q}$, have k collisions in the viable space and are eventually lost from boundaries or absorbed. Such random walks are defined by the set of coordinates in the phase space reached by the particles. For the sake of simplicity, from now on the coordinates in the phase space will be denoted by the point $z = (\mathbf{r},\mathbf{v})$.

The construction of the random walk is the basic step to be performed in order to simulate the Monte Carlo simulation of the particles. Once the particle is created from the source $\mathcal{Q}$, it travels through the phase space via the $K(z',z)$ kernel. Assuming that the kernels are exactly known at each point of the viable phase space, the random walks can be then generated by

i. sampling the travelled distance from the continuous density function of the transfer kernel T;

ii. sampling the collision event from the discrete probability function p_i;

iii. sampling the state of the secondary particle(s) ν_i after the collision from the continuous distribution function f_{C_i} associated to the sampled event.

Once an ensemble of random walks has been sampled, the purpose of a Monte Carlo simulation is in general to define the appropriate *random variable* $\omega(\alpha)$ associated to the random walk α, whose expected value provides an estimate for the quantity

$$\mathbb{E}[\omega(\alpha)] \equiv \left\langle \psi(z) \middle| g(z) \right\rangle = \int \psi(z) g(z) dz, \tag{2.63}$$

which represents the inner product of the collision density $\psi(z)$ times a general test function $g(z)$ [157–159]. The function $g(z)$ is precisely the *score* that is desired, and $\langle \psi | g \rangle$ represents the *collision density-averaged* score over the volume of interest. The quantity $\omega(\alpha)$, which must be properly chosen so to ensure the convergence to $\mathbb{E}[\omega] = \langle \psi | g \rangle$, takes the name of Monte Carlo estimator [157–159]. The expected value of an ensemble of M random walks can be computed as

$$\mathbb{E}[\omega(\alpha)] = \frac{\sum_{i=1}^{M} \omega(\alpha_i)}{M}, \tag{2.64}$$

where α_i is the i-th random walk and $\omega(\alpha_i)$ is the associated random variable. It can be shown that convergence of the estimator as a function of the number of simulated random walks goes with the square root of M [157, 158].

A frequently used estimator is the so-called *collision* estimator, defined as

$$\omega_{coll}(\alpha) = \sum_m g(z_m), \tag{2.65}$$

where the index m is extended to all the collisions performed by the walker during its history. If we are interested in evaluating a score in a portion V of the phase space, the test function must be zero everywhere but in V; in other words, the test function must be multiplied by the *marker function* $\chi_V(z)$, i.e., $\chi_V(z) = 1$ for $z \in V$ and $\chi_V(z) = 0$ for $z \notin V$ [157, 158]. By progressively reducing the size of such volume V, we can obtain the value of the score evaluated at a single point of the phase space. On the other hand, the smaller the volume, the smaller is the probability to obtain a sample of the event in that position. Special techniques exist to obtain an estimate of the point-wise distribution of a physical quantity in the phase space (the so-called point-flux estimation: here we will not address this issue) [157]. The collision estimator for the particle flux $\varphi = \psi/\Sigma$ can be similarly obtained from

$$\omega_{coll}(\alpha) = \sum_m \frac{g(z_m)}{\Sigma(v_m)}, \tag{2.66}$$

where $\Sigma(v_m)$ is the total cross section of the particle at the m-th collision, when the incident velocity is v_m. In this case, $\mathbb{E}[\omega_{coll}] = \langle \varphi | g \rangle$. Finally, the estimator for the particle density-averaged scores is defined as

$$\omega_{coll}(\alpha) = \sum_m \frac{g(z_m)}{\Sigma(v_m) v_m}, \tag{2.67}$$

from the definition $N = \psi/(\Sigma v)$ for the stationary particle density in phase space. In this case, $\mathbb{E}[\omega_{coll}] = \langle N | g \rangle$. As an alternative to the collision estimator, the so-called *track length estimator* is defined as [157, 158]

$$\omega_{track}(\alpha) = \sum_m g(z_m) t_m, \tag{2.68}$$

where t_m is the time spent by the m-th particle in the volume V of the phase space. This estimator is such that $\mathbb{E}[\omega_{track}] = \langle N | g \rangle$. For the flux-averaged scores, we can then define

$$\omega_{track}(\alpha) = \sum_m g(\vec{x}_m) d_m, \tag{2.69}$$

where d_m is the track of the m-th particle in the volume V, whence $\mathbb{E}[\omega_{track}] = \langle\varphi|g\rangle$.

It can be shown that for exponential flights we have $\mathbb{E}[\omega_{track}(\alpha)] \equiv \mathbb{E}[\omega_{coll}(\alpha)]$ for any given g (by virtue of the Markovian nature of the underlying stochastic process), which implies that the two estimators converge to each other when $M \to \infty$ [157, 158]. The variance associated to the estimators depends on the problem we want to solve. In general, the collision estimators have a smaller variance in large volumes, whereas the track estimators are better suited for small volumes [157, 158].

2.5.2 Other physical observables

The theory of Monte Carlo methods as applied to the transport of exponential (and more generally random) flights has known a huge development since 1940 [157–160], following the pioneering works of Metropolis, Fermi, Von Neumann and Ulam [161–164]. A prominent and distinct advantage of Monte Carlo methods as applied to the study of stochastic processes is that they do not require the knowledge of the deterministic evolution equation for the desired observables. To quote T. E. Booth: *Monte Carlo simulation can be conceived directly from the abstracted physical process without ever even considering a transport equation. Average particle behavior in the Monte Carlo process certainly is described by the transport equation, just as a ball's motion is described by Newton's equation. But as a philosophical matter, saying that Monte Carlo is 'solving' the transport equation seems a bit like saying that a ball is 'solving' Newton's equation* [165].

On the other hand, knowledge of the Boltzmann equation has largely inspired since the beginning of the method (and still keeps inspiring) the Monte Carlo algorithms used for computing the particle densities $N_t(\mathbf{r}, \mathbf{v})$ and $\psi_g(\mathbf{r}, \mathbf{v})$, and turns out to be highly useful during both their conception and their subsequent analysis. Moreover, almost all of the existing schemes for accelerating the convergence of the Monte Carlo algorithms for $N_t(\mathbf{r}, \mathbf{v})$ and $\psi_g(\mathbf{r}, \mathbf{v})$ are based on the associated Boltzmann equation and/or its adjoint form [5, 157–159]. Within this framework, the analysis of the phase space densities by Monte Carlo simulation may benefit from both efficient algorithms and a solid theoretical background.

While the particle densities $N_t(\mathbf{r}, \mathbf{v})$ and $\psi_g(\mathbf{r}, \mathbf{v})$ in most cases provide a satisfactory description of the average behaviour of the random walkers, a number of interesting questions concerning the examined system can not be simply answered in terms of these sole quantities. In particular, we have remarked that no information concerning higher moments of the phase space distribution of the particles can be extracted from either $N_t(\mathbf{r}, \mathbf{v})$ or $\psi_g(\mathbf{r}, \mathbf{v})$, because the transport equation for the phase space densities ignores the correlations between particles [3, 5, 112, 115, 165]. Examples of such non-average observables emerge in several applications: one might for instance want to know how far in space a neutron will travel within a medium, once emitted from a source; how many gamma rays will arrive at a detector via coincidence events; how many collisions a nucleon will suffer during a cascade; how long it will take for a random search strategy to attain the desired target; whether and when an epidemic outbreak will eventually die out; how long it will take for a DNA filament to traverse a nano-pore during a translocation process; how long a fluctuating price will stay above a given threshold; and so on. Other physical observables are then needed, which might be roughly regrouped as

1. the *occupation statistics* of the particles within a volume of the phase space; depending on the specific boundary conditions, this quantity may represent the first passage time of the particles to a given barrier, or the residence time in a given region;

2. the distribution of the *number of descendant particles* that are within a region of the phase space at any given time, given a single initial walker emitted at the initial time;

3. the *survival probability*, i.e., the probability that at a given time the walker (or more generally at least a descendant of the original walker) is still alive. A closely related observable is the *escape probability*, i.e., the probability that at a given time the walker has left a domain.

In all such cases, the average densities alone are not sufficient to provide an answer, and the description of the transport process must be achieved in a framework that is necessarily broader than that of the Boltzmann equation. In Booth's words: *the conflation of 'solving a problem' and 'solving an equation' is so prevalent that Monte Carlo is often misleadingly described simply as a way to solve the Boltzmann equation, rather than the broader set of transport problems that the stochastic simulation can solve* [165]. Monte Carlo simulation, by virtue of its very nature, is ideally suited to assess the full distribution of a given collection of individuals undergoing a stochastic process: by adapting the estimators to the specific physical question, it is in principle possible to extract the full distribution of any observable (even those that are usually not accessible by means of experimental measurements). In this respect, Monte Carlo goes much further than just 'solving the Boltzmann equation' [165].

2.6 Structure of this work

When going beyond the realm of the Boltzmann equation and taking into consideration other physical observables such as those mentioned above, it would be therefore highly desirable to have the possibility of guiding the Monte Carlo simulation by means of the corresponding evolution equations for the observables. In particular, determining the equations governing a given arbitrary observable has a twofold aim: on one hand, it allows verifying the results of Monte Carlo simulation; on the other hand, it allows improving and accelerating the Monte Carlo methods by providing a better understanding of the underlying random walk behaviour.

Specific transport equations, of course, can be written so as to include the effects of correlations between particles: if a Monte Carlo practitioner wishes to use transport equations to analyze and/or improve his Monte Carlo calculation, it is important to understand which transport equations are relevant to the calculation [165].

In the remainder of this manuscript (Parts III and IV), we shall show that it is actually possible to explicitly derive a family of such evolution equations for a broad class of physical observables by resorting to the so-called *Feynman-Kac* backward formalism. This work is organized in *two parts*, the former related to the formal development of the backward approach for stochastic particle transport, and the latter focusing on the applications in nuclear reactor physics.

Concerning Part III, in Chapter 3 we will first consider the case of purely diffusive transport processes, and derive the corresponding Feynman-Kac equations for both the continuous-time and discrete-time evolution of a single particle. In Chapter 4, we will generalize these results to the case of branching processes, where particles can undergo reproduction and death. In particular, we will show that in the presence of branching the equations for the higher moments of the observables have additional source terms, which are the signature of increased fluctuations around the average. Finally, in Chapter 5 we will further extend the backward formalism to the analysis of the collective evolution of a stochastic population of particles.

Then, in Part IV we will apply the Feynman-Kac evolution equations to the analysis of some problems emerging in the field of radiation transport. In Chapter 6 we will determine the opacity of a body with respect to a flow of incoming neutrons or photons by relating this problem to the occupation statistics. We will show that it is possible to establish some universal properties for the opacity, the so-called generalized Cauchy formulas, that do not depend on the specific features of the underlying branching random walks. In Chapter 7 we will characterize the random spatial extension of a burst of diffusing and branching particles injected into a system, and explicitly determine the

perimeter and the area of the burst at and close to the critical regime. Finally, in Chapter 8 we will consider the spatial correlations affecting the neutron population in a prototype model of a nuclear reactor, and show that correlations actually induce a spontaneous spatial segregation of neutrons, the so-called clustering: this phenomenon stems from the subtle asymmetry between birth events by fission and death events by absorption. The effects of such correlations will be assessed by exactly computing the pair correlation function by the backward approach. In this context, we shall also evaluate the impact of equilibrium between the neutrons and the precursors on the global and local fluctuations of fission chains close to criticality.

The contents of Part III and IV mostly stem from gathering, reorganizing and sharpening part of the material published in international peer-reviewed journals and presented at several conferences and seminars in France and abroad, in preparation of the *Habilitation* degree at the Université Paris XI Orsay. The detailed list of the published works can be found in the *bibliography* included at the end of Part I of the present manuscript (see **??**). In particular, the material of Chapter 3 comes from

1. A. Zoia, E. Dumonteil, A. Mazzolo, Phys. Rev. E **83**, 041137 (2011)
2. A. Zoia, E. Dumonteil, A. Mazzolo, Phys. Rev. Lett. **106**, 220602 (2011)
3. A. Zoia, E. Dumonteil, A. Mazzolo, Phys. Rev. E **84**, 021139 (2011)
4. A. Zoia, E. Dumonteil, A. Mazzolo, Phys. Rev. E **84**, 061130 (2011)
5. A. Zoia, E. Dumonteil, A. Mazzolo, Phys. Rev. E **85**, 011132 (2012).

The material of Chapters 4 and 5 comes from

1. A. Zoia, E. Dumonteil, A. Mazzolo, EuroPhys. Lett. **98**, 40012 (2012)
2. A. Zoia, E. Dumonteil, A. Mazzolo S. Mohamed, J. Phys. A: Math. Theor. **45**, 425002 (2012)
3. A. Zoia, E. Brun, F. Malvagi, Ann. Nucl. Energy **63**, 276-284 (2014)
4. A. Zoia, E. Dumonteil, A. Mazzolo, C. de Mulatier, A. Rosso, Phys. Rev. E **90**, 042118 (2014)
5. A. Zoia, E. Brun, F. Damian, F. Malvagi, Annals of Nuclear Energy **75**, 627 (2015).

The material of Chapter 6 comes from

1. A. Zoia, E. Dumonteil, A. Mazzolo, EuroPhys. Lett. **100**, 40002 (2012)
2. A. Mazzolo, C. de Mulatier, A. Zoia, J. Math. Phys. **55**, 083308 (2014)
3. C. de Mulatier, A. Mazzolo, A. Zoia, EPL **107**, 30001 (2014). *Editor's choice.*

The material of Chapter 7 comes from

1. E. Dumonteil, S. Majumdar, A. Rosso, A. Zoia, PNAS **110**, 4239-4244 (2013).

Finally, the material of Chapter 8 comes from

1. E. Dumonteil, F. Malvagi, A. Zoia, A. Mazzolo, D. Artusio, C. Dieudonné, C. De Mulatier, Ann. Nucl. Energy **63**, 612-618 (2014)
2. C. de Mulatier, E. Dumonteil, A. Rosso, A. Zoia, J. Stat. Mech. P08021 (2015)
3. B. Houchmandzadeh, E. Dumonteil, A. Mazzolo, A. Zoia, Phys. Rev. E **92**, 052114 (2015).

Part II

The Feynman-Kac formalism

Chapter 3

The backward equations: a primer

The formulation is mathematically equivalent to the more usual formulations. There are, therefore, no fundamentally new results. However, there is a pleasure in recognizing old things from a new point of view.

R. P. Feynman, Rev. Mod. Phys. **20**, 367 (1948).

3.1 Introduction

In the previous Chapter we have established the physical picture of systems composed of particles randomly flowing through a medium. In this context, a fundamental question concerns the *occupation statistics* of the transported particles within the crossed body: *i*) the distribution of the total travelled *length* ℓ, which is directly proportional to the radiation flux, and *ii*) the distribution of the number n of performed *collisions*, which is related to the power density deposited in the traversed region [5, 113]. Precisely quantifying the flow of radiation such as neutrons or photons through a structural material or a living body represents a long-standing problem in statistical physics [5, 66, 113] and is key to mastering relevant technological issues encompassing the design of nuclear reactors [30], light distribution in tissues for medical diagnosis [77], and radiative heat transfer [67], only to name a few. In this respect, occupation statistics is intimately connected to the well known and long studied problem of the *sojourn time* of a random walker in a given domain [7, 97, 98, 102, 107–109, 145, 166–177], and is naturally formulated in the framework of the stochastic process underlying the evolution of the random particle flow.

Linear transport (where particles are fairly diluted, i.e., interact with the surrounding medium but not with each other) is modeled in terms of *Pearson random flights*: particles move at constant speed along straight paths of random length, interrupted by collisions with the medium, whereupon directions are randomly redistributed [5, 113, 148]. Generally speaking, stochastic transport may be coupled to a birth-death mechanism (think for example of neutron multiplication in fissile materials, photon cascades, the reproduction of bacteria and epidemics): a random number of particles may emerge from a collision, which leads to branching particle trajectories [28, 29, 32, 33, 39, 61].

A powerful and far-reaching approach that allows quantifying the occupation statistics of random flights can be established by resorting to the *Feynman-Kac formalism* [178–180], which

has been originally proposed by Feynman [181] and made rigorous on mathematical grounds by Kac [182–187]. The approach was first introduced for computing the residence times of a one-dimensional regular Brownian motion by slightly adapting the Feynman path integrals from quantum mechanics, and was then extended to general continuous-time Markov processes in a series of seminal papers. In these works, a profound connection between the underlying stochastic dynamics and the deterministic equations governing the evolution of some functionals defined over the particle trajectories was established. More recently, the Feynman-Kac formalism has been generalized to non-Markovian continuous-time processes, such as in the case of particles undergoing anomalous diffusion [188–190]. In the following, we first recall the basics of the Feynman-Kac formalism for a standard Brownian particle, which allows illustrating this technique, and then derive the corresponding formulas for exponential and random flights.

3.2 Functionals of Brownian motion

In [183, 184], a method for computing the distribution of the stochastic integral

$$\mathcal{I}_f = \int_0^t f(X_{t'})dt' \tag{3.1}$$

was first proposed, where f is an arbitrary (positive) function, and X_t is a regular one-dimensional Brownian motion starting at some x_0 at time $t = 0$, i.e., $X_0 = x_0$. Later, it was shown that the method used for characterizing $\mathcal{I}_f$ actually applied to more general Markov processes [182, 185–187]. For our scopes, we will assume that the underlying process is a regular d-dimensional Brownian motion $\mathbf{X}_t$ with diffusion coefficient D, starting at $\mathbf{x}_0$ at time $t = 0$, and evolving in a domain B [2]. This is a reasonable hypothesis for living organisms (as far as the support is sufficiently homogeneous) [6–8, 39], and holds also for neutrons in the so-called diffusion regime (in the absence of localized sources or sinks, and when scattering dominates over absorption) [3, 4, 30, 32].

3.2.1 Residence time in a volume V

Assume that the function f is the marker function $f = \mathbb{1}_V$ of a domain $V \subset B$: thus, the stochastic integral in Eq. (3.1) represents the *residence time* t_V of the Brownian particle within the region V when observed up to the time t, i.e, the portion of the time that the particle spends in V while moving around in the domain B [179, 180, 182]. The residence time

$$t_V(t) = \int_0^t \mathbb{1}_V(\mathbf{X}_{t'})dt' \tag{3.2}$$

is clearly a stochastic variable, which depends on the random realization of the underlying trajectory, as well as on the starting point $\mathbf{x}_0$ and on the observation time t [182, 185–187]. In principle, one would be interested in determining the full probability density function $P_t(t_V|\mathbf{x}_0)$ that the residence time lies between t_V and $t_V + dt_V$, when the particle starts at $\mathbf{x}_0$, and the trajectory is observed up to time t. In practice, it turns out much more convenient to write down an equation for the generating function associated to $P_t(t_V|\mathbf{x}_0)$, and this is precisely what the Feynman-Kac approach allows obtaining [179, 180, 182].

Define the *moment generating function*

$$Q_t(s|\mathbf{x}_0) = \mathbb{E}[e^{-st_V(t)}](\mathbf{x}_0), \tag{3.3}$$

where $\mathbb{E}[\cdot]$ denotes the ensemble average over possible realizations [2]. The quantity $Q_t(s|\mathbf{x}_0)$ can be seen as the Laplace transform of the probability density $P_t(t_V|\mathbf{x}_0)$, the transformed variable being s. By definition, the moment generating function is such that

$$(-1)^k \frac{\partial^k}{\partial s^k} Q_t(s|\mathbf{x}_0)|_{s=0} = \mathbb{E}_t[t_V^k](\mathbf{x}_0), \tag{3.4}$$

i.e., by taking the k-th derivative of $Q_t(s|\mathbf{x}_0)$ and evaluating the resulting function at $s = 0$ one obtains the k-th moment of the variable t_V [2]. Now, since knowledge of the moments of a distribution at any order k is equivalent to knowing the distribution itself, it follows that determining an evolution equation for the generating function $Q_t(s|\mathbf{x}_0)$ allows the distribution $P_t(t_V|\mathbf{x}_0)$ to be fully characterized. The *backward* evolution equation for the generating function $Q_t(s|\mathbf{x}_0)$ is derived in Appendix A.2.1 and reads

$$\boxed{\frac{\partial}{\partial t} Q_t(s|\mathbf{x}_0) = D\nabla^2_{\mathbf{x}_0} Q_t(s|\mathbf{x}_0) - s\,\mathbb{1}_V(\mathbf{x}_0) Q_t(s|\mathbf{x}_0),} \tag{3.5}$$

Equation (3.5) takes the name of *Feynman-Kac equation*. Boundary conditions on $Q_t(s|\mathbf{x}_0)$ depend on the problem at hand, for instance leakage or reflecting conditions at the boundary ∂B of B. As for the initial condition, we have $t_V = 0$ for $t = 0$, which implies also

$$Q_0(s|\mathbf{x}_0) = \mathbb{E}[e^{-st_V(0)}](\mathbf{x}_0) = 1. \tag{3.6}$$

Remark that we have $Q_t(0|\mathbf{x}_0) = 1$ from normalization.

The moments of the residence time $t_V(t)$ can be finally obtained by taking the derivatives with respect to s as in Eq. (3.4), which by recursion yields the following formula

$$\boxed{\frac{\partial}{\partial t} \mathbb{E}_t[t_V^k](\mathbf{x}_0) = D\nabla^2_{\mathbf{x}_0} \mathbb{E}_t[t_V^k](\mathbf{x}_0) + k\mathbb{E}_t[t_V^{k-1}](\mathbf{x}_0),} \tag{3.7}$$

for $k \geq 1$, with the conditions

$$\mathbb{E}_0[t_V^k](\mathbf{x}_0) = 0, \tag{3.8}$$

and

$$\mathbb{E}_t[t_V^0](\mathbf{x}_0) = 1 \tag{3.9}$$

from normalization [180, 182].

This argument is easily extended in Appendix A.2.1 to a Brownian motion *with absorption*. Assume that the Brownian particle diffusing within the domain B undergoes absorption at a rate γ: in this case, we get the Feynman-Kac equation

$$\frac{\partial}{\partial t} Q_t(s|\mathbf{x}_0) = \mathcal{L}^\dagger_{\mathbf{x}_0} Q_t(s|\mathbf{x}_0) - s\,\mathbb{1}_V(\mathbf{x}_0) Q_t(s|\mathbf{x}_0) + \gamma, \tag{3.10}$$

where

$$\mathcal{L}^\dagger_{\mathbf{x}_0} = D\nabla^2_{\mathbf{x}_0} - \gamma. \tag{3.11}$$

is the backward operator for diffusion with absorption, and the boundary and initial conditions are the same as in Eq. (3.5). By taking the k-th derivative of Eq. (3.10), we obtain the moments of the residence time t_V for a medium with absorption, namely

$$\frac{\partial}{\partial t} \mathbb{E}_t[t_V^k](\mathbf{x}_0) = \mathcal{L}^\dagger_{\mathbf{x}_0} \mathbb{E}_t[t_V^k](\mathbf{x}_0) + k\,\mathbb{1}_V(\mathbf{x}_0) \mathbb{E}_t[t_V^{k-1}](\mathbf{x}_0), \tag{3.12}$$

for $k \geq 1$, which has the same structure as Eq. (3.7).

3.2.2 Green's function and the general solution

Equations (3.12) have the general form

$$\frac{\partial}{\partial t} f_t(\mathbf{x}_0) = \mathcal{L}^\dagger_{\mathbf{x}_0} f_t(\mathbf{x}_0) + a_t(\mathbf{x}_0), \tag{3.13}$$

where $a_t(\mathbf{x}_0)$ is some known source term with $a_0(\mathbf{x}_0) = 0$, and initial condition $f_0(\mathbf{x}_0) = b(\mathbf{x}_0)$ for $t = 0$. Equations of this kind admit the solution

$$f_t(\mathbf{x}_0) = \int d\mathbf{x}' b(\mathbf{x}') \mathcal{G}_t(\mathbf{x}'; \mathbf{x}_0) + \int_0^t dt' \int d\mathbf{x}' a_{t-t'}(\mathbf{x}') \mathcal{G}_{t'}(\mathbf{x}'; \mathbf{x}_0), \tag{3.14}$$

where $\mathcal{G}_t(\mathbf{x}; \mathbf{x}_0)$ is the Green's function [2, 191] satisfying the backward equation

$$\frac{\partial}{\partial t} \mathcal{G}_t(\mathbf{x}; \mathbf{x}_0) = \mathcal{L}^\dagger_{\mathbf{x}_0} \mathcal{G}_t(\mathbf{x}; \mathbf{x}_0), \tag{3.15}$$

with $\mathcal{G}_0(\mathbf{x}; \mathbf{x}_0) = \delta(\mathbf{x} - \mathbf{x}_0)$ and the boundary conditions of the problem at hand. By identifying

$$a_t(\mathbf{x}) = k \mathbb{1}_V(\mathbf{x}) \mathbb{E}_t[t_V^{k-1}](\mathbf{x}) \tag{3.16}$$

and

$$b(\mathbf{x}) = \mathbb{E}_0[t_V^k](\mathbf{x}_0) = 0, \tag{3.17}$$

we then formally express the solution $\mathbb{E}_t[t_V^k](\mathbf{x}_0)$ in terms of the Green's function as

$$\mathbb{E}_t[t_V^k](\mathbf{x}_0) = k \int_0^t dt' \int d\mathbf{x}' \mathbb{1}_V(\mathbf{x}') \mathbb{E}_{t-t'}[t_V^{k-1}](\mathbf{x}') \mathcal{G}_{t'}(\mathbf{x}'; \mathbf{x}_0). \tag{3.18}$$

In particular, for the average residence time ($k = 1$) we have

$$\mathbb{E}_t[t_V^1](\mathbf{x}_0) = \int_0^t dt' \int_V d\mathbf{x}' \mathcal{G}_{t'}(\mathbf{x}'; \mathbf{x}_0), \tag{3.19}$$

and for the second moment of the residence time ($k = 2$) we have

$$\begin{aligned} \mathbb{E}_t[t_V^2](\mathbf{x}_0) &= 2 \int_0^t dt' \int_V d\mathbf{x}' \mathbb{E}_{t-t'}[t_V^1](\mathbf{x}') \mathcal{G}_{t'}(\mathbf{x}'; \mathbf{x}_0) \\ &= 2 \int_0^t dt' \int_V d\mathbf{x}' \int_0^{t-t'} dt'' \int_V d\mathbf{x}'' \mathcal{G}_{t''}(\mathbf{x}''; \mathbf{x}') \mathcal{G}_{t'}(\mathbf{x}'; \mathbf{x}_0). \end{aligned} \tag{3.20}$$

3.2.3 Number of individuals in a volume V

Consider again a d-dimensional Brownian motion with diffusion coefficient D and absorption rate γ. A single walker starts from position $\mathbf{x}_0$ at time $t_0 = 0$. Let $m_V = m_V(\mathbf{x}_0, t)$ be the number of particles that are found in a volume $V \subseteq B$ of the viable space when the process is observed at a time $t > t_0$. We are interested in determining the detection probability $\mathcal{P}_t(m_V|\mathbf{x}_0)$ of finding m_V particles in volume $V \subseteq B$ at time t, for a single particle starting at $\mathbf{x}_0$ at time t_0. It is convenient to introduce the associated probability generating function

$$W_t(u|\mathbf{x}_0) = \mathbb{E}[u^{m_V(\mathbf{x}_0, t)}]. \tag{3.21}$$

The k-th (factorial) moments of m_V can be then obtained by derivation with respect to u, namely,

$$\mathbb{E}_t[(m_V)_k(\mathbf{x}_0)] = \frac{\partial^k}{\partial u^k} W_t(u|\mathbf{x}_0)|_{u=1}, \tag{3.22}$$

where

$$\mathbb{E}_t[(m)_k] = \mathbb{E}_t[m(m-1)\cdots(m-k+1)] \tag{3.23}$$

is the falling factorial moment of order k [192,193]. In particular, the average particle number reads

$$\mathbb{E}_t[m_V|\mathbf{x}_0] = \frac{\partial}{\partial u} W_t(u|\mathbf{x}_0)|_{u=1}. \tag{3.24}$$

For the second factorial moment we have

$$\mathbb{E}_t[(m_V)_2|\mathbf{x}_0] = \mathbb{E}_t[m_V^2|\mathbf{x}_0] - \mathbb{E}_t[m_V|\mathbf{x}_0] = \frac{\partial^2}{\partial u^2} W_t(u|\mathbf{x}_0)|_{u=1}. \tag{3.25}$$

By following the same argument as for the residence time, it can be shown [1] that $W_t(u|\mathbf{x}_0)$ satisfies the backward equation

$$\frac{\partial}{\partial t} W_t = \mathcal{L}^\dagger_{\mathbf{x}_0} W_t + \gamma, \tag{3.26}$$

where the backward operator $\mathcal{L}^\dagger_{\mathbf{x}_0}$ has been defined in Eq. (3.11). By taking the k-th derivative of Eq. (3.26) we get the moment equation

$$\frac{\partial}{\partial t} \mathbb{E}_t[(m_V)_k|\mathbf{x}_0] = \mathcal{L}^\dagger_{\mathbf{x}_0} \mathbb{E}_t[(m_V)_k|\mathbf{x}_0] \tag{3.27}$$

for $k \geq 1$, which must be solved together with the initial condition $\mathbb{E}_0[(m_V)_k|\mathbf{x}_0] = \mathbb{1}_V(\mathbf{x}_0)$ when $k = 1$ and $\mathbb{E}_0[(m_V)_k|\mathbf{x}_0] = 0$ when $k > 1$.

Then, the average particle number can be again expressed in terms of the Green's function and reads

$$\mathbb{E}_t[m_V|\mathbf{x}_0] = \int_V d\mathbf{x}' \mathcal{G}_t(\mathbf{x}'; \mathbf{x}_0). \tag{3.28}$$

For the second factorial moment we obtain

$$\mathbb{E}_t[(m_V)_2|\mathbf{x}_0] = 0, \tag{3.29}$$

which implies $\mathbb{E}_t[m_V^2|\mathbf{x}_0] = \mathbb{E}_t[m_V|\mathbf{x}_0]$. By recurrence, it is not difficult to show that more generally $\mathbb{E}_t[m_V^k|\mathbf{x}_0] = \mathbb{E}_t[m_V|\mathbf{x}_0]$, for $k \geq 1$. Thus, from the moments of any order being all equal to $\mathbb{E}_t[m_V|\mathbf{x}_0]$, the occupation probability $\mathcal{P}_t(m_V|\mathbf{x}_0)$ can be explicitly identified as being a Bernoulli distribution of parameter $\mathbb{E}_t[m_V|\mathbf{x}_0] \leq 1$, namely,

$$\mathcal{P}_t(m_V = 1|\mathbf{x}_0) = \mathbb{E}_t[m_V|\mathbf{x}_0] = \int_V d\mathbf{x}' \mathcal{G}_t(\mathbf{x}'; \mathbf{x}_0) \tag{3.30}$$

and

$$\mathcal{P}_t(m_V = 0|\mathbf{x}_0) = 1 - \mathbb{E}_t[m_V|\mathbf{x}_0]. \tag{3.31}$$

Since the two events are mutually exclusive, by centering the volume V at a site $\mathbf{x}_i$ and taking $|V| \to 0$, the probability density P of finding a particle born at $\mathbf{x}_0$ at position $\mathbf{x}_i$ after a time t is given by $P_t(\mathbf{x}|\mathbf{x}_0) = \mathcal{G}_t(\mathbf{x}_i; \mathbf{x}_0)$.

[1] See, for instance, the derivation in [26,32] or the sketch of proof in [210].

3.3 Functionals of exponential flights

Let us now turn our attention to the case of d-dimensional *exponential flights*. Consider a single walker initially emitted from a point source at time $t_0 = 0$ at position $\mathbf{r}_0$, with velocity $\mathbf{v}_0$. Once emitted, the walker undergoes a sequence of displacements (at constant speed), separated by collisions with the surrounding medium. As discussed in the previous Chapters, when the scattering centers encountered by the travelling particle are spatially uniform, the inter-collision lengths are exponentially distributed [7,8], so that the displacements from $\mathbf{r}'$ to $\mathbf{r}$ in direction $\boldsymbol{\omega} = \mathbf{v}/|\mathbf{v}|$ between any two collisions obey the probability density

$$T(\mathbf{r}' \to \mathbf{r}|\mathbf{v}) = \Sigma(\mathbf{r}, v) e^{-\int_0^{\boldsymbol{\omega}\cdot(\mathbf{r}-\mathbf{r}')} \Sigma(\mathbf{r}'+s\boldsymbol{\omega}, v) ds}, \tag{3.32}$$

with $v = |\mathbf{v}|$ [157,158]. The total cross section $\Sigma(\mathbf{r}, v)$ represents the interaction rate per unit length: $\Sigma(\mathbf{r}, v)$ typically depends on the particle position and speed [157]. In the following, we introduce a few simplifying hypotheses, whose main advantage is to keep notation to a minimum, yet retaining the key physical mechanisms. Thus, we assume that displacements are performed at a constant speed $v = v_0$, i.e., that only the walker directions $\boldsymbol{\omega}$ do change after collisions. Furthermore, we assume that at each collision the walker can either be absorbed with probability $p_a(\mathbf{r}) = \Sigma_a(\mathbf{r})/\Sigma(\mathbf{r})$, or be *isotropically* scattered with probability $p_s(\mathbf{r}) = 1 - p_a(\mathbf{r}) = \Sigma_s(\mathbf{r})/\Sigma(\mathbf{r})$. Here $\Sigma_a(\mathbf{r})$ and $\Sigma_s(\mathbf{r})$ denote the absorption and scattering cross sections, respectively. With these assumptions, we have

$$T(\mathbf{r}' \to \mathbf{r}|\mathbf{v}) = T(\mathbf{r}' \to \mathbf{r}|\boldsymbol{\omega}) \tag{3.33}$$

$$f_C(\mathbf{v}' \to \mathbf{v}) = f_C(\boldsymbol{\omega}' \to \boldsymbol{\omega}) = \frac{1}{\Omega_d}. \tag{3.34}$$

Exponential flights, as defined above, are a Markovian stochastic process that can be observed both as a function of time t and discrete generations g (this latter case corresponds to recording the particle position and direction at collision events only). Markovianity is granted by the fact that displacements between collisions are exponentially distributed [32, 157, 158], and implies that knowledge of the phase space variables $\mathbf{r}, \boldsymbol{\omega}$ at time t or generation g is sufficient to determine the future evolution of the walker [2]. We would like characterize the *occupation statistics* of such process within a given region V: this is naturally formulated in terms of the number of visits n_V and of the travelled lengths ℓ_V in V. To begin with, we address first the *average* physical observables.

3.3.1 The average total travelled length $\mathbb{E}[\ell_V]$

Let $N_t(\mathbf{r}, \boldsymbol{\omega})$ be the average number of particles that at time t are found in the phase space element $d\mathbf{r}d\boldsymbol{\omega}$ around $\mathbf{r}, \boldsymbol{\omega}$, starting from a source $N_0(\mathbf{r}, \boldsymbol{\omega}) = \mathcal{Q}$ at time $t_0 = 0$. Under the previous assumptions, the Boltzmann equation for the average particle density in phase space reads

$$\frac{\partial}{\partial t} N_t + v\boldsymbol{\omega} \cdot \nabla_{\mathbf{r}} N_t = -v\Sigma(\mathbf{r}) N_t + \int \frac{d\boldsymbol{\omega}'}{\Omega_d} v\Sigma_s(\mathbf{r}) N_t(\mathbf{r}, \boldsymbol{\omega}'). \tag{3.35}$$

Boundary conditions on $N_t(\mathbf{r}, \boldsymbol{\omega})$ depend on the specific problem under analysis. The stationary behaviour of the particle density is provided by integrating over time, and for the *stationary flux* $\varphi_t = vN_t$

$$\varphi(\mathbf{r}, \boldsymbol{\omega}) = \int_0^\infty dt \varphi_t(\mathbf{r}, \boldsymbol{\omega}) \tag{3.36}$$

[2] Conversely, knowledge of the position $\mathbf{r}$ alone does not ensure Markovianity, as is instead the case for Brownian motion [2].

we get in particular

$$\boldsymbol{\omega} \cdot \nabla_{\mathbf{r}} \varphi + \Sigma(\mathbf{r})\varphi = \int \frac{d\boldsymbol{\omega}'}{\Omega_d} \Sigma_s(\mathbf{r})\varphi(\mathbf{r}, \boldsymbol{\omega}') + \mathcal{Q}. \tag{3.37}$$

Eq. (3.37) can be recast in the more compact formula

$$\mathcal{L}\varphi(\mathbf{r}, \boldsymbol{\omega}) = -\mathcal{Q}, \tag{3.38}$$

where

$$\mathcal{L} = -\boldsymbol{\omega} \cdot \nabla_{\mathbf{r}} - \Sigma(\mathbf{r}) + \int \frac{d\boldsymbol{\omega}'}{\Omega_d} \Sigma_s(\mathbf{r}) \tag{3.39}$$

takes the name of *(forward) transport operator* [30, 113, 157]. The quantity $\varphi(\mathbf{r}, \boldsymbol{\omega})$ physically represents the stationary density of the total length travelled by the particles in the phase space element $d\mathbf{r}d\boldsymbol{\omega}$ around $\mathbf{r}, \boldsymbol{\omega}$ for a given source $\mathcal{Q}$ [5, 14, 113, 157, 158]: hence, the average travelled length in a given volume V will be given by

$$\mathbb{E}[\ell_V](\mathcal{Q}) = \int_V d\mathbf{r} \int d\boldsymbol{\omega} \varphi(\mathbf{r}, \boldsymbol{\omega}), \tag{3.40}$$

where the integral over directions is extended over the unit d-dimensional spherical surface Ω_d.

3.3.2 The average total number of visits $\mathbb{E}[n_V]$

If generations are considered instead of time, the density $\psi_g(\mathbf{r}, \boldsymbol{\omega})$ of particles that at the g-th generation enter a collision at $\mathbf{r}$, having direction $\boldsymbol{\omega}$, satisfies the recursive Chapman-Kolmogorov equation

$$\psi_{g+1} = \int d\mathbf{r}' \int \frac{d\boldsymbol{\omega}'}{\Omega_d} T(\mathbf{r}' \to \mathbf{r}|\boldsymbol{\omega}) p_s(\mathbf{r}') \psi_g(\mathbf{r}', \boldsymbol{\omega}'), \tag{3.41}$$

with the uncollided density

$$\psi_1(\mathbf{r}, \boldsymbol{\omega}) = \int d\mathbf{r}' T(\mathbf{r}' \to \mathbf{r}|\boldsymbol{\omega}) \mathcal{Q}(\mathbf{r}', \boldsymbol{\omega}). \tag{3.42}$$

The stationary behavior of $\psi_g(\mathbf{r}, \boldsymbol{\omega})$ is obtained by summing over all generations: as customary, we define the *stationary collision density* as being [30]

$$\psi(\mathbf{r}, \boldsymbol{\omega}) = \sum_{g=1}^{\infty} \psi_g(\mathbf{r}, \boldsymbol{\omega}), \tag{3.43}$$

and we thus get the stationary integral equation

$$\psi = \int d\mathbf{r}' \int \frac{d\boldsymbol{\omega}'}{\Omega_d} T(\mathbf{r}' \to \mathbf{r}|\boldsymbol{\omega}) p_s(\mathbf{r}') \psi(\mathbf{r}', \boldsymbol{\omega}') + \psi_1. \tag{3.44}$$

The quantity $\psi(\mathbf{r}, \boldsymbol{\omega})$ physically represents the stationary density of particles entering a collision at $\mathbf{r}, \boldsymbol{\omega}$ for a given source $\mathcal{Q}$ [5, 14, 113, 157, 158]: then, the average number of visits to a given volume V will be given by

$$\mathbb{E}[n_V](\mathcal{Q}) = \int_V d\mathbf{r} \int d\boldsymbol{\omega} \psi(\mathbf{r}, \boldsymbol{\omega}). \tag{3.45}$$

From $\mathbb{E}[n_V](\mathcal{Q})$ and $\mathbb{E}[\ell_V](\mathcal{Q})$ being two average observables of the same stochastic process, the quantities ψ and φ must be intimately connected to each other as well. Actually, by comparing Eqs. (3.37) and (3.44), it can be shown that [30, 157]

$$\psi(\mathbf{r}, \boldsymbol{\omega}) = \Sigma(\mathbf{r})\varphi(\mathbf{r}, \boldsymbol{\omega}). \tag{3.46}$$

This provides the relation between the stationary densities ψ and φ. As a consequence, we have also

$$\mathbb{E}[n_V](\mathcal{Q}) = \int_V d\mathbf{r} \int d\boldsymbol{\omega} \Sigma(\mathbf{r}) \varphi(\mathbf{r}, \boldsymbol{\omega}). \tag{3.47}$$

The approach proposed in this Section so to assess the behavior of the average quantities $\mathbb{E}[\ell_V]$ and $\mathbb{E}[n_V]$ can not be straightforwardly extended to higher moments (which are often necessary to quantify the statistical fluctuations around the average), nor to other observables. In the following, we will show that this difficulty can be overcome by resorting to the Feynman-Kac formalism, similarly as done above for Brownian motion.

3.3.3 Total travelled length in V

Consider a *single particle* emitted at $\mathbf{r}_0$ in direction $\boldsymbol{\omega}_0$ at time $t_0 = 0$. We formally define the total length $\ell_V(t)$ travelled by an exponential flight in a given volume V, when observed up to a time t, as

$$\ell_V(t) = \int_0^t \mathbb{1}_V(\mathbf{r}') v dt', \tag{3.48}$$

where the integral is intended over the path of a distinct realization up to time t, and $\mathbb{1}_V(\mathbf{r})$ denotes the marker function of the volume V, i.e., $\mathbb{1}_V(\mathbf{r}) = 1$ when $\mathbf{r} \in V$, and $\mathbb{1}_V(\mathbf{r}) = 0$ elsewhere. The quantity $\ell_V(t)$ is clearly a stochastic variable, which depends on the realizations of the underlying process, as well as on the initial conditions. Instead of studying the probability density function $P_t(\ell_V|\mathbf{r}_0, \boldsymbol{\omega}_0)$, it is more convenient to introduce the associated moment generating function

$$Q_t(s|\mathbf{r}_0, \boldsymbol{\omega}_0) = \mathbb{E}[e^{-s\ell_V(t)}](\mathbf{r}_0, \boldsymbol{\omega}_0), \tag{3.49}$$

where s is the transformed variable with respect to ℓ_V. The derivation of a backward equation for $Q_t(s|\mathbf{r}_0, \boldsymbol{\omega}_0)$ closely follows the path integral approach for Brownian motion [183] and is sketched in Appendix A.2.2. This yields the Feynman-Kac equation

$$\boxed{\frac{1}{v_0}\frac{\partial}{\partial t} Q_t = \mathcal{L}^\dagger Q_t - s\mathbb{1}_V(\mathbf{r}_0) Q_t + \Sigma_a(\mathbf{r}_0),} \tag{3.50}$$

where

$$\mathcal{L}^\dagger = \boldsymbol{\omega}_0 \cdot \nabla_{\mathbf{r}_0} - \Sigma(\mathbf{r}_0) + \Sigma_s(\mathbf{r}_0) \int \frac{d\boldsymbol{\omega}_0'}{\Omega_d} \tag{3.51}$$

is the *(backward) transport operator* adjoint to $\mathcal{L}$ [30]. Equation (3.50) is completed by the initial condition $Q_0(s|\mathbf{r}_0, \boldsymbol{\omega}_0) = 1$ and by the appropriate boundary conditions, which depend on the problem at hand.

3.3.4 Moment equations for ℓ_V

Equation (3.50) is a partial differential equation with an integral term, for which explicit solutions are hardly available. Moreover, one would still need to invert the solution Q_t so to obtain the probability density of ℓ_V in the direct space. A somewhat simpler approach consists in deriving the corresponding moment equations [107, 109, 145, 175, 177]: by the definition of Q_t, the moments of the travelled length can be obtained from

$$\mathbb{E}_t[\ell_V^k](\mathbf{r}_0, \boldsymbol{\omega}_0) = (-1)^k \frac{\partial^k}{\partial s^k} Q_t(s|\mathbf{r}_0, \boldsymbol{\omega}_0)|_{s=0}. \tag{3.52}$$

By taking the k-th derivative of Eq. (3.50), we get the following recursive formula for the moments of the travelled length

$$\frac{1}{v_0}\frac{\partial}{\partial t}\mathbb{E}_t[\ell_V^k] = \mathcal{L}^\dagger \mathbb{E}_t[\ell_V^k] + k\mathbb{1}_V(\mathbf{r}_0)\mathbb{E}_t[\ell_V^{k-1}], \tag{3.53}$$

for $k \geq 1$. The recurrence is initiated with the conditions $\mathbb{E}_t[\ell_V^0] = 1$ (from normalization), and $\mathbb{E}_0[\ell_V^k] = 0$.

Define now the Green's function $\mathcal{G}_t(\mathbf{r}, \boldsymbol{\omega}; \mathbf{r}_0, \boldsymbol{\omega}_0)$ satisfying the backward equation

$$\frac{1}{v_0}\frac{\partial}{\partial t}\mathcal{G}_t(\mathbf{r}, \boldsymbol{\omega}; \mathbf{r}_0, \boldsymbol{\omega}_0) = \mathcal{L}^\dagger \mathcal{G}_t(\mathbf{r}, \boldsymbol{\omega}; \mathbf{r}_0, \boldsymbol{\omega}_0), \tag{3.54}$$

with $\mathcal{G}_0(\mathbf{r}, \boldsymbol{\omega}; \mathbf{r}_0, \boldsymbol{\omega}_0) = \delta(\mathbf{r} - \mathbf{r}_0)\delta(\boldsymbol{\omega} - \boldsymbol{\omega}_0)$ and the boundary conditions of the problem at hand. Then, by analogy with the case of Brownian motion, the moments of the travelled length can be formally expressed in terms of the Green's function as

$$\mathbb{E}_t[\ell_V^k](\mathbf{r}_0, \boldsymbol{\omega}_0) = k\int_0^t dt' \int d\mathbf{r}' \int d\boldsymbol{\omega}' v_0 \mathbb{1}_V(\mathbf{r}')\mathbb{E}_{t-t'}[\ell_V^{k-1}](\mathbf{r}', \boldsymbol{\omega}')\mathcal{G}_{t'}(\mathbf{r}', \boldsymbol{\omega}'; \mathbf{r}_0, \boldsymbol{\omega}_0). \tag{3.55}$$

3.3.5 Stationary behaviour of $\mathbb{E}[\ell_V^k]$

Often, the observation time t is much longer than the characteristic time scale of the system dynamics, which means that trajectories are followed up to $t \to \infty$. In this case, the time derivative in Eq. (3.53) vanishes. We therefore get a recursive formula for the stationary moments $\mathbb{E}[\ell_V^k] = \lim_{t\to\infty} \mathbb{E}_t[\ell_V^k]$, namely,

$$\mathcal{L}^\dagger \mathbb{E}[\ell_V^k](\mathbf{r}_0, \boldsymbol{\omega}_0) = -U_{k-1}(\mathbf{r}_0, \boldsymbol{\omega}_0) \tag{3.56}$$

for $k \geq 1$, where

$$U_{k-1}(\mathbf{r}_0, \boldsymbol{\omega}_0) = k\mathbb{1}_V(\mathbf{r}_0)\mathbb{E}[\ell_V^{k-1}](\mathbf{r}_0, \boldsymbol{\omega}_0) \tag{3.57}$$

can be interpreted as a (known) source term that depends at most on the moments of order $k-1$. Now, from $\mathcal{L}^\dagger$ being the adjoint operator with respect to $\mathcal{L}$, i.e.,

$$\langle \mathcal{L}f, g\rangle = \langle \mathcal{L}^\dagger g, f\rangle, \tag{3.58}$$

Eq. (3.56) can be explicitly inverted, and gives

$$\mathbb{E}[\ell_V^k](\mathcal{Q}) = \int d\mathbf{r} \int d\boldsymbol{\omega} U_{k-1}(\mathbf{r}, \boldsymbol{\omega})\varphi(\mathbf{r}, \boldsymbol{\omega}), \tag{3.59}$$

which means that the stationary moments of the travelled length can be obtained by convoluting the stationary flux with the source term U_{k-1}. In particular, for the average length travelled in V, i.e., $k = 1$, we recover the formula

$$\mathbb{E}[\ell_V](\mathcal{Q}) = \int_V d\mathbf{r} \int d\boldsymbol{\omega}\varphi(\mathbf{r}, \boldsymbol{\omega}), \tag{3.60}$$

since $U_0(\mathbf{r}, \boldsymbol{\omega}) = \mathbb{1}_V(\mathbf{r})$.

3.3.6 Total number of visits to V

We address then the statistical properties of the total number of visits $n_V(g)$ performed by an exponential flight in a given volume V, when observed up to the g-th generation. We formally define

$$n_V(g) = \sum_i \mathbb{1}_V(\mathbf{r}_i), \tag{3.61}$$

where the sum is over all the points visited by the path up to entering the g-th generation (the source not being taken into account). The quantity $n_V(g)$ is again a stochastic variable depending on the realizations of the underlying process and on the initial conditions. Similarly as done for ℓ_V, instead of studying the probability $P_g(n_V|\mathbf{r}_0, \boldsymbol{\omega}_0)$, it is more convenient to introduce the associated moment generating function

$$Q_g(u|\mathbf{r}_0, \boldsymbol{\omega}_0) = \mathbb{E}[e^{-un_V(g)}](\mathbf{r}_0, \boldsymbol{\omega}_0), \tag{3.62}$$

where u is the transformed variable with respect to n_V. The backward evolution for $Q_g(u|\mathbf{r}_0, \boldsymbol{\omega}_0)$ is derived in Appendix A.2.3, which yields the *discrete Feynman-Kac equation* in integral-differential form

$$\boxed{-\boldsymbol{\omega}_0 \cdot \nabla_{\mathbf{r}_0} Q_{g+1}(u|\mathbf{r}_0, \boldsymbol{\omega}_0) + \Sigma Q_{g+1}(u|\mathbf{r}_0, \boldsymbol{\omega}_0) = e^{-u\mathbb{1}_V(\mathbf{r}_0)} \left[\Sigma_a + \Sigma_s \langle Q_g \rangle_\Omega\right],} \tag{3.63}$$

where we have used the short-hand notation

$$\langle f \rangle_\Omega = \int \frac{d\boldsymbol{\omega}_0'}{\Omega_d} f(\boldsymbol{\omega}_0') \tag{3.64}$$

for the average over directions. The initial condition is provided by

$$Q_1(u|\mathbf{r}_0, \boldsymbol{\omega}_0) = \int e^{-u\mathbb{1}_V(\mathbf{r}_1)} T^\dagger(\mathbf{r}_1 \to \mathbf{r}_0|\boldsymbol{\omega}_0) d\mathbf{r}_1, \tag{3.65}$$

$T^\dagger$ being the adjoint density associated to T [113, 157], and the appropriate boundary conditions.

3.3.7 Moment equations for n_V

Equation (3.63) is an integral-differential and finite differences equation for the generating function. Similarly as in the case of ℓ_V, the analysis of the distribution of n_V can be simplified by deriving the corresponding moment equations: by the definition of Q_g, the moments of the number of visits can be obtained from

$$\mathbb{E}_g[n_V^k](\mathbf{r}_0, \boldsymbol{\omega}_0) = (-1)^k \frac{\partial^k}{\partial u^k} Q_g(u|\mathbf{r}_0, \boldsymbol{\omega}_0)|_{u=0}. \tag{3.66}$$

Then, by taking the k-th derivative of Eq. (3.63), we get the following recursive formula for the moments of the number of visits

$$-\boldsymbol{\omega}_0 \cdot \nabla_{\mathbf{r}_0} \mathbb{E}_{g+1}[n_V^k] + \Sigma \mathbb{E}_{g+1}[n_V^k] = \Sigma_s \langle \mathbb{E}_g[n_V^k] \rangle_\Omega + \Sigma_s \sum_{j=1}^{k-1} \binom{k}{j} \mathbb{1}_V(\mathbf{r}_0) \langle \mathbb{E}_g[n_V^j] \rangle_\Omega, \tag{3.67}$$

for $k \geq 1$. The recurrence is initiated with the conditions $\mathbb{E}_g[n_V^0] = 1$ (from normalization), and

$$\mathbb{E}_1[n_V^k] = \int \mathbb{1}_V(\mathbf{r}_1) T^\dagger(\mathbf{r}_1 \to \mathbf{r}_0|\boldsymbol{\omega}_0) d\mathbf{r}_1. \tag{3.68}$$

3.3.8 Stationary behaviour of $\mathbb{E}[n_V^k]$

Consider now trajectories that are followed up to $g \to \infty$. We therefore get a recursive formula for the stationary moments $\mathbb{E}[n_V^k] = \lim_{g\to\infty} \mathbb{E}_g[n_V^k]$, namely,

$$\mathcal{L}^\dagger \mathbb{E}[n_V^k](\mathbf{r}_0, \boldsymbol{\omega}_0) = -H_{k-1}(\mathbf{r}_0, \boldsymbol{\omega}_0), \tag{3.69}$$

where

$$H_{k-1} = \Sigma_s \sum_{j=1}^{k-1} \binom{k}{j} \mathbb{1}_V(\mathbf{r}_0) \langle \mathbb{E}[n_V^j] \rangle_\Omega \tag{3.70}$$

is a source term. When $k = 1$, the quantity H_0 is simply proportional to U_0, namely, $H_0 = \Sigma U_0$. Similarly as done for the moments of travelled lengths, the relation between $\mathcal{L}$ and $\mathcal{L}^\dagger$ allows explicitly inverting Eq. (3.69) in terms of the corresponding stationary flux φ, which yields

$$\mathbb{E}[n_V^k](\mathcal{Q}) = \int d\mathbf{r} \int d\boldsymbol{\omega} H_{k-1}(\mathbf{r}, \boldsymbol{\omega}) \varphi(\mathbf{r}, \boldsymbol{\omega}). \tag{3.71}$$

This means that the stationary moments of the number of visits can be obtained by convoluting the stationary flux with the source term H_{k-1}. In particular, for the average number of visits to V ($k = 1$) we recover the formula

$$\mathbb{E}[n_V](\mathcal{Q}) = \int_V d\mathbf{r} \int d\boldsymbol{\omega} \Sigma(\mathbf{r}) \varphi(\mathbf{r}, \boldsymbol{\omega}) = \int_V d\mathbf{r} \int d\boldsymbol{\omega} \psi(\mathbf{r}, \boldsymbol{\omega}), \tag{3.72}$$

since $H_0 = \Sigma \mathbb{1}_V$. The simple proportionality between the average values $\mathbb{E}[n_V^1](\mathcal{Q})$ and $\mathbb{E}[\ell_V^1](\mathcal{Q})$ does not apply to higher moments.

3.3.9 Number of individuals

The quantities ℓ_V and n_V, as defined above, are cumulative, i.e., their knowledge integrates the whole history of the walk, from the source to the time (or generation) at which the measurement is performed. Sometimes, it is necessary to provide information about *instantaneous statistics*, namely the number $m_V(t)$ and $m_V(g)$ of particles in the volume V when an observation is performed at time t, or at generation g, respectively.

Let us introduce the probability generating function of the number of particles at a given time

$$W_t(s|\mathbf{r}_0, \boldsymbol{\omega}_0) = \mathbb{E}[s^{m_V(t)}]. \tag{3.73}$$

Now, from the same arguments as above, it follows that $W_t(s|\mathbf{r}_0, \boldsymbol{\omega}_0)$ satisfies

$$\boxed{\frac{1}{v_0} \frac{\partial}{\partial t} W_t(s|\mathbf{r}_0, \boldsymbol{\omega}_0) = \mathcal{L}^\dagger W_t + \Sigma_a(\mathbf{r}_0),} \tag{3.74}$$

with the initial condition $W_0(s|\mathbf{r}_0, \boldsymbol{\omega}_0) = s^{\mathbb{1}_V(\mathbf{r}_0)}$. Furthermore, again from the same argument as above, it follows that the probability generating function

$$W_g(u|\mathbf{r}_0, \boldsymbol{\omega}_0) = \mathbb{E}[u^{m_V(g)}] \tag{3.75}$$

for the number of particles at a given generation satisfies

$$\boxed{-\boldsymbol{\omega}_0 \cdot \nabla_{\mathbf{r}_0} W_{g+1}(u|\mathbf{r}_0, \boldsymbol{\omega}_0) + \Sigma(\mathbf{r}_0) W_{g+1}(u|\mathbf{r}_0, \boldsymbol{\omega}_0) = \Sigma_a(\mathbf{r}_0) + \Sigma_s(\mathbf{r}_0) \langle W_g \rangle_\Omega,} \tag{3.76}$$

with initial condition $W_1(u|\mathbf{r}_0, \boldsymbol{\omega}_0) = \int u^{\mathbb{1}_V(\mathbf{r}_1)} T^\dagger(\mathbf{r}_1 \to \mathbf{r}_0|\boldsymbol{\omega}_0) d\mathbf{r}_1$.

3.4 Generalization to random flights

Most of what said concerning exponential flights can be carried over to the broader class of discrete Pearson walks with arbitrarily distributed jump lengths. Such walks are not Markovian in time but at collision points (i.e., generations), so that it will be convenient to analyze their statistical properties by resorting to the discrete Feynman-Kac formalism. To simplify the matter, in the following we will assume that the point source $\mathcal{Q}$ emits isotropically.

Our starting point is the integral equation (A.35) for the moment generating function of exponential flights, namely,

$$Q_{g+1}(u|\mathbf{r}_0,\boldsymbol{\omega}_0) = \int d\mathbf{r}_1 T^\dagger(\mathbf{r}_1 \to \mathbf{r}_0|\boldsymbol{\omega}_0) e^{-u\mathbb{1}_V(\mathbf{r}_1)} \left[p_a(\mathbf{r}_1) + p_s(\mathbf{r}_1)\langle Q_g\rangle_\Omega\right] \tag{3.77}$$

with the initial condition

$$Q_1(u|\mathbf{r}_0,\boldsymbol{\omega}_0) = \int e^{-u\mathbb{1}_V(\mathbf{r}_1)} T^\dagger(\mathbf{r}_1 \to \mathbf{r}_0|\boldsymbol{\omega}_0) d\mathbf{r}_1. \tag{3.78}$$

In Eq. (3.77) we have not yet used the fact that $T^\dagger$ is the adjoint of an exponential kernel, so that Eq. (3.77) actually holds for arbitrary displacement kernels. Inspection of Eq. (A.35) by a change of variables shows that the probability generating function

$$F_g(u|\mathbf{r}_0,\boldsymbol{\omega}_0) = \mathbb{E}[u^{n_V}](\mathbf{r}_0,\boldsymbol{\omega}_0) \tag{3.79}$$

satisfies

$$F_{g+1}(u|\mathbf{r}_0,\boldsymbol{\omega}_0) = \int d\mathbf{r}_1 T^\dagger(\mathbf{r}_1 \to \mathbf{r}_0|\boldsymbol{\omega}_0) u^{\mathbb{1}_V(\mathbf{r}_1)} \left[p_a(\mathbf{r}_1) + p_s(\mathbf{r}_1)\langle F_g\rangle_\Omega\right] \tag{3.80}$$

with the initial condition

$$F_1(u|\mathbf{r}_0,\boldsymbol{\omega}_0) = \int u^{\mathbb{1}_V(\mathbf{r}_1)} T^\dagger(\mathbf{r}_1 \to \mathbf{r}_0|\boldsymbol{\omega}_0) d\mathbf{r}_1. \tag{3.81}$$

Now, by averaging both equations with respect to the initial isotropic direction $\boldsymbol{\omega}_0$, we get

$$F_{g+1}(u|\mathbf{r}_0) = \int d\mathbf{r}_1 T^\dagger(\mathbf{r}_1 \to \mathbf{r}_0) e^{-u\mathbb{1}_V(\mathbf{r}_1)} \left[p_a(\mathbf{r}_1) + p_s(\mathbf{r}_1) F_g(u|\mathbf{r}_1)\right] \tag{3.82}$$

and

$$F_1(u|\mathbf{r}_0) = \int e^{-u\mathbb{1}_V(\mathbf{r}_1)} T^\dagger(\mathbf{r}_1 \to \mathbf{r}_0) d\mathbf{r}_1, \tag{3.83}$$

where we have defined the direction-averaged probability generating function

$$F_g(u|\mathbf{r}_0) = \int \frac{d\boldsymbol{\omega}_0}{\Omega_d} F_g(u|\mathbf{r}_0,\boldsymbol{\omega}_0), \tag{3.84}$$

and the direction-averaged adjoint displacement kernel

$$T^\dagger(\mathbf{r}_1 \to \mathbf{r}_0) = \int \frac{d\boldsymbol{\omega}_0}{\Omega_d} T^\dagger(\mathbf{r}_1 \to \mathbf{r}_0|\boldsymbol{\omega}_0). \tag{3.85}$$

Once $F_g(u|\mathbf{r}_0)$ is known, the occupation statistics of the underlying random flights can be assessed in terms of the probability $P_g(n_V|\mathbf{r}_0)$ of performing exactly n_V collisions in V up to the g-th generation, which is obtained by taking the derivatives

$$P_g(n_V = k|\mathbf{r}_0) = \frac{1}{k!}\frac{\partial^k}{\partial u^k} F_g(u|\mathbf{r}_0)|_{u=0}. \tag{3.86}$$

3.5 Diffusion limit

The scaling limit of the discrete Feynman-Kac equation is achieved when n_V is large, and at the same time the typical jump length δx is vanishing small. We set $t_V = n_V dt$ and $t = gdt$, where dt is some small time scale, related to δx by the usual diffusion scaling $(\delta x)^2 = 2Ddt$, the constant D playing the role of a diffusion coefficient. By taking the limit of large n_V and vanishing dt, t_V converges to the residence time in V. It is natural to set $p_a = \gamma dt$, the quantity γ being the absorption rate. Observe that, when δx is small, for any (symmetric) displacement kernel T we have the Taylor expansion

$$\int T^\dagger(\mathbf{r}'_0 \to \mathbf{r}_0) f(\mathbf{r}'_0) d\mathbf{r}'_0 \simeq f(\mathbf{r}) + \frac{1}{2}(\delta x)^2 \nabla^2_{\mathbf{r}} f(\mathbf{r}), \tag{3.87}$$

where the first-order derivative vanishes if the kernel is symmetric. It is expedient to introduce the quantity $Q_t(s|\mathbf{r}_0) = F_t(e^{-st_V}|\mathbf{r}_0)$, which is the moment generating function of $t_V = n_V dt$, i.e.,

$$\mathbb{E}[t_V^k](\mathbf{r}_0) = (-1)^k \frac{\partial^k}{\partial u^k} Q_t(s|\mathbf{r}_0)|_{s=0}, \tag{3.88}$$

when trajectories are observed up to $t = gdt$. Under the previous hypotheses, combining Eqs. (3.82) and (3.83) yields

$$Q_{t+dt}(s|\mathbf{r}_0) - Q_t(s|\mathbf{r}_0) \simeq \mathcal{L}^\dagger_{\mathbf{r}_0} Q_t(s|\mathbf{r}_0) dt - s\mathbb{1}_V(\mathbf{r}_0) Q_t(s|\mathbf{r}_0) dt + \gamma dt, \tag{3.89}$$

where $\mathcal{L}^\dagger_{\mathbf{r}_0} = D\nabla^2_{\mathbf{r}_0} - \gamma$, and we have neglected all terms vanishing faster than dt. Taking the limit $dt \to 0$, we recognize then the Feynman-Kac equation for a Brownian motion with diffusion coefficient D and absorption rate γ, namely

$$\frac{\partial}{\partial t} Q_t(s|\mathbf{r}_0) = \mathcal{L}^\dagger_{\mathbf{r}_0} Q_t(s|\mathbf{r}_0) - s\mathbb{1}_V(\mathbf{r}_0) Q_t(u|\mathbf{r}_0) + \gamma. \tag{3.90}$$

In other words, in the diffusion limit the statistical properties of the number of visits in V behave as those of the residence time of a Brownian motion, as is quite naturally expected on physical grounds [97, 98, 109, 168, 177].

3.6 The gambler's ruin and the arcsine law

Direct calculations based on the discrete Feynman-Kac formulae, Eqs. (3.82) and (3.83), are in some cases amenable to exact results concerning $P_g(n_V|\mathbf{r}_0)$, at least for simple geometries and displacement kernels. As said above, knowledge of $F_g(u|\mathbf{r}_0)$ allows explicitly determining $P_g(n_V|\mathbf{r}_0)$. Indeed, by construction the probability generating function $F_g(u|\mathbf{r}_0)$ is a polynomial in the variable u, the coefficient of each power u^k being $P_g(n_V = k|\mathbf{r}_0)$. In particular, the probability that the particles never touch (or come back to, if the source $\mathbf{r}_0 \in V$) the domain V is obtained by evaluating $F_g(u|\mathbf{r}_0)$ at $u = 0$, i.e., $P_g(0|\mathbf{r}_0) = F_g(0|\mathbf{r}_0)$. In this Section, we shall discuss some relevant examples related to the occupation statistics of a random walk, namely, the gambler's ruin and the so-called arcsine law.

3.6.1 The gambler's ruin

Consider a gambler whose initial amount of money is $x_0 \geq 0$. At each (discrete) time step g, the gambler either wins or loses a fair bet, and his capital increases or decreases, respectively, by some

fixed quantity h with equal probability. One might be interested in knowing the probability that the gambler is not ruined (i.e., that his capital has not reached zero, yet) at the g-th bet, starting from the initial capital x_0. This well-known problem [2] can be easily recast in the Feynman-Kac formalism by setting a particle in motion on a straight line, starting from x_0, with scattering probability $p_s = 1$ and a discrete displacement kernel $T(x' \to x) = \delta(x - x' - h)/2 + \delta(x - x' + h)/2$. Setting $h = 1$ amounts to expressing the capital x_0 in multiple units of the bet, and entails no loss of generality. The counting condition is imposed by assuming a Kronecker delta $\mathbb{1}_V(x) = \delta_{x,0}$ in Eq. (3.82): since the walker can not cross $x = 0$ without touching it, solving the resulting equation for the quantity $F_g(0|x_0)$ gives therefore the required probability that the gambler is not ruined at the g-th bet. We integrate now Eq. (3.82) and use Eq. (3.83): we start from the initial condition $u^{\mathbb{1}_V(x_1)} = u^{\delta_{x_1,0}}$. Then, by observing that by symmetry T and $T^\dagger$ have the same functional form, and performing the integrals Eq. (3.83) over the delta functions, we obtain

$$F_1(u|x_0) = \frac{u^{\delta_{x_0+1,0}} + u^{\delta_{x_0-1,0}}}{2}. \tag{3.91}$$

By injecting thus this expression in Eq. (3.82) and integrating again over the delta functions, we get

$$F_2(u|x_0) = \frac{u^{\delta_{x_0-1,0}} u^{\delta_{x_0-2,0}} + u^{\delta_{x_0+1,0}} u^{\delta_{x_0,0}} + u^{\delta_{x_0-1,0}} u^{\delta_{x_0,0}} + u^{\delta_{x_0+1,0}} u^{\delta_{x_0+2,0}}}{4}. \tag{3.92}$$

Proceeding by recursion, and identifying the coefficient of the zero-th order term in the polynomial yields then the first terms in the series

$$\begin{aligned}
P_g(0|1) &= \left\{ \frac{1}{2}, \frac{2}{4}, \frac{3}{8}, \frac{6}{16}, \frac{10}{32}, \frac{20}{64}, \frac{35}{128}, \frac{70}{256}, ... \right\} \\
P_g(0|2) &= \left\{ \frac{2}{2}, \frac{3}{4}, \frac{6}{8}, \frac{10}{16}, \frac{20}{32}, \frac{35}{64}, \frac{70}{128}, \frac{126}{256}, ... \right\} \\
P_g(0|3) &= \left\{ \frac{2}{2}, \frac{4}{4}, \frac{7}{8}, \frac{14}{16}, \frac{25}{32}, \frac{50}{64}, \frac{91}{128}, \frac{182}{256}, ... \right\} \\
P_g(0|4) &= \left\{ \frac{2}{2}, \frac{4}{4}, \frac{8}{8}, \frac{15}{16}, \frac{30}{32}, \frac{56}{64}, \frac{112}{128}, \frac{210}{256}, ... \right\}
\end{aligned} \tag{3.93}$$

for $x_0 = 1, 2, 3, ...$, respectively [3]. After some rather lengthy algebra, by induction one can finally recognize the formula

$$P_g(0|x_0) = \sum_{k=0}^{\lceil (g+x_0-1)/2 \rceil} \left[\binom{g}{k} - \binom{g}{k - x_0} \right] 2^{-g}, \tag{3.94}$$

where $\lceil \cdot \rceil$ denotes the integer part.

The quantity $P_g(0|x_0)$ is displayed in Fig. 3.1 as a function of g for a few values of x_0. The larger the initial capital x_0, the longer $P_g(0|x_0) \simeq 1$ before decreasing. At large g, taking the limit of Eq. (3.94) leads to the scaling

$$P_g(0|x_0) \simeq \sqrt{\frac{2}{\pi}} \frac{x_0}{\sqrt{g}}, \tag{3.95}$$

in agreement with the findings in [173]. This means that asymptotically the gambler is almost sure not to be ruined, yet, up to $g \simeq 2x_0^2/\pi$ bets. Note that Eq. (3.94) is the survival probability of

[3] The quantity $u^{\delta_{x,0}}$ evaluated at $u = 0$ is equal to 1 when $x = 0$, and vanishes otherwise.

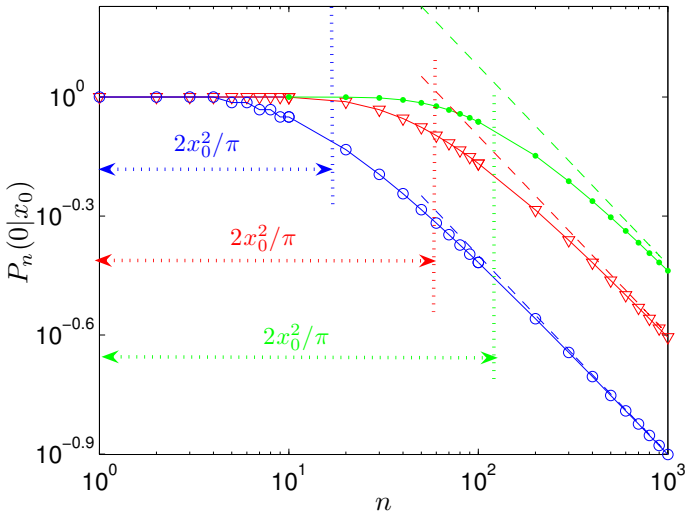

Figure 3.1: The probability $P_g(0|x_0)$ that the gambler is not ruined at the g-th bet, given an initial capital x_0. Bets are modeled by discrete random increments of fixed size $s = \pm 1$. Blue circles: $x_0 = 5$; red triangles: $x_0 = 10$; green dots: $x_0 = 15$. Lines have been added to guide the eye. Dashed lines correspond to the asymptotic result $P_g(0|x_0) \simeq \sqrt{2/\pi} x_0 g^{-1/2}$. The interval $2x_0^2/\pi$ is also shown for each x_0.

the gambler: the first passage probability $J_g(0|x_0)$, i.e., the probability that the gambler is ruined exactly at the g-th bet, can be obtained from $J_g(x_0) = P_{g-1}(0|x_0) - P_g(0|x_0)$. As a particular case, for $0 < x_0 \leq g$ and $n + x_0$ even, we recover the result in [2], namely

$$J_g(x_0) = \frac{x_0}{2^g g} \binom{g}{\frac{g+x_0}{2}}. \tag{3.96}$$

Finally, observe that when $x_0 = 0$

$$P_g(0|0) = \left\{1, \frac{1}{2}, \frac{2}{4}, \frac{3}{8}, \frac{6}{16}, \frac{10}{32}, \frac{20}{64}, \frac{35}{128}, \ldots\right\} \tag{3.97}$$

for $g \geq 1$. This is easily recognized as being the series

$$P_g(0|0) = \binom{g-1}{\lceil \frac{g-1}{2} \rceil} 2^{1-g}, \tag{3.98}$$

which is though unphysical, since the gambler should not be allowed betting when lacking an initial amount of money.

3.6.2 The arcsine law with discrete jumps

Consider a walker on a straight line, starting from x_0. We are interested in assessing the distribution $P_g(n_V|x_0)$ of the number of collisions n_V that the walker performs at the right of the starting point, when observed up to the g-th collision. This amounts to choosing $\mathbb{1}_V(x) = H(x - x_0)$, H being the Heaviside step function, in Eq. (3.82). To fix the ideas, without loss of generality we set $x_0 = 0$, and we initially assume that $p_s = 1$, i.e., the walker can not be

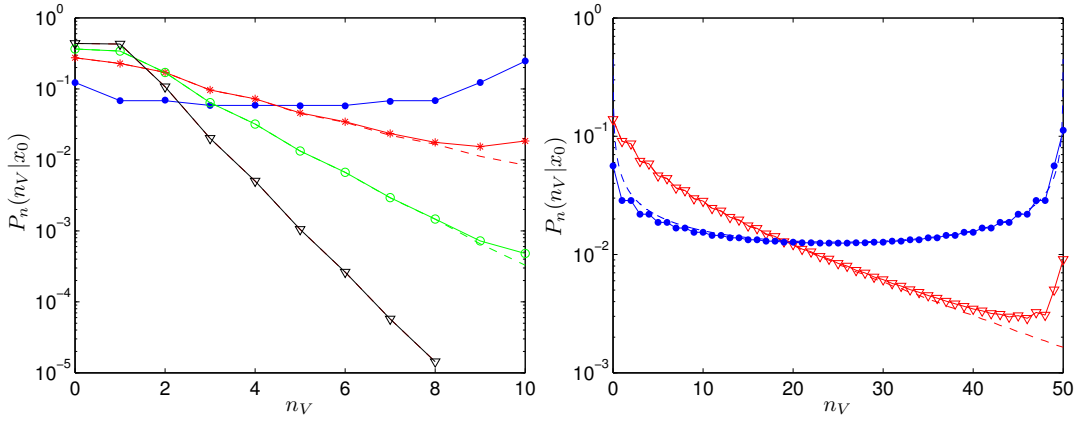

Figure 3.2: The arcsine law $P_g(n_V|x_0)$ with discrete jump lengths, as a function of n_V. The starting point is $x_0 = 0$. Left. Curves are diplayed for $g = 10$. Blue dots: $p_s = 1$ (dots); red stars: $p_s = 3/4$; green circles: $p_s = 1/2$; black triangles: $p_s = 1/4$. Lines have been added to guide the eye. Dashed curves are the asymptotic Eq. (3.104) for the correponding value of p_s. Right. Curves are diplayed for $g = 50$. Blue dots: $p_s = 1$; dashed line: the asymptotic distribution $1/\sqrt{n_V(g-n_V)}\pi$. Red triangles: $p_s = 0.95$; dashed asymptotic Eq. (3.104).

absorbed along the trajectory. This is a well known and long studied problem, for both Markovian and non-Markovian processes [2, 172, 174, 194–197]: for Brownian motion, the average residence time in V is simply $\mathbb{E}[t_V] = t/2$, whereas t_V itself is known to obey the so called Lévy's arcsine law $P_t(t_V) = 1/\sqrt{t_V(t-t_V)}\pi$, whose U shape basically implies that the particle will most often spend its time being always either on the positive or negative side of the axis [2, 173, 209]. This counterintuitive result has been shown to asymptotically hold also for discrete-time random walks without absorption, for which one expects

$$P_g(n_V|0) \simeq \frac{1}{\sqrt{n_V(g-n_V)}\pi} \tag{3.99}$$

when g and n_V are large (see for instance [173]).

The Feynman-Kac approach allows explicitly deriving $P_g(n_V|0)$. Again, assume a displacement kernel with discrete jumps $T(x' \to x) = \delta(x-x'-h)/2+\delta(x-x'+h)/2$, with jump size $h = 1$. Then, by integrating Eq. (3.82) and subsequently using Eq. (3.83) we compute the coefficients of the polynomial, which can be organized in an infinite triangle, whose first terms read

g	$n_V = 0$	1	2	3	4	5	6	7
0	1							
1	$\frac{1}{2}$	$\frac{1}{2}$						
2	$\frac{1}{4}$	$\frac{1}{4}$	$\frac{2}{4}$					
3	$\frac{2}{8}$	$\frac{1}{8}$	$\frac{2}{8}$	$\frac{3}{8}$				
4	$\frac{3}{16}$	$\frac{2}{16}$	$\frac{2}{16}$	$\frac{3}{16}$	$\frac{6}{16}$			
5	$\frac{6}{32}$	$\frac{3}{32}$	$\frac{4}{32}$	$\frac{3}{32}$	$\frac{6}{32}$	$\frac{10}{32}$		
6	$\frac{10}{64}$	$\frac{6}{64}$	$\frac{6}{64}$	$\frac{6}{64}$	$\frac{6}{64}$	$\frac{10}{64}$	$\frac{20}{64}$	
7	$\frac{20}{128}$	$\frac{10}{128}$	$\frac{12}{128}$	$\frac{9}{128}$	$\frac{12}{128}$	$\frac{10}{128}$	$\frac{20}{128}$	$\frac{35}{128}$

Actually, this result does not depend on the choice of h. To identify the elements $P_g(n_V|0)$,

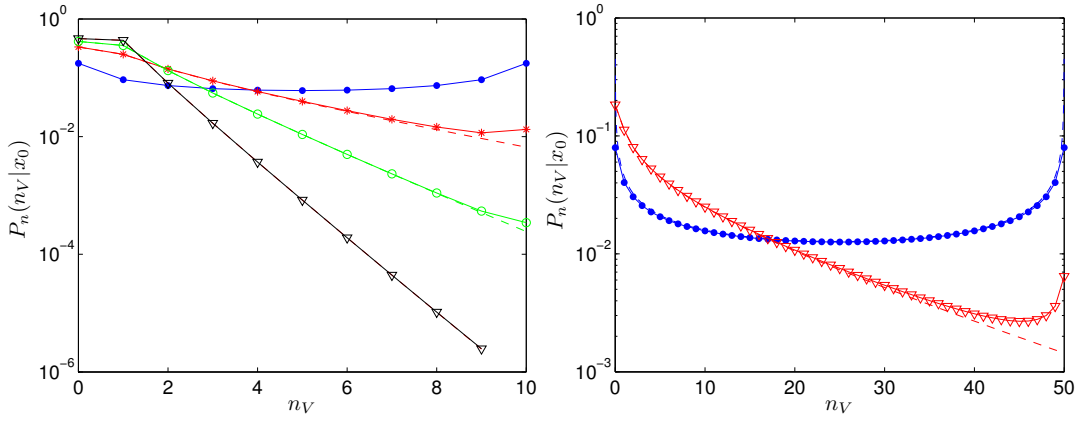

Figure 3.3: The arcsine law $P_g(n_V|x_0)$ with exponential jump lengths, as a function of n_V. The starting point is $x_0 = 0$. Left. Curves are displayed for $g = 10$. Blue dots: $p_s = 1$; red stars: $p_s = 3/4$; green circles: $p_s = 1/2$; black triangles: $p_s = 1/4$. Lines have been added to guide the eye. Dashed curves are the asymptotic Eq. (3.111) for the correponding value of p_s. Right. Curves are displayed for $g = 50$. Blue dots: $p_s = 1$; dashed line: the asymptotic distribution $1/\sqrt{n_V(g-n_V)}\pi$. Red triangles: $p_s = 0.95$; dashed line: asymptotic Eq. (3.111).

we initially inspect the column $n_V = 1$ of the triangle, and recognize the underlying series as being given by terms of the kind $\binom{g-2}{\lceil (g-2)/2 \rceil} 2^{-g}$. Then we realize that columns with $n_V \geq 2$ are related to the first column by a shift in the index g. The column $n_V = 0$ can be obtained from normalization. Proceding by induction, the elements in the triangle can be finally recast in the compact formula

$$P_g(n_V|0) = \binom{g-n_V-1}{\lceil \frac{g-n_V-1}{2} \rceil} \binom{n_V}{\lceil \frac{n_V}{2} \rceil} 2^{-g}. \tag{3.100}$$

Note that our result is slightly different from [2], where collisions are counted in pairs. When both g and n_V are large, we obtain the limit curve $P_g(n_V|0) \simeq 1/\sqrt{n_V(g-n_V)}\pi$.

When the scattering probability can vary in $0 \leq p_s \leq 1$, the triangle can be generated as above, and the first few terms read

g	$n_V = 0$	1	2	3	4
0	1				
1	$\frac{1}{2}$	$\frac{1}{2}$			
2	$\frac{2-p_s}{4}$	$\frac{2-p_s}{4}$	$\frac{2p_s}{4}$		
3	$\frac{4-2p_s}{8}$	$\frac{4-2p_s-p_s^2}{8}$	$\frac{2p_s(2-p_s)}{8}$	$\frac{3p_s^2}{8}$	
4	$\frac{8-4p_s-p_s^3}{16}$	$\frac{8-4p_s-2p_s^2}{16}$	$\frac{2p_s(4-2p_s-p_s^2)}{16}$	$\frac{3p_s^2(2-p_s)}{16}$	$\frac{6p_s^3}{16}$

Now, the identification of the polynomial coefficients $P_g(n_V|0)$ becomes more involved, because each coefficient is itself a polynomial with respect to p_s. The strategy in the identification is the same as above. By induction, the column for $n_V = 1$ can be identified as being

$$P_g(1|0) = \frac{1-p_s+\sqrt{1-p_s^2}}{4} + \left(\frac{p_s}{2}\right)^{4+2y} \binom{2+2y}{1+y} \frac{{}_2F_1\left(1, \frac{3}{2}+y, 3+y, p_s^2\right)}{2(2+y)} \tag{3.101}$$

for $g \geq 2$, with $y = \lceil (g-3)/2 \rceil$, and $p_s(1|0) = 1/2$. Once $P_g(1|0)$ is known, by inspection one realizes

that the other columns $P_g(n_V|0)$ are related by

$$P_g(n_V|0) = \left(\frac{p_s}{2}\right)^{n_V-1} \binom{n_V}{\lceil \frac{n_V}{2} \rceil} P_{g-n_V+1}(1|0) \tag{3.102}$$

for $n_V \geq 2$. The probability $P_g(0|0)$ is finally obtained from normalization, and reads

$$P_g(0|0) = \frac{p_s - 1 + \sqrt{1-p_s^2}}{2p_s} + \left(\frac{p_s}{2}\right)^{2+2z} \binom{2z}{z} \frac{{}_2F_1\left(\frac{1}{2}+z, 1, 2+z, p_s^2\right)}{p_s(1+z)}, \tag{3.103}$$

with $z = \lceil g/2 \rceil$. These results generalize Eq. (3.100), and are illustrated in Fig. 3.2 (left), where we compare $P_g(n_V|0)$ as a function of n_V for $g = 10$ and different values of p_s. When $p_s = 1$ the distribution approaches a U shape, as expected. As soon as $p_s < 1$, the shape changes considerably, and in particular $P_g(n_V|0)$ becomes strongly peaked at $n_V = 0$ as the effects of absorption overcome scattering. The presence of a second peak at $n_V = g$ is visible when $p_s \simeq 1$ and progressively disappear as p_s decreases: when p_s is small, $P_g(n_V|0)$ has an exponential tail. When g is large, $P_g(n_V|0)$ approaches the asymptotic curve

$$P_\infty(n_V|0) = \left(\frac{p_s}{2}\right)^{n_V-1} \binom{n_V}{\lceil \frac{n_V}{2} \rceil} \frac{1 - p_s + \sqrt{1-p_s^2}}{4} \tag{3.104}$$

for $n_V \geq 1$, and

$$P_\infty(0|0) = \frac{p_s - 1 + \sqrt{1-p_s^2}}{2p_s}. \tag{3.105}$$

Remark that when $p_s = 1$ this means that the U shape for large g collapses on the two extremes at $n_V = 0$ and $n_V = g$. Equation (3.104) is an excellent approximation of $P_(n_V|0)$ when the scattering probability is not too close to $p_s \simeq 1$: as expected, the discrepancy between the exact and aymptotic probability is most evident when $n_V \simeq g$, as shown in Fig. 3.2 (left). Fig. (3.2) (right) displays $P_g(n_V|0)$ as a function of n_V for $g = 50$, in order to emphasize the effects of p_s: when $p_s = 1$ the probability $P_g(n_V|0)$ is almost superposed to the asymptotic curve $P_g(n_V|0) \simeq 1/\sqrt{n_V(g-n_V)}\pi$, whereas a deviation in the scattering probability as small as $p_s = 0.95$ is sufficient to radically change the shape of the collision number distribution. Finally, observe that when n_V is also large, which implies $p_a \ll 1$, Eq. (3.104) behaves as

$$P_\infty(n_V|0) \simeq \sqrt{\frac{1-p_s}{\pi n_V}} e^{-(1-p_s)n_V}. \tag{3.106}$$

3.6.3 The arcsine law with continuous jumps

When the displacement kernel $T(x' \to x)$ is continuous and symmetric, $p_s = 1$, and $x_0 = 0$, the distribution of the number of collisions n_V falling in $x \geq x_0$ is universal, in that it does not depend on the specific functional form of $T(x' \to x)$ (see [173] and references therein). This strong and surprising result stems from a Sparre Andersen theorem [198], whose proof is highly non trivial (and does not apply to discrete jumps) [173]. This leaves the choice on the form of kernel $T(x' \to x)$, as far as it satisfies the hypotheses of the theorem. For the sake of simplicity, we have assumed an exponential distribution of jump lengths, i.e., $T(x' \to x) = \exp(-|x - x'|)/2$. Starting from Eq. (3.82) and Eq. (3.83) we can generate the infinite triangle

g	$n_V=0$	1	2	3	4	5	6	7
0	1							
1	$\frac{1}{2}$	$\frac{1}{2}$						
2	$\frac{3}{8}$	$\frac{2}{8}$	$\frac{3}{8}$					
3	$\frac{3}{16}$	$\frac{5}{16}$	$\frac{5}{16}$	$\frac{3}{16}$				
4	$\frac{35}{128}$	$\frac{20}{128}$	$\frac{18}{128}$	$\frac{20}{128}$	$\frac{35}{128}$			
5	$\frac{63}{256}$	$\frac{35}{256}$	$\frac{30}{256}$	$\frac{30}{256}$	$\frac{35}{256}$	$\frac{63}{256}$		
6	$\frac{231}{1024}$	$\frac{126}{1024}$	$\frac{105}{1024}$	$\frac{100}{1024}$	$\frac{105}{1024}$	$\frac{126}{1024}$	$\frac{231}{1024}$	
7	$\frac{429}{2048}$	$\frac{231}{2048}$	$\frac{189}{2048}$	$\frac{175}{2048}$	$\frac{175}{2048}$	$\frac{189}{2048}$	$\frac{231}{2048}$	$\frac{429}{2048}$

It is easy to verify that the triangle indeed does not depend on the jump kernel, and that other functional forms of $T(x' \to x)$ would lead to the same coefficients for the polynomials $P_g(n_V|0)$. This holds true also for Lévy flights, where $T(x' \to x)$ is a Lévy stable law and jump lengths are unbounded [173]. We start from the column $n_V = 1$, observe the relation with the subsequent columns $n_V \geq 2$, and finally derive the case $n_V = 0$ from normalization. Proceding therefore by induction we recognize that the elements of the triangle obey

$$P_g(n_V|0) = \binom{2g-2n_V}{g-n_V}\binom{2n_V}{n_V}2^{-2g}. \tag{3.107}$$

We recover here the celebrated results of the collision number distribution for discrete-time walks with symmetric continuous jumps, in absence of absorption [2,173]. When both g and n_V are large, it is possible to show that Eq. (3.107) converges to the U shape $1/\sqrt{n_V(g-n_V)}\pi$.

When the scattering probability is allowed to vary in $0 \leq p_s \leq 1$, it turns out that the polynomial coefficients $P_g(n_V|0)$ are the same for several different continuous symmetric kernels $T(x' \to x)$ (Lévy flights included), and we are therefore led to conjecture that the universality result for the case $p_s = 1$ carries over to to random walks with absorption. This allows generalizing the Sparre Andersen theorem for the collision number distribution on the half-line to a broader class of Markovian discrete-time processes. The first few terms in the triangle (which for practical purposes we have generated by resorting to $T(x' \to x) = \exp(-|x-x'|)/2$) read

g	$n_V=0$	1	2	3	4
0	1				
1	$\frac{1}{2}$	$\frac{1}{2}$			
2	$\frac{4-p_s}{8}$	$\frac{4-2p_s}{8}$	$\frac{3p_s}{8}$		
3	$\frac{8-2p_s-p_s^2}{16}$	$\frac{8-4p_s-p_s^2}{16}$	$\frac{3p_s(2-p_s)}{16}$	$\frac{5p_s^2}{16}$	
4	$\frac{64-16p_s-8p_s^2-5p_s^3}{128}$	$\frac{64-32p_s-8p_s^2-4p_s^3}{128}$	$\frac{6p_s(8-4p_s-p_s^2)}{128}$	$\frac{20p_s^2(2-p_s)}{128}$	$\frac{35p_s^3}{128}$

As above, identification of the terms $P_g(n_V|0)$ becomes more involved, because each coefficient is itself a polynomial with respect to p_s. By induction, the column for $n_V = 1$ can be identified as being

$$P_g(1|0) = \frac{\sqrt{1-p_s}}{2} + \left(\frac{p_s}{4}\right)^g \binom{2g-2}{g-1} \frac{{}_2F_1\left(-\frac{1}{2}+g, 1, 1+g, p_s\right)}{g} \tag{3.108}$$

for $g \geq 1$. Once $P_g(1|0)$ is known, the subsequent columns $P_(n_V|0)$ are observed to obey

$$P_g(n_V|0) = \left(\frac{p_s}{4}\right)^{n_V-1} \binom{2n_V-1}{n_V} P_{g-n_V+1}(1|0) \tag{3.109}$$

for $n_V \geq 2$. The probability $P_n(0|0)$ is finally obtained from normalization, and reads

$$P_g(0|0) = \frac{p_s - 1 + \sqrt{1-p_s}}{p_s} + \left(\frac{p_s}{4}\right)^g \binom{2g}{g} \frac{{}_2F_1\left(\frac{1}{2}+g, 1, 2+g, p_s\right)}{2(1+g)}. \tag{3.110}$$

These results are illustrated in Fig. 3.3 (left), where we compare $P_g(n_V|0)$ as a function of n_V for $g = 10$ and different values of p_s. The findings for continuous jumps closely resemble those for discrete displacements. When $p_s = 1$ the distribution approaches a U shape, as expected. As soon as $p_s < 1$, the shape again changes abruptly, and in particular $P_n(n_V|0)$ becomes strongly peaked at $n_V = 0$ when absorption dominates scattering. When p_s is small, $P_g(n_V|0)$ decreases exponentially at large n_V. When n is large, $P_g(n_V|0)$ approaches the asymptotic curve

$$P_\infty(n_V|0) = \left(\frac{p_s}{4}\right)^{n_V-1} \binom{2n_V-1}{n_V} \frac{\sqrt{1-p_s}}{2} \tag{3.111}$$

for $n_V \geq 1$, and

$$P_\infty(0|0) = \frac{p_s - 1 + \sqrt{1-p_s}}{p_s}. \tag{3.112}$$

Again, Eq. (3.111) is an excellent approximation of $P_g(n_V|0)$ when the scattering probability is not too close to $p_s \simeq 1$, as shown in Fig. 3.3 (left). Fig. 3.3 (right) displays $P_g(n_V|0)$ as a function of n_V for $g = 50$, in order to emphasize the effects of p_s: when $p_s = 1$ the probability $P_g(n_V|0)$ is almost superposed to the asymptotic curve $P_g(n_V|0) \simeq 1/\sqrt{n_V(g-n_V)}\pi$, whereas a deviation in the scattering probability as small as $p_s = 0.95$ is sufficient to radically change the shape of the collision number distribution. Finally, observe that when n_V is also large, which implies $p_a \ll 1$, Eq. (3.111) yields the same scaling as Eq. (3.106). All analytical calculations discussed here have been verified by comparison with Monte Carlo simulations with 10^6 particles.

Chapter 4

Branching processes

The fundamental point in fabricating a chain reacting machine is of course to see to it that each fission produces a certain number of neutrons and some of these neutrons will again produce fission.

E. Fermi, Phys. Today **8**, 12 (1955).

4.1 Introduction

So far, we have assumed that the only source of randomness for the transported particles was in their stochastic displacements. Often, the spatial displacements of systems occurring in physics and in biology are coupled to some random reproduction-disappearance mechanism [4, 6, 28, 29, 32, 33, 38, 39, 61]. The evolution of the neutron population in a nuclear reactor in the presence of multiplication due to fission events provides a central example [4, 25, 26, 32, 112]. In the context of life sciences, models of diffusion with birth-death events of the Galton-Watson type [199–201] (the so-called 'Brownian bugs') have been successfully applied to, among others, the dynamics of bacterial colonies [6, 39, 49, 51–53], the spread of epidemics [38, 61, 62, 65], the mutation-propagation of genes [43, 44, 46–48], and the spatial patterns of ecological communities [40–42]. Because of the interplay between displacements and reproduction-disappearance events, generally speaking these systems display an increased randomness with respect to purely diffusive processes.

In the presence of reproduction and disappearance, the paths performed by the individuals result in a ramified structure, as shown in Fig. 4.1: for this reason, such random walks are usually called *branching processes*. The theory of branching processes has been thoroughly explored, and the related bibliography is extremely rich [28, 29, 32, 33]. Nonetheless, deriving precise asymptotic estimates for branching processes often demands a great amount of ingenuity [202–209], and this subject is still an area of very active investigation. As shown in the following, because of the very nature of the underlying process most physical quantities obey non-linear evolution equations, which prevent in most cases exact solutions to be obtained. This is true even for the very simplest systems [202–208].

A systematic approach to the physical observables associated to branching processes can be derived by suitably generalizing the Feynman-Kac formalism introduced in the previous Chapter. Similarly as done before, in the following we first recall the basics of the Feynman-Kac approach for

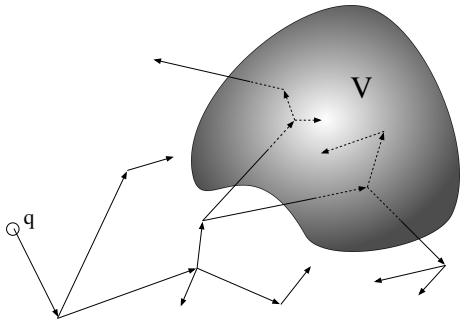

Figure 4.1: An illustration of branching exponential flights starting from a point source $\mathcal{Q}$ and traversing a volume V in phase space.

branching Brownian motion, and then derive the corresponding formulas for branching exponential and random flights.

4.2 Branching Brownian motion

Consider a particle initially located at $\mathbf{x}_0$ at time $t_0 = 0$. The walker obeys a regular d-dimensional Brownian motion with diffusion coefficient D. At rate γ, the individual is absorbed and disappears. At rate β, the individual undergoes a Galton-Watson reproduction event [29, 201]: the particle disappears and is replaced by a random number i of identical and independent descendants, whose number obeys the probability p_i. We assume that each descendant, once created, behaves as the parent particle and evolves indepedently of the other individuals. Such kind of stochastic process defines a *branching Brownian motion* [28,29,33]. We would like to compute the distribution of stochastic integrals of the form

$$\mathcal{I}_f = \# \int_0^t f(\mathbf{X}_{t'}) dt' \tag{4.1}$$

where f is an arbitrary (positive) function and $\mathbf{X}_t$ is a d-dimensional branching Brownian motion starting at $\mathbf{x}_0$ at time $t = 0$, and evolving in a domain B. The symbol # is used to recall that the integral is over all branching paths.

4.2.1 Residence time in a volume V

We initially address the distribution of the *residence time* t_V of the branching Brownian particle within the region V when observed up to the time t, which corresponds to the function f being the marker function $f = \mathbb{1}_V$ of a domain $V \subset B$. The residence time

$$t_V(t) = \# \int_0^t \mathbb{1}_V(\mathbf{X}_{t'}) dt' \tag{4.2}$$

is again a stochastic variable, which depends on the random realization of the underlying trajectory, as well as on the starting point $\mathbf{x}_0$ and on the observation time t.

Let us recall the definition of the *moment generating function*

$$Q_t(s|\mathbf{x}_0) = \mathbb{E}[e^{-st_V(t)}](\mathbf{x}_0), \tag{4.3}$$

where $\mathbb{E}[\cdot]$ denotes the ensemble average over possible realizations. The backward Feynman-Kac evolution equation for $Q_t(s|\mathbf{x}_0)$ in the case of a branching Brownian motion is derived in Appendix A.2.4, and reads

$$\boxed{\frac{\partial}{\partial t}Q_t(s|\mathbf{x}_0) = D\nabla^2_{\mathbf{x}_0}Q_t(s|\mathbf{x}_0) - (\gamma+\beta)Q_t(s|\mathbf{x}_0) - s\mathbb{1}_V(\mathbf{x}_0)Q_t(s|\mathbf{x}_0) + \gamma + \beta G[Q_t(s|\mathbf{x}_0)],} \tag{4.4}$$

where we have introduced the probability generating function

$$G[z] = p_0 + p_1 z + p_2 z^2 + \cdots = \sum_i p_i z^i \tag{4.5}$$

associated to the number of descendant particles per reproduction event.

4.2.2 Moments of residence time: Green's function and general solution

Equation (4.4) can hardly admit explicit solutions, because of the non-linear term due to the function G. A somewhat simpler approach to the analysis of the residence time is provided by the moment equations. By taking the k-th order derivative of Eq. (4.4) with respect to the conjugate variable s we get the moments

$$\mathbb{E}[t_V^k](\mathbf{x}_0) = (-1)^k \frac{\partial^k}{\partial s^k} Q_t(s|\mathbf{x}_0)|_{s=0}. \tag{4.6}$$

We apply then Eq. (4.6) to Eq. (4.4), and use Faà di Bruno's formula for multiple derivatives of composite functions [192], namely,

$$\frac{d^k}{dx^k} f[g(x)] = \sum_{j=1}^{k} f^{(k)}[g(x)]\, \mathcal{B}_{k,j}\left[g'(x), g''(x), \ldots, g^{(k-j+1)}(x)\right], \tag{4.7}$$

where

$$\mathcal{B}_{k,j}[z_i] = \mathcal{B}_{k,j}\left[z_1, z_2, \cdots, z_{k-j+1}\right] \tag{4.8}$$

are the so-called *Bell's polynomials* [192, 193]. The first few polynomials read [192]:

$$\mathcal{B}_{0,0} = 1; \tag{4.9}$$
$$\mathcal{B}_{1,1}[z_1] = z_1; \tag{4.10}$$
$$\mathcal{B}_{2,1}[z_1, z_2] = z_2, \quad \mathcal{B}_{2,2}[z_1, z_2] = z_1^2; \tag{4.11}$$
$$\mathcal{B}_{3,1}[z_1, z_2, z_3] = z_3, \quad \mathcal{B}_{3,2}[z_1, z_2, z_3] = 3z_1 z_2, \quad \mathcal{B}_{3,3}[z_1, z_2, z_3] = z_1^3. \tag{4.12}$$

Such polynomials commonly appear in connection with the combinatorics of branched structures [192]. We thus obtain the following recursive formula for the moments, namely,

$$\frac{\partial}{\partial t}\mathbb{E}_t[t_V^k] = \mathcal{L}^\dagger_{\mathbf{x}_0}\mathbb{E}_t[t_V^k] + k\mathbb{1}_V(\mathbf{r}_0)\mathbb{E}_t[t_V^{k-1}] + \beta\sum_{j=2}^{k}\nu_j\mathcal{B}_{k,j}[\mathbb{E}_t[t_V^i]], \tag{4.13}$$

where we have introduced the backward operator

$$\mathcal{L}^\dagger_{\mathbf{x}_0} = D\nabla^2_{\mathbf{x}_0} + \beta(\nu_1 - 1) - \gamma, \tag{4.14}$$

and

$$\nu_1 = \frac{\partial}{\partial z} G[z]|_{z=1} = \sum_i i p_i \tag{4.15}$$

is the *average number of secondary particles* per reproduction event. The quantities

$$\nu_j = \frac{\partial^j}{\partial z^j} G[z]|_{z=1} = \langle i(i-1)...(i-j+1) \rangle \tag{4.16}$$

are the *falling factorial moments* of the number of descendants per reproduction event [192, 193], with $\nu_0 = 1$. Equations (4.4) are *linear*, because the non-linear contributions coming from the Bell's polynomials are at most of order $k-1$ and can be then considered as a known source term in the equation of order k.

Similarly as done in the previous Chapter, it is expedient to introduce the Green's function $\mathcal{G}_t(\mathbf{x}; \mathbf{x}_0)$ satisfying the backward equation

$$\frac{\partial}{\partial t} \mathcal{G}_t(\mathbf{x}; \mathbf{x}_0) = \mathcal{L}^\dagger_{\mathbf{x}_0} \mathcal{G}_t(\mathbf{x}; \mathbf{x}_0), \tag{4.17}$$

with $\mathcal{G}_0(\mathbf{x}; \mathbf{x}_0) = \delta(\mathbf{x} - \mathbf{x}_0)$ and the boundary conditions of the problem at hand. Then, the moments of the residence time can be formally expressed in terms of the Green's function as

$$\begin{aligned} \mathbb{E}_t[t_V^k](\mathbf{x}_0) = k \int_0^t dt' \int d\mathbf{x}' \mathbb{1}_V(\mathbf{x}') \mathbb{E}_{t-t'}[t_V^{k-1}](\mathbf{x}') \mathcal{G}_{t'}(\mathbf{x}'; \mathbf{x}_0) \\ + \beta \sum_{j=2}^{k} \nu_j \int_0^t dt' \int d\mathbf{x}' \mathcal{B}_{k,j}[\mathbb{E}_{t-t'}[t_V^i(\mathbf{x}')]] \mathcal{G}_{t'}(\mathbf{x}'; \mathbf{x}_0). \end{aligned} \tag{4.18}$$

For $k \geq 2$, branching events provide an additional source (depending on moments up to order $k-1$) that contributes to moments of order k. In particular, the fluctuations of the residence time ($k = 2$) are thus higher than in the case of a purely diffusive Brownian motion.

4.2.3 Number of individuals in a volume V

Consider a d-dimensional branching Brownian motion starting from position $\mathbf{x}_0$ at time $t_0 = 0$. Let $m_V = m_V(\mathbf{x}_0, t)$ be the number of particles that are found in a volume $V \subseteq B$ of the viable space when the process is observed at a time $t > t_0$. We are interested in determining the detection probability $\mathcal{P}_t(m_V|\mathbf{x}_0)$ of finding m_V particles in volume $V \subseteq B$ at time t, for a *single particle* starting at $\mathbf{x}_0$ at time t_0. It is convenient to introduce the associated probability generating function

$$W_t(u|\mathbf{x}_0) = \mathbb{E}[u^{m_V(\mathbf{x}_0, t)}], \tag{4.19}$$

from which the k-th falling factorial moments of m_V can be obtained by derivation with respect to u. In particular, the average particle number reads

$$\mathbb{E}_t[m_V|\mathbf{x}_0] = \frac{\partial}{\partial u} W_t(u|\mathbf{x}_0)|_{u=1}. \tag{4.20}$$

For the second factorial moment we take the derivative twice, namely,

$$\mathbb{E}_t[(m_V)_2|\mathbf{x}_0] = \mathbb{E}_t[m_V^2|\mathbf{x}_0] - \mathbb{E}_t[m_V|\mathbf{x}_0] = \frac{\partial^2}{\partial u^2} W_t(u|\mathbf{x}_0)|_{u=1}. \tag{4.21}$$

By following the same strategy as above, it can be shown that $W_t(u|\mathbf{x}_0)$ satisfies the backward equation

$$\boxed{\frac{\partial}{\partial t}W_t = D\nabla^2_{\mathbf{x}_0}W_t - (\beta+\gamma)W_t + \gamma + \beta G[W_t],} \tag{4.22}$$

By taking the derivative of Eq. (4.22) once we get the equation for the average particle number

$$\frac{\partial}{\partial t}\mathbb{E}_t[m_V|\mathbf{x}_0] = \mathcal{L}^\dagger_{\mathbf{x}_0}\mathbb{E}_t[m_V|\mathbf{x}_0]. \tag{4.23}$$

Equation (4.23) must be solved together with the initial condition $\mathbb{E}_0[m_V|\mathbf{x}_0] = \mathbb{1}_V(\mathbf{x}_0)$. Then, for the average particle number we get

$$\mathbb{E}_t[m_V|\mathbf{x}_0] = \int_V d\mathbf{x}'\mathcal{G}_t(\mathbf{x}';\mathbf{x}_0). \tag{4.24}$$

4.2.4 Multi-type branching processes

In some physical systems, a (random) fraction of the particles emerging from a reproduction event is emitted with a *random time delay*. Examples emerge for instance in neutron transport and in epidemics [4]. Conceptually, delayed emission can be represented by assuming that at each reproduction event a parent particle of type A creates a random number of independent and identically distributed (*prompt*) descendants of type A, plus a random number of so-called *precursors*, which we will denote by type B. Immediately thereafter, the descendants of type A will start to diffuse and replicate as the parent particle. As for the precursors B, they will stay in place during an exponential waiting time with rate λ, and will subsequently decay to particles of type A. Upon decay, each precursor will generate exactly one regular particle. This mechanism can be described in terms of multi-type branching processes [4, 32]. The backward formalism described above can be extended to multi-type branching by introducing the following notation: we will define

$$W^A_t(u|\mathbf{x}_0) = \mathbb{E}^A[u^{n_V(\mathbf{x}_0,t)}] \tag{4.25}$$

the probability generating function of detecting n_V particles of type A at V for a single particle of type A starting from $\mathbf{x}_0$ at time $t_0 = 0$; similarly, we will define

$$W^B_t(u|\mathbf{x}_0) = \mathbb{E}^B[u^{n_V(\mathbf{x}_0,t)}] \tag{4.26}$$

the probability generating function of detecting n_V particles of type A at V for a single particle of type B starting from $\mathbf{x}_0$ at time $t_0 = 0$. By following the same strategy as before, it can be shown that $W^A_t(u|\mathbf{x}_0)$ and $W^B_t(u|\mathbf{x}_0)$ satisfy the system of coupled equations

$$\begin{aligned}
\frac{\partial}{\partial t}W^A_t &= D\nabla^2_{\mathbf{x}_0}W^A_t - (\gamma+\beta)W^A_t + \gamma + \beta G^A[W^A_t]G^B[W^B_t] \\
\frac{\partial}{\partial t}W^B_t &= -\lambda W^B_t + \lambda W^A_t,
\end{aligned} \tag{4.27}$$

where $G^A[z]$ is the generating function of the number of descendants of type A per reproduction event and $G^B[z]$ is the generating function of the number of precursors B per reproduction event. We have used here the hypothesis of independence for the probability of generating a given number of descendants and of precursors, whence the product of the generating functions in the former evolution equation. These equations can accommodate any kind of distributions for the number of descendants and precursors, as well as arbitrary boundary conditions. The moments of the physical observables can be finally obtained by taking the derivatives of the generating functions.

4.3 Occupation statistics of branching exponential flights

Let us now turn our attention to the case of d-dimensional branching exponential flights. Consider a single walker initially emitted from a point source at time $t_0 = 0$ at position $\mathbf{r}_0$, with direction $\boldsymbol{\omega}_0$. Similarly as done in the previous Chapter, in order to keep notation to a minimum we assume that the particle speed $v = v_0$ is constant, i.e., that only the walker directions $\boldsymbol{\omega}$ do change after collisions, and that scattering is isotropic. At each collision, the incident particle can alternatively be captured with probability $p_a(\mathbf{r}) = \Sigma_a(\mathbf{r})/\Sigma(\mathbf{r})$, be scattered with probability $p_s(\mathbf{r}) = \Sigma_s(\mathbf{r})/\Sigma(\mathbf{r})$, or give rise to fission with probability $p_f(\mathbf{r}) = \Sigma_f(\mathbf{r})/\Sigma(\mathbf{r})$. In the case of fission, the incident particle disappears and i new particles (the descendants) are isotropically emitted with probability $p_i(\mathbf{r})$. Each descendant will then behave as the mother particle, and undergo a new sequence of displacements and collisions.

Branching exponential flights, as defined above, are a Markovian stochastic process (because of the exponential distribution of the jumps) that can be observed both as a function of time t and discrete generations g. We would like to characterize the occupation statistics of such process within a given region V, namely the number of visits n_V and of the travelled lengths ℓ_V in V. To begin with, we address first the average physical observables of exponential flights.

4.3.1 The average total travelled length $\mathbb{E}[\ell_V]$

The time-dependent Boltzmann equation for the the average particle density in phase space $N_t(\mathbf{r}, \boldsymbol{\omega})$ for a source $\mathcal{Q}$ at time $t_0 = 0$ can be obtained with a slight modification of Eq. (3.35). The mass balance along a line oriented as $\boldsymbol{\omega}$ in a small time dt yields

$$\frac{\partial}{\partial t} N_t + v\boldsymbol{\omega} \cdot \nabla_{\mathbf{r}} N_t = -v\Sigma N_t + \int \frac{d\boldsymbol{\omega}'}{\Omega_d} v\Sigma_s(\mathbf{r}) N_t(\mathbf{r}) + \int \frac{d\boldsymbol{\omega}'}{\Omega_d} v\nu_1(\mathbf{r})\Sigma_f(\mathbf{r}) N_t(\mathbf{r}, \boldsymbol{\omega}'), \tag{4.28}$$

where the quantity $\nu_1(\mathbf{r}) = \sum_i i p_i(\mathbf{r})$ is the *average number of secondary particles* emitted per fission event. Boundary conditions on $N_t(\mathbf{r}, \boldsymbol{\omega})$ depend on the specific problem under analysis. For the stationary flux $\varphi(\mathbf{r}, \boldsymbol{\omega}) = \int_0^\infty dt \varphi_t(\mathbf{r}, \boldsymbol{\omega})$ we get in particular

$$\boldsymbol{\omega} \cdot \nabla_{\mathbf{r}} \varphi + \Sigma(\mathbf{r})\varphi = \int \frac{d\boldsymbol{\omega}'}{\Omega_d} \Sigma_s(\mathbf{r})\varphi(\mathbf{r}, \boldsymbol{\omega}') + \int \frac{d\boldsymbol{\omega}'}{\Omega_d} \nu_1(\mathbf{r})\Sigma_f(\mathbf{r})\varphi(\mathbf{r}, \boldsymbol{\omega}') + \mathcal{Q}, \tag{4.29}$$

which can be again rewritten as

$$\mathcal{L}\varphi(\mathbf{r}, \boldsymbol{\omega}) = -\mathcal{Q}, \tag{4.30}$$

where now the forward transport operator for *isotropic* branching exponential flights reads

$$\mathcal{L} = -\boldsymbol{\omega} \cdot \nabla_{\mathbf{r}} - \Sigma(\mathbf{r}) + \int \frac{d\boldsymbol{\omega}'}{\Omega_d} \Sigma_s(\mathbf{r}) + \int \frac{d\boldsymbol{\omega}'}{\Omega_d} \nu_1(\mathbf{r})\Sigma_f(\mathbf{r}). \tag{4.31}$$

The average travelled length in a given volume V of phase space follows then from

$$\mathbb{E}[\ell_V](\mathcal{Q}) = \int_V d\mathbf{r} \int d\boldsymbol{\omega} \varphi(\mathbf{r}, \boldsymbol{\omega}). \tag{4.32}$$

4.3.2 The average total number of visits $\mathbb{E}[n_V]$

For the collision density $\psi_g(\mathbf{r}, \boldsymbol{\omega})$ at the g-th generation we get

$$\psi_{g+1}(\mathbf{r}, \boldsymbol{\omega}) = \int d\mathbf{r}' \int \frac{d\boldsymbol{\omega}'}{\Omega_d} T(\mathbf{r}' \to \mathbf{r}|\boldsymbol{\omega})[p_s(\mathbf{r}) + \nu_1(\mathbf{r}) p_f(\mathbf{r})]\psi_g(\mathbf{r}', \boldsymbol{\omega}'), \tag{4.33}$$

with the uncollided density

$$\psi_1(\mathbf{r},\boldsymbol{\omega}) = \int d\mathbf{r}' T(\mathbf{r}' \to \mathbf{r}|\boldsymbol{\omega}) \mathcal{Q}(\mathbf{r}',\boldsymbol{\omega}). \tag{4.34}$$

The stationary collision density $\psi(\mathbf{r},\boldsymbol{\omega}) = \sum_{g=1}^{\infty} \psi_g(\mathbf{r},\boldsymbol{\omega})$ satisfies

$$\psi = \int d\mathbf{r}' \int \frac{d\boldsymbol{\omega}'}{\Omega_d} T(\mathbf{r}' \to \mathbf{r}|\boldsymbol{\omega})[p_s(\mathbf{r}) + \nu_1(\mathbf{r}) p_f(\mathbf{r})]\psi(\mathbf{r}',\boldsymbol{\omega}') + \psi_1. \tag{4.35}$$

The average number of visits to a given volume V of phase space follows again from

$$\mathbb{E}[n_V](\mathcal{Q}) = \int_V d\mathbf{r} \int d\boldsymbol{\omega} \psi(\mathbf{r},\boldsymbol{\omega}). \tag{4.36}$$

Remark that Eq. (4.35) can still be equivalently recast into Eq. (4.29) by setting $\psi = \Sigma\varphi$. As a consequence, we have also

$$\mathbb{E}[n_V](\mathcal{Q}) = \int_V d\mathbf{r} \int d\boldsymbol{\omega} \Sigma(\mathbf{r}) \varphi(\mathbf{r},\boldsymbol{\omega}). \tag{4.37}$$

It follows that the average observables associated to branching exponential flights are ruled by the same equations as in the previous Chapter. In order to assess the higher moments of the travelled length and the number of visits we have to resort to the Feynman-Kac formalism.

4.3.3 Total travelled length in V

We formally define the total length $\ell_V(t)$ travelled by a branching exponential flight in a given volume V of the phase space, when observed up to a time t, as

$$\ell_V(t) = \# \int_0^t \mathbb{1}_V(\mathbf{r}') v dt', \tag{4.38}$$

where the integral is now intended over all the branching paths of a single realization up to time t. Let us introduce the associated moment generating function

$$Q_t(s|\mathbf{r}_0,\boldsymbol{\omega}_0) = \mathbb{E}[e^{-s\ell_V(t)}](\mathbf{r}_0,\boldsymbol{\omega}_0) \tag{4.39}$$

for a single walker initially at $\mathbf{r}_0,\boldsymbol{\omega}_0$ at observation time $t = 0$. The derivation of the backward evolution equation for $Q_t(s|\mathbf{r}_0,\boldsymbol{\omega}_0)$ is sketched in Appendix A.2.5, and yields

$$\boxed{\frac{1}{v_0}\frac{\partial}{\partial t} Q_t = \boldsymbol{\omega}_0 \cdot \nabla_{\mathbf{r}_0} Q_t - \Sigma Q_t - s\mathbb{1}_V(\mathbf{r}_0) Q_t + \Sigma_a + \Sigma_s \langle Q_t \rangle_\Omega + \Sigma_f G[\langle Q_t \rangle_\Omega],} \tag{4.40}$$

with $G[z] = \sum_i p_i z^i$. Equation (4.40) is completed by the initial condition $Q_0(s|\mathbf{r}_0,\boldsymbol{\omega}_0) = 1$ and by the appropriate boundary conditions, which depend on the problem at hand.

4.3.4 Moment equations for ℓ_V

Equation (4.40) is a partial differential equation with a nonlinear integral term, for which explicit solutions are hardly available. The corresponding (linear) moment equations can be obtained from

$$\mathbb{E}_t[\ell_V^k](\mathbf{r}_0,\boldsymbol{\omega}_0) = (-1)^k \frac{\partial^k}{\partial s^k} Q_t(s|\mathbf{r}_0,\boldsymbol{\omega}_0)|_{s=0}. \tag{4.41}$$

By taking the k-th derivative of Eq. (4.40) and resorting to the Faà di Bruno's formula for multiple derivatives of composite functions [192], we get the following recursive expression for the moments of the trace length

$$\frac{1}{v_0}\frac{\partial}{\partial t}\mathbb{E}_t[\ell_V^k] = \mathcal{L}^\dagger \mathbb{E}_t[\ell_V^k] + k\mathbb{1}_V(\mathbf{r}_0)\mathbb{E}_t[\ell_V^{k-1}] + \Sigma_f \sum_{j=2}^{k} \nu_j \mathcal{B}_{k,j}\left[\langle \mathbb{E}_t[\ell_V^i]\rangle_\Omega\right], \tag{4.42}$$

for $k \geq 1$, where

$$\mathcal{L}^\dagger = \boldsymbol{\omega}_0 \cdot \nabla_{\mathbf{r}_0} - \Sigma + \Sigma_s \int \frac{d\boldsymbol{\omega}_0'}{\Omega_d} + \Sigma_f \nu_1 \int \frac{d\boldsymbol{\omega}_0'}{\Omega_d} \tag{4.43}$$

is the *(backward) transport operator* adjoint to $\mathcal{L}$ [5,30,113], and $\mathcal{B}_{k,j}$ are again the Bell's polynomials. The recurrence is initiated with the conditions $\mathbb{E}_t[\ell_V^0] = 1$ (from normalization), and $\mathbb{E}_0[\ell_V^k] = 0$.

Define now the Green's function $\mathcal{G}_t(\mathbf{r}, \boldsymbol{\omega}; \mathbf{r}_0, \boldsymbol{\omega}_0)$ satisfying the backward equation

$$\frac{1}{v_0}\frac{\partial}{\partial t}\mathcal{G}_t(\mathbf{r}, \boldsymbol{\omega}; \mathbf{r}_0, \boldsymbol{\omega}_0) = \mathcal{L}^\dagger \mathcal{G}_t(\mathbf{r}, \boldsymbol{\omega}, \mathbf{r}_0, \boldsymbol{\omega}_0), \tag{4.44}$$

with $\mathcal{G}_0(\mathbf{r}, \boldsymbol{\omega}; \mathbf{r}_0, \boldsymbol{\omega}_0) = \delta(\mathbf{r} - \mathbf{r}_0)\delta(\boldsymbol{\omega} - \boldsymbol{\omega}_0)$ and the boundary conditions of the problem at hand. Then, by analogy with the case of Brownian motion, the moments of the travelled length can be formally expressed in terms of the Green's function as

$$\begin{aligned}\mathbb{E}_t[\ell_V^k](\mathbf{r}_0, \boldsymbol{\omega}_0) = {} & k \int_0^t dt' \int d\mathbf{r}' \int d\boldsymbol{\omega}' v_0 \mathbb{1}_V(\mathbf{r}') \mathbb{E}_{t-t'}[\ell_V^{k-1}](\mathbf{r}', \boldsymbol{\omega}') \mathcal{G}_{t'}(\mathbf{r}', \boldsymbol{\omega}'; \mathbf{r}_0, \boldsymbol{\omega}_0) \\ & + \Sigma_f v_0 \sum_{j=2}^{k} \nu_j \int_0^t dt' \int d\mathbf{r}' \int d\boldsymbol{\omega}' \mathcal{B}_{k,j}\left[\langle \mathbb{E}_{t-t'}[\ell_V^i]\rangle_\Omega(\mathbf{r}')\right] \mathcal{G}_{t'}(\mathbf{r}', \boldsymbol{\omega}'; \mathbf{r}_0, \boldsymbol{\omega}_0).\end{aligned} \tag{4.45}$$

4.3.5 Stationary behaviour

When the observation time t is much longer than the characteristic time scale of the system dynamics ($t \to \infty$), the time derivative in Eq. (4.42) vanishes, provided that the moment $\mathbb{E}_t[\ell_V^k]$ does not diverge. We therefore get a recursive formula for the stationary moments $\mathbb{E}[\ell_V^k] = \lim_{t\to\infty} \mathbb{E}_t[\ell_V^k]$, namely,

$$\mathcal{L}^\dagger \mathbb{E}[\ell_V^k](\mathbf{r}_0, \boldsymbol{\omega}_0) = -U_{k-1}(\mathbf{r}_0, \boldsymbol{\omega}_0), \tag{4.46}$$

where

$$U_{k-1}(\mathbf{r}_0, \boldsymbol{\omega}_0) = k\mathbb{1}_V(\mathbf{r}_0)\mathbb{E}[\ell_V^{k-1}] + \Sigma_f \sum_{j=2}^{k} \nu_j \mathcal{B}_{k,j}\left[\langle \mathbb{E}[\ell_V^i]\rangle_\Omega\right] \tag{4.47}$$

is a source term that depends at most on the moments of order $k-1$.

Now, from $\mathcal{L}^\dagger$ being the adjoint operator with respect to $\mathcal{L}$, i.e.,

$$\langle \mathcal{L} f, g\rangle = \langle \mathcal{L}^\dagger g, f\rangle, \tag{4.48}$$

Eq. (4.46) can be explicitly inverted, and gives

$$\mathbb{E}[\ell_V^k](\mathcal{Q}) = \int d\mathbf{r} \int d\boldsymbol{\omega} U_{k-1}(\mathbf{r}, \boldsymbol{\omega}) \varphi(\mathbf{r}, \boldsymbol{\omega}), \tag{4.49}$$

which means that the stationary moments of the travelled length can be obtained by convoluting the stationary flux with the source term U_{k-1}. Finally, for the average length travelled in V, i.e., $k = 1$, we recover the formula

$$\mathbb{E}[\ell_V](\mathcal{Q}) = \int_V d\mathbf{r} \int d\boldsymbol{\omega} \varphi(\mathbf{r}, \boldsymbol{\omega}), \tag{4.50}$$

since $U_0(\mathbf{r}, \boldsymbol{\omega}) = \mathbb{1}_V(\mathbf{r})$.

4.3.6 Total number of visits to V

We address then the statistical properties of the total number of visits $n_V(g)$ performed by a branching exponential flight in a given volume V, when observed up to the g-th generation. We formally define

$$n_V(g) = \# \sum_i \mathbb{1}_V(\mathbf{r}_i), \tag{4.51}$$

where the sum is intended over all the points visited by the branching path up to entering the g-th generation. We adopt the convention that the source is not taken into account. We introduce the associated moment generating function

$$Q_g(u|\mathbf{r}_0, \boldsymbol{\omega}_0) = \mathbb{E}[e^{-un_V(g)}](\mathbf{r}_0, \boldsymbol{\omega}_0), \tag{4.52}$$

where u is the transformed variable with respect to n_V, for a single walker initially at $\mathbf{r}_0, \boldsymbol{\omega}_0$. The derivation of the evolution equation for $Q_g(u|\mathbf{r}_0, \boldsymbol{\omega}_0)$ is provided in Appendix A.2.6, and yields

$$\boxed{-\boldsymbol{\omega}_0 \cdot \nabla_{\mathbf{r}_0} Q_{g+1}(u|\mathbf{r}_0, \boldsymbol{\omega}_0) + \Sigma Q_{g+1}(u|\mathbf{r}_0, \boldsymbol{\omega}_0) = e^{-u\mathbb{1}_V(\mathbf{r}_0)} \left[\Sigma_a + \Sigma_s \langle Q_g \rangle_\Omega + \Sigma_f G\left[\langle Q_g \rangle_\Omega\right]\right],} \tag{4.53}$$

with the initial condition

$$Q_1(u|\mathbf{r}_0, \boldsymbol{\omega}_0) = \int d\mathbf{r}_1 e^{-u\mathbb{1}_V(\mathbf{r}_1)} T^\dagger(\mathbf{r}_1 \to \mathbf{r}_0|\boldsymbol{\omega}_0), \tag{4.54}$$

and the appropriate boundary conditions.

4.3.7 Moment equations for n_V

Equation (4.53) is a nonlinear integro-differential and finite differences equation. The corresponding moment equations can be obtained from

$$\mathbb{E}_g[n_V^k](\mathbf{r}_0, \boldsymbol{\omega}_0) = (-1)^k \frac{\partial^m}{\partial u^k} Q_g(u|\mathbf{r}_0, \boldsymbol{\omega}_0)|_{u=0}. \tag{4.55}$$

Then, by taking the k-th derivative of Eq. (4.53), we get the following recursive formula for the moments of number of visits

$$\begin{aligned} &-\boldsymbol{\omega}_0 \cdot \nabla_{\mathbf{r}_0} \mathbb{E}_{g+1}[n_V^k] + \Sigma \mathbb{E}_{g+1}[n_V^k] = \Sigma_s \langle \mathbb{E}_g[n_V^k] \rangle_\Omega + \Sigma_s \sum_{j=1}^{k-1} \binom{k}{j} \mathbb{1}_V(\mathbf{r}_0) \langle \mathbb{E}_g[n_V^j] \rangle_\Omega \\ &+ \Sigma_f \sum_{j=1}^{k} \nu_j \mathcal{B}_{k,j} \left[\langle \mathbb{E}_g[n_V^i] \rangle_\Omega\right] + \Sigma_f \sum_{i=1}^{k} \binom{k}{i} \mathbb{1}_V(\mathbf{r}_0) \sum_{j=0}^{k-i} \nu_j \mathcal{B}_{k-i,j} \left[\langle \mathbb{E}_g[n_V^q] \rangle_\Omega\right], \end{aligned} \tag{4.56}$$

for $k \geq 1$. Equation (4.56) relates the moments $\mathbb{E}_g[n_V^k]$ of the number of visits to the moments ν_j of the descendant number. The recurrence is initiated with the conditions $\mathbb{E}_g[n_V^0] = 1$ (from normalization), and $\mathbb{E}_1[n_V^k] = \int d\mathbf{r}_1 \mathbb{1}_V(\mathbf{r}_1) T^\dagger(\mathbf{r}_1 \to \mathbf{r}_0|\boldsymbol{\omega}_0)$.

4.3.8 Stationary behaviour

When trajectories are followed up to $g \to \infty$ (provided that the moment $\mathbb{E}_g[n_V^k]$ does not diverge) we get a recursive formula for the stationary moments $\mathbb{E}[n_V^k] = \lim_{g\to\infty} \mathbb{E}_g[n_V^k]$, namely,

$$\mathcal{L}^\dagger \mathbb{E}[n_V^k](\mathbf{r}_0, \boldsymbol{\omega}_0) = -H_{k-1}(\mathbf{r}_0, \boldsymbol{\omega}_0), \tag{4.57}$$

where

$$\begin{aligned} H_{k-1} = \Sigma_s \sum_{j=1}^{k-1} \binom{k}{j} \mathbb{1}_V(\mathbf{r}_0) \langle \mathbb{E}[n_V^j] \rangle_\Omega + \Sigma_f \sum_{j=2}^{k} \nu_j \mathcal{B}_{k,j} \left[\langle \mathbb{E}[n_V^i] \rangle_\Omega \right] \\ + \Sigma_f \sum_{i=1}^{k} \binom{k}{i} \mathbb{1}_V(\mathbf{r}_0) \sum_{j=0}^{k-i} \nu_j \mathcal{B}_{k-i,j} \left[\langle \mathbb{E}[n_V^q] \rangle_\Omega \right] \end{aligned} \tag{4.58}$$

is a source term, and we have singled out the terms of order k. When $k = 1$, we have $H_0 = \Sigma U_0$.

As done for the moments of travelled lengths, Eq. (4.57) can be explicitly inverted in terms of the corresponding stationary flux φ, and gives

$$\mathbb{E}[n_V^k](\mathcal{Q}) = \int d\mathbf{r} \int d\boldsymbol{\omega} H_{k-1}(\mathbf{r}, \boldsymbol{\omega}) \varphi(\mathbf{r}, \boldsymbol{\omega}), \tag{4.59}$$

which means that the stationary moments of the number of visits can be obtained by convoluting the stationary flux with the source term H_{k-1}. In particular, for the average number of visits to V ($k = 1$) we recover the formula

$$\mathbb{E}[n_V^1](\mathcal{Q}) = \int d\mathbf{r} \int d\boldsymbol{\omega} \mathbb{1}_V(\mathbf{r}_0) \Sigma \varphi(\mathbf{r}, \boldsymbol{\omega}), \tag{4.60}$$

since $H_0(\mathbf{r}, \boldsymbol{\omega}) = \Sigma(\mathbf{r}) \mathbb{1}_V(\mathbf{r})$. The simple proportionality between $\mathbb{E}[n_V^1]$ and $\mathbb{E}[\ell_V^1]$ does not carry over to higher moments.

4.4 Other physical observables

The Feynman-Kac approach proposed above can be extended to the analysis of other physical observables. We work out the probability of never visiting a region, the number of individuals and the survival probability.

4.4.1 Probability of never visiting a region V

One might be interested in determining the probability $\mathcal{R}_g(\mathbf{r}_0, \boldsymbol{\omega}_0)$ that an exponential flight coming from a point source at $\mathbf{r}_0, \boldsymbol{\omega}_0$ *never collides* in a given domain V, up to generation g. This is intimately related to the well-known *gambler's ruin* problem [2, 7, 8]. By definition,

$$\mathcal{R}_g(\mathbf{r}_0, \boldsymbol{\omega}_0) = \mathbb{E}[u^{n_V(g)}](\mathbf{r}_0, \boldsymbol{\omega}_0)|_{u=0}. \tag{4.61}$$

By comparing $\mathbb{E}[u^{n_V(g)}](\mathbf{r}_0, \boldsymbol{\omega}_0)$ to $Q_g(u|\mathbf{r}_0, \boldsymbol{\omega}_0)$, it is apparent that $\mathcal{R}_g(\mathbf{r}_0, \boldsymbol{\omega}_0)$ satisfies

$$-\boldsymbol{\omega}_0 \cdot \nabla_{\mathbf{r}_0} \mathcal{R}_{g+1}(\mathbf{r}_0, \boldsymbol{\omega}_0) + \Sigma \mathcal{R}_{g+1}(\mathbf{r}_0, \boldsymbol{\omega}_0) = \bar{\mathbb{1}}_V(\mathbf{r}_0) \Big[\Sigma_a + \Sigma_s \langle \mathcal{R}_g \rangle_\Omega + \Sigma_f G \left[\langle \mathcal{R}_g \rangle_\Omega \right] \Big], \tag{4.62}$$

where $\bar{\mathbb{1}}_V(\mathbf{r}_0) = 1 - \mathbb{1}_V(\mathbf{r}_0)$. As for the initial conditions, we have

$$\mathcal{R}_1(\mathbf{r}_0, \boldsymbol{\omega}_0) = \int d\mathbf{r}_1 \bar{\mathbb{1}}_V(\mathbf{r}_1) T^\dagger(\mathbf{r}_1 \to \mathbf{r}_0 | \boldsymbol{\omega}_0). \tag{4.63}$$

When $g \to \infty$, we get the stationary probability equation

$$-\boldsymbol{\omega}_0 \cdot \nabla_{\mathbf{r}_0} \mathcal{R}(\mathbf{r}_0, \boldsymbol{\omega}_0) + \Sigma \mathcal{R}(\mathbf{r}_0, \boldsymbol{\omega}_0) = \bar{\mathbb{1}}_V(\mathbf{r}_0) \Big[\Sigma_a + \Sigma_s \langle \mathcal{R} \rangle_\Omega + \Sigma_f G \left[\langle \mathcal{R} \rangle_\Omega \right] \Big], \tag{4.64}$$

where we have set $\mathcal{R}(\mathbf{r}_0, \boldsymbol{\omega}_0) = \lim_{g \to \infty} \mathcal{R}_g(\mathbf{r}_0, \boldsymbol{\omega}_0)$.

4.4.2 Number of individuals

From the same argument as above, the probability generating function $W_t = \mathbb{E}[s^{m_V(t)}]$ for the *number of individuals* $m_V(t)$ in V at a given time t satisfies

$$\frac{1}{v_0} \frac{\partial}{\partial t} W_t(s|\mathbf{r}_0, \boldsymbol{\omega}_0) - \boldsymbol{\omega}_0 \cdot \nabla_{\mathbf{r}_0} W_t(s|\mathbf{r}_0, \boldsymbol{\omega}_0) + \Sigma W_t(s|\mathbf{r}_0, \boldsymbol{\omega}_0) = \Sigma_a + \Sigma_s \langle W_t \rangle_\Omega + \Sigma_f G[\langle W_t \rangle_\Omega], \tag{4.65}$$

with initial condition $W_0(s|\mathbf{r}_0, \boldsymbol{\omega}_0) = s^{\mathbb{1}_V(\mathbf{r}_0)}$. Equation (4.65) is known in reactor physics as the *Pál-Bell equation* [25, 26, 32].

Furthermore, again from the same argument as above, the probability generating function $W_g = \mathbb{E}[u^{m_V(g)}]$ for the number of individuals $m_V(g)$ at a given generation g satisfies

$$-\boldsymbol{\omega}_0 \cdot \nabla_{\mathbf{r}_0} W_{g+1}(u|\mathbf{r}_0, \boldsymbol{\omega}_0) + \Sigma W_{g+1}(u|\mathbf{r}_0, \boldsymbol{\omega}_0) = \Sigma_a + \Sigma_s \langle W_g \rangle_\Omega + \Sigma_f G[\langle W_g \rangle_\Omega], \tag{4.66}$$

with initial condition $W_1(u|\mathbf{r}_0, \boldsymbol{\omega}_0) = \int d\mathbf{r}_1 u^{\mathbb{1}_V(\mathbf{r}_1)} T^\dagger(\mathbf{r}_1 \to \mathbf{r}_0 | \boldsymbol{\omega}_0)$.

4.4.3 Survival probability

Assume now that the viable space B is bounded, that the volume V coincides with B and that particles are lost upon leaving the boundary ∂V. We would like to assess the *survival probability* at time t or generation g, due to the interplay between diffusion, absorption and branching. As particles can not re-enter V after crossing the boundaries, if $m_V(t) = 0$, then also $m_V(t') = 0$ for $t' \geq t$ (i.e., the process goes to extinction), and the same holds true for $m_V(g)$. Hence, by definition, the probability of having zero particles in the volume V at a time t is given by $W_t(s = 0|\mathbf{r}_0, \boldsymbol{\omega}_0)$, which equivalently yields the probability that extinction is reached for times smaller than t, since V is bounded [2, 4, 32]. We define then the survival probability of an exponential flight as

$$\mathcal{S}_t(\mathbf{r}_0, \boldsymbol{\omega}_0) = 1 - W_t(s = 0|\mathbf{r}_0, \boldsymbol{\omega}_0), \tag{4.67}$$

which by direct substitution in Eq. (4.65) satisfies

$$\frac{1}{v_0} \frac{\partial}{\partial t} \mathcal{S}_t(\mathbf{r}_0, \boldsymbol{\omega}_0) - \boldsymbol{\omega}_0 \cdot \nabla_{\mathbf{r}_0} \mathcal{S}_t(\mathbf{r}_0, \boldsymbol{\omega}_0) + \Sigma \mathcal{S}_t(\mathbf{r}_0, \boldsymbol{\omega}_0) = \Sigma_s \langle \mathcal{S}_t \rangle_\Omega + \Sigma_f F[\langle \mathcal{S}_t \rangle_\Omega], \tag{4.68}$$

where we have set [26]

$$F[z] = \sum_{k=1}^{\infty} (-1)^{k+1} \frac{\nu_k}{k!} z^k. \tag{4.69}$$

At the boundaries, $\mathcal{S}_t$ must vanish when $\boldsymbol{\omega}_0$ is directed towards the exterior of V.

The survival probability as a function of generations is defined as

$$\mathcal{S}_g(\mathbf{r}_0, \boldsymbol{\omega}_0) = 1 - W_g(u = 0|\mathbf{r}_0, \boldsymbol{\omega}_0), \tag{4.70}$$

which by direct substitution in Eq. (4.66) satisfies

$$-\boldsymbol{\omega}_0 \cdot \nabla_{\mathbf{r}_0} \mathcal{S}_{g+1}(\mathbf{r}_0, \boldsymbol{\omega}_0) + \Sigma \mathcal{S}_{g+1}(\mathbf{r}_0, \boldsymbol{\omega}_0) = \Sigma_s \langle \mathcal{S}_g \rangle_\Omega + \Sigma_f F \left[\langle \mathcal{S}_g \rangle_\Omega \right], \tag{4.71}$$

where $\mathcal{S}_g$ must again vanish at the boundaries when $\boldsymbol{\omega}_0$ is directed towards the exterior of V. Finally, by either taking the limit $\mathcal{S} = \lim_{t\to\infty} \mathcal{S}_t(\mathbf{r}_0, \boldsymbol{\omega}_0)$ or $\mathcal{S} = \lim_{g\to\infty} \mathcal{S}_g(\mathbf{r}_0, \boldsymbol{\omega}_0)$, respectively, the *probability of ultimate survival* $\mathcal{S}(\mathbf{r}_0, \boldsymbol{\omega}_0)$ satisfies

$$-\boldsymbol{\omega}_0 \cdot \nabla_{\mathbf{r}_0} \mathcal{S} + \Sigma \mathcal{S} = \Sigma_s \langle \mathcal{S} \rangle_\Omega + \Sigma_f F[\langle \mathcal{S} \rangle_\Omega]. \tag{4.72}$$

Observe that in principle $\mathcal{S} = 0$ is always a solution to Eq. (4.72), which would imply a vanishing probability that infinitely long branching chains exist in V. However, it may happen that the population growth is not sufficiently compensated by the particle loss due to finite geometry and absorption: in this case, the solution $\mathcal{S} = 0$ would become unstable, and $\mathcal{S}_t$ (or $\mathcal{S}_g$) would converge towards a non-trivial ultimate survival probability $\mathcal{S} = \mathcal{S}_\infty > 0$ [4, 28, 29, 32]. The stability analysis of the solution $\mathcal{S} = 0$ can be carried out by introducing a small perturbation [210], for instance in the form

$$\hat{\mathcal{S}} \simeq 0 + \delta X(t) Y(\mathbf{r}_0, \boldsymbol{\omega}_0), \tag{4.73}$$

the amplitude $\delta > 0$ being a small positive constant, with $X(t) > 0$ and $Y(\mathbf{r}_0, \boldsymbol{\omega}_0) > 0$. Now, if we inject $\hat{\mathcal{S}}$ into Eq. (4.68), and take the limit $\delta \to 0$, we obtain an equation for the perturbation amplitude

$$\frac{1}{v_0} \frac{1}{X(t)} \frac{\partial X(t)}{\partial t} = \frac{\boldsymbol{\omega}_0 \cdot \nabla_{\mathbf{r}_0} Y - \Sigma Y + \Sigma_s \langle Y \rangle_\Omega + \Sigma_f \nu_1 \langle Y \rangle_\Omega}{Y}, \tag{4.74}$$

where at the numerator of the right hand side we recognize the adjoint operator $\mathcal{L}^\dagger$. From the separation of the variables, Eq. (4.74) shows that the evolution of the perturbation amplitude with respect to time is determined by the ratio $\alpha = \mathcal{L}^\dagger Y / Y$, hence by the eigenvalue equation

$$\boldsymbol{\omega}_0 \cdot \nabla_{\mathbf{r}_0} Y - \Sigma Y + \Sigma_s \langle Y \rangle_\Omega + \Sigma_f \nu_1 \langle Y \rangle_\Omega = \alpha Y. \tag{4.75}$$

The spectrum of the eigenvalues of $\mathcal{L}^\dagger$ depends on the geometry of V and on the boundary conditions. If all eigenvalues α are negative, the amplitude of the small perturbation will shrink in time, so that eventually $\mathcal{S} \to 0$; if on the contrary at least one eigenvalue is positive, then the small perturbation will grow in time, which means that $\mathcal{S} = 0$ is unstable, and eventually $\mathcal{S} \to \mathcal{S}_\infty$. For a given branching process, the crossover between these two regimes depends on the size and shape of the volume V, and generally speaking one would expect that $\mathcal{S} \to \mathcal{S}_\infty$ for a volume size larger than some critical value V_c [29, 30, 32, 210], which is attained when the largest eigenvalue attains $\alpha = 0$.

The stability analysis of $\hat{\mathcal{S}} \simeq 0 + \delta X_g Y(\mathbf{r}_0, \boldsymbol{\omega}_0)$ in Eq. (4.71) leads to

$$\frac{X_{g+1}}{X_g} = -\frac{\Sigma_s \langle Y \rangle_\Omega + \Sigma_f \nu_1 \langle Y \rangle_\Omega}{\boldsymbol{\omega}_0 \cdot \nabla_{\mathbf{r}_0} Y(\mathbf{r}_0, \boldsymbol{\omega}_0) - \Sigma Y(\mathbf{r}_0, \boldsymbol{\omega}_0)}. \tag{4.76}$$

The evolution of the perturbation amplitude is determined then by the eigenvalue equation

$$-\boldsymbol{\omega}_0 \cdot \nabla_{\mathbf{r}_0} Y(\mathbf{r}_0, \boldsymbol{\omega}_0) + \Sigma Y(\mathbf{r}_0, \boldsymbol{\omega}_0) = \frac{1}{k} \Big[\Sigma_s \langle Y \rangle_\Omega + \Sigma_f \nu_1 \langle Y \rangle_\Omega \Big], \tag{4.77}$$

where the fundamental eigenvalue k plays the role of an *effective multiplication factor*, expressing the ratio between the sizes of two successive generations: when $k < 1$ the perturbation shrinks and when $k > 1$ the perturbation grows, the crossover occurring for a critical volume V_c such that $k = 1$ [30, 210].

4.5 Branching random flights and the diffusion limit

Similarly as observed in the previous Chapter, most of what said concerning branching exponential flights can be carried over to the broader class of discrete branching Pearson walks with arbitrarily distributed jump lengths. Branching random flights emerge for instance in modelling the propagation of epidemics: n_V corresponds to the number of infections in a region V as a function of the position of the initial infected person (as long as the number of infected people is small, so that nonlinear effects due to the depletion of the susceptibles can be neglected, and that spatial displacements can be described by a simple random walk [61]). The quantity n_V occurs also in population genetics, where one might be interested in quantifying the number n_V of mutations of a given kind V, starting from a single character, as a function of the number of generations (this is closely related to the Ewens' formula for the mutation partition, when mutations are allowed to be recurrent [46]). Such walks are Markovian at collision points (i.e., generations), and their analysis can be carried out by resorting to the discrete Feynman-Kac formalism [211]. In the following we will assume that the source $\mathcal{Q}$ emits isotropically.

Inspection of Eq. (A.50) by a change of variables shows that the probability generating function

$$F_g(u|\mathbf{r}_0, \boldsymbol{\omega}_0) = \mathbb{E}[u^{n_V}](\mathbf{r}_0, \boldsymbol{\omega}_0) \tag{4.78}$$

satisfies

$$F_{g+1}(u|\mathbf{r}_0, \boldsymbol{\omega}_0) = \int d\mathbf{r}_1 T^\dagger(\mathbf{r}_1 \to \mathbf{r}_0|\boldsymbol{\omega}_0) u^{\mathbb{1}_V(\mathbf{r}_1)} \left[p_a + p_s \langle F_g \rangle_\Omega + p_f G\left[\langle F_g \rangle_\Omega\right]\right], \tag{4.79}$$

with the initial condition

$$F_1(u|\mathbf{r}_0, \boldsymbol{\omega}_0) = \int u^{\mathbb{1}_V(\mathbf{r}_1)} T^\dagger(\mathbf{r}_1 \to \mathbf{r}_0|\boldsymbol{\omega}_0) d\mathbf{r}_1. \tag{4.80}$$

Now, by averaging both equations with respect to the initial isotropic direction $\boldsymbol{\omega}_0$ we get

$$F_{g+1}(u|\mathbf{r}_0) = \int d\mathbf{r}_1 T^\dagger(\mathbf{r}_1 \to \mathbf{r}_0) e^{-u\mathbb{1}_V(\mathbf{r}_1)} \left[p_a + p_s F_g(u|\mathbf{r}_1) + p_f G\left[F_g(u|\mathbf{r}_1)\right]\right] \tag{4.81}$$

and

$$F_1(u|\mathbf{r}_0) = \int e^{-u\mathbb{1}_V(\mathbf{r}_1)} T^\dagger(\mathbf{r}_1 \to \mathbf{r}_0) d\mathbf{r}_1, \tag{4.82}$$

where $F_g(u|\mathbf{r}_0)$ is the direction-averaged probability generating function and $T^\dagger(\mathbf{r}_1 \to \mathbf{r}_0)$ the direction-averaged adjoint displacement kernel. Once $F_g(u|\mathbf{r}_0)$ is known, the occupation statistics of the underlying branching random flights can be again assessed in terms of the probability $P_g(n_V|\mathbf{r}_0)$ of performing exactly n_V collisions in V up to the g-th generation, which is obtained by taking the derivatives

$$P_g(n_V = k|\mathbf{r}_0) = \frac{1}{k!}\frac{\partial^k}{\partial u^k} F_g(u|\mathbf{r}_0)|_{u=0}. \tag{4.83}$$

4.5.1 Diffusion limit

We conclude by examining the scaling limit of the discrete Feynman-Kac equations for branching processes for large n_V, and vanishing small jump length δx. We set $t_V = n_V dt$ and $t = ndt$, where dt is some small time scale related to δx by the usual diffusion scaling $(\delta x)^2 = 2Ddt$. By taking large n_V and vanishing dt, t_V converges to the residence time in V. It is expedient to introduce the quantity $Q_t(u|\mathbf{r}_0) = F_t(e^u|\mathbf{r}_0)$, which is the moment generating function of t_V, i.e.,

$$\mathbb{E}_t[t_V^k](\mathbf{r}_0) = (-1)^k \frac{\partial^k}{\partial u^k} Q_t(u|\mathbf{r}_0)|_{u=0}, \tag{4.84}$$

when trajectories are observed up to time t. Combining Eqs. (4.81) and (4.82), using the Taylor expansion for small δx of the jump kernels and passing to the limit $dt \to 0$ yields

$$\frac{\partial}{\partial t} Q_t = \nabla^2_{\mathbf{r}_0} Q_t - (\gamma + \beta) Q_t - u \mathbb{1}_V(\mathbf{r}_0) Q_t + \gamma + \beta G\left[Q_t\right]. \tag{4.85}$$

4.6 The rod model

In this Section we will discuss a relevant example of branching stochastic process, namely neutron multiplication and diffusion in a prototype model of nuclear fuel rod. During reactor start-up analysis, one is interested in determining the time evolution of the neutron flux φ_t in a system, starting from a given initial condition [30,32,123,124,126]. The full description of such behaviour is obtained by solving the time-dependent Boltzmann equation for the flux, together with the equations for the precursors concentrations $c_t^{i,j}$. Alternatively, one could perform a *spectral analysis* of the Boltzmann operator and thus reconstruct the time behaviour of the system. As shown in Sec. 1.5, this corresponds to solving the *coupled system of eigenvalue equations*

$$\frac{\alpha}{v}\varphi_\alpha(\mathbf{r},\mathbf{v}) + L\,\varphi_\alpha(\mathbf{r},\mathbf{v}) = F_p\,\varphi_\alpha(\mathbf{r},\mathbf{v}) + \sum_{i,j} \chi_d^{i,j}(\mathbf{r},v)\lambda_{i,j} c_\alpha^{i,j}(\mathbf{r}) \tag{4.86}$$

and

$$\alpha c_\alpha^{i,j}(\mathbf{r}) = \int \nu_d^{i,j}(v')\Sigma_f^i(\mathbf{r},v')\varphi_\alpha(\mathbf{r},\mathbf{v}')\,\mathrm{d}\mathbf{v}' - \lambda_{i,j} c_\alpha^{i,j}(\mathbf{r}), \tag{4.87}$$

for the flux φ_α and the precursors $c_\alpha^{i,j}$. Since the α eigenvalues physically represent the characteristic frequencies of the system, they are often called the *natural* eigenvalues [5, 30]. Notation is taken from Sec. 1.5. Often, however, the system evolution may be characterized in terms of the long-time (asymptotic) behaviour [5, 30]. In this case, only the *algebraically largest* eigenvalue α must be found (i.e., the eigenvalue whose real part is larger than those of all other eigenvalues), so that the corresponding fundamental mode $\varphi_\alpha(\mathbf{r},\mathbf{v})$ will provide the space and velocity shape of the neutron flux at long times [5, 30, 137, 138]. It is customary to formally solve Eq. (4.87) for the precursor concentration and to replace the resulting $c_\alpha^{i,j}$ into Eq. (4.86). This yields the (nonlinear) eigenvalue problem for φ_α [30,140,141]

$$\boxed{\frac{\alpha}{v}\varphi_\alpha(\mathbf{r},\mathbf{v}) + L\,\varphi_\alpha(\mathbf{r},\mathbf{v}) = F_p\,\varphi_\alpha(\mathbf{r},\mathbf{v}) + \sum_{i,j} \frac{\lambda_{i,j}}{\lambda_{i,j}+\alpha} F_d^{i,j}\,\varphi_\alpha(\mathbf{r},\mathbf{v}),} \tag{4.88}$$

where we have defined the delayed fission operator

$$F_d^{i,j}\,f = \chi_d^{i,j}(\mathbf{r},v) \int \nu_d^{i,j}(v')\Sigma_f^i(\mathbf{r},v') f(\mathbf{r},\mathbf{v}')\,\mathrm{d}\mathbf{v}'. \tag{4.89}$$

The full Eq. (4.88) including delayed contributions (in which case α physically represents the *inverse of the asymptotic reactor period* [30,140,141]) has recently attracted renewed interest in view of its practical applications in reactor kinetics [122, 212–215].

The eigenvalue equation (4.88) can be solved by Monte Carlo methods. The key tool is the so-called α-k power iteration algorithm [1], whose specific details depend on the sign of the dominant eigenvalue α [217–220]. The structure of the algorithm, whose details are detailed in [215,220], is as follows.

[1] Actually, alternative algorithms have been also proposed, such as the weight correction methods for prompt [216] and delayed [214] α eigenvalues, or the transition rates matrix [122].

Positive dominant eigenvalue

The simplest approach consists in simulating the neutron population alone: we introduce a fictitious factor k and rewrite the nonlinear eigenvalue Eq. (4.88) as follows

$$L_\alpha \, \varphi_\alpha(\mathbf{r},\mathbf{v}) = \frac{1}{k} \left[F_p \, \varphi_\alpha(\mathbf{r},\mathbf{v}) + \sum_{i,j} w_{i,j}(\alpha) \, F_d^{i,j} \, \varphi_\alpha(\mathbf{r},\mathbf{v}) \right], \tag{4.90}$$

where $L_\alpha = L + \Sigma_\alpha$ is a modified transport operator, $\Sigma_\alpha = \alpha/v$ can be interpreted as an additional sterile capture cross-section (the so-called time absorption) added to the total cross section, and we have a factor

$$w_{i,j}(\alpha) = \frac{\lambda_{i,j}}{\lambda_{i,j} + \alpha} > 0 \tag{4.91}$$

appearing in front of the $F_d^{i,j}$ operator. This term actually acts as a population control tool (depending on the value of α at the current generation) to be applied to each delayed fission neutron. In other words, the average number of delayed neutrons emitted per fission is modified to $w_{i,j}(\alpha)\nu_d^{i,j}(v')$ for an incident neutron of speed v'. Alternatively, $\nu_d^{i,j}(v')$ delayed neutrons are emitted, but their statistical weight is multiplied by a factor $w_{i,j}(\alpha)$ before being assigned to the next generation. Keeping in mind these precautions, Eq. (4.90) can be solved by resorting to α-k power iteration algorithm, i.e., by searching for α such that $k = k(\alpha) = 1$. We start from a tentative distribution $\varphi_\alpha^{(0)}$ (zero-*th* iteration) for the neutrons and provide a guess value for $\alpha^{(0)}$. Then, we search for the corresponding k eigenvalue by standard power iteration, which will depend on the current value of α. Neutrons are simulated within a generation until they leak, get absorbed, or give rise to new fissions, as customary. On the basis of k, we will then adjust the value of α for the next generation (for instance, one can take $\alpha^{(g+1)} = k\alpha^{(g)}$). This procedure is iterated until $k(\alpha)$ converges to $k = 1$: the corresponding value of α will provide the fundamental prompt eigenvalue, and the associated φ_α the fundamental eigenmode. Convergence on $k(\alpha)$ could be monitored by defining an appropriate criterion, e.g., $|k(\alpha) - 1| \leq \epsilon$, with a desired accuracy ϵ. A discussion on the convergence of the algorithm towards the fundamental eigenvalue can be found in [214].

Negative dominant eigenvalue

When $\alpha < 0$, the standard α-k power iteration algorithm is known to be numerically unstable and usually leads to abnormal code termination [217]. In [215, 220] we have provided an improved algorithm for negative α that has been shown to be numerically stable. Starting from the nonlinear eigenvalue Eq. (4.88) for the neutron population alone, we can rewrite

$$L_{\alpha,\eta} \, \varphi_\alpha(\mathbf{r},\mathbf{v}) = \frac{1}{k} \, F_p \, \varphi_\alpha(\mathbf{r},\mathbf{v}) + \frac{1}{k} \, F_{\alpha,\eta} \, \varphi_\alpha(\mathbf{r},\mathbf{v}) + \frac{1}{k} \sum_{i,j} w_{i,j}(\alpha) \, F_d^{i,j} \, \varphi_\alpha(\mathbf{r},\mathbf{v}), \tag{4.92}$$

where $L_{\alpha,\eta} = L + \Sigma_{\alpha,\eta}$ is a modified transport operator, with $\Sigma_{\alpha,\eta} = -\eta\alpha/v$ (η being an arbitrary positive constant). We formally define the creation operator

$$F_{\alpha,\eta} \, f = \int \nu_\eta \delta(\mathbf{v} - \mathbf{v}') \Sigma_{\alpha,\eta} f(\mathbf{r},\mathbf{v}') \, \mathrm{d}\mathbf{v}', \tag{4.93}$$

with

$$\nu_\eta = \frac{\eta + 1}{\eta} > 0. \tag{4.94}$$

The term $\Sigma_{\alpha,\eta}$ acts here as an additional creation cross-section (the so-called time production), whose associated creation operator $F_{\alpha,\eta}$ appears at the right hand side of the equation with a delta-spectrum in velocity and an average number of produced neutrons equal to ν_η.

The factor $w_{i,j}(\alpha)$ in front of the $F_d^{i,j}$ terms acts as a population control tool. However, one can observe that now $w_{i,j}(\alpha)$ introduces singularities in Eq. (4.92) at the values $\alpha = -\lambda_{i,j}$, α being negative. If we restrict our search to the dominant α eigenvalue, this implies that α must be found in the interval $-\lambda^\star < \alpha < 0$, where $\lambda^\star = \min_{i,j} \lambda_{i,j}$ is the smallest decay constant over all fissile isotopes and over all precursor families. Bearing this consideration in mind, the treatment of delayed neutrons proceeds as above, i.e., the average number of delayed neutrons emitted per fission is modified to $w_{i,j}(\alpha)\nu_d^{i,j}(v')$ for an incident neutron of speed v'.

Then, Eq. (4.92) satisfies a balance between creation terms (at the right hand side) and destruction terms (at the left hand side), and can be solved by applying the α-k power iteration as above.

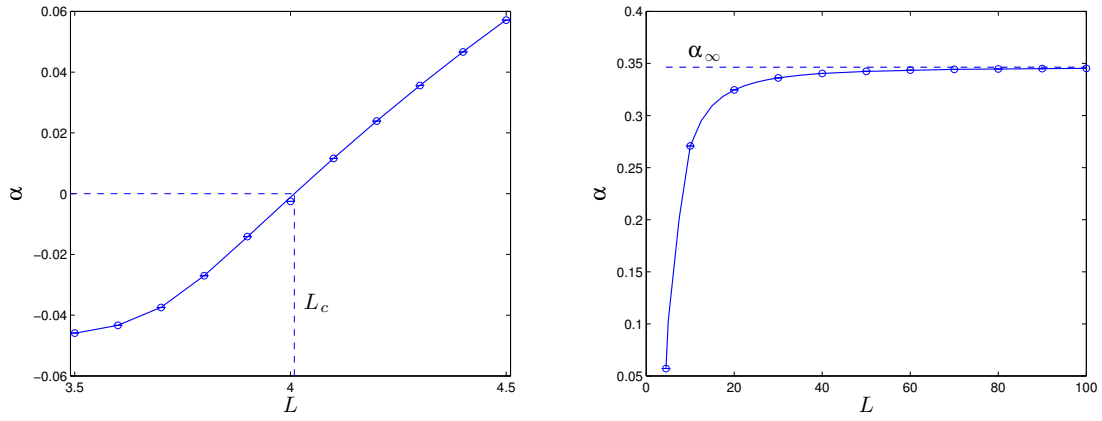

Figure 4.2: Left. Behaviour of the fundamental α eigenvalue as a function of the domain size L. Monte Carlo estimates based on the α-k power iteration are displayed as symbols; exact values are shown as solid line. For this example the critical size is $L_c = 4.00886$ (dashed line). Right. Behaviour of the fundamental α eigenvalue as a function of the domain size L. Monte Carlo estimates based on the α-k power iteration are displayed as symbols; exact values are shown as solid line. The dashed line represents the asymptotic eigenvalue $\alpha_\infty = 0.34628$ for an infinite domain, $L \to \infty$.

4.6.1 Finding the eigenvalues of the rod model

The *rod model* is possibly the simplest example of space- and direction-dependent transport problem [221]: particles move at constant speed v along a line (the rod) and undergo collision events at a rate $v\Sigma_t$. Because of the geometric constraints, only two directions of flight are allowed, namely forward ($\omega = +$) and backward ($\omega = -$); here, we furthermore assume that scattering and fission are isotropic, i.e., that directions taken by the particles after a collision are sampled with equal probability, and a single fissile isotope is present. If we define $\varphi_\alpha(x, +)$ the angular flux in the positive direction and $\varphi_\alpha(x, -)$ in the negative direction, respectively, where x is the spatial

coordinate, Eq. (4.88) becomes

$$\pm\frac{\partial}{\partial x}\varphi_\alpha(x,\pm)+\frac{\alpha}{v}\varphi_\alpha(x,\pm)+\Sigma_t\varphi_\alpha(x,\pm)$$
$$=\Sigma_s\varphi_\alpha(x)+(1-\beta)\nu_f\Sigma_f\varphi_\alpha(x)+\sum_{j=1}^{M}\frac{\lambda_j}{\lambda_j+\alpha}\beta_j\nu_f\Sigma_f\varphi_\alpha(x), \tag{4.95}$$

where $\varphi_\alpha(x)=[\varphi_\alpha(x,+)+\varphi_\alpha(x,-)]/2$ is the scalar flux integrated over the allowed directions. Here we have defined β the total fraction of delayed fission neutrons, and β_j the fraction of delayed fission neutrons for family j, ν_f being the average (prompt plus delayed) number of neutrons per fission.

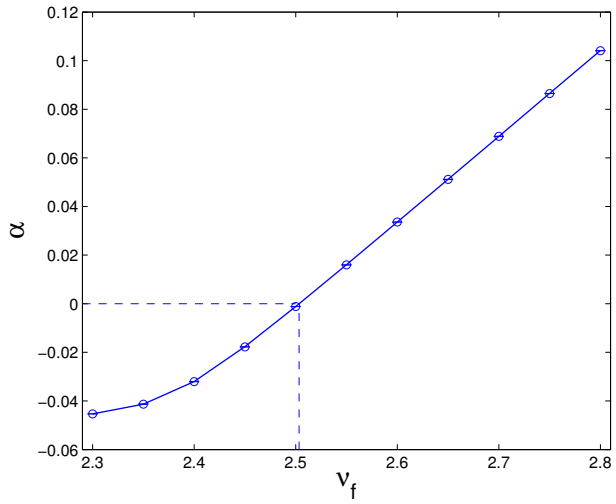

Figure 4.3: The rod model. Behaviour of the fundamental α eigenvalue as a function of ν_f, the average number of neutrons per fission, when $L=4$. Monte Carlo estimates based on the α-k power iteration are displayed as symbols; exact values are shown as solid line. The critical configuration is attained for $\nu_f=2.5034$ (dashed line).

When vacuum boundary conditions are imposed, the viable space is a segment $[0,L]$, with boundary conditions $\varphi_\alpha(x=0,+)=0$ and $\varphi_\alpha(x=L,-)=0$: following the same strategy as in [221], a dispersion relation can be explicitly derived, whose roots α are the eigenvalues of the transport problem. Introducing the dimensionless eigenvalue $\psi=1+\alpha/(v\Sigma_t)$ and the dimensionless length $z=L\Sigma_t$ yields the dispersion relation

$$\cosh\left(z\sqrt{\psi\left(\psi-\nu_\alpha\right)}\right)+\frac{\left(\psi-\frac{\nu_\alpha}{2}\right)\sinh\left(z\sqrt{\psi\left(\psi-\nu_\alpha\right)}\right)}{\sqrt{\psi\left(\psi-\nu_\alpha\right)}}=0, \tag{4.96}$$

where

$$\nu_\alpha=\bar{\nu}_p+\sum_{j=1}^{m}\frac{\lambda_j}{\lambda_j+\alpha}\bar{\nu}_d^j, \tag{4.97}$$

the quantity

$$\bar{\nu}_p=\frac{\Sigma_s+\nu_f(1-\beta)\Sigma_f}{\Sigma_t} \tag{4.98}$$

being the average number of secondary prompt particles per collision, and

$$\bar{\nu}_d^j = \frac{\beta_j \nu_f \Sigma_f}{\Sigma_t} \tag{4.99}$$

the average number of secondary delayed particles in family j per collision. The zeros of Eq. (4.96), solved as a function of α, form the spectrum of the nonlinear eigensystem (4.95).

When precursors are neglected, there exists a finite number of real eigenvalues, plus a countable infinity of complex eigenvalues associated to oscillating modes [221]; in the presence of precursors, additional eigenvalues are introduced by the m singularities at $\alpha = -\lambda_j$. When the dominant eigenvalue satisfies $\alpha = 0$, the system is exactly critical, i.e., the neutron population will stay constant. From Eq. (4.96), this happens for a (dimensionless) critical segment length $z_c = L_c \Sigma_t$

$$z_c = 2 \frac{\tan^{-1}\left(\frac{1}{\sqrt{\bar{\nu}-1}}\right)}{\sqrt{\bar{\nu}-1}}, \tag{4.100}$$

where $\bar{\nu} = \bar{\nu}_p + \sum_{j=1}^m \bar{\nu}_d^j$. For very large systems, $z \gg 1$, Eq. (4.96) becomes independent of the spatial effects and the eigenvalues $\alpha_\infty = \lim_{L\to\infty} \alpha$ satisfy the simpler relation

$$\alpha_\infty = v\Sigma_t \left(\bar{\nu}_p + \sum_{j=1}^m \frac{\lambda_j}{\lambda_j + \alpha_\infty} \bar{\nu}_d^j - 1 \right). \tag{4.101}$$

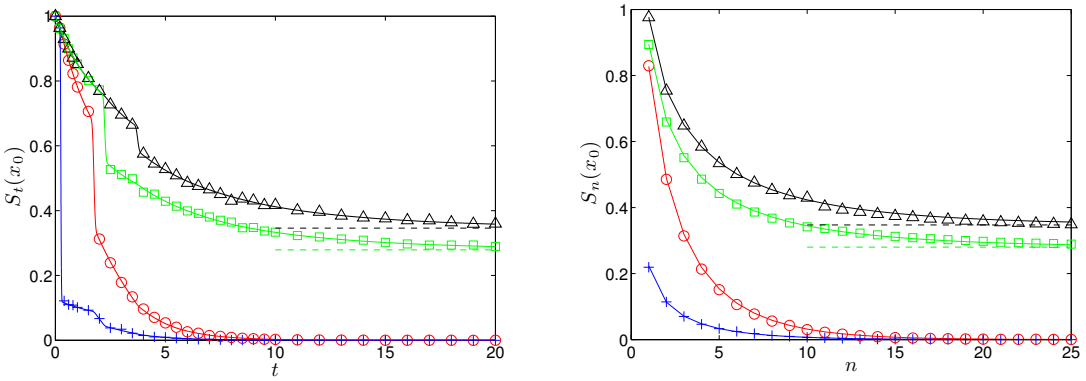

Figure 4.4: Left. Survival probabilities $\mathcal{S}_t^{\pm}(x_0)$ for $\Sigma_a = 0.2$, $\Sigma_s = 0.3$, $\Sigma_f = 0.5$ and $\nu_f = 2$ ($L_c = 3.9987$). Blue crosses and red circles: $\mathcal{S}_t^{+}(x_0)$ and $\mathcal{S}_t^{-}(x_0)$, respectively, with $x_0 = 1.75$ and $L = 2$ ($\alpha < 0$). Green squares and black triangles: $\mathcal{S}_t^{+}(x_0)$ and $\mathcal{S}_t^{-}(x_0)$, respectively, with $x_0 = 3.75$ and $L = 6$ ($\alpha > 0$). Solid lines are numerical integrals of Eq. (4.68), symbols Monte Carlo simulations with 10^6 histories. Dashed curves: asymptotic survival probabilities $\mathcal{S}_\infty$ from Eq. (4.72). Right. Survival probabilities $\mathcal{S}_g^{\pm}(x_0)$ for $p_0 = 0.2$, $p_1 = 0.3$, and $p_2 = 0.5$ ($\nu_1 = 1.3$, and $L_c = 3.9987$). Blue crosses and red circles: $\mathcal{S}_g^{+}(x_0)$ and $\mathcal{S}_g^{-}(x_0)$, respectively, with $x_0 = 1.75$ and $L = 2$ ($k < 1$). Green squares and black triangles: $\mathcal{S}_g^{+}(x_0)$ and $\mathcal{S}_g^{-}(x_0)$, respectively, with $x_0 = 3.75$ and $L = 6$ ($k > 1$). Solid lines are numerical integrals of Eq. (4.71), symbols Monte Carlo simulations with 10^6 histories. Dashed curves: asymptotic survival probabilities S_∞ from Eq. (4.72).

Equation (4.96) can be solved numerically by any root tracking algorithm, and in particular the dominant eigenvalue α can be easily determined to a high degree of accuracy. As such, the rod

model is ideally suited to test the Monte Carlo α-k power iteration detailed above. To proceed, we choose the following physical parameters: $\Sigma_s = 0.2$, $\Sigma_a = 0.1$, $\Sigma_f = 0.3$ and $v = 1$; we take two delayed groups ($m = 2$), with $\beta_1 = 0.003$, $\beta_2 = 0.0035$, $\lambda_1 = 0.2$ and $\lambda_2 = 0.05$. We illustrate then the results of Monte Carlo simulations as compared with the numerical solutions for the fundamental α eigenvalue stemming from Eq. (4.96). Simulations have been run with 10^6 particles per cycle over 2000 cycles, which for every choice of parameters examined here ensures a convergence of the order of a few pcm (after discarding the first 1000 cycles from inspection of the series $\alpha^{(g)}$).

As a first example, we study the evolution of α as a function of the domain size L, for a given $\nu_f = 2.5$: results are displayed in Fig. 4.2. For this example, the critical size is $L_c = 4.00886$ (from Eq. (4.100)), and for very large L the dominant eigenvalue approaches $\alpha_\infty = 0.34628$ (from Eq. (4.101)). In both cases, the Monte Carlo power iteration algorithm (displayed as symbols) neatly converges to the exact results (displayed in solid line). Then, we consider the evolution of the eigenvalue α as a function of the average number of neutrons per fission, ν_f. For this example, we set $L = 4$ and we make ν_f vary around the reference value $\nu_f = 2.5$ adopted in the previous example. Results are displayed in Fig. 4.3. The Monte Carlo power iteration algorithm (displayed as symbols) again neatly converges to the exact results (displayed in solid line).

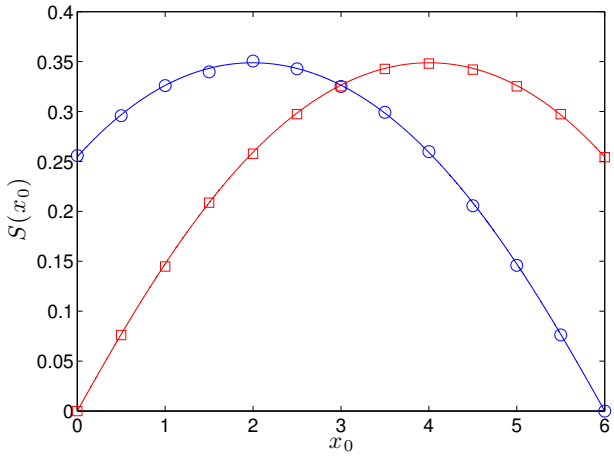

Figure 4.5: Ultimate survival probabilities $\mathcal{S}^{\pm}(x_0)$ for $\Sigma_a = 0.2$, $\Sigma_s = 0.3$, $\Sigma_f = 0.5$ and $\nu_f = 2$ ($L_c = 3.9987$). Blue circles and red squares: $\mathcal{S}^{+}(x_0)$ and $\mathcal{S}^{-}(x_0)$, respectively, with $L = 6$ ($\alpha > 0$). Solid lines are numerical integrals from Eq. (4.72), symbols Monte Carlo simulations with 10^6 histories.

4.6.2 Relation to survival probabilities

As explained in the previous Chapters, there exists a deep connection between the dominant eigenvalues of the Boltzmann operator and the survival probabilities of the underlying branching exponential flights. In particular, we have previously shown that when the dominant eigenvalue $\alpha < 0$ the survival probability asymptotically vanishes, namely, $\mathcal{S}_t \to 0$, and the branching exponential flights will come to extinction because of leakages and possibly absorptions; when on the contrary $\alpha > 0$, then $\mathcal{S}_t \to \mathcal{S}_\infty$, and there exists a finite non-trivial probability $\mathcal{S}_\infty > 0$ that branching exponential flights be persistent, as particles born from fission are not sufficiently compensated by leakages and absorptions. The crossover between these two regimes is reached for $\alpha = 0$, which

therefore defines the portion of the parameter space for which the branching process will attain ultimate extinction.

The survival probabilities for the rod model with leakage boundary conditions can be deduced from Eq. (4.68) and (4.71). For the sake of simplicity, we have here neglected the contributions due to delayed neutrons. These equations can be integrated numerically: in Fig. 4.4 we compare the resulting curves (as a function of time or generations, respectively) with Monte Carlo simulations for different configurations. In particular, once the physical properties of the system have been chosen, by varying the rod size L it is possible to impose $L < L_c$ or $L > L_c$. In the former case, the survival probabilities converge to zero independent of the starting direction, as expected, whereas in the latter the survival probabilities saturate to an asymptotic value $\mathcal{S}_\infty$ that depends on the starting point as well as on the initial direction of the walker.

Observe that $\mathcal{S}_t^+$ up to a time of the order of $\tau^+ \simeq |L - x_0|/v$ does not feel the effects of the boundaries, yet, and the same holds for S_t^- up to a time of the order of $\tau^- \simeq x_0/v$. Therefore, we expect $\mathcal{S}_t^+ \simeq \mathcal{S}_t^-$ up to $\min(\tau^+, \tau^-)$. For the configuration where $L > L_c$, the ultimate survival probability as a function of starting point and initial direction is displayed in Fig. 4.5.

Chapter 5

Stochastic populations

A large nation, of whom we will only concern ourselves with adult males, N in number, and who each bear separate surnames colonise a district. Their law of population is such that, in each generation, a_0 per cent of the adult males have no male children who reach adult life; a_1 have one such male child; a_2 have two; and so on up to a_5 who have five.
Find
(1) what proportion of their surnames will have become extinct after r generations; and (2) how many instances there will be of the surname being held by m persons.

H. W. Watson and F. Galton, J. Anthropol. Inst. Great Britain **4**, 138 (1875).

5.1 Introduction

In the previous Chapters, we have examined the statistical properties of the physical quantities related to a *single initial walker* among those composing the system under investigation. In this Chapter, we will focus of the *collective* behaviour of a collection $\mathcal{Q}$ of particles undergoing branching random walks in a region V. We will assume that N such individuals are initially present at $t_0 = 0$. In order to characterize the statistical properties of such a system, we are in principle interested in determining the full distribution of the events induced by the particles and recorded at multiple 'detectors' (i.e., at some portions of the viable phase space). In practice, it turns out that the first few moments of the event distribution convey most of the required information, which reduces the burden in calculations.

The relevant physical observables are thus *i*) the *average number of particles* that are found at a given detector located at V_i, namely, $\mathbb{E}_t[m_{V_i}|\mathcal{Q}]$, and *ii*) the *correlations between two detectors* located respectively at V_i and V_j, namely, $\mathbb{E}_t[m_{V_i} m_{V_j}|\mathcal{Q}]$, when the process is observed at a time $t > t_0$ (see Fig. 5.1).

The local particle concentration c at a site $\mathbf{x}_i$ is defined by centering the volume V_i at $\mathbf{x}_i$ and taking the volume size $V_i \to 0$, namely,

$$c_t(\mathbf{x}_i) = \lim_{V_i \to 0} \frac{\mathbb{E}_t[m_{V_i}|\mathcal{Q}]}{V_i}. \tag{5.1}$$

The quantity $c_t(\mathbf{x}_i)d\mathbf{x}_i$ represents by definition the average number of particles to be found in a small volume $d\mathbf{x}_i$ around position $\mathbf{x}_i$ at time t. The local correlations h between a site $\mathbf{x}_i$ and a site

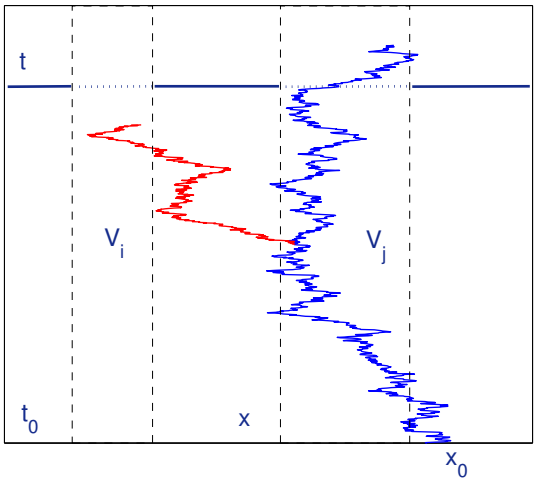

Figure 5.1: Example of realization of a branching Brownian motion in one dimension. A single walker starts to diffuse from position x_0 at time $t_0 = 0$. At a later time, a branching event occurs, and a new independent Brownian motion starts to diffuse. At the observation time t, one of the two walkers is found in the region V_j, whereas the other has been absorbed at an earlier time and does not contribute to the counting process.

$\mathbf{x}_j$ are similarly defined by centering the volume V_i at $\mathbf{x}_i$ and the volume V_j at $\mathbf{x}_j$, respectively, and taking $V_i \to 0$ and $V_j \to 0$, namely,

$$h_t(\mathbf{x}_i, \mathbf{x}_j) = \lim_{\substack{V_i \to 0 \\ V_j \to 0}} \frac{\mathbb{E}_t[m_{V_i} m_{V_j} | \mathcal{Q}]}{V_i V_j}. \tag{5.2}$$

The quantity $h_t(\mathbf{x}_i, \mathbf{x}_j) d\mathbf{x}_i d\mathbf{x}_j$ is proportional to the probability of finding *a pair of particles* whose first member has coordinates $\mathbf{x}_i$ and the second has coordinates $\mathbf{x}_j$ at time t. Actually, it is customary to introduce the (dimensionless) normalized and centered pair correlation function g, which is obtained from h by subtracting the product of the concentrations and the self-correlation and by dividing by the product of the concentrations [53, 116], namely,

$$g_t(\mathbf{x}_i, \mathbf{x}_j) = \frac{h_t(\mathbf{x}_i, \mathbf{x}_j) - c_t(\mathbf{x}_i) c_t(\mathbf{x}_j) - \delta(\mathbf{x}_i - \mathbf{x}_j) c_t(\mathbf{x}_i)}{c_t(\mathbf{x}_i) c_t(\mathbf{x}_j)}. \tag{5.3}$$

The evolution equations for these physical observables can be derived by resorting to either forward or backward formalism [4, 32, 34, 36]. Here, we will establish the evolution equations for the first two moments by suitable extending the backward formalism discussed in the previous Chapter. The key result is that the solutions of the resulting equations can be formally obtained in terms of the Green's function.

5.2 Coincidence detection

In order to fix the ideas, in the following we will assume that each walker undergoes a d-dimensional branching Brownian motion with absorption rate γ, reproduction rate β and diffusion

coefficient D. We assume that reproduction is governed by a regular Galton-Watson process: the particle disappears and is replaced by a random number k of identical and independent descendants, distributed according to the probability p_k and behaving as the parent particle [28, 29, 33].

Consider first a single walker starting from position $\mathbf{x}_0$ at time $t_0 = 0$. Let $m_{V_i} = m_{V_i}(\mathbf{x}_0, t)$ be the number of particles that are found in a volume $V_i \subseteq V$ of the viable space when the process is observed at a time $t > t_0$. We are interested in determining the simultaneous detection probability $\mathcal{P}_t(m_{V_i}, m_{V_j}|\mathbf{x}_0)$ of finding m_{V_i} particles in volume $V_i \subseteq V$ and m_{V_j} particles in volume $V_j \subseteq V$, at time t, for a single particle starting at $\mathbf{x}_0$ at time t_0. It is convenient to introduce the associated two-volume probability generating function

$$W_t(u_i, u_j|\mathbf{x}_0) = \mathbb{E}[u_i^{m_{V_i}(\mathbf{x}_0,t)} u_j^{m_{V_j}(\mathbf{x}_0,t)}], \tag{5.4}$$

from which the m-th (factorial) moments of m_{V_i} and m_{V_j} can be obtained by derivation with respect to u_i and u_j, respectively. In particular, the average particle number reads

$$\mathbb{E}_t[m_{V_i}|\mathbf{x}_0] = \frac{\partial}{\partial u_i} W_t(u_i, u_j|\mathbf{x}_0)|_{u_i=1,u_j=1}. \tag{5.5}$$

For the two-volume correlations we take the mixed derivative, namely,

$$\mathbb{E}_t[m_{V_i} m_{V_j}|\mathbf{x}_0] = \frac{\partial^2}{\partial u_i \partial u_j} W_t(u_i, u_j|\mathbf{x}_0)|_{u_i=1,u_j=1}. \tag{5.6}$$

By generalizing the arguments used in the previous Chapter, it can be shown that $W_t(u_i, u_j|\mathbf{x}_0)$ satisfies again the backward equation

$$\frac{\partial}{\partial t} W_t = D\nabla^2_{\mathbf{x}_0} W_t - (\gamma + \beta) W_t + \gamma + \beta G[W_t], \tag{5.7}$$

identical to Eq. (4.22). By taking the derivative of Eq. (5.7) once we get the equation for the average particle number

$$\frac{\partial}{\partial t} \mathbb{E}_t[m_{V_i}|\mathbf{x}_0] = \mathcal{L}^\dagger_{\mathbf{x}_0} \mathbb{E}_t[m_{V_i}|\mathbf{x}_0], \tag{5.8}$$

where we have used the backward operator $\mathcal{L}^\dagger_{\mathbf{x}_0}$

$$\mathcal{L}^\dagger_{\mathbf{x}_0} = D\nabla^2_{\mathbf{x}_0} - \gamma + \beta(\nu_1 - 1), \tag{5.9}$$

and $\nu_1 = \sum_k k p_k$. Equation (5.8) must be solved together with the initial condition $\mathbb{E}_0[m_{V_i}|\mathbf{x}_0] = \mathbb{1}_{V_i}(\mathbf{x}_0)$.

As for the correlations, by taking the mixed derivative of Eq. (5.7) we obtain

$$\frac{\partial}{\partial t} \mathbb{E}_t[m_{V_i} m_{V_j}|\mathbf{x}_0] = \mathcal{L}^\dagger_{\mathbf{x}_0} \mathbb{E}_t[m_{V_i} m_{V_j}|\mathbf{x}_0] + \beta\nu_2 \mathbb{E}_t[m_{V_i}|\mathbf{x}_0] \mathbb{E}_t[m_{V_j}|\mathbf{x}_0], \tag{5.10}$$

where $\nu_2 = \sum_k k(k-1)p_k$. Equation (5.10) must be solved together with the initial condition $\mathbb{E}_0[m_{V_i} m_{V_j}|\mathbf{x}_0] = \mathbb{1}_{V_i}(\mathbf{x}_0)\mathbb{1}_{V_j}(\mathbf{x}_0)$.

Let us now introduce the Green's function $\mathcal{G}_t(\mathbf{x}; \mathbf{x}_0)$ satisfying the backward equation

$$\frac{\partial}{\partial t} \mathcal{G}_t(\mathbf{x}; \mathbf{x}_0) = \mathcal{L}^\dagger_{\mathbf{x}_0} \mathcal{G}_t(\mathbf{x}; \mathbf{x}_0), \tag{5.11}$$

with $\mathcal{G}_0(\mathbf{x}; \mathbf{x}_0) = \delta(\mathbf{x} - \mathbf{x}_0)$ and the boundary conditions of the problem at hand. Then, by closely following the same strategy as in the previous Chapters, for the average particle number we get

$$\mathbb{E}_t[m_{V_i}|\mathbf{x}_0] = \int_{V_i} d\mathbf{x}' \mathcal{G}_t(\mathbf{x}'; \mathbf{x}_0). \tag{5.12}$$

As for the correlations, we find

$$\mathbb{E}_t[m_{V_i} m_{V_j}|\mathbf{x}_0] = \int_{V_i\cap V_j} d\mathbf{x}' \mathcal{G}_t(\mathbf{x}';\mathbf{x}_0) + \beta\nu_2 \int_0^t dt' \int_V d\mathbf{x}' \mathcal{F}_{t'}(V_i, V_j, \mathbf{x}') \mathcal{G}_{t-t'}(\mathbf{x}';\mathbf{x}_0), \tag{5.13}$$

where $V_i \cap V_j$ denotes the intersection of V_i and V_j and we have set

$$\mathcal{F}_t(V_i, V_j, \mathbf{x}) = \int_{V_i} d\mathbf{x}' \mathcal{G}_t(\mathbf{x}';\mathbf{x}) \int_{V_j} d\mathbf{x}'' \mathcal{G}_t(\mathbf{x}'';\mathbf{x}). \tag{5.14}$$

5.3 From one-particle to N-particle observables

Let us now consider a collection $\mathcal{Q}$ of N such individuals initially located at $\mathbf{x}_0^1$, $\mathbf{x}_0^2$, $\mathbf{x}_0^3$, $\cdots$, $\mathbf{x}_0^N$ with density $Q(\mathbf{x}_0^1, \mathbf{x}_0^2, \cdots, \mathbf{x}_0^N)$ at time $t_0 = 0$. Since particles evolve independently of each other, the contributions of each particle to the counting process $m_{V_i} = m_{V_i}(\mathbf{x}_0^1, \mathbf{x}_0^2, \mathbf{x}_0^3, \cdots, \mathbf{x}_0^N, t)$ are additive, and the probability generating function satisfies

$$W_t(u_i, u_j|\mathbf{x}_0^1, \mathbf{x}_0^2, \cdots, \mathbf{x}_0^N) = \prod_{k=1}^N W_t(u_i, u_j|\mathbf{x}_0^k). \tag{5.15}$$

Suppose that the initial positions are independently and identically distributed and obey the factorized density

$$Q(\mathbf{x}_0^1, \mathbf{x}_0^2, \cdots, \mathbf{x}_0^N) = \prod_{k=1}^N q(\mathbf{x}_0^k). \tag{5.16}$$

The corresponding probability generating function $W_t(u_i, u_j|\mathcal{Q})$ satisfies then

$$W_t(u_i, u_j|\mathcal{Q}) = \prod_{k=1}^N \int_V d\mathbf{x}_0^k q(\mathbf{x}_0^k) W_t(u_i, u_j|\mathbf{x}_0^k), \tag{5.17}$$

which can be finally rewritten as

$$W_t(u_i, u_j|\mathcal{Q}) = \langle W_t(u_i, u_j|\mathbf{x}_0)\rangle_q^N, \tag{5.18}$$

where we have denoted $\langle f(\mathbf{x}_0)\rangle_q = \int_V d\mathbf{x}_0 q(\mathbf{x}_0) f(\mathbf{x}_0)$ the average over the distribution of the initial coordinates.

The moments of the N-particle observables can be again obtained as above. In particular, for the average particle number we get

$$\mathbb{E}_t[m_{V_i}|\mathcal{Q}] = N \langle \mathbb{E}_t[m_{V_i}|\mathbf{x}_0]\rangle_q. \tag{5.19}$$

Hence, from Eqs. (5.19) and (5.1) we obtain the local concentration

$$\boxed{c_t(\mathbf{x}_i) = N \int_V d\mathbf{x}_0 q(\mathbf{x}_0) \mathcal{G}_t(\mathbf{x}_i;\mathbf{x}_0),} \tag{5.20}$$

where we have used $\mathbb{1}_{V_i}(\mathbf{x})/V_i \to \delta(\mathbf{x}-\mathbf{x}_i)$. Equation (5.20) basically expresses a linear superposition of effects from single-particle contributions.

As for the correlations, we have

$$\mathbb{E}_t[m_{V_i} m_{V_j}|\mathcal{Q}] = N(N-1)\langle \mathbb{E}_t[m_{V_i}|\mathbf{x}_0]\rangle_q \langle \mathbb{E}_t[m_{V_j}|\mathbf{x}_0]\rangle_q + N\langle \mathbb{E}_t[m_{V_i} m_{V_j}|\mathbf{x}_0]\rangle_q. \tag{5.21}$$

Hence, from Eqs. (5.21) and (5.2) we obtain

$$h_t(\mathbf{x}_i,\mathbf{x}_j) = \frac{N(N-1)}{N^2} c_t(\mathbf{x}_i)c_t(\mathbf{x}_j) + \delta(\mathbf{x}_i-\mathbf{x}_j)c_t(\mathbf{x}_i) + \beta\nu_2 \int_0^t dt' \int_V d\mathbf{x}' \mathcal{G}_{t'}(\mathbf{x}_i;\mathbf{x}')\mathcal{G}_{t'}(\mathbf{x}_j;\mathbf{x}')c_{t-t'}(\mathbf{x}'), \tag{5.22}$$

where we have used

$$\lim_{\substack{V_i\to 0\\ V_j\to 0}} \frac{\mathcal{F}_t(V_i,V_j,\mathbf{x})}{V_iV_j} = \mathcal{G}_t(\mathbf{x}_i;\mathbf{x})\mathcal{G}_t(\mathbf{x}_j;\mathbf{x}). \tag{5.23}$$

For $N \gg 1$, $g_t(\mathbf{x}_i,\mathbf{x}_j)$ reads then

$$\boxed{g_t(\mathbf{x}_i,\mathbf{x}_j) = \frac{\beta\nu_2}{c_t(\mathbf{x}_i)c_t(\mathbf{x}_j)} \int_0^t dt' \int_V d\mathbf{x}' \mathcal{G}_{t'}(\mathbf{x}_i;\mathbf{x}')\mathcal{G}_{t'}(\mathbf{x}_j;\mathbf{x}')c_{t-t'}(\mathbf{x}').} \tag{5.24}$$

Equation (5.24) represents the (normalized) contributions to the correlations due to particles freely evolving from t_0 to $t-t'$, having a branching event in $\mathbf{x}'$ and whose descendants independently reach the points $\mathbf{x}_i$ and $\mathbf{x}_j$ at time t. Observe that when $\beta = 0$ the normalized pair correlation function g vanishes, which denotes the absence of correlations between particle positions in the absence of branching. Deviations of g from zero are the signature of strong non-Poissonian fluctuations induced by the reproduction-disappearance mechanism [42,53]. When $g \geq 1$, fluctuations are of the same order of magnitude as the concentration, which means that the information conveyed in the concentration alone (i.e., a purely deterministic approach) is useless.

5.3.1 Variance-to-mean ratio

The pair correlation function g provides local information about the fluctuations. A useful integral estimator so as to assess the entity of the fluctuations with respect to the average in a given region V_i is the so-called *variance-to-mean ratio* χ [4,32,222], which is defined as

$$\chi = \frac{\mathbb{E}_t[n_{V_i}^2|\mathcal{Q}] - \mathbb{E}_t[n_{V_i}|\mathcal{Q}]^2}{\mathbb{E}_t[n_{V_i}|\mathcal{Q}]}. \tag{5.25}$$

By replacing the definitions of $\mathbb{E}_t[n_{V_i}^2|\mathcal{Q}]$ and $\mathbb{E}_t[n_{V_i}|\mathcal{Q}]$, when $N \gg 1$ the variance-to-mean ratio can be expressed in terms of the Green's function, namely,

$$\chi = 1 + \beta\nu_2 \frac{\int_0^t dt' \left\langle \int_V d\mathbf{x}' \mathcal{F}_{t'}(V_i,V_i,\mathbf{x}')\mathcal{G}_{t-t'}(\mathbf{x}';\mathbf{x}_0)\right\rangle_q}{\left\langle \int_{V_i} d\mathbf{x}' \mathcal{G}_t(\mathbf{x}';\mathbf{x}_0)\right\rangle_q}.$$

Observe that in the absence of reproduction events ($\beta = 0$) the variance-to-mean ratio is identically equal to unit (i.e., fluctuations are Poissonian), which follows from the particle histories being uncorrelated. A departure from unit is the signature of non-Poissonian fluctuations due to correlations [51–53]. In the context of reactor physics, the variance-to-mean ratio is intimately related to the so-called Feynman alpha method [223], which is used for the analysis of the correlations in neutron detectors due to fission chains [4,32].

5.4 Other kinds of sources

In many practical applications, the initial number of particles is not known in advance and is itself a random quantity M, with distribution $\mathcal{Z}(M)$. Assuming again independent and identically distributed coordinates $\mathbf{x}_0^k$, $k = 1, 2, \cdots, M$, Eq. (5.17) can be then generalized by averaging over the realizations of M, namely,

$$W_t(u_i, u_j|\mathcal{Z}) = \sum_M \mathcal{Z}(M) \prod_{k=1}^{M} \int_V d\mathbf{x}_0^k q(\mathbf{x}_0^k) W_t(u_i, u_j|\mathbf{x}_0^k). \tag{5.26}$$

Often, the initial configuration is assumed to be a Poisson point process [26, 32], which means that the total number M of starting particles obeys a Poisson distribution, i.e.,

$$\mathcal{Z}(M) = \frac{\mu^M}{M!} e^{-\mu}, \tag{5.27}$$

where $\mu = \mathbb{E}[M]$ is the average number of source particles. In this case, using the independence property as above, the sum in Eq. (5.26) can be explicitly carried out, which yields

$$W_t(u_i, u_j|\mathcal{Z}) = \exp\left(\mu \left\langle W_t(u_i, u_j|\mathbf{x}_0) - 1 \right\rangle_q\right). \tag{5.28}$$

This result takes the name of Campbell's theorem [26]. In particular, if we choose $\mu = N$, by taking the derivatives of the probability generating function the average particle number would be left unchanged with respect to the case of fixed N (as expected), namely, $\mathbb{E}_t[n_{V_i}|\mathcal{Q}_Q] = \mathbb{E}_t[n_{V_i}|\mathcal{Q}]$. As for the correlations, $\mathbb{E}_t[n_{V_i} n_{V_j}|\mathcal{Q}_Q]$ would be still given by Eq. (5.21), provided that the factor $N(N-1)$ is replaced by N^2: this means that the correlations associated to a Poisson point source with $\mu = N$ would appreciably differ from those associated to a source with a fixed number N of particles only when N is relatively small.

5.5 Fluctuations around equilibrium

Once the Green's function $\mathcal{G}_t(\mathbf{x}; \mathbf{x}_0)$ of the problem has been determined, then by integration Eqs. (5.20) and (5.24) allow explicitly characterizing the evolution of the particle concentration and of the correlations of the particle number, respectively. Formulas (5.20) and (5.24) hold for any geometries and spatial source distributions, and can accommodate arbitrary boundary and initial conditions (which affect the shape of $\mathcal{G}_t(\mathbf{x}; \mathbf{x}_0)$). A situation of particular interest is that of individuals prepared *at equilibrium* with respect to the spatial variable at time $t_0 = 0$.

5.5.1 Thermodynamic limit

The so-called *thermodynamic limit* is attained by considering a large number N of particles in a large volume V, and imposing that the particle density

$$\mathcal{C} = \lim_{\substack{N\to\infty \\ V\to\infty}} \frac{N}{V} \tag{5.29}$$

is finite [42, 44, 51–53]. The Green's function for a d-dimensional infinite system is the Gaussian density

$$\mathcal{G}_t(\mathbf{x}; \mathbf{x}_0) = \frac{e^{-\frac{r^2}{4Dt} + [\beta(\nu_1 - 1) - \gamma]t}}{(4\pi D t)^{d/2}}, \tag{5.30}$$

which spatially depends only on the relative particle distance $r = |\mathbf{x} - \mathbf{x}_0|$. As for the spatial density of the source particles, equilibrium imposes the uniform distribution $q^{\mathrm{eq}}(\mathbf{x}_0) = 1/V$. From Eq. (5.20), the concentration then reads

$$c_t^{\infty}(\mathbf{x}_i) = \lim_{\substack{N\to\infty \\ V\to\infty}} c_t^{\mathrm{eq}}(\mathbf{x}_i) = \mathcal{C} e^{[\beta(\nu_1-1)-\gamma]t}, \tag{5.31}$$

where we have used the normalization of the Gaussian density. When reproduction is exactly compensated by absorption, i.e., $\gamma = \beta(\nu_1 - 1)$, the system is said to be *critical* and the concentration is stationary, namely, $c_t^{\infty}(\mathbf{x}_i) = \mathcal{C}$. As for the pair correlation function, from Eq. (5.24) we get

$$g_t^{\infty}(r) = \lim_{\substack{N\to\infty \\ V\to\infty}} g_t^{\mathrm{eq}}(\mathbf{x}_i, \mathbf{x}_j) = \frac{\beta\nu_2}{\mathcal{C}} e^{[\gamma-\beta(\nu_1-1)]t} \int_0^t dt' \frac{e^{-\frac{r^2}{8Dt'}+[\beta(\nu_1-1)-\gamma]t'}}{(8\pi D t')^{d/2}}, \tag{5.32}$$

and we recover the result previously obtained in [53]. In particular, for exactly critical systems with $\gamma = \beta(\nu_1 - 1)$ the integral in the pair correlation function can be carried out explicitly [53], and yields

$$g_t^{\infty}(r) = \frac{\beta\nu_2}{8\pi^{d/2} D\mathcal{C}} r^{2-d} \Gamma_{d/2-1}\left(\frac{r^2}{8Dt}\right), \tag{5.33}$$

where $\Gamma_a(z) = \int_z^{\infty} e^{-u} u^{a-1} du$ is the incomplete Gamma function [224]. The asymptotic time behaviour of Eq. (5.33) depends on the dimension d: it is known that $g_t^{\infty}(r) \sim \sqrt{t}$ for $d = 1$, $g_t^{\infty}(r) \sim \log(t)$ for $d = 2$, and $g_t^{\infty}(r) \sim$ const for $d > 2$ [53].

5.5.2 Confined geometries

We will now focus on particles evolving in confined geometries, whose analysis can be carried out by resorting to the eigenfunction expansion of the Green's function. Generally speaking, when the domain V is open, bounded and connected it is possible to solve for the Green's function of Eq. (5.11) by evoking the separation of variables [191]. If this is the case, then the Green's function $\mathcal{G}_t(\mathbf{x}; \mathbf{x}_0)$ can be expanded in terms of a discrete sum of eigenfunctions $\varphi_{\mathbf{k}}$ of the operator $\mathcal{L}^{\dagger}_{\mathbf{x}_0}$ [191], in the form

$$\mathcal{G}_t(\mathbf{x}; \mathbf{x}_0) = \sum_{\mathbf{k}} \varphi_{\mathbf{k}}(\mathbf{x}) \varphi_{\mathbf{k}}(\mathbf{x}_0) e^{\alpha_{\mathbf{k}} t}, \tag{5.34}$$

where $\alpha_{\mathbf{k}}$ are the associated eigenvalues [191], depending on the physical parameters and on the boundary conditions at ∂V. We assume that such expansion is complete, which means that

$$\sum_{\mathbf{k}} \varphi_{\mathbf{k}}(\mathbf{x}) \varphi_{\mathbf{k}}(\mathbf{x}_0) = \delta(\mathbf{x} - \mathbf{x}_0), \tag{5.35}$$

and that the eigenvalues can be ordered so that $\alpha_{\mathbf{0}} > |\alpha_{\mathbf{1}}| \geq \cdots \geq |\alpha_{\mathbf{k}}| \geq \cdots$. The functions $\varphi_{\mathbf{k}}(\mathbf{x})$ and $\varphi_{\mathbf{k}}(\mathbf{x}_0)$ satisfy the boundary conditions and are ortho-normal, with

$$\int d\mathbf{x}' \varphi_{\mathbf{k}_i}(\mathbf{x}') \varphi_{\mathbf{k}_j}(\mathbf{x}') = \delta_{\mathbf{k}_i, \mathbf{k}_j}. \tag{5.36}$$

The eigenvalues and the eigenfunctions depend on the specific boundary conditions. In most physical applications, one is often led to consider either (perfectly) reflecting or absorbing boundaries: in the former case, individuals reaching the walls bounce off and their trajectories are otherwise undisturbed (Neumann boundary condition); in the latter, individuals hitting the boundaries leak

out and are thus lost (Dirichlet boundary condition). Neumann boundary condition would be representative, e.g., of neutrons multiplication in the presence of highly scattering shielding barriers, such as beryllium or heavy water [30], or the evolution of a bacterial colony confined on a Petri box with impermeable walls [52]. Absorbing boundaries are frequently met in radiation transport when the diffusing particles are free to escape upon crossing the external surface (the so-called geometrical leakage) [30].

5.5.3 Concentration and correlation function at equilibrium

Assuming that the individuals are prepared at equilibrium basically amounts to sampling the initial N-particle distribution on the fundamental spatial eigenstate of this system. In this case, we have $q^{\mathrm{eq}}(\mathbf{x}_0) \propto \varphi_{\mathbf{0}}(\mathbf{x}_0)$, and we obtain

$$c_t^{\mathrm{eq}}(\mathbf{x}_i) = N q^{\mathrm{eq}}(\mathbf{x}_i) e^{\alpha_{\mathbf{0}} t}, \tag{5.37}$$

where $\alpha_{\mathbf{0}}$ is the fundamental eigenvalue. Then, the spatial shape of the concentration would not vary, namely, $c_t(\mathbf{x}_i) \propto q^{\mathrm{eq}}(\mathbf{x}_i)$, and its amplitude would evolve exponentially in time, with a rate $\alpha_{\mathbf{0}}$. The sign of the fundamental eigenvalue $\alpha_{\mathbf{0}}$ determines the asymptotic behaviour of the concentration: when $\alpha_{\mathbf{0}} > 0$ the population diverges in time and the system is said to be supercritical; when $\alpha_{\mathbf{0}} < 0$ the population shrinks to zero and the system is said to be subcritical. When $\alpha_{\mathbf{0}} = 0$, the system is said to be critical and the concentration simplifies to

$$c_t^{\mathrm{eq}}(\mathbf{x}_i) = N q^{\mathrm{eq}}(\mathbf{x}_i), \tag{5.38}$$

which means that, once prepared in the fundamental eigenstate, the system will stay in that eigenstate (on average). Nuclear systems are typically operated at or close to the critical regime $\alpha_{\mathbf{0}} = 0$, so as to have a constant power output [32].

Concerning the pair correlation function, when the initial configuration is sampled on the fundamental eigenstate, from Eq. (5.24) we get

$$g_t^{\mathrm{eq}}(\mathbf{x}_i, \mathbf{x}_j) = \frac{\beta \nu_2 e^{-\alpha_{\mathbf{0}} t}}{N q^{\mathrm{eq}}(\mathbf{x}_i) q^{\mathrm{eq}}(\mathbf{x}_j)} \int_0^t dt' e^{-\alpha_{\mathbf{0}} t'} \int_V d\mathbf{x}' q^{\mathrm{eq}}(\mathbf{x}') \mathcal{G}_{t'}(\mathbf{x}_i; \mathbf{x}') \mathcal{G}_{t'}(\mathbf{x}_j; \mathbf{x}'). \tag{5.39}$$

Then, by using the eigenfunction expansion of the Green's functions and explicitly performing the time integral we are led to

$$g_t^{\mathrm{eq}}(\mathbf{x}_i, \mathbf{x}_j) = \frac{\beta \nu_2 e^{-\alpha_{\mathbf{0}} t}}{N q^{\mathrm{eq}}(\mathbf{x}_i) q^{\mathrm{eq}}(\mathbf{x}_j)} \sum_{\mathbf{k}_i, \mathbf{k}_j} \frac{e^{(\alpha_{\mathbf{k}_i} + \alpha_{\mathbf{k}_j} - \alpha_{\mathbf{0}}) t} - 1}{\alpha_{\mathbf{k}_i} + \alpha_{\mathbf{k}_j} - \alpha_{\mathbf{0}}} A_{\mathbf{k}_i, \mathbf{k}_j} \varphi_{\mathbf{k}_i}(\mathbf{x}_i) \varphi_{\mathbf{k}_j}(\mathbf{x}_j), \tag{5.40}$$

where the coefficients $A_{\mathbf{k}_i, \mathbf{k}_j}$ are given by

$$A_{\mathbf{k}_i, \mathbf{k}_j} = \int_V d\mathbf{x}' q^{\mathrm{eq}}(\mathbf{x}') \varphi_{\mathbf{k}_i}(\mathbf{x}') \varphi_{\mathbf{k}_j}(\mathbf{x}'). \tag{5.41}$$

Equation (5.40) has a fairly involved structure: in order to get some physical insight on the behaviour of the pair correlation function in bounded domains, it is convenient to perform a frequency analysis in the Laplace domain [4], namely,

$$g_s^{\mathrm{eq}}(\mathbf{x}_i, \mathbf{x}_j) = \int_0^\infty e^{-st} g_t^{\mathrm{eq}}(\mathbf{x}_i, \mathbf{x}_j) dt. \tag{5.42}$$

Without loss of generality, we can single out the fundamental mode, from which stems

$$g_s^{\mathrm{eq}}(\mathbf{x}_i,\mathbf{x}_j)=\frac{\beta\nu_2}{Nq^{\mathrm{eq}}(\mathbf{x}_i)q^{\mathrm{eq}}(\mathbf{x}_j)}\frac{1}{\alpha_{\mathbf{0}}+s}\frac{1}{s}\times \\ \Big[A_{\mathbf{0},\mathbf{0}}\varphi_{\mathbf{0}}(\mathbf{x}_i)\varphi_{\mathbf{0}}(\mathbf{x}_j)+s\sum_{\mathbf{k}_i,\mathbf{k}_j\neq\mathbf{0}}\frac{A_{\mathbf{k}_i,\mathbf{k}_j}}{2\alpha_{\mathbf{0}}-\alpha_{\mathbf{k}_i}-\alpha_{\mathbf{k}_j}+s}\varphi_{\mathbf{k}_i}(\mathbf{x}_i)\varphi_{\mathbf{k}_j}(\mathbf{x}_j)\Big]. \tag{5.43}$$

As expected on physical grounds, the overall intensity of the correlations is inversely proportional to the number of particles contained in the volume. The pre-factor $1/[(\alpha_{\mathbf{0}}+s)s]$ determines the ultimate fate of the pair correlation function at long times (small s), and depends on the rate $\alpha_{\mathbf{0}}$ at which the average population is increasing or decreasing. When the system is supercritical, i.e., $\alpha_{\mathbf{0}}>0$, upon taking the inverse Laplace transform the pair correlation function for long times asymptotically converges to the constant

$$g_{t\to\infty}^{\mathrm{eq}}(\mathbf{x}_i,\mathbf{x}_j)\to\frac{\beta\nu_2}{N\alpha_{\mathbf{0}}}\mathcal{M}, \tag{5.44}$$

where

$$\mathcal{M}=A_{\mathbf{0},\mathbf{0}}\frac{\varphi_{\mathbf{0}}(\mathbf{x}_i)\varphi_{\mathbf{0}}(\mathbf{x}_j)}{q^{\mathrm{eq}}(\mathbf{x}_i)q^{\mathrm{eq}}(\mathbf{x}_j)} \tag{5.45}$$

is a normalization factor. This means that fluctuations will be equally distributed at any spatial scale. In the supercritical regime, the average population is exponentially increasing at a rate $\alpha_{\mathbf{0}}$, thus contributing to the mixing of the individuals: for sufficiently large N one typically expects the amplitude of the pair correlation function to be $g\ll 1$, and fluctuations to be safely neglected. However, it may still happen that $g\geq 1$, when the number of initial particles is $N\ll\beta\nu_2\mathcal{M}/\alpha_{\mathbf{0}}$. This can be understood as a competition between the growth rate $\alpha_{\mathbf{0}}$ of the average population and the growth rate $\beta\nu_2$ of branching-induced fluctuations: if $\alpha_{\mathbf{0}}$ is rather small, strong correlations may have enough time to develop, despite the smoothing effect induced by the appearance of an increasing number of new particles. When the system is subcritical, i.e., $\alpha_{\mathbf{0}}<0$, the pair correlation function at long times grows unbounded exponentially fast, as $g_{t\to\infty}^{\mathrm{eq}}(\mathbf{x}_i,\mathbf{x}_j)\sim\exp(-\alpha_{\mathbf{0}}t)$: for negative $\alpha_{\mathbf{0}}$, the average population is rapidly decreasing, which enhances the relative importance of fluctuations due to correlations. When the system is exactly critical, the pair correlation function asymptotically diverges with a linear scaling in time, namely,

$$g_{t\to\infty}^{\mathrm{eq}}(\mathbf{x}_i,\mathbf{x}_j)\sim\frac{\beta\nu_2}{N}\mathcal{M}t. \tag{5.46}$$

This linear scaling reflects the nature of the underlying Galton-Watson birth-death mechanism: when $\alpha_{\mathbf{0}}=0$ a collection of N individuals will go to extinction ($g\geq 1$) over a typical time $\sim N/(\beta\nu_2)$ [51, 53, 199].

The features displayed here are the signature of systems composed of a finite number of individuals in bounded geometries. The coefficients $A_{\mathbf{k}_i,\mathbf{k}_j}/(2\alpha_{\mathbf{0}}-\alpha_{\mathbf{k}_i}-\alpha_{\mathbf{k}_j}+s)$ determine the relevance of the contributions of higher-order eigenfunctions to the spatial behaviour of the pair correlation function: we expect fluctuations to become spatially flat after the mixing time required by the particles to diffuse over the characteristic (finite) system size.

5.5.4 Reflecting boundaries

For reflecting (Neumann) boundary conditions the fundamental eigenstate is spatially flat [191], and the associated fundamental eigenvalue is

$$\alpha_{\mathbf{0}}=-\gamma+\beta(\nu_1-1). \tag{5.47}$$

Thus, if we choose $p^{\text{eq}}(\mathbf{x}_0) = 1/V$, from Eq. (5.37) for the concentration we would simply have

$$c_t^{\text{eq}}(\mathbf{x}_i) = \frac{N}{V} e^{\alpha_{\mathbf{0}} t}. \tag{5.48}$$

At criticality, $c_t^{\text{eq}}(\mathbf{x}_i) = N/V$. As for the pair correlation function, from Eq. (5.39) we obtain

$$g_t^{\text{eq}}(\mathbf{x}_i, \mathbf{x}_j) = \beta \nu_2 \frac{V}{N} e^{-\alpha_{\mathbf{0}} t} \int_0^t dt' e^{-\alpha_{\mathbf{0}} t'} \mathcal{G}_{2t'}(\mathbf{x}_i; \mathbf{x}_j), \tag{5.49}$$

where we have used the Markov property of the Green's functions, namely,

$$\int d\mathbf{x}' \mathcal{G}_t(\mathbf{x}_i; \mathbf{x}') \mathcal{G}_t(\mathbf{x}_j; \mathbf{x}') = \mathcal{G}_{2t}(\mathbf{x}_i; \mathbf{x}_j). \tag{5.50}$$

By resorting to the eigenfunction expansion, we get

$$g_t^{\text{eq}}(\mathbf{x}_i, \mathbf{x}_j) = \beta \nu_2 \frac{V}{N} e^{-\alpha_{\mathbf{0}} t} \sum_{\mathbf{k}} \frac{e^{(2\alpha_{\mathbf{k}} - \alpha_{\mathbf{0}})t} - 1}{2\alpha_{\mathbf{k}} - \alpha_{\mathbf{0}}} \varphi_{\mathbf{k}}(\mathbf{x}_i) \varphi_{\mathbf{k}}(\mathbf{x}_j), \tag{5.51}$$

which we could have directly derived from Eq. (5.40) by imposing ortho-normality, i.e.,

$$A_{\mathbf{k}_i, \mathbf{k}_j} = \frac{\delta_{\mathbf{k}_i, \mathbf{k}_j}}{V}. \tag{5.52}$$

By singling out the fundamental mode and passing to the Laplace transform, from Eq. (5.51) we have

$$g_s^{\text{eq}}(\mathbf{x}_i, \mathbf{x}_j) = \frac{\beta \nu_2}{N} \frac{1}{\alpha_{\mathbf{0}} + s} \frac{1}{s} \Big[1 + s \sum_{\mathbf{k} \neq \mathbf{0}} \frac{V}{2\alpha_{\mathbf{0}} - 2\alpha_{\mathbf{k}} + s} \varphi_{\mathbf{k}}(\mathbf{x}_i) \varphi_{\mathbf{k}}(\mathbf{x}_j) \Big]. \tag{5.53}$$

Part III

Applications to radiation transport

Chapter 6

Opacity of bounded media: Cauchy's formulas

Les jeux & les questions de conjecture ne roulent ordinairement que sur des rapports de quantités discrètes ; l'esprit humain plus familier avec les nombres qu'avec les mesures de l'étendue les a toujours préférés ; les jeux en sont une preuve, car leurs loix sont une arithmétique continuelle ; pour mettre donc la Géométrie en possession de ses droits sur la science du hasard, il ne s'agit que d'inventer des jeux qui roulent sur l'étendue & sur ces rapports [...] ; le jeu du franc-carreau peut nous servir d'exemple.

Georges-Louis Leclerc, compte de Buffon, *Essai d'arithmétique morale* (1778).

6.1 Introduction

In the previous Chapters, we have provided a general approach to the analysis of the length ℓ_V travelled by a walker within a domain V and to the number of visits n_V of the walker to the domain, for a single starting particle. In the following, we will show that when branching random flights evolve within confined geometries it is possible to derive a set of remarkably simple *Cauchy-like formulas* relating the surface and volume averages of $L = \mathbb{E}[\ell_V]$ and $N = \mathbb{E}[n_V]$, namely,

$$\langle L \rangle_S = \eta_d \frac{V}{S} \left[1 + \frac{p_s + \nu_1 p_f - 1}{\langle l \rangle} \langle L \rangle_V \right] \tag{6.1}$$

$$\langle N \rangle_S = \frac{\eta_d}{\langle l \rangle} \frac{V}{S} \left[1 + (p_s + \nu_1 p_f - 1) \langle N \rangle_V \right]. \tag{6.2}$$

Here, $\mathbb{E}[\cdot]$ denotes the ensemble average over realizations, $\langle \cdot \rangle_S$ the spatial average over trajectories entering the medium through the outer surface S of the body, $\langle \cdot \rangle_V$ the spatial average over trajectories starting from within the volume V; $\langle l \rangle$ is the mean free path of the walkers, p_s the scattering probability, p_f the fission probability, ν_1 the average number of descendants per fission, and η_d a dimension-dependent constant ($\eta_2 = \pi$ and $\eta_3 = 4$). To keep notation simple, we will assume that the physical parameters are spatially constant. As a particular case, we will show that when $p_s + \nu_1 p_f = 1$ the average travelled length reads

$$\langle L \rangle_S = \eta_d \frac{V}{S}, \tag{6.3}$$

depending only on a purely geometric ratio and not on the specific details of the process.

The dimensionless quantities $\langle L\rangle_S/\langle l\rangle$ and $\langle N\rangle_S$ play a prominent role, in that they allow assessing the *opacity* of the body, i.e., its 'size' with respect to the traversing walks [5,113]. Eqs. (6.1) and (6.2) generalize the elegant Cauchy formulas previously obtained for purely diffusive exponential Pearson walks [106, 107, 109, 175] and will be shown to apply to the very broad class of branching random flights.

6.2 The equilibrium condition

Consider an isotropic source of particles uniformly distributed in space. Walkers leaving from the source move at constant speed and undergo jumps of random length l distributed according to the density $T(l)$, with finite *mean free path*

$$\langle l\rangle = \int_0^{+\infty} l\, T(l)\, dl. \tag{6.4}$$

Upon collision, each walker can be scattered with probability $p_s = \Sigma_s/\Sigma$, be absorbed with probability $p_a = \Sigma_a/\Sigma$, or give rise to fission with probability $p_f = \Sigma_f/\Sigma$. In the case of fission, the particle disappears and with probability p_i gives rise to a random number i of descendants, with $\nu_1 = \sum_i i p_i$. We assume that the directions $\boldsymbol{\omega}$ taken after scattering and fission are isotropic, i.e., obey Ω_d^{-1}, where $\Omega_d = 2\pi^{d/2}/\Gamma(d/2)$ is the surface of the unit sphere in dimension d. Each descendant behaves independently as the progenitor particle, thus resulting in a ramified structure for the stochastic paths (see Fig. 6.1).

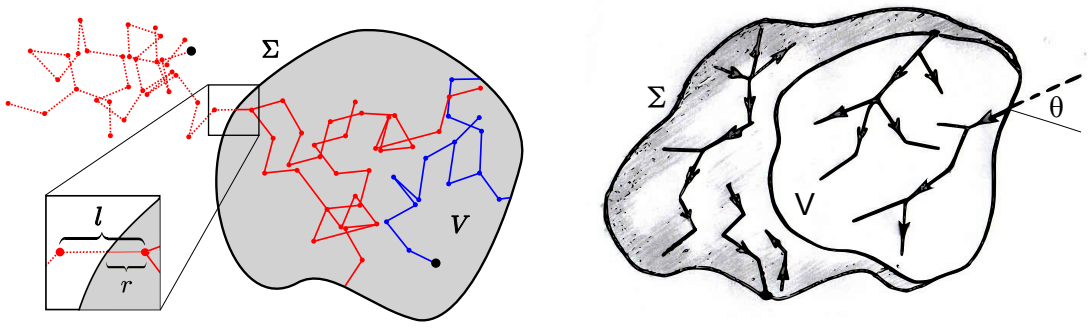

Figure 6.1: *Left.* Trajectories born outside the body and entering through the surface S (red) and trajectories born inside the body (blue) for a branching Pearson random walk with jumps of constant size. Source points are marked as black dots. The inset displays the distinct behaviour of the first jump across S for particles coming from outside, which is distributed according to $H(r)$ instead of $T(l)$. *Right.* A schematic representation of branching random flights in a bounded domain, starting on the surface S or inside the volume V. For trajectories starting on the surface, the angle θ between the normal to the surface and the incoming trajectory obeys a density function depending on dimensionality.

Consider now a sub-domain of finite volume V and regular surface $S = \partial V$ immersed in the particle flow. Trajectories are observed from the entrance of a single particle through S until the disappearance of the particle and all its descendants by either absorption in V or escape from S (see Fig. 6.1). The previous assumptions ensure an equilibrium condition for the source, and we can

safely assume that the walkers will enter the body from S with a uniform distribution of entry points $\mathbf{r}_0$ and an isotropic distribution of incident directions $\boldsymbol{\omega}_0$ [106, 107]. The final ingredient needed to fully characterize the particle inflow through S is the density $H(r)$ of the first jump length r through the body for walkers crossing the surface (see Fig. 6.1). Since the walkers come from outside the body, they must necessarily have performed a jump of length l larger than r. As a consequence, the density $H(r)$ must be proportional to the probability that the jump from outside V is larger than r, namely, $H(r) \propto \int_r^\infty T(l)dl$ [225]. By imposing normalization and using $\langle l \rangle = \int_0^\infty dr \int_r^\infty T(l)dl$, we get the first jump length density [226]

$$H(r) = \frac{1}{\langle l \rangle} \int_r^{+\infty} T(l)\, dl \; . \tag{6.5}$$

For *exponential flights*, we have in particular

$$H(r) = T(r) = \frac{1}{\langle l \rangle} e^{-r/\langle l \rangle}, \tag{6.6}$$

which is the signature of the *Markovian nature* of this process: trajectories crossing S have no memory of their past history, so that the first jump distribution does not differ from the others [227].

6.3 Opacity of homogeneous media

We will begin our analysis by the case of d-dimensional *exponential* flights. Branching Pearson random walks with exponentially distributed jumps stem from assuming that the traversed medium is homogeneous at the length scale seen by the walkers along their paths. If scattering centers are completely uncorrelated, the probability of occurrence of particle-medium interactions per unit length is independent of the travelled distance and the flights are therefore Poissonian, i.e., exponential [5,113]. In this case, the Markovian (memoryless) nature of the transport process allows resorting to the Feynman-Kac formalism that we have discussed in the previous Chapters.

Consider a single walker initially emitted from a point source at $\mathbf{r}_0$ with direction $\boldsymbol{\omega}_0$ and performing exponential flights with mean free path $\langle l \rangle$ [1]. Consider then a bounded domain of non-zero volume V (with finite diameter) and non-zero measurable surface $S = \partial V$. In order to keep notation simple, yet retaining the key features of the process, we will assume in the following that particles evolve at constant speed v, descendants are emitted isotropically and independently from each other, and $\langle l \rangle$ is constant over the volume V.

6.3.1 Travelled lengths

To start with, we denote by

$$L_t^k(\mathbf{r}_0, \boldsymbol{\omega}_0) = \mathbb{E}_t[\ell_V^k](\mathbf{r}_0, \boldsymbol{\omega}_0) \tag{6.7}$$

the k-th moment of the total length travelled in V by the particle and all its descendants when observed up to time t, starting from a single walker in $\mathbf{r}_0$ with direction $\boldsymbol{\omega}_0$ at time $t = 0$. As shown in the previous Chapter, the Feynman-Kac formalism allows deriving

$$\frac{1}{v_0}\frac{\partial}{\partial t} L_t^k(\mathbf{r}_0, \boldsymbol{\omega}_0) = \mathcal{L}^\dagger L_t^k(\mathbf{r}_0, \boldsymbol{\omega}_0) + k \mathbb{1}_V L_t^{k-1}(\mathbf{r}_0, \boldsymbol{\omega}_0) + \Sigma_f \sum_{j=2}^{k} \nu_j \mathcal{B}_{k,j} \left[\langle L_t^i \rangle_\Omega \right], \tag{6.8}$$

[1] When the physical parameters are constant, the mean free path $\langle l \rangle$ is related to the cross section Σ by $\langle l \rangle = 1/\Sigma$.

for $k \geq 1$, starting with $L_0^k(\mathbf{r}_0, \boldsymbol{\omega}_0) = 0$ and $L_t^0(\mathbf{r}_0, \boldsymbol{\omega}_0) = 1$ from normalization. Here

$$\mathcal{L}^\dagger = \boldsymbol{\omega}_0 \cdot \nabla_{\mathbf{r}_0} - \Sigma + \Sigma_s \int \frac{d\boldsymbol{\omega}_0}{\Omega_d} + \Sigma_f \nu_1 \int \frac{d\boldsymbol{\omega}_0}{\Omega_d} \tag{6.9}$$

is the backward transport operator [113]. Recall that we have defined

$$\langle h_t \rangle_\Omega(\mathbf{r}_0) \equiv \int \frac{d\boldsymbol{\omega}_0}{\Omega_d} h_t(\mathbf{r}_0, \boldsymbol{\omega}_0) \tag{6.10}$$

the average over directions. Finally, $\mathcal{B}_{m,j}[z_i] = \mathcal{B}_{m,j}[z_1, z_2, \cdots, z_{m-j+1}]$ stand for the Bell's polynomials [192], and $\nu_j = \langle k(k-1)...(k-j+1) \rangle$ are the falling factorial moments of the descendant number, with $\nu_0 = 1$. When trajectories are observed up to a time t much longer than the characteristic time scale of the system dynamics, we can define the stationary moments

$$L^k(\mathbf{r}_0, \boldsymbol{\omega}_0) = \lim_{t \to +\infty} L_t^k(\mathbf{r}_0, \boldsymbol{\omega}_0), \tag{6.11}$$

provided that the limit exists. Intuitively, this condition is satisfied when the particle losses due to absorptions and leakages from the boundaries are larger than the gain due to population growth, which is always the case if V is below some critical size V_c [113]. In the following we will assume that $V < V_c$, unless differently specified: the time derivative in Eq. (6.8) then vanishes at large times, and we get

$$\mathcal{L}^\dagger L^k(\mathbf{r}_0, \boldsymbol{\omega}_0) + k \mathbb{1}_V L^{k-1}(\mathbf{r}_0, \boldsymbol{\omega}_0) + \Sigma_f \sum_{j=2}^{k} \nu_j \mathcal{B}_{k,j}\left[\langle L^i \rangle_\Omega(\mathbf{r}_0)\right] = 0, \tag{6.12}$$

with the boundary conditions $L^k(\mathbf{r}_0 \in S, \boldsymbol{\omega}_0) = 0$ when $\boldsymbol{\omega}_0$ is directed outward.

Following [109], our aim is now to average Eq. (6.12) over the starting position and direction of the walker. As the domain V is bounded, we can safely define the probability measures for trajectories born in the domain and for those starting on the surface. Choosing the starting coordinates uniformly distributed inside V imposes the uniform volume probability measure

$$\frac{d\boldsymbol{\Omega}}{\Omega_d} \frac{dV}{V}, \tag{6.13}$$

where $d\boldsymbol{\Omega}$ is the solid angle element [2]. Similarly, an isotropic incident flux uniformly distributed on the frontier S imposes the surface probability measure

$$\frac{d\boldsymbol{\Omega}}{\alpha_d} \frac{dS}{S} (\boldsymbol{\Omega} \cdot \mathbf{n}), \tag{6.14}$$

where

$$\alpha_d = \frac{2\pi^{(d-1)/2}}{d-1} \Gamma\left(\frac{d-1}{2}\right) \tag{6.15}$$

is the inward isotropic flux through a unit sphere [109, 229] and $\mathbf{n}$ is the inward surface normal [3].

This allows precisely defining the volume average appearing in Eqs. (6.1) and (6.2) for any function $h(\mathbf{r}_0, \boldsymbol{\omega}_0)$:

$$\langle h \rangle_V = \int_V \frac{d\mathbf{r}_0}{V} \int \frac{d\boldsymbol{\omega}_0}{\Omega_d} h(\mathbf{r}_0, \boldsymbol{\omega}_0). \tag{6.16}$$

[2] A $\mu-$ or equivalently $\nu-$randomness in the language of stochastic geometry [228, 229].

[3] A $\mu-$randomness [228, 229]. The term $\cos\theta = (\boldsymbol{\Omega} \cdot \mathbf{n})$ implies that in polar coordinates trajectories starting on the surface must enter the domain with density $\theta = \arcsin(2\xi - 1)$ in two dimensions and $\theta = 1/2 \arccos(1 - 2\xi)$ in three dimensions, ξ being uniformly distributed in $(0, 1]$.

over uniform starting positions $\mathbf{r}_0 \in V$ and isotropic directions $\boldsymbol{\omega}_0$ [109, 229]. Analogously, the surface average of $h(\mathbf{r}_0, \boldsymbol{\omega}_0)$ is defined as

$$\langle\, h \,\rangle_S = \int_S \frac{dS(\mathbf{r}_0)}{S} \int \frac{d\boldsymbol{\omega}_0}{\alpha_d}\, \boldsymbol{\omega}_0 \cdot \mathbf{n}\, h(\mathbf{r}_0, \boldsymbol{\omega}_0)\,. \tag{6.17}$$

We integrate then Eq. (6.12) uniformly over all possible initial positions and directions (taking into account the isotropy property), and apply the Gauss divergence theorem. This yields the recursive formula

$$\langle L^k \rangle_S = \eta_d \frac{V}{S}\Big[k\langle L^{k-1}\rangle_V + (\Sigma_s + \nu_1\Sigma_f - \Sigma)\langle L^k\rangle_V + \Sigma_f \sum_{j=2}^{k} \nu_j \langle \mathcal{B}_{k,j}\left[\langle L^i\rangle_\Omega(\mathbf{r}_0)\right]\rangle_V\Big], \tag{6.18}$$

where we have set

$$\eta_d = \frac{\Omega_d}{\alpha_d} = \sqrt{\pi}(d-1)\frac{\Gamma\left(\frac{d-1}{2}\right)}{\Gamma\left(\frac{d}{2}\right)}. \tag{6.19}$$

Equation (6.18) relates the k-th moment of trajectories starting on the surface to the different moments (up to order k) of trajectories born inside the volume, and as such extends to branching random flights the formulas

$$\langle L\rangle_S = \eta_d \frac{V}{S} \quad \text{and} \quad \langle L^{k-1}\rangle_V = \frac{\langle L^k\rangle_S}{k\langle L\rangle_S} \quad \text{for} \quad k \geq 1 \tag{6.20}$$

previously obtained for diffusive exponential Pearson walks with $\Sigma_a = \Sigma_f = 0$ [106, 109, 175]. In particular, using $\langle l\rangle = 1/\Sigma$, from Eq. (6.18) the average length ($k = 1$) yields Eq. (6.1), namely,

$$\langle L\rangle_S = \eta_d \frac{V}{S}\left[1 + \frac{p_s + \nu_1 p_f - 1}{\langle l\rangle}\langle L\rangle_V\right], \tag{6.21}$$

which generalizes the celebrated *Cauchy's formula* (also known as the mean chord length property)

$$\langle L\rangle_S = \eta_d \frac{V}{S}, \tag{6.22}$$

originally established for random straight lines drawn from the surface of the volume [229] and recently shown to rather surprisingly apply also to exponential Pearson random flights with $p_s = 1$ [106, 109, 175, 230].

The term $\langle L\rangle_S/\langle l\rangle$ is a measure of the opacity of the volume, in that it expresses the ratio between the average length travelled in V when an isotropic particle flux is imposed at the surface S and the mean free path. Another quantity of interest is $\langle L\rangle_S/(\eta_d V/S)$, which is the ratio between the average length travelled in the actual medium V and the length that the particle would elapse if V were empty and the paths were straight lines (the meaning of the denominator stems from Cauchy's formula).

In general, Eq. (6.21) depends on the fine details of the process and of the geometry, since the term $\langle L\rangle_V$ is not universal. However, when the underlying branching process has $p_s + \nu_1 p_f = 1$, Eq. (6.21) yields precisely the Cauchy's formula. In this case, thus, the quantity $\langle L\rangle_S$ would depend only on the geometrical ratio V/S and not on the specific details of the random walk. In particular, $\langle L\rangle_S$ would be independent of the characteristic jump size $\langle l\rangle$. This simple property unfortunately does not carry over to higher moments of the travelled length. Indeed, for $k = 2$ we have $\mathcal{B}_{2,2}[z_1, z_2] = z_1^2$, and Eq. (6.18) then gives

$$\langle L^2\rangle_S = \eta_d \frac{V}{S}\left[2\langle L\rangle_V + (\Sigma_s + \nu_1\Sigma_f - \Sigma)\langle L^2\rangle_V + \Sigma_f\nu_2\langle\langle L\rangle_\Omega^2(\mathbf{r}_0)\rangle_V\right]. \tag{6.23}$$

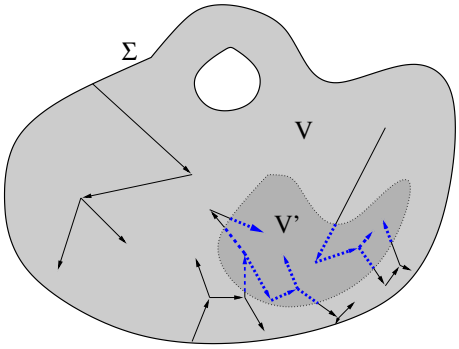

Figure 6.2: Branching random flights born in the volume V (or on the surface S) and traversing a sub-domain V' of V. The portion of the trajectories spent in V' is displayed as blue dashed lines.

Bell's polynomials in Eq. (6.18) are the signature of branching, and for $k \geq 2$ introduce some extra non-vanishing terms ($\nu_2 > 0$) with respect to Eq. (6.20) even when $p_s + \nu_1 p_f = 1$.

In the absence of branching, i.e., when random flights can be either scattered or absorbed, with $p_a + p_s = 1$, explicit relations for the probability density functions of the travelled length can be also derived. Under these hypotheses, Eq. (6.18) reduces to

$$\langle L^k \rangle_S = \eta_d \frac{V}{S} \left[k \langle L^{k-1} \rangle_V - \Sigma_a \langle L^k \rangle_V \right]. \tag{6.24}$$

In the presence of absorption, then, $\langle L \rangle_S < \eta_d V/S$, as expected. We denote by $f(l)$ and $g(r)$ the probability density of the total travelled length for a trajectory started on the surface or inside the volume, respectively. Then, Eq. (6.24) can be identically rewritten as

$$\int_0^\infty l^k f(l) dl = \eta_d \frac{V}{S} \int_0^\infty \left[\frac{k}{r} - \Sigma_a \right] r^k g(r) dr. \tag{6.25}$$

Integrating Eq. (6.25) by parts and using normalization $\int_0^\infty g(r)dr = 1$ yields the relation

$$g(r) = \frac{1}{\eta_d \frac{V}{S}} \left[1 + \eta_d \frac{V}{S} \Sigma_a - \int_0^r f(l) e^{\Sigma_a l} dl \right] e^{-\Sigma_a r}, \tag{6.26}$$

between the two densities $f(l)$ and $g(r)$. In the limit of purely diffusive processes ($p_s \to 1$), Eq. (6.26) reduces to

$$g(r) = \frac{1}{\eta_d \frac{V}{S}} \int_r^\infty f(l) dl, \tag{6.27}$$

a relation originally established for straight paths [231] and later extended to exponential Pearson walks [175].

6.3.2 Excursions in sub-domains

Considerable efforts have been devoted to the study of the occupation statistics of some sub-domain V' included in V. This issue has been thoroughly investigated, e.g., in the context of residence times for Brownian motion (with or without branching; see, e.g., [44, 48, 97, 168, 191]) and exponential Pearson walks [109]. Consider a branching exponential flight emitted in V: the particle and its descendants may enter V', spend some time inside, branch, possibly die in V' or

escape, then re-enter V', and so on, as illustrated in Fig. 6.2. The total length travelled in V' can be straightforwardly assessed by resorting to the Feynman-Kac formalism mentioned above. Indeed, its moments $L'^k(\mathbf{r}_0, \boldsymbol{\omega}_0)$ satisfy Eq. (6.12), the marker function being restricted to the sub-domain V'. Then, averaging over all angles and positions inside V yields

$$\langle L'^k \rangle_S = \eta_d \frac{V}{S} \Big[k \frac{V'}{V} \langle L'^{k-1} \rangle_{V'} + (\Sigma_s + \nu_1 \Sigma_f - \Sigma) \langle L'^k \rangle_V + \Sigma_f \sum_{j=2}^{k} \nu_j \langle \mathcal{B}_{k,j} \left[\langle L'^i \rangle_\Omega (\mathbf{r}_0) \right] \rangle_V \Big]. \quad (6.28)$$

For $k = 1$ we have in particular

$$\langle L' \rangle_S = \eta_d \frac{V}{S} \left[\frac{V'}{V} + \frac{p_s + \nu_1 p_f - 1}{\langle l \rangle} \langle L' \rangle_V \right]. \quad (6.29)$$

As a consequence, for trajectories starting on the surface, the ratio $\langle L' \rangle_S / \langle L \rangle_S$ between the length travelled in V' and that travelled in V generally depends on the geometry as well as on the walk features. However, for branching exponential flights with $p_s + \nu_1 p_f = 1$, we have

$$\frac{\langle L' \rangle_S}{\langle L \rangle_S} = \frac{V'}{V} \quad (6.30)$$

i.e., we recover the elegant *ergodic-type* property that applies to purely diffusive exponential flights [109].

6.3.3 Number of collision events

The k-th stationary moment

$$N^k(\mathbf{r}_0, \boldsymbol{\omega}_0) = \lim_{g \to \infty} \mathbb{E}_g[n_V^k](\mathbf{r}_0, \boldsymbol{\omega}_0) \quad (6.31)$$

of the number of collisions in V performed by a branching exponential flight starting from $\mathbf{r}_0$ in direction $\boldsymbol{\omega}_0$ can be also assessed by resorting to the Feynman-Kac formalism: as shown in the previous Chapter, N^k satisfies

$$\mathcal{L}^\dagger N^k(\mathbf{r}_0, \boldsymbol{\omega}_0) + \Sigma_s \mathbb{1}_V \sum_{j=1}^{k-1} \binom{k}{j} \langle N^j \rangle_\Omega + \Sigma_f \sum_{j=2}^{k} \nu_j \mathcal{B}_{k,j} \left[\langle N^i \rangle_\Omega \right] + \Sigma_f \mathbb{1}_V \sum_{q=1}^{k} \binom{k}{q} \sum_{j=0}^{k-q} \nu_j \mathcal{B}_{k-q,j} \left[\langle N^i \rangle_\Omega \right] = 0, \quad (6.32)$$

which closely resembles Eq. (6.12). At the boundaries, we have $N^k(\mathbf{r}_0 \in S, \boldsymbol{\omega}_0) = 0$ when $\boldsymbol{\omega}_0$ is directed outward. Then, by averaging Eq. (6.32) over starting positions and directions in V we get

$$\langle N^k \rangle_S = \eta_d \frac{V}{S} \Sigma \Big[(p_s + p_f \nu_1 - 1) \langle N^k \rangle_V + p_s \sum_{j=1}^{k-1} \binom{k}{j} \langle N^j \rangle_\Omega (\mathbf{r}_0) + p_f \sum_{j=2}^{k} \nu_j \langle \mathcal{B}_{k,j} \left[\langle N^i \rangle_\Omega (\mathbf{r}_0) \right] \rangle_V + p_f \sum_{q=1}^{k} \binom{k}{q} \sum_{j=0}^{k-q} \nu_j \langle \mathcal{B}_{k-q,j} \left[\langle N^i \rangle_\Omega (\mathbf{r}_0) \right] \rangle_V \Big], \quad (6.33)$$

which generalizes the results previously found for diffusive exponential Pearson walks [232]. In particular, for the average collision number ($k = 1$) we recover Eq. (6.2), namely,

$$\langle N \rangle_S = \frac{\eta_d}{\langle l \rangle} \frac{V}{S} \left[1 + (p_s + \nu_1 p_f - 1) \langle N \rangle_V \right]. \quad (6.34)$$

Now, from exponential flights being a Markovian process it follows that $\langle l\rangle\langle N\rangle_V = \langle L\rangle_V$ [210]. Hence, we have also $\langle L\rangle_S = \langle l\rangle\langle N\rangle_S$, which amounts to saying that the opacity can be expressed in terms of the mean number of collisions performed by the walkers in V when entering from the surface. Similarly as done for the lengths, the number of collisions in a sub-domain V' can again be computed by using $\mathbb{1}_{V'}$ in Eq. (6.32).

For non-branching flights, $p_s + p_a = 1$ and we have

$$\langle N^k\rangle_S = \eta_d \frac{V}{S}\Sigma\left[p_s \sum_{j=1}^{k}\binom{k}{j}\langle N^j\rangle_V + (p_s-1)\langle N^k\rangle_V\right] \tag{6.35}$$

for $k \geq 1$. By making use of the binomial formula, we finally get

$$\langle N^k\rangle_S = \eta_d \frac{V}{S}\Sigma\left[p_s\langle (N+1)^k\rangle_V - \langle N^k\rangle_V + p_a\right]. \tag{6.36}$$

In the absence of branching, it is also possible to explicitly derive the collision probabilities. We denote by $f(i)$ and $g(j)$ the collision number probability for a trajectory started on the surface or inside the volume, respectively. Then, Eq. (6.36) can be identically rewritten as

$$\sum_{i=0}^{\infty} i^k f(i) = \eta_d \frac{V}{S}\Sigma\left[\sum_{j=0}^{\infty}\left[p_s(j+1)^k - j^k\right] g(j) + p_a\right]. \tag{6.37}$$

By equating the terms of the series, and imposing that the relation holds for arbitrary $k \geq 1$, we get then

$$f(j) = \eta_d \frac{V}{S}\Sigma\left[p_s g(j-1) - g(j) + p_a\delta_{j,1}\right], \tag{6.38}$$

$\delta_{i,j}$ being the Kronecker delta. Resumming over j yields in particular $f(0) = 1 - \eta_d\frac{V}{S}\Sigma g(0)$. For exponential Pearson walks, $p_s \to 1$ and we obtain

$$f(j) = \eta_d \frac{V}{S}\Sigma\left[g(j-1) - g(j)\right]. \tag{6.39}$$

6.3.4 Escape probability

Recall from the previous Chapter that when the volume V is bounded, the probability $\mathcal{R}(\mathbf{r}_0, \boldsymbol{\omega}_0)$ that a trajectory starting from $\mathbf{r}_0$ in direction $\boldsymbol{\omega}_0$ never visits the exterior of V satisfies

$$-\boldsymbol{\omega}_0 \cdot \nabla_{\mathbf{r}_0}\mathcal{R}(\mathbf{r}_0,\boldsymbol{\omega}_0) + \Sigma\mathcal{R}(\mathbf{r}_0,\boldsymbol{\omega}_0) = \mathbb{1}_V\left[\Sigma_a + \Sigma_s\langle\mathcal{R}\rangle_\Omega + \Sigma_f G\left[\langle\mathcal{R}\rangle_\Omega\right]\right], \tag{6.40}$$

where $G[z] = \sum_i p_i z^i$ is the generating function associated to the fission particle distribution p_i and $\mathcal{R}(\mathbf{r}_0 \in S, \boldsymbol{\omega}_0) = 0$ when $\boldsymbol{\omega}_0$ is directed outward. By definition, the quantity $\mathcal{E} = 1 - \mathcal{R}$ represents the escape probability from the volume V. Then, averaging Eq. (6.40) over all initial positions and directions yields

$$\langle\mathcal{R}\rangle_S = \frac{\eta_d}{\langle l\rangle}\frac{V}{S}\left[p_a + p_s\langle\mathcal{R}\rangle_\Omega + p_f\langle G\left[\langle\mathcal{R}\rangle_\Omega\right]\rangle_V - \langle\mathcal{R}\rangle_V\right]. \tag{6.41}$$

The terms $\langle\mathcal{R}\rangle_V$ and and $\langle\mathcal{R}\rangle_S$ have a simple probabilistic meaning, namely, the probability that a particle born uniformly and isotropically in the volume V, or entering the body isotropically from the boundary, respectively, is absorbed with all its descendants in V [113]. Similarly, $\langle\mathcal{R}\rangle_\Omega(\mathbf{r}_0)$ represents the probability that a particle born isotropically at $\mathbf{r}_0$ is absorbed (with all its descendants) in V.

When walkers can not be absorbed in the domain ($p_a = 0$, and $p_0 = 0$ in $G[z]$), trajectories must necessarily escape from the boundaries, and we have $\langle \mathcal{R} \rangle_S = 0$. This rather intuitive result can be understood as follows: developing Eq. (6.41) and using $\langle \mathcal{R} \rangle_\Omega^k \leq \langle \mathcal{R} \rangle_\Omega$ ($\langle \mathcal{R} \rangle_\Omega$ is a probability), we immediately get that $\langle \mathcal{R} \rangle_S \leq 0$: then, the probability that a particle entering the body isotropically from the boundary is absorbed with all its descendants in V must vanish, as expected. The same applies to $\langle \mathcal{R} \rangle_V$.

In the absence of branching, we get

$$\langle \mathcal{R} \rangle_S = \eta_d \frac{V}{S} \Sigma_a \left[1 - \langle \mathcal{R} \rangle_V \right], \tag{6.42}$$

a d-dimensional generalization of a theorem originally derived for purely absorbing media [113] and extended to diffusive and absorbing media in three dimensions in [175].

6.3.5 Survival probability

Recall from the previous Chapter that for branching exponential flights in bounded domains when $V > V_c$ the probability of ultimate survival $\mathcal{S}(\mathbf{r}_0, \boldsymbol{\omega}_0)$ satisfies

$$-\boldsymbol{\omega}_0 \cdot \nabla_{\mathbf{r}_0} \mathcal{S}(\mathbf{r}_0, \boldsymbol{\omega}_0) + \Sigma \mathcal{S}(\mathbf{r}_0, \boldsymbol{\omega}_0) = \Sigma_s \langle \mathcal{S} \rangle_\Omega + \Sigma_f F[\langle \mathcal{S} \rangle_\Omega], \tag{6.43}$$

where

$$F[z] = \sum_{k=1}^{\infty} (-1)^{k+1} \frac{\nu_k}{k!} z^k. \tag{6.44}$$

At the boundaries, $\mathcal{S}$ must vanish when $\boldsymbol{\omega}_0$ is directed towards the exterior of V. Averaging Eq. (6.43) over all initial positions and directions yields then

$$\langle \mathcal{S} \rangle_S = \frac{\eta_d}{\langle l \rangle} \frac{V}{S} \left[p_s \langle \langle \mathcal{S} \rangle_\Omega \rangle_V + p_f \langle F \left[\langle \mathcal{S} \rangle_\Omega \right] \rangle_V - \langle \mathcal{S} \rangle_V \right]. \tag{6.45}$$

Unfortunately, the complex nature of the alternating series in $F[z]$ seems to prevent from drawing general conclusions based on Eq. (6.45).

6.4 Universality of Cauchy's formulas

In many important applications of linear transport theory, including light propagation through engineered optical materials [70–72] or turbid media [73–75], neutron diffusion in pebble-bed reactors [76], and radiation trapping in hot atomic vapours [79], the hypothesis of uncorrelated scattering centers is deemed to fail, which thus calls for models based on *non-exponential* random walks. One is then naturally led to wonder whether similar general results for L and N can be established in such circumstances. In the attempt of addressing this issue, in the following we will derive two key results: first, we will show that under mild hypotheses Cauchy-like formulas (6.1) and (6.2) have a *universal character*, and quite surprisingly carry over to branching Pearson walks with arbitrary jumps [4]. Second, we will also establish a *local version* of formulas (6.1) and (6.2), namely,

$$\langle \varphi \rangle_S (\mathbf{r}, \boldsymbol{\omega}) = \eta_d \frac{V}{S} \left[\frac{1}{V \Omega_d} + \frac{p_s + \nu_1 p_f - 1}{\langle l \rangle} \langle \varphi \rangle_V (\mathbf{r}, \boldsymbol{\omega}) \right] \tag{6.46}$$

$$\langle \psi \rangle_S (\mathbf{r}, \boldsymbol{\omega}) = \frac{\eta_d}{\langle l \rangle} \frac{V}{S} \left[\frac{1}{V \Omega_d} + (p_s + \nu_1 p_f - 1) \langle \psi \rangle_V (\mathbf{r}, \boldsymbol{\omega}) \right], \tag{6.47}$$

[4] This result has been hinted on physical grounds for purely diffusive Pearson walks [107, 226].

a stronger result that directly relates the surface- and volume-averaged travelled length density $\langle\varphi\rangle$ and collision density $\langle\psi\rangle$ at any point $\{\mathbf{r},\boldsymbol{\omega}\}$ of the phase space. As discussed in the following, the proposed formalism is fairly broad and applies more generally to physical and biological systems with diffusion, reproduction and death.

6.4.1 Number of collisions

Let us define the collision density $\psi(\mathbf{r},\boldsymbol{\omega}|\mathbf{r}_0,\boldsymbol{\omega}_0)$ such that

$$N(\mathbf{r}_0,\boldsymbol{\omega}_0)=\int_V d\mathbf{r}\int d\boldsymbol{\omega}\,\psi(\mathbf{r},\boldsymbol{\omega}|\mathbf{r}_0,\boldsymbol{\omega}_0) \tag{6.48}$$

is the average number of particles having a collision within V, for a single walker starting from $\mathbf{r}_0$ in direction $\boldsymbol{\omega}_0$ [113]. The collision density satisfies the linear Boltzmann equation [5, 113]

$$\psi(\mathbf{r},\boldsymbol{\omega}|\mathbf{r}_0,\boldsymbol{\omega}_0)=\int_0^u ds\,T(s)\int\frac{d\boldsymbol{\omega}'}{\Omega_d}(p_s+\nu_1 p_f)\psi(\mathbf{r}-s\boldsymbol{\omega},\boldsymbol{\omega}'|\mathbf{r}_0,\boldsymbol{\omega}_0)+\psi_1(\mathbf{r},\boldsymbol{\omega}|\mathbf{r}_0,\boldsymbol{\omega}_0), \tag{6.49}$$

where $u=u(\mathbf{r},\boldsymbol{\omega})$ is the distance from the point $\mathbf{r}$ to the surface S in the direction of $-\boldsymbol{\omega}$ (see Fig. 6.3). The quantity ψ_1 appearing at the right hand side of Eq. (6.49) is the so called first-collision density, which represents the contributions to ψ due to particles having their first collision in V with coordinates $\{\mathbf{r},\boldsymbol{\omega}\}$ [113]. Let us begin by considering the trajectories coming from outside V and entering the body by crossing the surface S at $\mathbf{r}_0\in S$. In this case,

$$\psi_1(\mathbf{r},\boldsymbol{\omega}|\mathbf{r}_0,\boldsymbol{\omega}_0)=\int_0^u ds\,H(s)\mathcal{Q}(\mathbf{r}-s\boldsymbol{\omega},\boldsymbol{\omega}), \tag{6.50}$$

where we have set $\mathcal{Q}(\mathbf{r},\boldsymbol{\omega})=\delta(\mathbf{r}-\mathbf{r}_0)\delta(\boldsymbol{\omega}-\boldsymbol{\omega}_0)$. Then, applying the surface average (6.17) to Eq. (6.49) and using the divergence theorem yields

$$\langle\,\psi\,\rangle_S(\mathbf{r},\boldsymbol{\omega})=\int_0^u ds\,T(s)\langle\,\chi\,\rangle_S(\mathbf{r}-s\boldsymbol{\omega})-\frac{1}{\alpha_d S}\int_V d\mathbf{r}_0\,\nabla\Big[\boldsymbol{\omega}\,H((\mathbf{r}-\mathbf{r}_0)\cdot\boldsymbol{\omega})\Big]. \tag{6.51}$$

As customary in transport theory, we have here introduced the outgoing collision density

$$\chi(\mathbf{r}|\mathbf{r}_0,\boldsymbol{\omega}_0)=\int\frac{d\boldsymbol{\omega}'}{\Omega_d}(p_s+\nu_1 p_f)\psi(\mathbf{r},\boldsymbol{\omega}'|\mathbf{r}_0,\boldsymbol{\omega}_0), \tag{6.52}$$

which is defined such that $\int_V d\mathbf{r}\chi(\mathbf{r}|\mathbf{r}_0,\boldsymbol{\omega}_0)$ represents the average number of particles re-emitted after a collision in V, for a single walker starting from $\mathbf{r}_0$ in direction $\boldsymbol{\omega}_0$ [113]. The integral in the second term at the right hand side of Eq. (6.51) can be explicitly computed in terms of the density H and yields $-H(u)$, so that from Eq. (6.51) we are led to the following integral equation

$$\langle\psi\rangle_S(\mathbf{r},\boldsymbol{\omega})=\int_0^u\langle\chi\rangle_S(\mathbf{r}-s\boldsymbol{\omega})T(s)\,ds+\frac{1}{\alpha_d S}H(u). \tag{6.53}$$

Instead of solving directly Eq. (6.53), the idea is to relate the surface averages to the volume averages. To this aim, consider next the trajectories born within the body. In this case, $\mathbf{r}_0\in V$ and the first-collision density reads

$$\psi_1(\mathbf{r},\boldsymbol{\omega}|\mathbf{r}_0,\boldsymbol{\omega}_0)=\int_0^u ds\,T(s)\mathcal{Q}(\mathbf{r}-s\boldsymbol{\omega},\boldsymbol{\omega}), \tag{6.54}$$

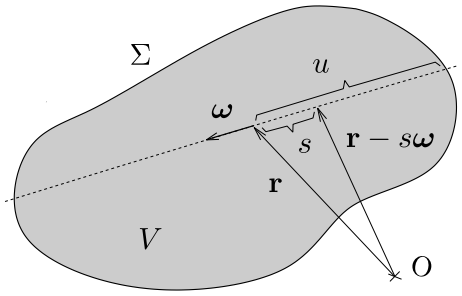

Figure 6.3: A two-dimensional illustration of the coordinate s and the distance $u = u(\mathbf{r}, \boldsymbol{\omega})$ from the point $\mathbf{r}$ to the surface S in the direction of $-\boldsymbol{\omega}$.

Then, applying the volume average (6.16) to Eq. (6.49) yields the integral equation

$$\langle \psi \rangle_V(\mathbf{r}, \boldsymbol{\omega}) = \int_0^u \left[\langle \chi \rangle_V(\mathbf{r} - s\boldsymbol{\omega}) + \frac{1}{V\Omega_d} \right] T(s)\, ds. \tag{6.55}$$

From inspection, it can be seen that Eqs. (6.53) and (6.55) can be both recast as a system of integral equations of the form

$$\begin{cases} F_{S,V}(\mathbf{r}, \boldsymbol{\omega}) = \displaystyle\int_0^u \left[p_s + \nu_1 p_f - 1 + G_{S,V}(\mathbf{r} - s\boldsymbol{\omega}) \right] T(s)\, ds \\ G_{S,V}(\mathbf{r}) = \displaystyle\int \frac{d\boldsymbol{\omega}'}{\Omega_d} (p_s + \nu_1 p_f) F_{S,V}(\mathbf{r}, \boldsymbol{\omega}'), \end{cases}$$

where $F_S(\mathbf{r}, \boldsymbol{\omega}) = \langle l \rangle \alpha_d S \langle \psi \rangle_S(\mathbf{r}, \boldsymbol{\omega}) - 1$ and $F_V(\mathbf{r}, \boldsymbol{\omega}) = (\nu_1 - 1)\Omega_d V \langle \psi \rangle_V(\mathbf{r}, \boldsymbol{\omega})$, respectively. Generally speaking, integral equations of this kind can not be solved explicitly, but it can be shown that their solution is unique [2]. It thus follows the equality

$$\langle l \rangle \alpha_d S \langle \psi \rangle_S(\mathbf{r}, \boldsymbol{\omega}) = 1 + (p_s + \nu_1 p_f - 1) V \Omega_d \langle \psi \rangle_V(\mathbf{r}, \boldsymbol{\omega}), \tag{6.56}$$

whence Eq. (6.47). Finally, by recalling the definition in Eq. (6.48), integrating Eq. (6.47) over volume V and over directions Ω_d yields Eq. (6.2) as announced. Actually, the result obtained in Eq. (6.47) is stronger than Eq. (6.2), in that it represents a *local property* which is valid for any pair of coordinates $\mathbf{r}$ and $\boldsymbol{\omega}$. Observe that when $p_s + \nu_1 p_f = 1$ Eq. (6.56) does not depend on $\langle \psi \rangle_V$, and the corresponding surface-averaged collision density is constant over the body, namely,

$$\langle \psi \rangle_S(\mathbf{r}, \boldsymbol{\omega}) = \frac{1}{\langle l \rangle \alpha_d S}. \tag{6.57}$$

In this case, it follows that the average number of collisions in any sub-region $V' \subseteq V$ is simply proportional to V', an *ergodic-like* property already exhibited for branching exponential flights [227].

6.4.2 Travelled lengths

Let us define the angular flux $\varphi(\mathbf{r}, \boldsymbol{\omega} | \mathbf{r}_0, \boldsymbol{\omega}_0)$ such that

$$L(\mathbf{r}_0, \boldsymbol{\omega}_0) = \int_V d\mathbf{r} \int d\boldsymbol{\omega} \varphi(\mathbf{r}, \boldsymbol{\omega} | \mathbf{r}_0, \boldsymbol{\omega}_0) \tag{6.58}$$

is the average length travelled in V, for a given walker starting from $\mathbf{r}_0$ in direction $\boldsymbol{\omega}_0$ [113]. The angular flux is related to the outgoing density by [5, 113]

$$\varphi(\mathbf{r},\boldsymbol{\omega}|\mathbf{r}_0,\boldsymbol{\omega}_0) = \int_0^u ds\, \mathcal{P}_{_V}(s) \int \frac{d\boldsymbol{\omega}'}{\Omega_d}(p_s + \nu_1 p_f)\psi(\mathbf{r}-s\boldsymbol{\omega},\boldsymbol{\omega}'|\mathbf{r}_0,\boldsymbol{\omega}_0) + \varphi_1(\mathbf{r},\boldsymbol{\omega}|\mathbf{r}_0,\boldsymbol{\omega}_0), \tag{6.59}$$

where $\mathcal{P}_V(s) = 1 - \int_0^s T(l)dl = \langle l\rangle H(s)$ is the probability for a particle to perform a flight length larger than s once emitted at a collision, and $\varphi_1(\mathbf{r},\boldsymbol{\omega}|\mathbf{r}_0,\boldsymbol{\omega}_0)$ represents the contributions to the angular flux due to uncollided particles. Consider first the trajectories coming from outside V and crossing the surface S at $\mathbf{r}_0 \in S$. In this case, the uncollided flux reads

$$\varphi_1(\mathbf{r},\boldsymbol{\omega}|\mathbf{r}_0,\boldsymbol{\omega}_0) = \int_0^u ds\, \mathcal{P}_{_S}(s)\mathcal{Q}(\mathbf{r}-s\boldsymbol{\omega},\boldsymbol{\omega}), \tag{6.60}$$

where $\mathcal{P}_S(s) = 1 - \int_0^s H(l)dl$ is the probability that the uncollided length of the walker after crossing S is larger that s. Then, by taking the surface average of Eq. (6.59) and using the same arguments as for Eq. (6.51), we get the integral equation

$$\alpha_d S\langle\varphi\rangle_{_S}(\mathbf{r},\boldsymbol{\omega}) - 1 = \int_0^u \big[\langle l\rangle \alpha_d S\langle\chi\rangle_{_S}(\mathbf{r}-s\boldsymbol{\omega}) - 1\big] H(s)ds. \tag{6.61}$$

Consider next the trajectories born within the body. In this case, $\mathbf{r}_0 \in V$ and the uncollided angular flux reads

$$\varphi_1(\mathbf{r},\boldsymbol{\omega}|\mathbf{r}_0,\boldsymbol{\omega}_0) = \int_0^u ds\, \mathcal{P}_{_V}(s)\mathcal{Q}(\mathbf{r}-s\boldsymbol{\omega},\boldsymbol{\omega}). \tag{6.62}$$

Then, applying the volume average (6.16) to Eq. (6.59) yields the integral equation

$$\langle\varphi\rangle_{_V}(\mathbf{r},\boldsymbol{\omega}) = \int_0^u \left[\frac{1}{V\Omega_d} + \langle\chi\rangle_{_V}(\mathbf{r}-s\boldsymbol{\omega})\right] \langle l\rangle H(s)ds. \tag{6.63}$$

Equations (6.61) and (6.63) form a coupled system relating $\langle\varphi\rangle_{S,V}(\mathbf{r},\boldsymbol{\omega})$ to $\langle\chi\rangle_{S,V}(\mathbf{r})$. The integrals involving the outgoing collision densities appearing at the right hand side of Eqs. (6.61) and (6.63) can be simplified by resorting to Eqs. (6.53) and (6.55), respectively. Then, by combining the two equations, the surface average $\langle\varphi\rangle_{_S}(\mathbf{r},\boldsymbol{\omega})$ can be directly solved in terms of the volume average $\langle\varphi\rangle_{_V}(\mathbf{r},\boldsymbol{\omega})$, from which stems the identity

$$\langle l\rangle \alpha_d S\langle\varphi\rangle_{_S}(\mathbf{r},\boldsymbol{\omega}) = \langle l\rangle + (p_s + \nu_1 p_f - 1)V\Omega_d\langle\varphi\rangle_{_V}(\mathbf{r},\boldsymbol{\omega}), \tag{6.64}$$

whence Eq. (6.46). Finally, by recalling the definition in Eq. (6.58), integrating Eq. (6.46) over volume V and over directions Ω_d yields Eq. (6.1) as announced. Similarly as for the collision densities in Eq. (6.47), observe that Eq. (6.46) is valid for any pair of coordinates $\mathbf{r}$ and $\boldsymbol{\omega}$ and represents thus a result *stronger* than Eq. (6.1). In particular, when $p_s + \nu_1 p_f = 1$ Eq. (6.64) does not depend on $\langle\varphi\rangle_V$: the corresponding surface-averaged angular flux is constant over the body, namely,

$$\langle\varphi\rangle_S(\mathbf{r},\boldsymbol{\omega}) = \frac{1}{\alpha_d S}, \tag{6.65}$$

which is a purely geometrical quantity, independent of the features of the underlying random walk. In this case, the average travelled length in any sub-region $V' \subseteq V$ is simply proportional to V' and thus satisfies the *ergodic-like* property previously established for branching exponential flights [227].

Formulas (6.1) and (6.2) relate surface- to volume-averaged quantities. Surface and volume terms can be also separately singled out by algebraic manipulations of Eqs. (6.53), (6.55), (6.61) and (6.63). For the former, we have

$$\alpha_d S\big[\langle\varphi\rangle_S(\mathbf{r},\boldsymbol{\omega}) - \langle l\rangle\,\langle\psi\rangle_S(\mathbf{r},\boldsymbol{\omega})\big] = \int_0^u \big[\langle l\rangle\alpha_d S\,\langle\chi\rangle_S(\mathbf{r}-s\boldsymbol{\omega}) - 1\big]\big[H(s)-T(s)\big]ds. \tag{6.66}$$

The right hand side of Eq. (6.66) vanishes when $H(s) = T(s)$ for any s (i.e., for exponential flights), or more generally for any class of branching Pearson walks when $p_s + \nu_1 p_f = 1$ (for which $\langle\chi\rangle_S(\mathbf{r}) = 1/\langle l\rangle\alpha_d S$). In either case, we obtain the simple local relation $\langle\varphi\rangle_S(\mathbf{r},\boldsymbol{\omega}) = \langle l\rangle\langle\psi\rangle_S(\mathbf{r},\boldsymbol{\omega})$, from which stems also $\langle L\rangle_S = \langle l\rangle\langle N\rangle_S$. As for the latter, we get

$$\Omega_d V\big[\langle\varphi\rangle_V(\mathbf{r},\boldsymbol{\omega}) - \langle l\rangle\langle\psi\rangle_V(\mathbf{r},\boldsymbol{\omega})\big] = \langle l\rangle\int_0^u \big[1 + V\Omega_d\langle\chi\rangle_V(\mathbf{r}-s\boldsymbol{\omega})\big]\big[H(s)-T(s)\big]ds. \tag{6.67}$$

The quantity $1 + V\Omega_d\langle\chi\rangle_V$ is strictly positive, so that $\langle\varphi\rangle_V - \langle l\rangle\langle\psi\rangle_V$ vanishes only if $H(s) = T(s) = \exp(-s/\langle l\rangle)/\langle l\rangle$. Thus, it follows that the local relation $\langle\varphi\rangle_V(\mathbf{r},\boldsymbol{\omega}) = \langle l\rangle\langle\psi\rangle_V(\mathbf{r},\boldsymbol{\omega})$, whence also $\langle L\rangle_V = \langle l\rangle\langle N\rangle_V$, demands the Markov property of exponential flights, for any value of $p_s + \nu_1 p_f$.

6.5 Discussion and perspectives

As observed above, the form of the distribution $T(r)$ reflects the nature of the traversed medium. Neutrons and photons freely stream in the empty spaces between obstacles, which act as scattering centers. When the mean distance between such obstacles is much larger than the average size of the obstacles, and the spatial positions are uncorrelated, then the medium (i.e., the mixture of vacuum and scattering centers) may be considered homogeneous at the scale of a mean free path $\langle l\rangle$, which ensures an exponential jump length distribution $T(r)$ [5, 71, 76, 113]. The hypothesis of homogeneity may break down because of spatial correlations in the scattering centers, or because of strong heterogeneities in the size of the obstacles.

Optical materials with engineered obstacle sizes provide a fundamental tool for the analysis of light propagation in disordered media: when the non-scattering regions have a wide distribution spanning several orders of magnitude (fractal heterogeneity), $T(r)$ has been reported to follow a power-law decay of the kind $T(r) \sim r^{-1-\alpha}$, with $0 < \alpha < 2$ [70, 71]. This distribution is compatible with Lévy flights (anomalous) diffusion, whose properties are notoriously difficult to determine for confined geometries [233, 234]. In the case of radiative transfer in turbulent clouds, the measured jump lengths also display a power-law decay, due to the long-range correlations affecting the positions of the water droplets encountered by photons [73–75].

Quenched disorder in the form of non-scattering regions similarly induces correlations between steps [72]: this issue is central for neutron transport in pebble-bed reactors, whose core is filled with about $5 \cdot 10^5$ randomly packed spheres composed of nuclear fuel and graphite, having a radius comparable to the mean free path: jump distributions appear wider than exponential, and free paths enhanced [76]. The description of neutron and photon propagation in such heterogeneous systems is particularly challenging, and a comprehensive theoretical framework is still missing, especially in the presence of boundaries [71, 72, 76]. In this respect, formulas (6.1) and (6.2) contribute to the investigation of non-exponential particle transport, in that they accommodate for arbitrary geometries and jump length distributions $T(r)$ (we require however that $\langle l\rangle < +\infty$, which for Lévy flights would impose the restriction $\alpha > 1$). For illustration, a numerical example based on Monte Carlo simulation is discussed in Fig. 6.4.

So far, we have assumed that the surface of the body is transparent to the incoming particle flow. Each re-entry from the surface (if any) is taken into account as a new trajectory, which formally

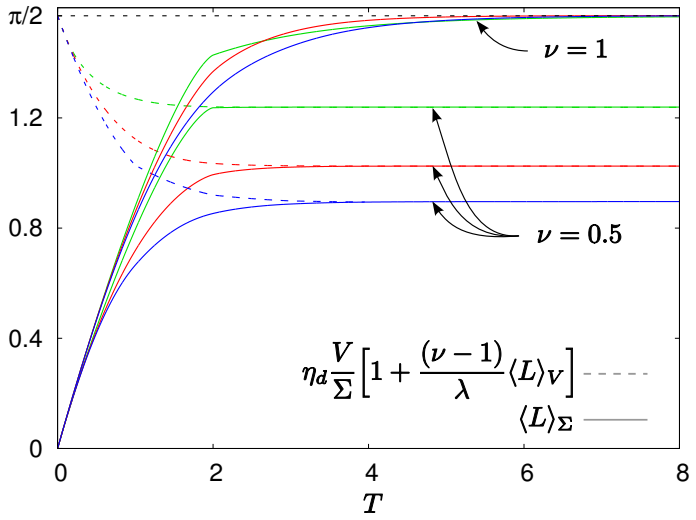

Figure 6.4: The length spent in a disk of unit radius ($d = 2$ and $\eta_2 V/\Sigma = \pi/2$) by branching Pearson walks with various kinds of jump distributions and various ν, as obtained by Monte Carlo simulation. We consider constant flights $T(u) = \delta(u-1)$ (blue), exponential flights $T(u) = \exp(-u)$ (red), and Pareto power-law flights $T(u) = \gamma u_m^\gamma / u^{\alpha+1}$ with $\gamma = 1.1$, $u_m = 1/11$ and $u \geq u_m$ (green). All distributions have been normalized so that $\lambda = 1$. Solid lines correspond to $\langle L\rangle_\Sigma$ and dashed lines to $\eta_d(V/\Sigma)[1 + (p_s + \nu_1 p_f - 1)\langle L\rangle_V/\lambda]$. Both quantities are observed from the entrance of a trajectory through Σ until the disappearance of the particle and all its descendants by either absorption in V or escape through Σ. For long observation times t, they converge to the same value, in agreement with Eq. (6.1). In particular, for $p_s + \nu_1 p_f = 1$ this value is independent of the jump distribution and is given by $\eta_2 V/\Sigma = \pi/2$.

corresponds to imposing absorbing boundary conditions on S. This is coherent with the definition given for chords traversing non-convex bodies [235] and ensures the validity of the previous results for convex as well as non-convex domains. More generally, we might consider *mixed* boundary conditions, the surface S being composed of an arbitrary combination of reflecting portions S_r and absorbing portions S_a. Trajectories can enter the body (and escape) only through S_a. Collisions on S_r can be indifferently modelled by assuming that the inward direction angle equals the outward direction angle (perfect reflection), or that the surface acts an isotropic diffuser [109]. In either case, by following the same strategy as above, it can be shown that any of these boundary conditions can be straightforwardly taken into account in formulas (6.1) and (6.2) by replacing the term S by S_a [109], which further extends the applicability of our results.

Chapter 7

Spatial spread and convex hull

The lesson of Lord Rayleigh's solution is that in open country the most probable place to find a drunken man who is at all capable of keeping on his feet is somewhere near his starting point.

K. Pearson, Nature **27**, 294 (1905).

7.1 Introduction

Consider a single particle performing a branching random walk and injected into a system at a given position $\mathbf{r}$ at time $t_0 = 0$. In principle, the branching mechanism stems from the interactions of the particles with the medium: in the case of neutron transport, e.g., fission events result from neutrons breaking fissile nuclei in the surrounding medium. Explicitly considering such interactions (the so-called depletion) would lead to non-linear models. Of particular interest is the *outbreak phase*, i.e., the early times of the injection, when the host population N is much larger than the number of injected individuals. During this regime, the host population hardly evolves, so that non-linear effects can be safely neglected and one can just monitor the evolution of the *injected population alone*.

The evolution of such system has been generalized to a variety of both deterministic as well as stochastic models, whose distinct advantages and shortcomings are discussed at length in [38, 236, 237]. Generally speaking, stochastic models are more suitable in presence of a small number of injected individuals, when fluctuations around the average may be relevant [236, 237]. During the early phases, the injected population is typically small: in this regime, the evolution can be modeled by resorting to a stochastic birth-death branching process of the Galton-Watson type for the number of injected [38, 236, 237], where each injected individual undergoes a reproduction event at rate β and get absorbed at rate γ. For the sake of simplicity, we will assume in the following that the reproduction event is binary, so that exactly two individuals are produced. As discussed in the previous Chapters, the ultimate fate of the injected particle in an unbounded support depends on the *reproduction number* $R_0 = \beta/\gamma$. If $R_0 > 1$ the number of descendants explodes and invades a finite fraction of the host population; if $R_0 < 1$ the descendants go to extinction, and in the critical case $R_0 = 1$ the descendant population remains constant, but fluctuations are typically long lived and completely control the time evolution of the injected population [38, 40, 65].

How far in space can the outbreak spread? Branching processes alone are not sufficient

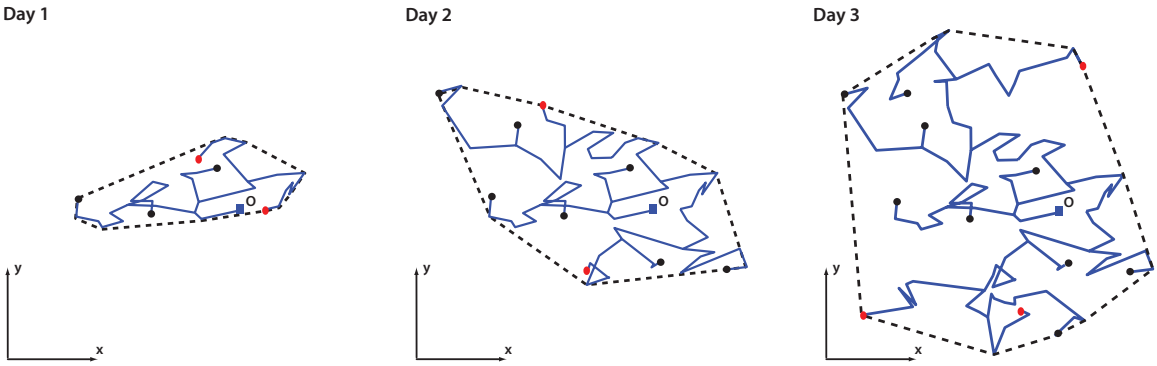

Figure 7.1: The snapshots of the trajectories of an assembly of injected particles at three different times (schematic), starting from a single individual at the origin O at time $t = 0$. Individuals that are still active at a given time t are displayed as red dots, while those already absorbed are shown as black dots. The convex hull enclosing the trajectories (shown as a dashed line) is a measure of geographical area covered by the spreading descendants. As the descendant particles grow in space, the associated convex hull also grows in time.

to describe this phenomenon, and spatial effects must necessarily be considered [38, 61, 238–240]. Quantifying the spatial spread of an outbreak is closely related to the modelling of the population displacements. Brownian motion is often considered as a paradigm for describing the migration of individuals, despite some well-known shortcomings: for instance, finite speed effects and preferential displacements are neglected. Nonetheless, as discussed in the previous Chapters, Brownian motion provides a reasonable basis for studying particle propagation.

While theoretical models based on branching Brownian motion have provided important insights on how the population size grows and fluctuates with time in a given domain [38,61,239,240], another fundamental question is how the spatial extension of the injected population evolves with time. The most popular and widely used method for quantifying such spatial spread consists in recording the set of positions of the injected particles and, at each time instant, construct a *convex hull*, i.e., a minimum convex polygon surrounding the positions (Fig. 7.1; for a precise definition of the convex hull, see below). The convex hull at time t then provides a rough measure of the area over which the injected particles have spread up to time t.

In this Chapter, we model the outbreak of a burst of injected particles as a Galton-Watson branching process in presence of Brownian spatial diffusion in dimension $d = 2$. Despite dynamics being relatively simple, the corresponding convex hull is a rather complex function of the trajectories of the individuals up to time t, whose statistical properties seem to be a formidable problem. Our main goal is to characterize the time evolution of the convex hull associated to this process, in particular its mean perimeter and area.

7.2 The model and the main results

Consider a population of N individuals, uniformly distributed in a two dimensional plane, with a single injected particle at the origin at the initial time. At the outbreak, it is sufficient to keep track of the positions of the injected particle and its descendants, which will be marked as 'particles'. The dynamics of these individuals is governed by a branching Brownian motion with the following stochastic rules. In a small time interval dt, each particle alternatively *(i)* get absorbed with

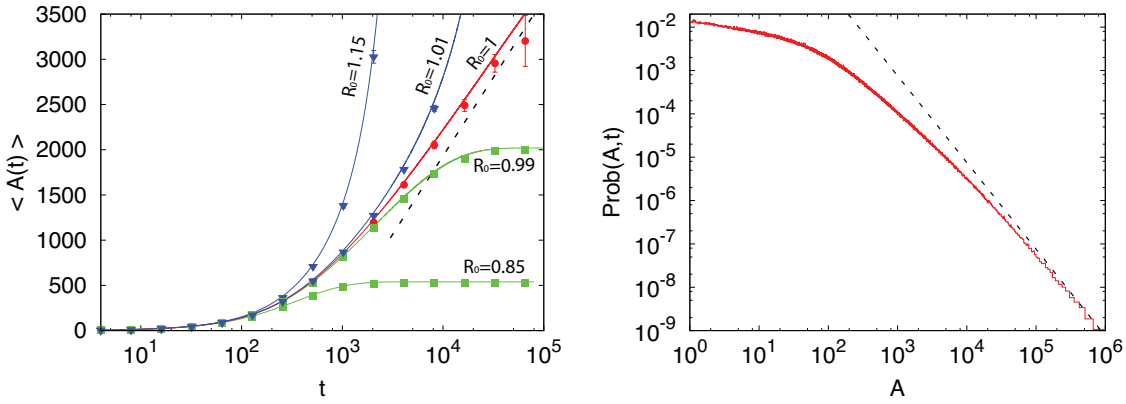

Figure 7.2: Left. The average area $\langle A(t)\rangle$ of the convex hull as a function of the observation time. For the parameter values, we have chosen $D = 1/2$ and $\beta = R_0\gamma = 0.01$. We considered five different values of R_0. We have obtained these results by two different methods: (i) via the numerical integration of Eqs. (7.11) and (7.16) and using Eq. (7.17). These results are displayed as solid lines. (ii) by Monte Carlo simulations of the two-dimensional branching Brownian motion with death with the same parameters, averaged over 10^5 samples. Monte Carlo are displayed as symbols. The dashed lines represent the asymptotic limits as given in Eq. (7.2) for the critical case $R_0 = 1$. Right. Distribution of the area of the convex hull for the critical case $R_0 = 1$, with $\gamma = 0.01$ and $D = 1/2$, as obtained by Monte Carlo simulations with $2 \cdot 10^6$ realizations. The dashed line corresponds to the power-law $(24\pi D/5\gamma)A^{-2}$ as predicted by Eq (7.33).

probability $\gamma\, dt$; *(ii)* undergoes reproduction with probability $\beta\, dt$. This conceptually corresponds to the birth of a new particle that can subsequently diffuse. The original particle still remains active, which means that the trajectory of the original particle branches into two new trajectories; *(iii)* diffuses with diffusion constant D with probability $1 - (\gamma + \beta)\, dt$. The coordinates $\{x(t), y(t)\}$ of the particle get updated to the new values $\{x(t) + \eta_x(t)\, dt, y(t) + \eta_y(t)\, dt\}$, where $\eta_x(t)$ and $\eta_y(t)$ are independent Gaussian white noises with zero mean and correlators $\langle \eta_x(t)\eta_x(t')\rangle = 2D\delta(t - t')$, $\langle \eta_y(t)\eta_y(t')\rangle = 2D\delta(t - t')$ and $\langle \eta_x(t)\eta_y(t')\rangle = 0$. The only dimensionless parameter in the model is the ratio $R_0 = \beta/\gamma$.

Consider now a particular history of the assembly of the trajectories of all the individuals up to time t, starting from a single injected particle initially at the origin (see Fig. 7.1). For every realization of the process, we construct the associated convex hull C. To visualize the convex hull, imagine stretching a rubber band so that it includes all the points of the set at time t inside it and then releasing the rubber band. It shrinks and finally gets stuck when it touches some points of the set, so that it can not shrink any further. This final shape is precisely the convex hull associated to this set.

In the following, we will show that the mean perimeter $\langle L(t)\rangle$ and the mean area $\langle A(t)\rangle$ of the convex hull are ruled by two coupled non-linear backward equations that can be solved numerically for all t (see Fig. 7.2). The asymptotic behaviour for large t can be determined analytically for the critical ($R_0 = 1$), subcritical ($R_0 < 1$) and supercritical ($R_0 > 1$) regimes. In particular, in the *critical* regime the mean perimeter *saturates* to a finite value as $t \to \infty$, while the mean area

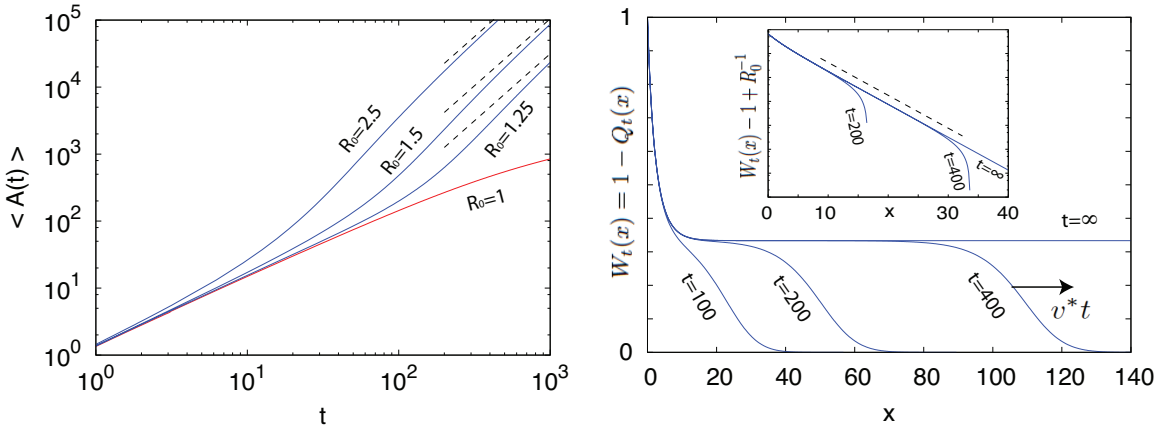

Figure 7.3: Left. The time behaviour of the average area in the supercritical regime for different values of $R_0 > 1$. Dashed lines represent the asymptotic scaling as in Eq. (7.4). The red curve corresponds to the critical regime. Right. The behaviour of $W_t(x) = 1 - Q_t(x)$ for $R_0 = 1.5$ at different times, as in Eq. (7.34). When $t \to \infty$, $W_t(x) \to 1 - R_0^{-1}$, and for large but finite times the travelling front behaviour is clearly visible. The inset displays the exponential convergence of $W_t(x)$ to the asymptotic limit. The dashed line represents $\xi = \sqrt{D/\gamma(R_0 - 1)}$.

diverges logarithmically for large t

$$\langle L(t \to \infty) \rangle = 2\pi \sqrt{\frac{6D}{\gamma}} + \mathcal{O}(t^{-1/2}) \tag{7.1}$$

$$\langle A(t \to \infty) \rangle = \frac{24\pi D}{5\gamma} \ln t + \mathcal{O}(1). \tag{7.2}$$

This prediction seems rather paradoxical at a first glance. How can the perimeter of a polygon be finite while its area is divergent? The resolution to this paradox owes its origin precisely to statistical fluctuations. The results in Eqs. (7.1) and (7.2) are true only on average. Of course, for each sample, the convex hull has a finite perimeter and a finite area. However, as we later show, the probability distributions of these random variables have power-law tails at long time limits. For instance, while $\text{Prob}(L, t \to \infty) \sim L^{-3}$ for large L (thus leading to a finite first moment), the area distribution behaves as $\text{Prob}(A, t \to \infty) \sim A^{-2}$ for large A. Hence the mean area is divergent as $t \to \infty$ (see Fig. 7.2).

When $R_0 \neq 1$, the evolution of the outbreak is controlled by a characteristic time t^*, which scales like $t^* \sim |R_0 - 1|^{-1}$. For times $t < t^*$ the descendants of the injected particle behave as in the critical regime. In the *subcritical* regime, for $t > t^*$ the quantities $\langle L(t) \rangle$ and $\langle A(t) \rangle$ rapidly saturate and the outbreak goes eventually to extinction. In contrast, in the *supercritical* regime, a new time-dependent behaviour emerges when $t > t^*$, since there exists a finite probability (namely $1 - 1/R_0$) that the outbreak never goes to extinction (Fig. 7.3). More precisely, we later show that

$$\langle L(t \gg t^*) \rangle = 4\pi \left(1 - \frac{1}{R_0}\right) \sqrt{D\,\gamma\,(R_0 - 1)}\, t \tag{7.3}$$

$$\langle A(t \gg t^*) \rangle = 4\pi \left(1 - \frac{1}{R_0}\right) D\,\gamma\,(R_0 - 1)\, t^2. \tag{7.4}$$

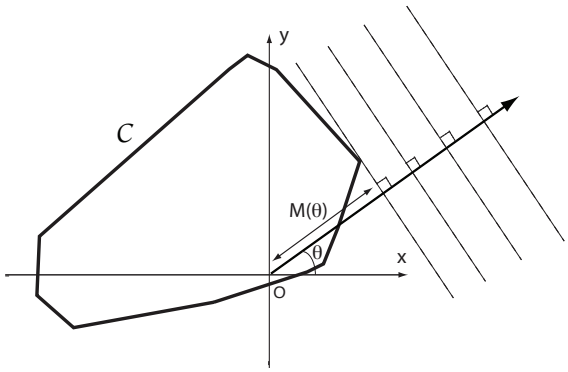

Figure 7.4: Cauchy's construction of the two-dimensional convex hull, with support function $M(\theta)$ representing the distance along the direction θ.

The ballistic growth of the convex hull stems from an underlying travelling front solution of the non-linear equation governing the convex hull behaviour. Indeed, the prefactor of the perimeter growth is proportional to the front velocity $v^* = 2\sqrt{D\,\gamma\,(R_0 - 1)}$. As time increases, the host population would decrease due to the growth of the individuals: this depletion effect leads to a breakdown of the outbreak regime and to a slowing down of the walker propagation.

7.3 The statistics of the convex hull

Characterizing the fluctuating geometry of C is a formidable task even in absence of branching ($\beta = 0$) and death ($\gamma = 0$), i.e., for purely diffusive process in two dimensions. Recent breakthroughs have nonetheless been obtained for diffusion processes [241, 242] by an adaptation of the Cauchy's integral geometric formulas for the perimeter and area of any closed convex curve in two dimensions. In fact, the problem of computing the mean perimeter and area of the convex hull of *any generic two dimensional* stochastic process can be mapped, using Cauchy's formulas, to the problem of computing the moments of the maximum and the time at which the maximum occurs for the associated one dimensional component stochastic process [241, 242]. This was used for computing, e.g., the mean perimeter and area of the convex hull of a two dimensional regular Brownian motion [241, 242] and of a two dimensional random acceleration process [243].

7.3.1 Cauchy's formula

Our main idea here is to extend this method to compute the convex hull statistics for the two dimensional branching Brownian motion. The problem of determining the perimeter and the area of the convex hull of any two-dimensional stochastic process $[x(\tau), y(\tau)]$ with $0 \leq \tau \leq t$ can be mapped to that of computing the statistics of the maximum and the time of occurrence of the maximum of the one dimensional component process $x(\tau)$ [241, 242]. This is achieved by resorting to a formula due to Cauchy, which applies to any closed convex curve C.

A sketch of the method is illustrated in Fig. 7.4. Choose the coordinates system such that the origin is inside the curve C and take a given direction θ. For fixed θ, consider a stick perpendicular to this direction and imagine bringing the stick from infinity and stop upon first touching the curve C. At this point, the distance $M(\theta)$ of the stick from the origin is called the

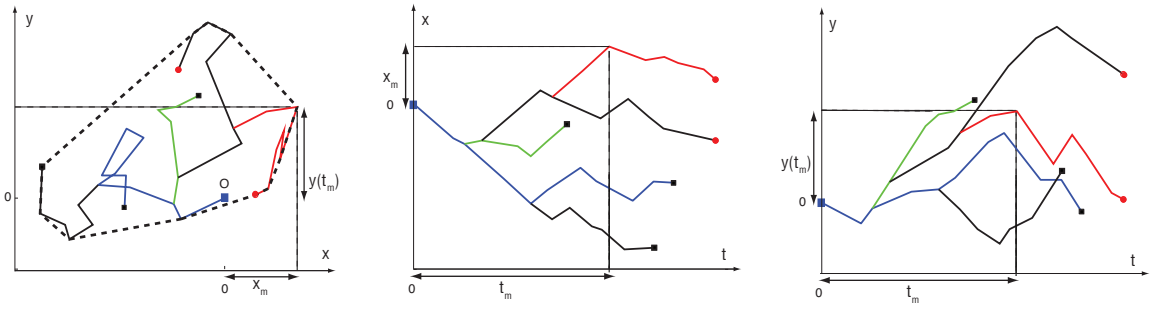

Figure 7.5: Left. A branching random walk composed of five individuals. At time $t = 0$, a single injected particle is at the origin O, and starts diffusing (blue line). At later times, this individual branches and gives rise to other individual. Among these, the red path reaches the maximum x_m along the x component up to the final time t. Active individuals at a given time t are displayed as red dots, whereas absorbed individuals as black dots. Center. The displacement along the x direction as a function of time. The red path reaches the global maximum x_m at time t_m. Right. The displacement along the y direction as a function of time. When the red path reaches the global maximum x_m at time t_m, its y coordinate attains the value $y(t_m)$. A crucial observation is that the y component of the trajectory connecting O to the red path is a regular Brownian motion. This is not the case for the x component, which is constrained to reach the global maximum of the branching process.

support function in the direction θ. Intuitively, the support function measures how close can one get to the curve C in the direction θ, coming from infinity. Once the support function $M(\theta)$ is known, then Cauchy's formulas [229, 244] give the perimeter L and the area A enclosed by C, namely,

$$L = \int_0^{2\pi} M(\theta)\, d\theta \tag{7.5}$$

$$A = \frac{1}{2}\int_0^{2\pi} \left[M^2(\theta) - (M'(\theta))^2\right] d\theta, \tag{7.6}$$

where $M'(\theta) = dM/d\theta$. For example, for a circle of radius $R = r$, $M(\theta) = r$, and one recovers the standard formulas: $L = 2\pi r$ and $A = \pi r^2$. When C is the convex hull of associated with the process at time t, we first need to compute its associated support function $M(\theta)$. A crucial point is to realize that actually $M(\theta) = \max_{0\le\tau\le t}\left[x(\tau)\cos(\theta) + y(\tau)\sin(\theta)\right]$ [241, 242]. Furthermore, if the process is rotationally invariant any average is independent of the angle θ. Hence for the average perimeter we can simply set $\theta = 0$ and write $\langle L(t)\rangle = 2\pi\langle M(0)\rangle$, where brackets denote the ensemble average over realizations. Similarly, for the average area $\langle A(t)\rangle = \pi\left[\langle M^2(0)\rangle - \langle M'(0)^2\rangle\right]$. Clearly, $M(0) = \max_{0\le\tau\le t}[x(\tau)]$ is then the maximum of the one dimensional component process $x(\tau)$ for $\tau \in [0, t]$.

Assume that $x(\tau)$ takes its maximum value $x(t_m)$ at time $\tau = t_m$ (see Fig. 7.5). Then, $M(0) = x(t_m) = x_m(t)$, and $M'(0) = y(t_m)$ [1]. Now, by taking the average over Cauchy's formulas,

[1] Actually, t_m implicitly depends on θ, hence formally $M'(\theta) = -x(t_m)\sin(\theta) + y(t_m)\cos(\theta) + \frac{dt_m}{d\theta}\left.\frac{dz_\theta(t)}{dt}\right|_{t=t_m}$. Nonetheless, since $z_\theta(t)$ is maximum at $t = t_m$, by definition $dz_\theta(t)/dt|_{t=t_m} = 0$.

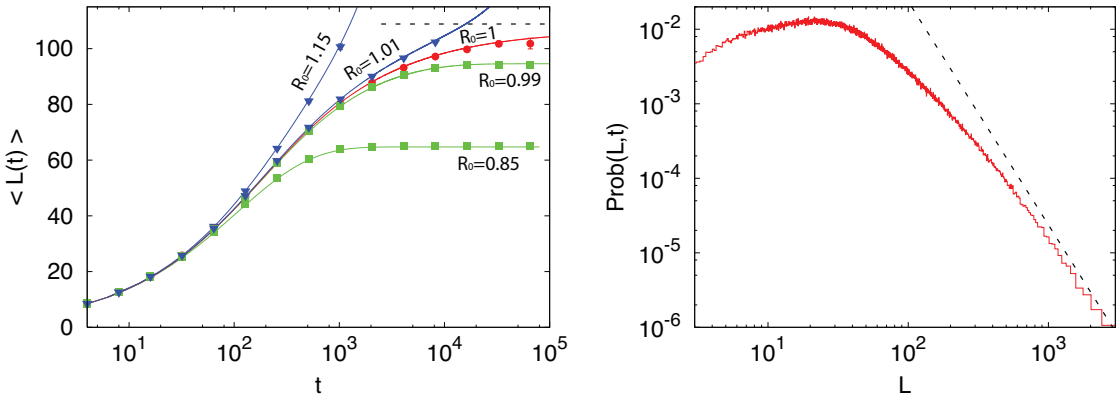

Figure 7.6: Left. The average perimeter $\langle L(t)\rangle$ of the convex hull as a function of the observation time. We have set $D = 1/2$ and $b = R_0\gamma = 0.01$, and consider different values of R_0. Results are obtained by: (i) numerical integration of the backward equation (solid lines, with $dt = 0.003125$ and $dx = 0.1768$). (ii) Monte Carlo simulation over 10^5 samples (symbols, with the same parameters and $dt = 0.25$). The asymptotic limits as given in Eq. (7.1) for the critical case $R_0 = 1$ are in dashed lines. Right. Distribution of the perimeter of the convex hull for the critical case $R_0 = 1$, with $\gamma = 0.01$ and $D = 1/2$, as obtained by Monte Carlo simulation over $2 \cdot 10^6$ realizations, with $dt = 1$ and $t = 4 \cdot 10^5$. The dashed line corresponds to the power-law L^{-3}.

and using isotropy in space, the average perimeter and area of the convex hull are given by

$$\langle L(t)\rangle = 2\pi\langle x_m(t)\rangle \tag{7.7}$$

$$\langle A(t)\rangle = \pi\left[\langle x_m^2(t)\rangle - \langle y^2(t_m)\rangle\right], \tag{7.8}$$

where x_m is the maximum displacement of our two-dimensional stochastic process in the x direction up to time t, t_m is the time at which the maximum displacement along x direction occurs and $y(t_m)$ is the ordinate of the process at t_m, i.e., when the displacement along the x direction is maximal. A schematic representation is provided in Fig. 7.5, where the global maximum x_m is achieved by one single injected individual, whose path is marked in red. Note that this argument is very general and is applicable to any rotationally invariant two dimensional stochastic process.

A crucial observation is that the y component of the trajectory connecting O to this red path is a regular one dimensional Brownian motion. Hence, given t_m and t, clearly $\langle y^2(t_m)\rangle = 2D\langle t_m\rangle$. Therefore,

$$\langle A(t)\rangle = \pi\left[\langle x_m^2(t)\rangle - 2D\langle t_m(t)\rangle\right]. \tag{7.9}$$

Equations (7.7) and (7.9) thus show that the mean perimeter and area of the outbreak are related to the extreme statistics of a one dimensional branching Brownian motion. Indeed, if we can compute the joint distribution $P_t(x_m, t_m)$, we can in turn compute the three moments $\langle x_m\rangle$, $\langle x_m^2\rangle$ and $\langle t_m\rangle$ that are needed in Eqs. (7.7) and (7.9). We show below that this can be performed exactly.

7.3.2 The convex hull perimeter and the maximum x_m

For the average perimeter, we just need the first moment $\langle x_m(t)\rangle = \int_0^\infty x_m\, q_t(x_m)\, dx_m$, where $q_t(x_m)$ denotes the probability density of the of the maximum of the one dimensional component process. It is convenient to consider the cumulative distribution $Q_t(x_m)$, i.e., the prob-

ability that the maximum x-displacement stays below a given value x_m up to time t. Then, $q_t(x_m) = dQ_t(x_m)/dx_m$ and$\langle x_m(t)\rangle = \int_0^\infty [1 - Q_t(x_m)]\, dx_m$. Since the process starts at the origin, its maximum x-displacement, for any time t, is necessarily nonnegative, i.e., $x_m \geq 0$. We next write down a backward Fokker-Planck equation describing the evolution of $Q_t(x_m)$ by considering the three mutually exclusive stochastic moves in a small time interval dt: starting at the origin at $t = 0$, the walker during the subsequent interval $[0, dt]$ is absorbed with probability γdt, branches with probability $\beta\, dt = R_0\gamma dt$, or diffuses by a random displacement $\Delta x = \eta_x(0)\, dt$ with probability $1-\gamma(1+R_0)dt$. In the last case, its new starting position is Δx for the subsequent evolution. Hence, for all $x_m \geq 0$, one can write

$$Q_{t+dt}(x_m) = \gamma dt + R_0\gamma dt Q_t^2(x_m) + [1 - \gamma(R_0 + 1)]dt\langle Q_t(x_m - \Delta x)\rangle, \tag{7.10}$$

where the expectation $\langle\rangle$ is taken with respect to the random displacements Δx. The first term means that if the process dies right at the start, its maximum up to t is clearly 0 and hence is necessarily less than x_m. The second term denotes the fact that in case of branching the maximum of each branch stays below x_m: since the branches are independent, one gets a square. The third term corresponds to diffusion. By using $\langle\Delta x\rangle = 0$ and $\langle\Delta x^2\rangle = 2Ddt$ and expanding Eq. (7.10) to the first order in dt and second order in Δx we obtain

$$\frac{\partial}{\partial t}Q = D\frac{\partial^2}{\partial x_m^2}Q - \gamma(R_0 + 1)Q + \gamma R_0 Q^2 + \gamma \tag{7.11}$$

for $x_m \geq 0$, satisfying the boundary conditions $Q_t(0) = 0$ and $Q_t(\infty) = 1$, and the initial condition $Q_0(x_m) = \Theta(x_m)$, where Θ is the Heaviside step function. Hence from Eq. (7.7)

$$\langle L(t)\rangle = 2\pi \int_0^\infty [1 - Q_t(x_m)]dx_m. \tag{7.12}$$

Equation (7.11) can be solved numerically for all t and all R_0, which allows subsequently computing $\langle L(t)\rangle$ in Eq. (7.12). The analysis of the statistical behaviour of the perimeter is illustrated in Figs. 7.6 and 7.7 for the critical and supercritical case, respectively.

7.3.3 The convex hull area

To compute the average area in Eq. (7.9), we need to evaluate $\langle x_m^2(t)\rangle$ as well as $\langle t_m\rangle$. Once the cumulative distribution $Q_t(x_m)$ is known, the second moment $\langle x_m^2(t)\rangle$ can be directly computed by integration, namely, $\langle x_m^2(t)\rangle = \int_0^\infty dx_m 2x_m(1 - Q_t(x_m))$. To determine $\langle t_m\rangle$, we need to also compute the probability density $p_t(t_m)$ of the random variable t_m. Unfortunately, writing down a closed equation for $p_t(t_m)$ is hardly feasible. Instead, we first define $P_t(x_m, t_m)$ as the joint probability density that the maximum of the x component achieves the value x_m at time t_m, when the full process is observed up to time t. Then, we derive a backward evolution equation for $P_t(x_m, t_m)$ and then integrate out x_m to derive the marginal density $p_t(t_m) = \int_0^\infty P_t(x_m, t_m)\, dx_m$. Following the same arguments as those used for $Q_t(x_m)$ yields a backward equation for $P_t(x_m, t_m)$:

$$P_{t+dt}(x_m, t_m) = [1 - \gamma(R_0 + 1)dt]\, \langle P_t(x_m - \Delta x, t_m - dt)\rangle + 2\gamma R_0 dt Q_t(x_m) P_t(x_m, t_m - dt). \tag{7.13}$$

The first term at the right hand side represents the contribution from diffusion. The second term represents the contribution from branching: we require that one of them attains the maximum x_m at the time $t_m - dt$, whereas the other stays below x_m ($Q_t(x_m)$ being the probability that this condition is satisfied). The factor 2 comes from the interchangeability of the particles. Developing Eq. (7.13) to leading order gives

$$\left[\frac{\partial}{\partial t} + \frac{\partial}{\partial t_m}\right] P_t = \left[D\frac{\partial^2}{\partial x_m^2} - \gamma(R_0 + 1) + 2\,\gamma\, R_0\, Q_t\right] P_t\,. \tag{7.14}$$

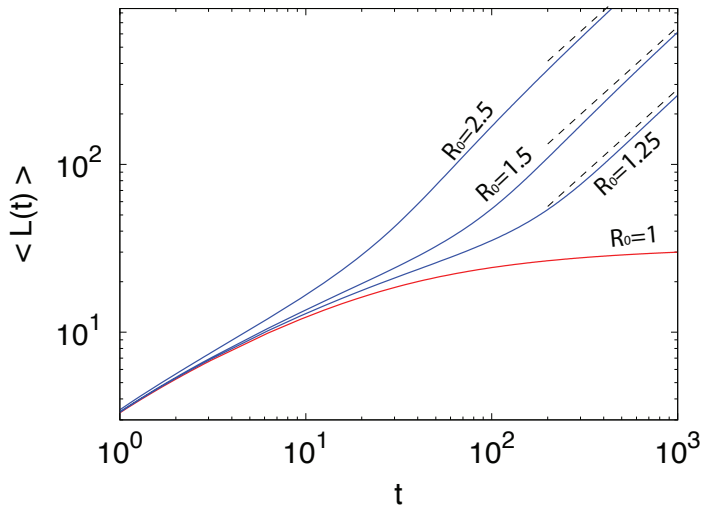

Figure 7.7: The time behaviour of the average perimeter in the supercritical regime for different values of $R_0 > 1$. Dashed lines represent the asymptotic scaling as in Eq. (7.4). The red curve corresponds to the critical regime.

This equation describes the time evolution of $P_t(x_m, t_m)$ in the region $x_m \geq 0$ and $0 \leq t_m \leq t$. It starts from the initial condition $P_0(x_m, t_m) = \delta(x_m)\,\delta(t_m)$ (since the process begins with a single infected with x component located at $x = 0$, it implies that at $t = 0$ the maximum $x_m = 0$ and also $t_m = 0$). For any $t > 0$ and $x_m > 0$, we have the condition $P_t(x_m, 0) = 0$. We need to also specify the boundary conditions at $x_m = 0$ and $x_m \to \infty$, which read (i) $P_t(\infty, t_m) = 0$ (since for finite t the maximum is necessarily finite) and (ii) $P_t(0, t_m) = \delta(t_m)\, q_t(x_m)|_{x_m=0}$. The latter condition comes from the fact that, if $x_m = 0$, this corresponds to the event that the x component of the entire process, starting at 0 initially, stays below 0 in the time interval $[0, t]$, which happens with probability $q_t(x_m)|_{x_m=0}$: consequently, t_m must necessarily be 0. Furthermore, by integrating $P_t(x_m, t_m)$ with respect to t_m we recover the marginal density $q_t(x_m)$.

Since we are only interested in $\langle t_m \rangle$, it is convenient to introduce

$$T_t(x_m) = \int_0^t t_m P_t(x_m, t_m) dt_m, \tag{7.15}$$

from which the average follows as $\langle t_m \rangle = \int dx_m T_t(x_m)$. Multiplying Eq. (7.14) by t_m and integrating by parts we get

$$\frac{\partial}{\partial t} T_t - q_t(x_m) = \left[D \frac{\partial^2}{\partial x_m^2} + 2\gamma R_0 Q_t - \gamma\,(R_0 + 1) \right] T_t, \tag{7.16}$$

with the initial condition $T_0(x_m) = 0$, and the boundary conditions $T_t(0) = 0$ and $T_t(\infty) = 0$. Eq. (7.16) can be integrated numerically, together with Eq. (7.11), and the behaviour of

$$\langle A(t) \rangle = \pi \int_0^\infty dx_m \left[2x_m (1 - Q_t(x_m)) - T_t(x_m) \right] \tag{7.17}$$

as a function of time is illustrated in Fig. 7.2.

7.4 The critical regime

We now focus on the critical regime $R_0 = 1$. We begin with the average perimeter: for $R_0 = 1$, Eq. (7.11) admits a stationary solution as $t \to \infty$, which can be obtained by setting $\partial Q/\partial t = 0$ and solving the resulting differential equation. In fact, this stationary solution is known from literature [48]. Taking the derivative of this solution with respect to x_m, we get the stationary probability density of the maximum x_m

$$q_\infty(x_m) = \partial_{x_m} Q_\infty(x_m) = \frac{2\sqrt{\frac{\gamma}{6D}}}{\left(1+\sqrt{\frac{\gamma}{6D}}x_m\right)^3}. \tag{7.18}$$

The average is $\langle x_m \rangle = \int_0^\infty x_m\, q_\infty(x_m)\, dx_m = \sqrt{6D/\gamma}$, which yields then Eq. (7.1) for the average perimeter of the convex hull at late times.

To compute the average area in Eq. (7.9), we need to also evaluate the second moment $\langle x_m^2(t)\rangle$, which diverges as $t \to \infty$, due to the power-law tail of the stationary probability density $q_\infty(x_m) \propto x_m^{-3}$ for large x_m. Hence, we need to consider large but finite t. In this case, the time dependent probability density $q_t(x_m)$ displays a scaling form which can be conveniently written as

$$q_t(x_m) \simeq q_\infty(x_m) f\left(\frac{x_m}{\sqrt{Dt}}\right), \tag{7.19}$$

where $f(z)$ is a rapidly decaying function with $f(z \ll 1) \simeq 1$, and $f(z \gg 1) \simeq 0$. Using the scaling form of Eq. (7.19) and Eq. (7.11) one can derive a differential equation for $f(z)$. But it turns out that we do not really need the solution of $f(z)$.

From Eq. (7.19) we see that the asymptotic power-law decay of $q_t(x_m)$ for large x_m has a cut-off around $x_m^* \sim \sqrt{Dt}$ and $f(z)$ is the cut-off function. The second moment at finite but large times t is given by $\langle x_m^2(t)\rangle = \int_0^\infty x_m^2 q_t(x_m)\, dx_m$. Substituting the scaling form and cutting off the integral over x_m at $x_m^* = c\sqrt{t}$ (where the constant c depends on the precise form of $f(z)$) we get, to leading order for large t,

$$\langle x_m^2(t)\rangle \simeq \int_0^{x_m^*} x_m^2\, q_\infty(x_m)\, dx_m \simeq \frac{6D}{\gamma}\ln t\ . \tag{7.20}$$

Thus, interestingly the leading order result is universal, i.e, independent of the details of the cut-off function $f(z)$ (the c-dependence is only in the subleading term). To complete the characterization of $\langle A(t)\rangle$ in Eq. (7.9), we still need to determine $\langle t_m \rangle$.

7.4.1 Analysis of t_m and the critical area

In the critical case $R_0 = 1$, the stationary joint probability density $P_\infty(x_m, t_m)$ satisfies (upon setting $\partial P_t/\partial t = 0$ in Eq. (7.14))

$$\frac{\partial}{\partial t_m} P_\infty(x_m, t_m) = \left[D\frac{\partial^2}{\partial x_m^2} - \frac{2\gamma}{\left[1+\sqrt{\frac{\gamma}{6D}}x_m\right]^2}\right] P_\infty(x_m, t_m)\ . \tag{7.21}$$

For any $x_m > 0$, we have the condition $P_\infty(x_m, 0) = 0$. The boundary conditions for Eq(7.21) are $P_\infty(x_m \to \infty, t_m) = 0$ and $P_\infty(0, t_m) = q_\infty(0)\,\delta(t_m) = 2\sqrt{\gamma/(6D)}\,\delta(t_m)$. We first take the Laplace transform of (7.21), namely,

$$\tilde{P}_\infty(x_m, s) = \int_0^\infty e^{-st_m} P_\infty(x_m, t_m)\, dt_m. \tag{7.22}$$

This gives for all $x_m > 0$

$$\frac{D}{s}\frac{\partial^2}{\partial x_m^2}\tilde{P}_\infty(x_m,s) = \left[1 + \frac{12}{\frac{s}{D}(\sqrt{\frac{6D}{\gamma}} + x_m)^2}\right]\tilde{P}_\infty(x_m,s), \tag{7.23}$$

where we have used the condition $P_\infty(x_m,0) = 0$ for any $x_m > 0$. This second order differential equation satisfies two boundary conditions: $\tilde{P}_\infty(\infty,s) = 0$ and $\tilde{P}_\infty(0,s) = 2\sqrt{\gamma/(6D)}$. The latter condition is obtained by Laplace transforming $P_\infty(0,t_m) = 2\sqrt{\gamma/(6D)}\,\delta(t_m)$. By setting

$$z = \left(\sqrt{\frac{6D}{\gamma}} + x_m\right)\sqrt{\frac{s}{D}}, \tag{7.24}$$

we rewrite the equation as

$$\frac{\partial^2}{\partial z^2}\tilde{P}_\infty - \tilde{P}_\infty - \frac{12}{z^2}\tilde{P}_\infty = 0. \tag{7.25}$$

Upon making the transformation $\tilde{P}_\infty(z) = \sqrt{z}\,F(z)$, the function $F(z)$ satisfies then the Bessel differential equation

$$\frac{d^2}{dz^2}F(z) + \frac{1}{z}\frac{d}{dz}F(z) - \left[1 + \frac{49}{4z^2}\right]F(z) = 0. \tag{7.26}$$

The general solution of this differential equation can be expressed as a linear combination of two independent solutions: $F(z) = A\,I_{7/2}(z) + B\,K_{7/2}(z)$ where $I_\nu(z)$ and $K_\nu(z)$ are modified Bessel functions. Since, $I_\nu(z) \sim e^z$ for large z, it is clear that to satisfy the boundary condition $\tilde{P}_\infty(\infty,s) = 0$ (which means $F(z\to\infty) = 0$), we need to choose $A = 0$. Hence we are left with $F(z) = BK_{7/2}(z)$, where the constant B is determined from the second boundary condition $\tilde{P}_\infty(0,s) = 2\sqrt{\gamma/(6D)}$. By reverting to the variable x_m, we finally get

$$\tilde{P}_\infty(x_m,s) = 2\sqrt{\frac{\gamma}{6D}}\sqrt{1+\frac{\gamma}{6D}\,x_m}\,\frac{K_{7/2}\left[\left(\sqrt{\frac{6D}{\gamma}} + x_m\right)\sqrt{\frac{s}{D}}\right]}{K_{7/2}\left[\sqrt{\frac{6s}{\gamma}}\right]}. \tag{7.27}$$

Now, we are interested in determining the Laplace transform of the marginal density $\tilde{p}_\infty(s) = \int_0^\infty e^{-s\,t_m}\,p_\infty(t_m)\,dt_m$ where $p_\infty(t_m) = \int_0^\infty P_\infty(x_m,t_m)\,dx_m$. Taking Laplace transform of this last relation with respect to t_m gives $\tilde{p}_\infty(s) = \int_0^\infty \tilde{P}_\infty(x_m,s)\,dx_m$. Once we know $\tilde{p}_\infty(s)$, we can invert it to obtain $p_\infty(t_m)$. Since we are interested only in the asymptotic tail of $p_\infty(t_m)$, it suffices to investigate the small s behavior of $\tilde{p}_\infty(s)$. Integrating Eq. (7.27) over x_m and taking the $s\to 0$ limit, we obtain after some algebra

$$\tilde{p}_\infty(s) = 1 + \frac{3}{5\gamma}\,s\,\ln(s) + \cdots. \tag{7.28}$$

We further note that

$$\int_0^\infty e^{-st_m}\,t_m^2\,p_\infty(t_m)\,dt_m = \frac{d^2}{ds^2}\tilde{p}_\infty(s) \simeq \frac{3}{5\gamma s}, \tag{7.29}$$

which can then be inverted to give the following asymptotic behavior for large t_m

$$p_\infty(t_m) \simeq \frac{3}{5\gamma t_m^2}\,. \tag{7.30}$$

Analogously as for $\langle x_m^2 \rangle$, the moment $\langle t_m \rangle \to \infty$, due to the power-law tail $p_\infty(t_m) \propto t_m^{-2}$. Hence we need to compute $\langle t_m \rangle$ for large but finite t: in this case, the time-dependent solution displays a scaling behavior

$$p_t(t_m) \simeq p_\infty(t_m)\, g\left(\frac{t_m}{t}\right), \tag{7.31}$$

where the scaling function $g(z)$ satisfies the conditions $g(z \ll 1) \simeq 1$ and $g(z \gg 1) = 0$.

Much like for the marginal density $q_t(x_m)$, we have a power-law tail of $p_t(t_m)$ for large t_m that has a cut-off at a scale $t_m^* \sim t$, and $g(z)$ is the cut-off function. As in the case of x_m, we do not need the precise form of $g(z)$ to compute the leading term of the first moment $\langle t_m \rangle = \int_0^\infty p_t(t_m)\, t_m\, dt_m$ for large t. Cutting off the integral at $t_m^* = c_1 t$ (where c_1 depends on the precise form of $g(z)$) and performing the integration gives

$$\langle t_m \rangle \simeq \int_0^t t_m\, p_\infty(t_m)\, dt_m \simeq \frac{3}{5\gamma} \ln t, \tag{7.32}$$

for large t, which leads again to a logarithmic divergence in time. Finally, substituting Eqs. (7.20) and (7.32) in Eq. (7.9) gives the result announced in Eq. (7.2).

7.4.2 Scaling arguments

A deeper understanding of the statistical properties of the process would demand knowing the full distribution $\mathrm{Prob}(L,t)$ and $\mathrm{Prob}(A,t)$ of the perimeter and area. These seem rather hard to compute, but one can obtain the asymptotic tails of the distributions by resorting to scaling arguments. Following the lines of Cauchy's formula, it is reasonable to assume that for each sample the perimeter scales as $L(t) \sim x_m(t)$. We have seen that the distribution of $x_m(t)$ has a power-law tail for large t: $q_\infty(x_m) \sim x_m^{-3}$ for large x_m. Then, assuming the scaling $L(t) \sim x_m(t)$ and using $\mathrm{Prob}(L, t \to \infty)\, dL \sim q_\infty(x_m)\, dx_m$, it follows that at late times the perimeter distribution also has a power-law tail: $\mathrm{Prob}(L, t \to \infty) \sim L^{-3}$ for large L. Similarly, using the Cauchy formula for the area, we can reasonably assume that for each sample $A(t) \sim x_m^2(t)$ in the scaling regime. Once again, using $\mathrm{Prob}(A, t \to \infty)\, dA = q_\infty(x_m)\, dx_m$, we find that the area distribution also converges, for large t, to a stationary distribution with a power-law tail: $\mathrm{Prob}(A, t \to \infty) \sim A^{-2}$ for large A. Moreover, the logarithmic divergence of the mean area calls for a precise ansatz on the tail of the area distribution, namely,

$$\mathrm{Prob}(A,t) \xrightarrow[A \gg 1]{} \frac{24\pi D}{5\gamma} A^{-2} h\left(\frac{A}{Dt}\right), \tag{7.33}$$

where the scaling function $h(z)$ satisfies the conditions $h(z \ll 1) = 1$, and $h(z \gg 1) \simeq 0$. It is possible to verify that this is the only scaling compatible with Eq. (7.2). These two results are consistent with the fact that for each sample typically $A(t) \sim L^2(t)$ at late times in the scaling regime. Our scaling predictions are in agreement with our Monte Carlo simulations (see Fig. 7.2). The power-law behaviour of $\mathrm{Prob}(A,t)$ implies that the average area is not representative of the typical behaviour of the epidemic area, which is actually dominated by fluctuations and rare events, with likelihood given by Eq. (7.33).

7.5 The supercritical regime

When $R_0 > 1$, it is convenient to rewrite Eq. (7.11) in terms of $W(x_m, t) = 1 - Q(x_m, t)$:

$$\frac{\partial}{\partial t} W = D\, \frac{\partial^2}{\partial x_m^2} W + \gamma(R_0 - 1) W - \gamma R_0 W^2 \tag{7.34}$$

starting from the initial condition $W(x_m, 0) = 0$ for all $x_m > 0$ (see Fig. 7.3). From Eq. (7.12), $\langle L(t)\rangle = 2\pi \int_0^\infty W(x_m, t)\, dx_m$ is just the area under the curve $W(x_m, t)$ vs. x_m, up to a factor 2π. As $t \to \infty$, the system approaches a stationary state for all $R_0 \geq 1$, which can be obtained by setting $\partial_t W = 0$ in Eq. (7.34). For $R_0 > 1$ the stationary solution $W(x_m, \infty)$ approaches the constant $1 - 1/R_0$ exponentially fast as $x_m \to \infty$, namely, $W(x_m, \infty) - 1 + R_0^{-1} \to \exp[-x_m/\xi]$, with a characteristic length scale $\xi = \sqrt{D/\gamma(R_0 - 1)}$. However, for finite but large t, $W(x_m, t)$ as a function of x_m has a two-step form: it first decreases from 1 to its asymptotic stationary value $1 - 1/R_0$ over the length scale ξ, and then decreases rather sharply from $1 - 1/R_0$ to 0. The frontier between the stationary asymptotic value $1 - 1/R_0$ (stable) and 0 (unstable) moves forward with time at constant velocity, thus creating a travelling front at the right end, which separates the stationary value $1 - 1/R_0$ to the left of the front and 0 to the right. This front advances with a constant velocity v^* that can be estimated using the standard velocity selection principle [203,205,245]. Near the front where the nonlinear term is negligible, the equation admits a travelling front solution: $W(x_m, t) \sim \exp[-\lambda(x_m - v\, t)]$, with a one parameter family of possible velocities $v(\lambda) = D\lambda + \gamma(R_0 - 1)/\lambda$, parametrized by λ. This dispersion relation $v(\lambda)$ has a minimum at$\lambda = \lambda^* = \sqrt{\gamma(R_0 - 1)/D}$, where $v^* = v(\lambda^*) = 2\sqrt{D\gamma(R_0 - 1)}$. According to the standard velocity selection principle [203, 205, 245], for a sufficiently sharp initial condition the system will choose this minimum velocity v^*. The width of the front remains of $\sim \mathcal{O}(1)$ at large t. Thus, due to this sharpness of the front, to leading order for large t one can approximate $W(x_m, t) \simeq (1 - 1/R_0)\Theta(v^* t - x_m)$ near the front. Hence, to leading order for large t one gets $\langle x_m(t)\rangle \simeq (1 - 1/R_0)v^* t$ and $\langle x_m^2\rangle \simeq (1 - 1/R_0)\,(v^* t)^2$. The former gives, from Eq. (7.7), the result announced in Eq. (7.4). For the mean area in Eq. (7.9), the term $\langle x_m^2\rangle \sim t^2$ for large t dominates over $\langle t_m\rangle \sim t$ (which can be neglected), and we get the result announced in Eq. (7.4).

We conclude with an additional remark. In our computations of the mean perimeter and area, we have averaged over all realizations of the epidemics up to time t, including those which are already absorbed at time t. It would also be interesting to consider averages only over the ensemble of individuals that are still active at time t. In this case we expect different scaling laws for the mean perimeter and the mean area of the convex hull. In particular, in the critical case, we believe that the behaviour would be much closer to that of a regular Brownian motion.

Chapter 8

Critical catastrophe and beyond

Where there is independence there must be the normal law.

M. Kac, *Enigmas of Chance* (1987).

8.1 Introduction

The evolution of a collection of individuals subject to reproduction and death can be effectively explained by the Galton-Watson model [29], if particle-particle correlations and non-linear effects can be safely neglected. When the death rate is larger than the birth rate, the system is said to be sub-critical: the population size decreases on average, and the ultimate fate is extinction. This occurs for instance for nuclear collision cascades, where charged particles are progressively scattered and absorbed by the medium [1, 29]. When on the contrary the birth rate is larger than the death rate, such as for bacteria reproducing on a Petri dish [52], the system is said to be super-critical. In this case, the population size grows on average. However, because of fluctuations on the number of individuals in the population, a non-trivial finite extinction probability exists for the whole system [29]. A super-critical regime is typically found also during the early stages of an epidemic (the so-called 'outbreak' phase), where a fast growth of the infected population is observed, until non-linear effects due to the depletion of susceptible individuals ultimately slow down the epidemic [62].

In the intermediate regime, the population stays constant on average, and the system is said to be exactly critical. A prominent example of a system operating at the critical point is provided by the self-sustaining chains of neutrons in nuclear reactors [4, 32]. Avalanches and self-organized criticality are other examples of system operating at or close to the critical point. At the critical or nearly critical regime, fluctuations due to birth and death may become particularly strong [29]. Assuming without loss of generality that the birth and death rates are Poissonian, from the Galton-Watson theory it is known that at criticality the total number $N(t)$ of particles in the system stays constant on average, i.e., $\mathbb{E}_t[N] = N_0$, whereas the variance grows in time, i.e., $Var[N] = \mathbb{E}_t[N^2] - \mathbb{E}_t^2[N] \propto \beta N_0 t$, where β is the birth rate [29]. This immediately implies that the typical fluctuations of the population size, say $\sqrt{Var[N]}$, will become comparable to the average population size N_0 over a time $\sim N_0/\beta$. Hence, a critical system will have a characteristic extinction time of the order of $\tau_E \simeq N_0/\beta$ [29]. This quite extreme behaviour has been observed for instance in avalanche dynamics. In the context of neutron multiplication, the shut-down of a reactor

operated in the critical regime due to the extinction of the fission chains has been theoretically investigated and goes under the name of *critical catastrophe* [4]. However, such observation is in open contradiction with the experience: the behaviour of nuclear reactors at the critical point is actually stable. This apparent paradox has been explained by pointing out that including feedback mechanisms (representing for instance human intervention) in the Galton-Watson model induces a stabilizing effect acting against the total population fluctuations [4].

The interplay between the fluctuations stemming from birth-death events and those stemming from random displacements will subtly affect the spatial distribution of the particles in such systems [33, 203, 204, 208]. In particular, it has been shown that at and close to the critical point a collection of such individuals, although spatially uniform at the initial time, may eventually display a wild patchiness (see Fig. 8.1), with particles closely packed together and empty spaces nearby [42, 52, 199, 200]. Spatial clustering phenomena have been first identified in connection with mathematical models of ecological communities [43, 44], and since then have been thoroughly investigated for both infinite and finite collections of individuals [42, 51, 53, 199, 200]. Non-uniform neutron densities in the reactor fuel elements might lead to local peaks in the deposited energy (hot spots) and represent thus a most unwanted event with respect to the safe operation of nuclear power plants [246]. In view of the findings concerning the impact of a feedback on the global neutron population, we might wonder whether imposing a global feedback on the total neutron population affects also the local spatial behaviour of the particles.

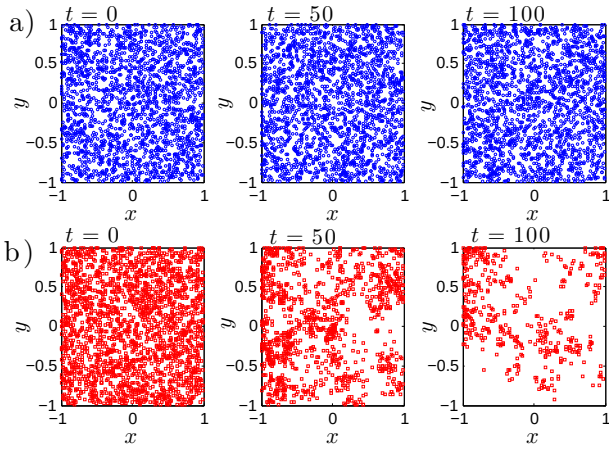

Figure 8.1: Monte Carlo simulation of the evolution of a collection of particles in a two-dimensional box. The particles are prepared at $t = 0$ on a uniform spatial distribution. In case a), particles follow regular Brownian motions: as time increases, positions are shuffled by diffusion, but the spatial distribution of the particles stays uniform. In case b), particles follow a branching Brownian motion with equal birth and death rates: as time increases, the population undergoes large fluctuations, and the particle density displays a wild patchiness. Eventually, the entire population goes to extinction.

8.2 A prototype model of nuclear reactor

To fix the ideas, here we will focus on the widely used light-water reactors. The nuclear fuel is made of uranium, arranged in a regular lattice and plunged in light water. A fission chain begins with a neutron emitted at high energy from a fission event (see Fig. 8.2). The neutron enters the surrounding water, slows down towards thermal equilibrium, and then starts diffusing. If the

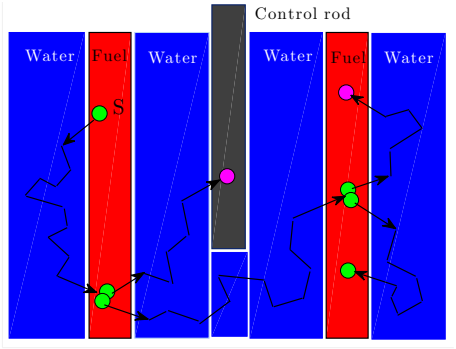

Figure 8.2: Simplified scheme of neutron propagation within a nuclear reactor. A fission chain begins with a source neutron (marked with S in the figure) born from a fission event in the fuel. The neutron diffuses in the water and may eventually come back to a fuel element. Then, it can either be absorbed (these events are marked by magenta circles), in which case the trajectory terminates; or it can give rise to a new fission, upon which additional neutrons are set free (these events are marked in green), and the fission chain is kept alive. The system is operated at the critical point when the average net number of neutrons produced at fission is exactly compensated by the losses by absorptions. A control rod can absorb the excess neutrons so as to adjust the total population and enforce the critical regime.

neutron eventually re-enters the fuel, it may *i*) be absorbed on the ^{238}U isotope of uranium, in which case the chain is terminated; or *ii*) give rise to a new fission event by colliding with the ^{235}U fissile isotope, whereupon a random number of high-energy neutrons are emitted. The water surrounding the fuel lattice acts as a reflector and prevents the neutrons from escaping from the core. A number of control rods are inserted into the core, with the aim of absorbing the excess neutrons and keep the population constant (this ensures a constant power output). When the neutron population grows, the control rods are inserted more deeply into the core, slowing down the chain reaction. On the contrary, when the population decreases, the control rods are raised, accelerating the chain reaction.

The energy- and spatial-dependent behaviour of a nuclear reactor can be fully assessed only by resorting to large-scale numerical simulations including a realistic description of the heterogeneous geometry [30,246]. However, here we will introduce a simplified prototype model of a nuclear reactor that yet retains all the key ingredients of a real system.

We will assume that the reactor can be represented as a collection of N neutrons undergoing diffusion, reproduction and absorption within an homogeneous d-dimensional box of finite volume V, with reflecting (mass-preserving) boundaries. It is reasonable to require that the initial neutron population has a uniform spatial distribution. The stochastic paths of neutrons are known to follow position- and velocity-dependent exponential flights [4]. For our model, we approximate these paths by d-dimensional branching Brownian motions with a constant diffusion coefficient D. The diffusing walker undergoes absorption at rate γ and reproduction at rate β. In this latter case, the neutron disappears and is replaced by a random number i of descendants, distributed according to a law p_i with average $\nu_1 = \sum_i i p_i$. In order for the reactor to be exactly critical, we must have $\gamma = \beta(\nu_1 - 1)$.

8.3 Fluctuations at criticality

Clustering phenomena have been mostly analysed either in the thermodynamic limit ($V \to \infty$ and $N \to \infty$, with finite N/V [44,53]) or in unbounded domains with finite N [199,200]. A re-

alistic description of actual physical systems demands however that the effects due to the finiteness of the viable volume V be explicitly taken into account. We will show that a neutron population within a finite-size reactor *at the critical regime* will ultimately undergo wild spatial fluctuations over the entire volume when population control is not applied. Population control may be enforced by imposing that the total number N of neutrons is preserved. The simplest way to impose such requirement is to correlate reproduction and absorption events: at each fission, a neutron disappears and is replaced by a random number $i \geq 1$ of descendants, and $i-1$ other neutrons are simultaneously removed from the collection in order to ensure the conservation of total population (see Fig. 8.3). This mechanism has been first introduced in the context of theoretical ecology (with binary branching), where similar large-scale constraints such as limited food resources have been shown to quench the wild fluctuations in the number of individuals that are expected for an unconstrained community [199, 200].

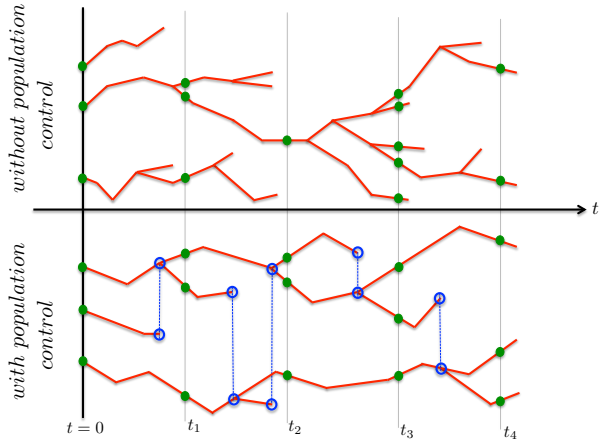

Figure 8.3: The evolution of a collection of critical branching random walks with binary fission. At time $t = 0$, $N = 3$ particles are present, and the system is observed at successive times $t_1 < t_2 < t_3 < t_4$. Top. When population control is not enforced, the number of particles present at the observation times fluctuates because births and deaths occur at random instants. Bottom. When population control is enforced, at each fission event a neutron is randomly chosen and removed, which exactly preserves N: at observation times, the total population is constant.

Let us denote by $n(\mathbf{x}_i, t)$ the instantaneous density of neutrons located at $\mathbf{x}_i$ at time t. For a *critical* reactor, the average neutron density at a point $\mathbf{x}_i$ reads

$$c_t(\mathbf{x}_i) = \mathbb{E}_t[n(\mathbf{x}_i, t)] = N \int d\mathbf{x}_0 q(\mathbf{x}_0) \mathcal{G}_t(\mathbf{x}_i; \mathbf{x}_0). \tag{8.1}$$

Here q is the spatial probability distribution function of the neutrons at time $t = 0$, and $\mathcal{G}_t(\mathbf{x}; \mathbf{x}_0)$ is the Green's function satisfying the backward equation

$$\frac{\partial}{\partial t} \mathcal{G}_t(\mathbf{x}; \mathbf{x}_0) = D \nabla^2_{\mathbf{x}_0} \mathcal{G}_t(\mathbf{x}; \mathbf{x}_0), \tag{8.2}$$

with the boundary conditions of the problem at hand. Note that at criticality the average neutron density becomes indistinguishable from that of N regular Brownian particles. This result holds true independently of whether population control is applied. For an initial uniform source of particles $q = 1/V$, it immediately follows that for a collection of N critical branching Brownian motions we simply have a uniform average density $c_t(\mathbf{x}_i) = N/V$, at any time.

In order to probe the spatial inhomogeneities of the neutron population due to clustering, we must therefore go beyond the average behaviour. A fundamental tool is provided by the two-point (or pair) correlation function $h_t(\mathbf{x}_i, \mathbf{x}_j)$ between positions $\mathbf{x}_i$ and $\mathbf{x}_j$, namely, the average density of pairs with the former particle in $\mathbf{x}_i$ and the latter in $\mathbf{x}_j$. This quantity is proportional to the joint probability density for $\mathbf{x}_i$ and $\mathbf{x}_j$. For N independent random walkers (in absence of branching and death) we simply have

$$h_t^i(\mathbf{x}_i, \mathbf{x}_j) = N(N-1) \int d\mathbf{x}_0 q(\mathbf{x}_0) \mathcal{G}_t(\mathbf{x}_i; \mathbf{x}_0) \int d\mathbf{x}_0 q(\mathbf{x}_0) \mathcal{G}_t(\mathbf{x}_j; \mathbf{x}_0). \tag{8.3}$$

In particular, if the particles are uniformly distributed, $h_t^i(\mathbf{x}_i, \mathbf{x}_j, t) = N(N-1)/V^2$. More generally, the spatial shape of $h_t(\mathbf{x}_i, \mathbf{x}_j)$ conveys information on the correlation range, whereas its amplitude is proportional to the correlation strength. A flat shape implies that the correlations have the same intensity everywhere; on the contrary, the presence of a peak at $\mathbf{x}_i \simeq \mathbf{x}_j$ reflects the increased probability of finding particles lying at short distances, which is the signature of spatial clustering [42, 52, 53]. A closely related quantity is the *average square distance between particles*, i.e.,

$$\langle r^2 \rangle(t) = \frac{\int d\mathbf{x}_i \int d\mathbf{x}_j |\mathbf{x}_i - \mathbf{x}_j|^2 h_t(\mathbf{x}_i, \mathbf{x}_j)}{\int d\mathbf{x}_i \int d\mathbf{x}_i h_t(\mathbf{x}_i, \mathbf{x}_j)}, \tag{8.4}$$

which is to be compared to the ideal average square distance of an uncorrelated population uniformly distributed in the available volume, namely,

$$\langle r^2 \rangle_{id} = \frac{1}{V^2} \int d\mathbf{x}_i \int d\mathbf{x}_j |\mathbf{x}_i - \mathbf{x}_j|^2 = \frac{d}{6} V^{\frac{2}{d}}, \tag{8.5}$$

where d denotes spatial dimension. Deviations of $\langle r^2 \rangle(t)$ from the reference value $\langle r^2 \rangle_{id}$ allow detecting spatial effects due to clustering [199, 200].

Analysis of the model detailed above shows that the population dynamics is governed by two distinct time scales: a mixing time $\tau_D \propto V^{2/d}/D$ and an extinction time $\tau_E \propto \beta/N$. The quantity τ_D physically represents the time over which a particle has explored the finite viable volume V by diffusion. Observe that the emergence of the time scale τ_D is a distinct feature of confined geometries having a finite spatial size: for unbounded domains, $\tau_D \to \infty$. The quantity τ_E has a different meaning according to whether population control is imposed [199]. For a free system, τ_E represents the time over which the fluctuations due to births and deaths lead to the extinction of the whole population. For a constrained system, τ_E represents the time over which the system has undergone a population renewal, and all the individuals descend from a single common ancestor. When the concentration N/V of individuals in the population is large (and the system is spatially bounded), it is reasonable to assume that $\tau_E > \tau_D$. Intuitively, the precise shape of the pair correlation function must then depend on the subtle interplay of τ_D and τ_E. Moreover, the pair correlation function will depend on whether population control is applied or not. In the following, we will denote by $h_t^f(\mathbf{x}_i, \mathbf{x}_j)$ the pair correlation function for the case without population control, and $h_t^c(\mathbf{x}_i, \mathbf{x}_j)$ for the case with population control.

The function $h_t^f(\mathbf{x}_i, \mathbf{x}_j)$ for an exactly critical free system has been derived in Sec. 5.3, and can be written as $h_t^f = h_t^{(f,1)} + h_t^{(f,2)}$, where $h_t^{(f,1)}(\mathbf{x}_i, \mathbf{x}_j) = h_t^i(\mathbf{x}_i, \mathbf{x}_j)$ is the contribution from

uncorrelated trajectories, and

$$h_t^{(f,2)}(\mathbf{x}_i,\mathbf{x}_j) = \beta\nu_2 N \int_0^t dt' \int_V d\mathbf{x}' \mathcal{G}_{t-t'}(\mathbf{x}_i;\mathbf{x}')\mathcal{G}_{t-t'}(\mathbf{x}_j;\mathbf{x}') \int d\mathbf{x}_0 q(\mathbf{x}_0)\mathcal{G}'_t(\mathbf{x}';\mathbf{x}_0) \tag{8.6}$$

is the contribution of the trajectories leading from the final positions at $\mathbf{x}_i$ and $\mathbf{x}_j$ at time t to the fission point $\mathbf{x}'$ at time t'. The coefficient $\nu_2 = \sum_i i(i-1)\,p_i$ is the mean number of pairs created at each collision [26]. Imposing a uniform spatial distribution $q = 1/V$ finally yields

$$h_t^f(\mathbf{x}_i,\mathbf{x}_j) = \frac{N\,(N-1)}{V^2} + \beta\nu_2 N \int_0^t dt' \mathcal{G}_{2t'}(\mathbf{x}_i;\mathbf{x}_j). \tag{8.7}$$

The integral of the Green's function appearing in Eq. 8.7 is unbounded, so that at long times the amplitude of the correlations is expected to diverge.

The pair correlation function h^c can be computed by closely following the arguments developed in [200]. Actually, the reactor model described above is basically identical to that proposed in [200], but for boundary conditions (neutrons evolve in a confined geometry, whereas in [200] the viable space was unbounded) and initial conditions (in [200], all the particles were located at the same point at $t = 0$, whereas here the spatial distribution ρ of the individuals at $t = 0$ is arbitrary). Let us choose a pair of (distinct) neutrons located at $\mathbf{x}_i$ and $\mathbf{x}_j$ at time t. These neutrons may, or may not, have had a common ancestor (from a branching event) at a previous time $0 < t' < t$. Because of particle number conservation, the fraction of new particle pairs created in the time interval $(t', t' + dt)$ is $\beta_p dt = \beta\nu_2 dt/(N-1)$, obtained as the ratio of the new particle pairs created in the time interval, i.e., $\beta\nu_2 N dt/2$, to the total number of pairs $N(N-1)/2$. The probability for a chosen pair of particles at time t not to have had a common ancestor is $U(t) = e^{-\beta_p t}$, so that the probability density for the ancestor to occur at time t' for a particle pair observed at t is

$$\psi_t(t') = \beta_p \frac{U(t)}{U(t')} = \beta_p e^{-\beta_p(t-t')}. \tag{8.8}$$

The function $h_t^c(\mathbf{x}_i,\mathbf{x}_j)$ can be again written as $h_t^c = h_t^{(c,1)} + h_t^{(c,2)}$, where $h_t^{(c,1)}(\mathbf{x}_i,\mathbf{x}_j) = U(t)\,h_t^i(\mathbf{x}_i,\mathbf{x}_j)$ is the contribution of neutrons having evolved freely with no common ancestors. The correlated contribution reads

$$h_t^{(c,2)}(\mathbf{x}_i,\mathbf{x}_j) = N(N-1)\int_0^t dt' \int_V d\mathbf{x}' \mathcal{G}_{t-t'}(\mathbf{x}_i;\mathbf{x}')\mathcal{G}_{t-t'}(\mathbf{x}_j;\mathbf{x}')\psi_t(t') \int d\mathbf{x}_0 q(\mathbf{x}_0)\mathcal{G}_{t'}(\mathbf{x}';\mathbf{x}_0). \tag{8.9}$$

where $N(N-1)\psi_t(t')dt'$ is the number of ordered particle pairs at time t that have a common ancestor in the time interval $(t', t' + dt')$. The pair correlation function finally yields

$$h_t^c(\mathbf{x}_i,\mathbf{x}_j) = \frac{N\,(N-1)}{V^2} e^{-\beta_p t} + \beta\nu_2 \frac{N}{V} \int_0^t dt' e^{-\beta_p t'} \mathcal{G}_{2t'}(\mathbf{x}_i;\mathbf{x}_j) \tag{8.10}$$

when imposing $q = 1/V$. The integral of the Green's function appearing in Eq. 8.10 is bounded thanks to the exponential term, and at long times the correlation function converges to an asymptotic shape.

The specific shape of the correlation functions depends on the Green's function, which can be computed once the dimension, geometry and boundary conditions of the problems have been assigned. The average square distance can be then obtained by direct integration by following Eq. 8.4. Once $h_t^{f,c}(\mathbf{x}_i,\mathbf{x}_j)$ has been determined, it is customary to introduce the normalized and centered pair correlation function, in the form

$$g_t^{f,c}(\mathbf{x}_i,\mathbf{x}_j) = \frac{h_t^{f,c}(\mathbf{x}_i,\mathbf{x}_j) - c_t(\mathbf{x}_i)c_t(\mathbf{x}_j)}{c_t(\mathbf{x}_i)c_t(\mathbf{x}_j}, \tag{8.11}$$

which allows more easily comparing the amplitude of the typical spatial fluctuations to the average particle density.

8.4 A critical fuel rod

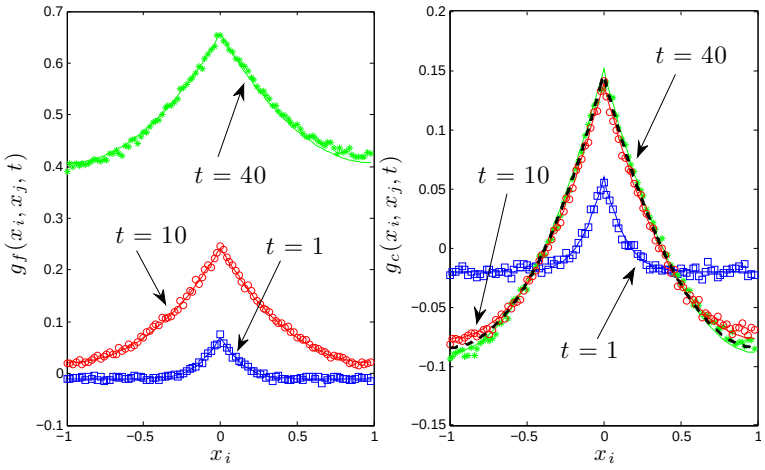

Figure 8.4: The normalized and centered pair correlation function $g_t^{f,c}(x_i, x_j)$ for a collection of $N = 10^2$ branching Brownian motions with diffusion coefficient $D = 10^{-2}$, death rate $\gamma = 1/2$ and binary reproduction rate $\beta = 1/2$, in a one-dimensional box of half-size $L = 1$. We take $x_j = 0$ and plot $g_t^{f,c}(x_i, x_j)$ with respect to x_i at successive times $t = 1$ (blue squares), $t = 10$ (red circles) and $t = 40$ (green stars). Symbols correspond to Monte Carlo simulations with 10^5 ensembles, solid lines to exact solutions (Eqs. 8.7 and 8.10, respectively). Left. For the case of a free system, $g_t^f(x_i, x_j)$ initially develops a peak at $x_i = x_j = 0$, which is the signature of particles undergoing spatial clustering. At later times, $g_t^f(x_i, x_j)$ takes an asymptotic spatial shape, and is translated upwards by a spatially uniform term growing linearly in time. Right. For the case of a system with population control, $g_t^c(x_i, x_j)$ initially develops again a peak at $x_i = x_j = 0$. Because of particle number conservation, an increased correlation about $x_i = 0$ implies negative correlations close to $x_i = \pm L$. At later times, $g_t^c(x_i, x_j)$ converges to an asymptotic spatial shape $g_\infty^c(x_i, x_j)$ (Eq. A.65), displayed as a black dashed curve.

For the purpose of physical analysis and illustration, let us consider a collection of $N = 10^2$ neutrons subject to diffusion, reproduction and death in a fuel rod, i.e., a one-dimensional bounded box $[-L, L]$, with $L = 1$ (thus, $V = 2$). To fix the ideas, we will set a diffusion coefficient $D = 10^{-2}$, death rate $\gamma = 1/2$ and binary reproduction rate $\beta = 1/2$. For this system, the mixing time reads $\tau_D \simeq 40.5$ and the extinction time reads $\tau_E \simeq 10^2$ (hence $\tau_D < \tau_E$; see Appendix A.3). The initial condition for the neutron population is a uniform spatial distribution on $[-L, L]$. In Fig. 8.4, we display the behaviour of the normalized and centered pair correlation functions $g_t^f(x_i, x_j)$ (left) and $g_t^c(x_i, x_j)$ (right) at successive times (their explicit expressions are reported in Appendix A.3). We set $x_j = 0$ and plot $g_t^{f,c}(x_i, x_j)$ as a function of $-L \leq x_i \leq L$. Solid curves represent the exact results given in Eqs. 8.7 and 8.10, respectively, at three increasing times $t = 1$, $t = 10$ and $t = 40$. Symbols represent Monte Carlo simulations performed with 10^5 ensembles of 10^2 neutrons.

For the free system, the pair correlation function $g_t^f(x_i, x_j)$ has three distinct regimes.

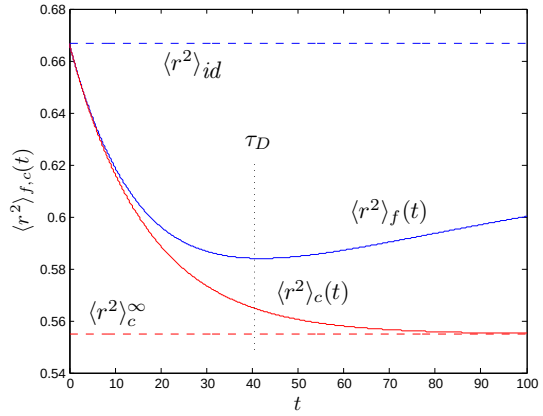

Figure 8.5: The average square distance between particles $\langle r^2\rangle_{f,c}(t)$ for the one-dimensional model with $N = 10^2$ neutrons, death rate $\gamma = 1/2$ and binary reproduction rate $\beta = 1/2$, $D = 10^{-2}$ and $L = 1$. The blue solid curve corresponds to the free case: at long times, $\langle r^2\rangle_f(t)$ asymptotically converges to the ideal average square distance $\langle r^2\rangle_{id} = (2/3)L^2$ for a spatially uniform population, which is displayed as a blue dashed line. The red solid line corresponds to the case of population control: at long times, $\langle r^2\rangle_c(t)$ asymptotically converges to the value $\langle r^2\rangle_c^\infty$ given in Eq. 8.13, which is displayed as a red dashed line.

Immediately after the initial time, $g_t^f(x_i, x_j)$ displays a peak at short distances $x_i \simeq x_j$, which mirrors the effects of local fluctuations responsible for spatial clustering. The amplitude of the peak is proportional to the ratio $\tau_D/\tau_E \propto \beta L^2/(ND)$ (see Eq. A.60), which precisely reflects the competition between migration and reproduction: the amplitude is larger for larger D and smaller β (for fixed L and N), and viceversa. The width of the peak, which is related to the correlation length of the system, is governed by diffusion, and is a growing function of D. For the limit case of non-diffusing particles ($D \to 0$), $g_t^f(x_i, x_j)$ would display a delta-like behaviour at $x_i = x_j$, as expected on physical grounds: for long times, all the descendant particles have died, except for a few point-like clusters composed of a very large number of individuals. For times shorter than the mixing time τ_D, the amplitude of the peak grows due to births and deaths dominating over diffusion, whereas its width increases due to diffusion. When $t \geq \tau_D$, the particles have explored the entire volume, and the tent-like shape of $g_t^f(x_i, x_j)$ freezes into its asymptotic behaviour (see Eq. A.58).

The total number of neutrons in the reactor also undergoes global fluctuations due to the absence of population control and to N being finite. These global fluctuations progressively lift upwards the shape of $g_t^f(x_i, x_j)$ by a spatially flat term that diverges linearly in time as $\sim \beta\nu_2 t/N$ (see Eq. A.60). Finally, for times larger than the extinction time τ_E, $g_t^f(x_i, x_j) \geq 1$ (see Eq. A.59). This physically means that, no matter how dense is the system is at time $t = 0$, global spatial fluctuations affect the whole volume with uniform (and increasing) intensity, and the neutrons are eventually doomed to extinction within a time $t \simeq N/(\beta\nu_2)$ in the absence of population control (see Fig. 8.3).

The average square distance between particles for the free system is displayed in Fig. 8.5: at time $t = 0$, the population is uniformly distributed and $\langle r^2\rangle_f(0) = \langle r^2\rangle_{id} = (2/3)L^2$. Immediately afterwards, $\langle r^2\rangle_f(t)$ starts to decrease due to spatial clustering. For times longer than τ_D, global fluctuations dominate, and correlations range over the whole box. Then, $\langle r^2\rangle_f(t)$ increases and asymptotically saturates again to the ideal average square distance: this can by understood by observing that $h_t^f(x_i, x_j)$ becomes spatially flat for $t \gg \tau_E$.

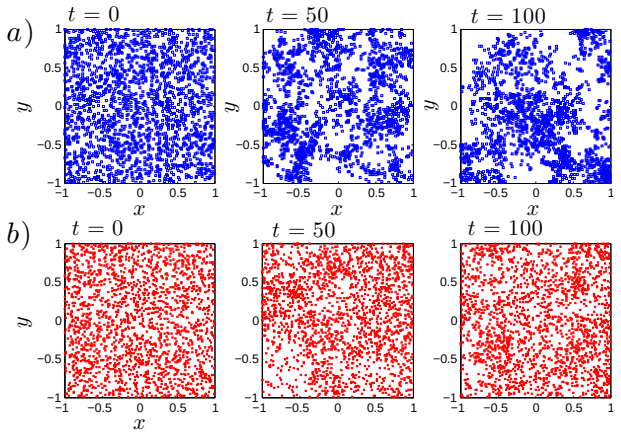

Figure 8.6: Monte Carlo simulation of the evolution of $N = 2 \times 10^3$ branching Brownian motions in a two-dimensional box of volume $V = 4$, subject to population control. The particles are prepared at $t = 0$ on a uniform spatial distribution, with specific square separation distance $\langle r^2 \rangle_{id}/N \simeq 6.67 \times 10^{-4}$. In case *a*), the migration area is $\ell^2_{\mathcal{A}} = 10^{-3}$: the ratio $\ell^2_{\mathcal{A}}/(\langle r^2 \rangle_{id}/N) \simeq 1.5$ is small and clustering phenomena dominate over diffusion (however, since the total particle number is preserved, the population can not go to extinction). In case *b*), the migration area is $\ell^2_{\mathcal{A}} = 10^{-2}$: the ratio $\ell^2_{\mathcal{A}}/(\langle r^2 \rangle_{id}/N) \simeq 15$ is large and spatial fluctuations are much milder.

When population control is enforced, the pair correlation function $g^c_t(x_i, x_j)$ has two distinct regimes. Immediately after the initial time, spatial clustering effects are again reflected in a peak at short distances $x_i \simeq x_j$ for $g^c_t(x_i, x_j)$. The amplitude and the width of the peak have the same behaviour as for the free system detailed above. However, due to the conservation of the number of particles, the positive correlations at the center of the box imply now negative correlations close to the boundaries $x_i = \pm L$. For times shorter than the mixing time τ_D, the amplitude of the peak grows and its width increases as in the previous case. Global spatial fluctuations are intrinsically suppressed by N being fixed due to population control. For times larger than τ_D, $g^c_t(x_i, x_j)$ converges to an asymptotic spatial shape $g^c_\infty(x_i, x_j)$ (see Eq. A.65). In this regime, the amplitude of the pair correlation function is bounded by (see Eq. A.66)

$$|g^c_t(x_i, x_j)| \leq \frac{\ell^2_{\mathcal{I}}}{\ell^2_{\mathcal{A}}}, \tag{8.12}$$

where $\ell^2_{\mathcal{A}} = D/\beta$ is the characteristic migration area of the particles, i.e., the square distance explored by diffusion during a generation, and $\ell^2_{\mathcal{I}} = \langle r^2 \rangle_{id}/N$ is the specific square separation distance between neutrons corresponding to a uniform spatial distribution within the finite box [42]. In order for the fluctuations to be small and prevent the emergence of spatial clustering, we must therefore have $\ell^2_{\mathcal{A}} \gg \ell^2_{\mathcal{I}}$, which occurs when the typical separation between particles is thoroughly explored within a single generation (see Fig. 8.6 for a numerical illustration). Observe that the equilibrium condition for a reactor to be operated at the critical point does not depend on the total neutron population N: therefore, in a system with population control, spatial clustering can be quenched by simply imposing that N is sufficiently large, namely, $N \gg \langle r^2 \rangle_{id}/\ell^2_{\mathcal{A}}$.

The average square distance between particles for the system with population control is displayed in Fig. 8.5: at time $t = 0$, the population is uniformly distributed and we recover $\langle r^2 \rangle_c(0) = \langle r^2 \rangle_{id} = (2/3)L^2$. Immediately afterwards, $\langle r^2 \rangle_c(t)$ starts to decrease due to the competition between

diffusion and birth-death. For times longer than τ_D, $\langle r^2\rangle_c(t)$ converges to the asymptotic value

$$\langle r^2\rangle_c^\infty = \lim_{t\to\infty}\langle r^2\rangle_c(t) = 4\frac{D}{\lambda_p}\left[1-\sqrt{\frac{2D}{\lambda_p L^2}}\tanh\left(\sqrt{\frac{\lambda_p L^2}{2D}}\right)\right], \tag{8.13}$$

which generalizes to confined geometries the findings for unbounded domains derived in [200] (see A.3).

8.5 Supercritical and subcritical regime

Consider again the one-dimensional reflected fuel rod of the previous Section and assume now that the system is *not critical*, i.e., $\gamma \neq \beta(\nu_1 - 1)$, and evolves *without population control*. In order to keep notation to a minimum, the f superscript will be dropped. When the initial particle distribution is uniform, namely, $q(x_0) = 1/2L$, the concentration can be readily obtained from Eq. (5.48), and yields

$$c_t(x_i) = \frac{N}{2L}e^{\alpha_0 t}, \tag{8.14}$$

where $\alpha_0 = \beta(\nu_1 - 1) - \gamma$ is the fundamental eigenvalue in the eigenfunction expansion for the Green's function (see Appendix A.3). Then, the concentration is independent of x_i and its amplitude grows or shrinks exponentially in time, at a rate α_0, regardless of the size of the box. If $\beta(\nu_1 - 1) > \gamma$, the concentration grows unbounded ($\alpha_0 > 0$), and for $\beta(\nu_1 - 1) < \gamma$ it shrinks to zero ($\alpha_0 < 0$). As for the pair correlation function, from Eq. (5.51) we get

$$g_t(x_i, x_j) = \frac{\beta\nu_2}{N}\Big[\frac{1-e^{-\alpha_0 t}}{\alpha_0} + 2Le^{-\alpha_0 t}\sum_{k=1}^{\infty}\frac{e^{(2\alpha_k-\alpha_0)t}-1}{2\alpha_k-\alpha_0}\varphi_k(x_i)\varphi_k(x_j)\Big], \tag{8.15}$$

with

$$\alpha_k = -\frac{k^2}{\tau_D} + \beta(\nu_1 - 1) - \gamma \tag{8.16}$$

and

$$\varphi_k(x) = \frac{1}{\sqrt{L}}\cos\left(k\pi\frac{L-x}{2L}\right) \tag{8.17}$$

for $k \geq 1$ [191, 247].

Correlations trivially vanish when $\beta = 0$. By averaging Eq. (8.15) over the box, we obtain

$$\frac{1}{(2L)^2}\int_{-L}^{L}\int_{-L}^{L} dx_i dx_j g_t(x_i, x_j) = \frac{\beta\nu_2}{N}\frac{1-e^{-\alpha_0 t}}{\alpha_0}, \tag{8.18}$$

which means that the fluctuations affecting the total number of particles contained in the box (regardless of their positions) will saturate exponentially fast to a constant for positive α_0, and will diverge exponentially fast for negative α_0. The analysis of the spatial behaviour of Eq. (8.15) demands a closer inspection. By taking the Laplace transform of Eq. (8.15) and replacing the eigenvalues defined in Eq. (8.16), from Eq. (5.53) we get

$$g_s(x_i, x_j) = \frac{\beta\nu_2}{N}\frac{1}{\alpha_0 + s}\frac{1}{s}\Big[1 + s\tau_D\sum_{k=1}^{\infty}\frac{2L}{2k^2 + s\tau_D}\varphi_k(x_i)\varphi_k(x_j)\Big]. \tag{8.19}$$

It is apparent that the quantity $s\tau_D$ is key to characterizing the space-dependent portion of $g_s(x_i, x_j)$. In particular, due to the competition between the birth-death rate α_0 and the mixing time τ_D, we

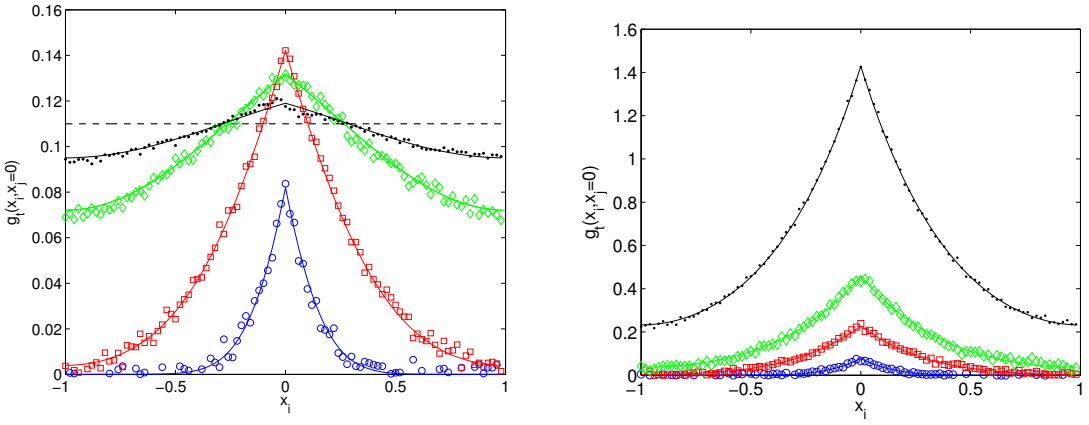

Figure 8.7: The pair correlation function $g_t(x_i, x_j = 0)$ for $N = 100$ particles in a one-dimensional box of half-side L with reflecting boundaries. The diffusion coefficient is $D = 10^{-2}$. The mixing time reads $\tau_D \simeq 40.5$. Left. The death rate is $\gamma = 0.45$ and binary reproduction rate is $\beta = 0.55$ (supercritical regime). The pair correlation function is displayed at times $t = 1$ (blue), $t = 5$ (red), $t = 20$ (green), and $t = 30$ (black). Solid lines correspond to numerical integration, symbols to Monte Carlo simulations with 10^5 realizations. The dashed line represents the asymptotic limit. Right. The death rate is $\gamma = 0.55$ and binary reproduction rate is $\beta = 0.45$ (subcritical regime). The pair correlation function is displayed at times $t = 1$ (blue), $t = 5$ (red), $t = 10$ (green), and $t = 20$ (black). Solid lines correspond to numerical integration, symbols to Monte Carlo simulations with 10^5 realizations.

expect the pair correlation function to display a rich behaviour. This is confirmed by numerical calculations: for illustration, we have computed $g_t(x_i, x_j)$ for supercritical (Fig. 8.7, left) and subcritical (Fig. 8.7, right) regimes and we have compared it to Monte Carlo simulations. In order to gain some physical insight, it is useful to single out distinct time scales. For $s\tau_D \ll 1$, i.e., for times longer than the mixing time scale τ_D, the second term between square brackets in Eq. (8.19) vanishes, and we have

$$g_s(x_i, x_j) \sim \frac{\beta\nu_2}{N} \frac{1}{\alpha_0 + s} \frac{1}{s}. \tag{8.20}$$

Then, by taking the inverse Laplace transform, we recognize that the pair correlation function is spatially flat and asymptotically behaves as

$$g_t(x_i, x_j) \sim \frac{\beta\nu_2}{N\alpha_0} \left(1 - e^{-\alpha_0 t}\right). \tag{8.21}$$

This basically means that in this regime the system is behaving as a whole, and fluctuations affect any spatial scale. For positive α_0, correlations at long times converge exponentially fast to a constant value, namely, $g_{t\to\infty}(x_i, x_j) \to \beta\nu_2/N\alpha_0$, which is small for large N (see Fig. 8.7, left); yet, correlations may be relevant (i.e., $g_t(x_i, x_j) \geq 1$) whenever the initial number of particles is relatively small, namely, $N \leq \nu_2/(\nu_1 - 1)$. For negative α_0, correlations at long times grow unbounded exponentially fast (see Fig. 8.7, right).

In the limit $s\tau_D \gg 1$, i.e., for times shorter than τ_D, the terms between square brackets in Eq. (8.19) become important, and $g_s(x_i, x_j)$ has a non-trivial spatial shape. In this regime, the

infinite sum in Eq. (8.19) can be approximated by an integral by resorting to the Euler-Maclaurin formula, which leads to the closed-form expression

$$g_s(x_i,x_j) \sim \frac{\beta\nu_2}{N}\frac{1}{\alpha_0+s}\frac{1}{s}\frac{\pi}{2}\sqrt{\frac{s\tau_D}{2}}\left[e^{-\frac{\pi}{2}\sqrt{\frac{s\tau_D}{2}}\frac{|x_i-x_j|}{L}}+e^{-\frac{\pi}{2}\sqrt{\frac{s\tau_D}{2}}\frac{(2L-|x_i+x_j|)}{L}}\right]. \tag{8.22}$$

For any given frequency s, $g_s(x_i,x_j)$ displays a tent-like shape, symmetrical with respect to the line $x_i = x_j$. For fixed x_i, $g_s(x_i,x_j)$ has a maximum at $x_j = x_i$. By virtue of the physical meaning of the pair correlation function, this behaviour reflects an enhanced probability of finding a pair of particles close to each other, which is the signature of clustering. Along the line $x_i = x_j$, $g_s(x_i,x_j)$ is symmetrical with respect to $x_i = x_j = 0$, where the function has a minimum, and the two global maxima are reached at the corners $x_j = x_i = \pm L$, which means that short-distance correlations are stronger when both particles are close to the boundaries of the box. Observe in particular that the short distance correlations for $x_i \simeq x_j \simeq \pm L$ (i.e., close to the boundaries) are twice as big as for $x_i \simeq x_j \simeq 0$ (i.e., at the center of the box).

Since $s\tau_D \gg 1$, the exponential terms in Eq. (8.22) are rapidly decaying, so that we expect the relevant contributions to the correlations to come from particles being not too far apart, namely, $|x_i - x_j|/L \ll 1$. By choosing $x_i \simeq x_j \simeq 0$, which corresponds to short-distance correlations at the center of the box, $g_t(x_i,x_j)$ can be obtained by inverting the Laplace transform, and reads

$$g_t(x_i,x_j) \sim \frac{\beta\nu_2}{N}\frac{\pi}{2}\frac{\tau_D}{\sqrt{2\alpha_0}}e^{-\alpha_0 t}\,erfi(\sqrt{\alpha_0 t}), \tag{8.23}$$

where erfi(z) is the imaginary error function [224]. In this regime, particles at the center of the box are not aware, yet, of the presence of the boundaries, so that we consistently recover the square root behaviour typical of one-dimensional critical systems in the thermodynamic limit (see Sec. 5.5.1). For $\alpha_0 \neq 0$, when $|\alpha_0|\tau_D \ll 1$, i.e., when the growth rate due to reproduction and disappearance is much shorter than that of mixing, then the short-distance correlations at the center of the box at early time yield again

$$g_t(x_i,x_j) \sim \frac{\beta\nu_2}{N}\sqrt{\frac{\pi}{2}\tau_D t}, \tag{8.24}$$

independent of α_0, because particles in this regime are not sensitive to the fluctuations due to births and deaths. When on the contrary $|\alpha_0|\tau_D \gg 1$, the effects due to reproduction and disappearance are in competition with mixing, and at longer times $1/|\alpha_0| \ll t \ll \tau_D$ the short-distance correlations at the center of the box yield

$$g_t(x_i,x_j) \sim \frac{\beta\nu_2}{N}\frac{\pi}{2}\left[\frac{e^{-\alpha_0 t}}{\sqrt{\frac{2|\alpha_0|}{\tau_D}}}+\frac{1}{\alpha_0}\frac{\tau_D}{\sqrt{2\pi t}}\right]. \tag{8.25}$$

8.6 The importance of delayed neutrons

In the simple reactor model described above, we have neglected the contribution of *delayed neutrons*. Actually, the fission fragments are usually left on an excited state and may later decay by a β^- nuclear reaction: the energy release on β-transformation is however in a number of cases sufficiently great to excite the product nucleus to a point where a supplementary high-energy neutron is sent out into the system. Since these extra neutrons are emitted after a (Poissonian) decay time of the excited states, they are labelled as *delayed*. By opposition, the neutrons emitted almost instantaneously at fission are labelled as *prompt*. Both prompt and delayed neutrons initiate new fission

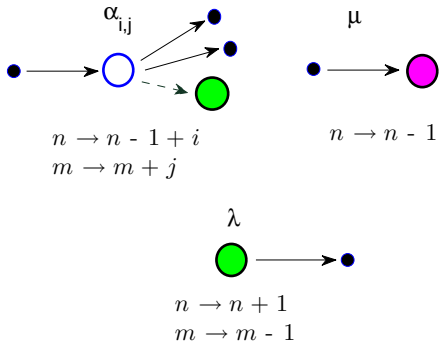

Figure 8.8: A scheme of the multi-type branching process involving neutrons and precursors, with the associated transition rates.

chains. We will assume that fission can be modelled as a *multi-type* Galton-Watson reproduction process [29]: the parent neutron disappears and is replaced by a random number i of identical and independent prompt neutrons, behaving as the parent particle, and a random number j of so-called *precursors*. The precursors conceptually represent the delayed neutrons being in a 'virtual state' before the nuclear decay of the fission fragments. There exists a joint probability $P_{i,j}$ of generating i neutrons and j precursors at the fission event, the realization $\{i,j\}$ being possibly correlated [4,32]. We will denote by λ the decay rate of the nuclear reaction, upon which the precursors disappear to give rise to a delayed neutron. In the following, we will examine the impact of the precursor population on the neutron fluctuations. In order to keep the notation burden to a minimum, we will focus on an *unbounded medium* without population control.

8.6.1 Statistical behaviour of the total populations

Let us initially consider the evolution of the whole neutron and precursor populations, by ignoring the spatial effects. The analysis of multi-type branching processes could be carried out by resorting to the backward evolution equations, as done in the previous Chapters [32]. However, here we will rather follow the forward approach, which allows more easily taking into account the presence of the initial particle distribution. The system dynamics can be formulated in terms of the transition rates between different discrete states of a two-dimensional Markov chain. Consider a state composed of n neutrons and m precursors at time t. Then, the system

(i) has a transition $\{n,m\} \to \{n-1,m\}$ with rate γn,

(ii) has a transition $\{n,m\} \to \{n-1+i,m+j\}$ with rate $\beta_{i,j} n = \beta P_{i,j} n$,

(iii) has a transition $\{n,m\} \to \{n+1,m-1\}$ with rate λm.

A scheme of the transitions between n and m is sketched in Fig. 8.8. Following these definitions, the *forward master equation* for the probability $\mathcal{P}_t(n,m)$ that at time t the system contains exactly n neutrons and m precursors is given by

$$\frac{\partial}{\partial t}\mathcal{P}_t(n,m) = -\gamma n \mathcal{P}_t(n,m) - \lambda m \mathcal{P}_t(n,m) + \lambda(m+1)\mathcal{P}_t(n-1,m+1)$$
$$-\sum_{i,j}\beta_{i,j} n \mathcal{P}_t(n,m) + \gamma(n+1)\mathcal{P}_t(n+1,m) + \sum_{i,j}\beta_{i,j}(n+1-i)\mathcal{P}_t(n+1-i,m-j). \qquad (8.26)$$

8.6.2 Average number of particles

By algebraic manipulations, from the master equation we can derive the evolution equations for the moments (see Appendix A.4.1). For the average number of particles $\langle n(t)\rangle = \sum_{n,m} n\mathcal{P}_t(n,m)$ and $\langle m(t)\rangle = \sum_{n,m} m\mathcal{P}_t(n,m)$, we get in particular the system

$$\begin{aligned}\frac{\partial}{\partial t}\langle n(t)\rangle &= (\rho-\beta\nu_m)\langle n(t)\rangle + \lambda\langle m(t)\rangle \\ \frac{\partial}{\partial t}\langle m(t)\rangle &= \beta\nu_m\langle n(t)\rangle - \lambda\langle m(t)\rangle,\end{aligned} \tag{8.27}$$

where we have introduced the average number

$$\nu_n = \sum_{i,j} iP_{i,j} \tag{8.28}$$

of prompt neutrons instantaneously emitted per reproduction event and the average number

$$\nu_m = \sum_{i,j} jP_{i,j} \tag{8.29}$$

of precursors created per reproduction event. The ratio $\nu_m/(\nu_n+\nu_m)$ for water-moderated reactors is about 0.6% [30]. The quantity $\rho = \beta(\nu_n+\nu_m-1)-\gamma$ physically represents the *net reactivity of the system per unit time* [30], i.e., the difference between the production rate and the loss rate. For safety reasons, the net reactivity of nuclear reactors is typically weak, in the form of small perturbations around $\rho = 0$: this is usually imposed by varying the position of the control elements in the core, which increases or decreases the neutron absorption within the nuclear reactor [30]. The system is said to be super-critical if $\rho > 0$, sub-critical if $\rho < 0$, and exactly critical if $\rho = 0$.

The evolution of $\langle n(t)\rangle$ and $\langle m(t)\rangle$ is fully determined by assigning the initial conditions $\langle n(0)\rangle = n_0$ and $\langle m(0)\rangle = m_0$. Nuclear reactors are operated at and close to the critical point, so that it is convenient to assume that at time $t = 0$ the average neutron and precursor populations are at equilibrium with zero reactivity: this condition is achieved by setting $\partial_t\langle n(t)\rangle|_{t=0} = \partial_t\langle m(t)\rangle|_{t=0} = 0$, which yields $\beta\nu_m n_0 = \lambda m_0$. The quantity $\vartheta = \lambda/(\beta\nu_m)$ physically represents the ratio between the rate at which precursors disappear by giving rise to delayed neutrons and the rate at which precursors are created by fission events. In the following, we will always assume that the system is prepared on a zero-reactivity equilibrium configuration at time $t = 0$, i.e., $n_0 = \vartheta m_0$, which implies the initial conditions

$$\langle n(0)\rangle = n_0, \quad \langle m(0)\rangle = \frac{n_0}{\vartheta}. \tag{8.30}$$

Actually, one could consider more generally a configuration where precursors are initially absent, and a neutron source is present at time $t = 0$. In this case, precursors will be created by fission. If the net reactivity of the system is zero, the number of neutrons will level off to a constant asymptotic value, and so will the number of precursors (see Appendix A.4.2). Once equilibrium is attained, one can verify that the ratio between the neutron and precursor population is again ϑ. In this respect, the main advantage of choosing an initial equilibrium configuration for the two populations is that it allows neglecting the convergence towards the asymptotic equilibrium.

Equations (8.27) can be solved exactly (see Appendix A.4.2). If the net reactivity is weak, as required above, expanding in small powers of $|\rho|$ yields the asymptotic solutions

$$\begin{aligned}\langle n(t)\rangle &\simeq n_0\frac{1+\vartheta+\epsilon}{1+\vartheta}e^{\omega t} \\ \langle m(t)\rangle &\simeq m_0\frac{1+\vartheta-\vartheta\epsilon}{1+\vartheta}e^{\omega t},\end{aligned} \tag{8.31}$$

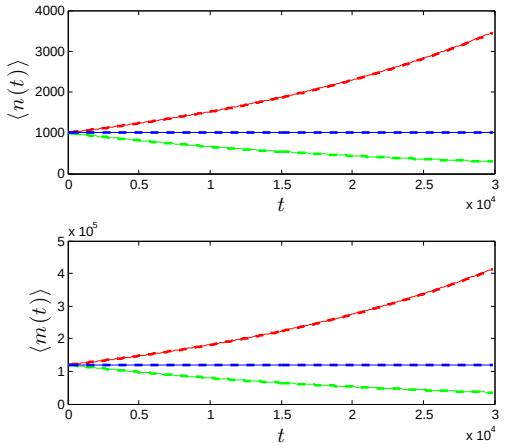

Figure 8.9: Evolution of the average neutron population $\langle n(t)\rangle$ (top) and the average precursor population $\langle m(t)\rangle$ (bottom), starting from a zero-reactivity equilibrium condition. Solid lines are the exact solutions in Eqs. (A.78), and dashed lines are the asymptotic solutions provided in Eqs. (8.31). The parameters are the following: $n_0 = 10^3$, $\vartheta = 8.333 \times 10^{-3}$, $\beta\nu_m = 1.2$ and $\lambda = 10^{-2}$. Red curves correspond to a supercritical reactor with $\rho = 5 \times 10^{-3}$, green curves correspond to a subcritical reactor with $\rho = -5 \times 10^{-3}$, and blue curves correspond to an exactly critical reactor with $\rho = 0$.

for long times, where

$$\omega = \frac{\vartheta}{1+\vartheta}\rho \tag{8.32}$$

is the *characteristic reactor period*, and for the sake of convenience we have introduced the rescaled reactivity

$$\epsilon = \frac{\rho}{\beta\nu_m}\frac{1}{1+\vartheta}. \tag{8.33}$$

The sign of the period ω depends on the net reactivity: for $\rho > 0$, $\omega > 0$ and the average populations asymptotically diverge in time; for $\rho < 0$, $\omega < 0$ and the average populations asymptotically shrink to zero; for $\rho = 0$, $\omega = 0$ and the populations stay exactly constant in time. For the three cases, the ratio

$$\frac{\langle n(t)\rangle}{\langle m(t)\rangle} \simeq \vartheta(1+\epsilon) \tag{8.34}$$

converges to a constant for long times.

Equations (8.31) are very effective in approximating the exact behaviour of the average neutron and precursor densities in the weak reactivity regime (see Fig. 8.9 for a numerical example). The accuracy of the approximation increases with decreasing ϑ. For typical nuclear systems, the coefficient ϑ is rather small, about $\vartheta \simeq 10^{-3}$ [30], which follows from the strong separation between the rate at which precursors are created ($\beta\nu_m$) and the rate at which precursors are converted to delayed neutrons (λ). This implies that at equilibrium the initial precursor population $m_0 = n_0/\vartheta$ is much larger than the initial neutron population n_0. Under this assumption, Eqs. (8.31) basically say that the average densities have an almost instantaneous jump $n_0 \to n_0(1+\vartheta+\epsilon)/(1+\vartheta)$

and $m_0 \to m_0(1+\vartheta-\vartheta\epsilon)/(1+\vartheta)$, respectively, followed by an exponential growth or decrease (depending on the sign of ρ) with an identical period ω. This result is due to the strong separation of the characteristic time scales of the system for small ϑ (see Appendix A.4.2), and is coherent with the classical results for average observables in reactor physics [30]. Indeed, when ϑ is small, precursors have a buffering effect on the evolution of the neutron population: this can be understood by summing up Eqs. (8.27), which yields

$$\frac{\partial}{\partial t}\left[\langle n(t)\rangle + \langle m(t)\rangle\right] = \rho\langle n(t)\rangle. \tag{8.35}$$

Then, from Eq. (8.34) at the leading order we have

$$\frac{1+\vartheta}{\vartheta}\frac{\partial}{\partial t}\langle n(t)\rangle = \rho\langle n(t)\rangle, \tag{8.36}$$

which implies that reactivity ρ is slowed down by a factor ϑ for small values of this parameter.

If the neutron and precursor populations were fully decoupled, and the reactor were to be run based on *prompt neutrons alone* ($\sum_i P_{i,j} = \delta_{j,0}$, so that $\nu_m = 0$, and $\lambda = 0$ for any m_0), the net reactivity would be $\rho_p = \beta(\nu_n - 1) - \gamma$, and we would have

$$\langle n(t)\rangle_p = n_0 e^{\omega_p t} \tag{8.37}$$

with $\omega_p = \rho_p$. We have used the subscript p to denote quantities related to purely *prompt* systems. Since $\nu_m \ll \nu_n$, then $\rho_p \simeq \rho$, whence also $\omega_p \simeq \omega/\vartheta$. By inspection, we thus have $\langle n(t)\rangle \simeq \langle n(\vartheta t)\rangle_p$ in the weak reactivity regime. In other words, in the presence of precursors the time at which the neutron population exponentially grows or shrinks is rescaled by a factor $t \to \vartheta t$, with $\vartheta \ll 1$. We rediscover here that delayed neutrons, despite their very small number, are therefore essential for reactor control thanks to the buffering effect of precursors [30].

8.6.3 Equations for the second moments

It is customary to introduce the normalized and centered second moments, in the form

$$u(t) = \frac{\langle n^2(t)\rangle - \langle n(t)\rangle^2}{\langle n(t)\rangle^2} \tag{8.38}$$

$$v(t) = \frac{\langle n(t)m(t)\rangle - \langle n(t)\rangle\langle m(t)\rangle}{\langle n(t)\rangle\langle m(t)\rangle} \tag{8.39}$$

$$w(t) = \frac{\langle m^2(t)\rangle - \langle m(t)\rangle^2}{\langle m(t)\rangle^2}. \tag{8.40}$$

The evolution equations for these quantities are derived in Appendix A.4.3, and read

$$\frac{\partial}{\partial t}u(t) = -2\frac{\lambda}{\chi_t}u(t) + 2\frac{\lambda}{\chi_t}v(t) + \frac{1}{\langle n(t)\rangle}\left(\beta\nu_n^{(2)} + \beta\nu_m + \frac{\lambda}{\chi_t} - \rho\right), \tag{8.41}$$

$$\frac{\partial}{\partial t}v(t) = \beta\nu_m\chi_t u(t) - \left(\frac{\lambda}{\chi_t} + \beta\nu_m\chi_t\right)v(t) + \frac{\lambda}{\chi_t}w(t) + \frac{1}{\langle n(t)\rangle}\left(\beta\nu_{nm}\chi_t - \beta\nu_m\chi_t - \lambda\right), \tag{8.42}$$

$$\frac{\partial}{\partial t}w(t) = 2\beta\nu_m\chi_t v(t) - 2\beta\nu_m\chi_t w(t) + \frac{1}{\langle n(t)\rangle}\left(\beta\nu_m^{(2)}\chi_t^2 + \beta\nu_m\chi_t^2 + \lambda\chi_t\right), \tag{8.43}$$

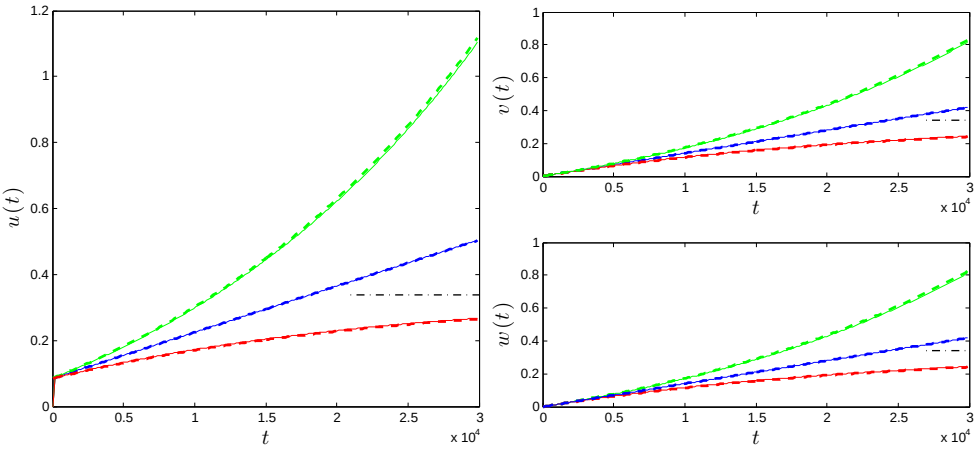

Figure 8.10: Left. Evolution of the normalized and centered second moment of the neutron population $u(t)$, starting from a zero-reactivity equilibrium condition. Solid lines are the numerical solutions of the exact Eq. (8.41), and dashed lines are the asymptotic solutions provided in Eqs. (8.46) and (8.51). Right. Evolution of the normalized and centered second moments $v(t)$ (top) and $w(t)$ (bottom), starting from a zero-reactivity equilibrium condition. Solid lines are the numerical solutions of the exact Eqs. (8.42) and (8.43), respectively, and dashed lines are the asymptotic solutions provided in Eq. (8.47) (Eq. (8.52) for the critical case) and Eq. (8.47) (Eq. (8.52) for the critical case), respectively, for small reactivities and $\vartheta \ll 1$. The parameters are the following: $n_0 = 10^3$, $\vartheta = 8.333 \times 10^{-3}$, $\beta\nu_m = 1.2$, $\lambda = 10^{-2}$, $\nu_n^{(2)} = 2$, $\nu_{nm} = 2.4 \times 10^{-2}$ and $\nu_m^{(2)} = 4 \times 10^{-3}$. Red curves correspond to a supercritical reactor with $\rho = 5 \times 10^{-3}$, green curves correspond to a subcritical reactor with $\rho = -5 \times 10^{-3}$, and blue curves correspond to an exactly critical reactor with $\rho = 0$. The dotted-dashed black lines correspond to the asymptotic values $u_\infty = v_\infty = w_\infty$ expected for the supercritical configuration, as given in Eq. (8.50).

where we have defined the factorial moments

$$\nu_n^{(2)} = \sum_{i,j} i(i-1)P_{i,j}, \quad \nu_m^{(2)} = \sum_{i,j} j(j-1)P_{i,j} \tag{8.44}$$

and the cross-moment

$$\nu_{nm} = \sum_{i,j} ijP_{i,j}, \tag{8.45}$$

and we have set $\chi_t = \langle n(t)\rangle/\langle m(t)\rangle$. The initial conditions are $u(0) = 0$, $v(0) = 0$, and $w(0) = 0$.

Even though Eqs. (8.41), (8.42) and (8.43) can be solved exactly, it is more instructive to focus on their long time behaviour, which is more appropriate for the physical analysis. The asymptotic expansion for small $|\rho|$ and small ϑ is detailed in Appendix A.4.4. In particular, under this assumption we can replace $\chi_t \simeq \vartheta(1+\epsilon)$. By retaining the leading order terms, for long times we have

$$u(t) \simeq \frac{A(1-\epsilon) + \vartheta(3A+2B)}{2n_0(1+\vartheta)(1+\vartheta-\epsilon)} e^{-\omega t} + \frac{\beta\nu_m}{n_0} \frac{\vartheta^2(A+2B+C)}{(1+\vartheta)(1+\vartheta-\epsilon)} \frac{1-e^{-\omega t}}{\omega}, \tag{8.46}$$

$$v(t) \simeq \frac{\vartheta(A+2B)}{2n_0(1+\vartheta)(1+\vartheta-\epsilon)}e^{-\omega t} + \frac{\beta\nu_m}{n_0}\frac{\vartheta^2(A+2B+C)}{(1+\vartheta)(1+\vartheta-\epsilon)}\frac{1-e^{-\omega t}}{\omega}, \tag{8.47}$$

$$w(t) \simeq \frac{\beta\nu_m}{n_0}\frac{\vartheta^2(A+2B+C)}{(1+\vartheta)(1+\vartheta-\epsilon)}\frac{1-e^{-\omega t}}{\omega}, \tag{8.48}$$

where the coefficients read

$$A = \frac{\nu_n^{(2)}}{\nu_m}\left(1-\frac{\epsilon}{1+\vartheta}\right) + 2\left(1-2\frac{\epsilon}{1+\vartheta}\right), \tag{8.49}$$

$B = \nu_{nm}/\nu_m - 2$, and $C = \nu_m^{(2)}/\nu_m + 2$. The asymptotic expressions in Eqs. (8.46), (8.47) and (8.48) are compared to the numerical solutions of the exact Eqs. (8.41), (8.42) and (8.43) in Figs. 8.10 left and right. The agreement of the asymptotic to the exact solutions in the weak reactivity regime is remarkable also for the second moments of the populations. When the reactor is subcritical, the average neutron and precursor populations decrease exponentially fast, so that $u(t)$, $v(t)$ and $w(t)$ diverge exponentially fast as $\sim \exp(|\omega|t)$. At some point, $u(t)$, $v(t)$ and $w(t)$ will become larger than 1, and the fluctuations will completely overrule the average behaviour of the individuals. On the contrary, when the reactor is supercritical the average neutron and precursor populations grow unbounded exponentially fast, and $u(t)$, $v(t)$ and $w(t)$ saturate to the asymptotic value

$$u_\infty = v_\infty = w_\infty \simeq \frac{\beta\nu_m}{n_0}\frac{\vartheta^2(A+2B+C)}{\omega(1+\vartheta)(1+\vartheta-\epsilon)}. \tag{8.50}$$

In this regime, the fluctuations may still be large when the initial neutron population n_0 is small. The case of an exactly critical system can be obtained from the previous equations by taking the limit for $\omega \to 0$, with $\epsilon = 0$. We thus obtain

$$u(t) \simeq \frac{A+\vartheta(3A+2B)}{2n_0(1+\vartheta)^2} + \frac{\beta\nu_m}{n_0}\frac{\vartheta^2(A+2B+C)}{(1+\vartheta)^2}t, \tag{8.51}$$

$$v(t) \simeq \frac{\vartheta(A+2B)}{2n_0(1+\vartheta)^2} + \frac{\beta\nu_m}{n_0}\frac{\vartheta^2(A+2B+C)}{(1+\vartheta)^2}t, \tag{8.52}$$

$$w(t) \simeq \frac{\beta\nu_m}{n_0}\frac{\vartheta^2(A+2B+C)}{(1+\vartheta)^2}t. \tag{8.53}$$

In the critical regime, the average populations stay constant, but the moments $u(t)$, $v(t)$ and $w(t)$ diverge linearly in time and will ultimately cross the threshold at one: this stems from the individuals being (almost surely) doomed to extinction [4]. The typical extinction time τ_E for the neutron population can be determined by imposing $u(\tau_E) \simeq 1$, which yields

$$\tau_E = \frac{n_0}{\beta\nu_m(A+2B+C)\vartheta^2} \tag{8.54}$$

by neglecting sub-leading order terms.

If the reactor were to be operated with prompt neutrons alone, we would have

$$u_p(t) = \frac{\beta\nu_n^{(2)}}{n_0}\frac{1-e^{-\omega_p t}}{\omega_p}, \tag{8.55}$$

for $\omega_p \neq 0$, and

$$u_p(t) = \frac{\beta \nu_n^{(2)}}{n_0} t \tag{8.56}$$

in the critical regime. By direct inspection, observing that the term $\nu_m(A + 2B + C)$ is dominated by $\nu_n^{(2)}$ since $\sum_i P_{i,j} \ll \sum_j P_{i,j}$ for $j \geq 1$, we have

$$u(t) \simeq \vartheta u_p(\vartheta t). \tag{8.57}$$

In other words, in the presence of precursors, the normalized and centered second moment of the neutron population has a much slower evolution in time ($t \to \vartheta t$, similarly as for the case of the average number of particles), and its amplitude is further rescaled by a factor ϑ. As for the extinction time, $\tau_E^p \simeq n_0/(\beta \nu_n^{(2)})$, and we would have $\tau_E \simeq \tau_E^p/\vartheta^2$. In this respect, precursors are extremely effective in *quenching the neutron fluctuations* at the scale of the global population.

8.7 Spatial correlations with prompt and delayed neutrons

We would like now to address the spatial behaviour of neutrons and precursors. For the sake of simplicity, let us initially consider a one-dimensional domain partitioned into cells of size ℓ, the cell of index k containing n_k neutrons and m_k precursors. The full state of the particles will be provided by the vectors $(\mathbf{n}, \mathbf{m})$, where $\mathbf{n} = \{..., n_k, ...\}$ and $\mathbf{m} = \{..., m_k, ...\}$. In order to manipulate a modified state where a particle has been added or removed from the site k with respect to $\mathbf{n}$, it is convenient to resort to the formalism proposed in [51, 248–250]: we will introduce the creation and annihilation operators $a_k^\dagger$ and a_k, whose action on $\mathbf{n}$ yields $a_k^\dagger \mathbf{n} = (..., n_{k-1}, n_k + 1, n_{k+1}, ...)$ and $a_k \mathbf{n} = (..., n_{k-1}, n_k - 1, n_{k+1}, ...)$, respectively, and the operators $b_k^\dagger$ and b_k that have identical action on $\mathbf{m}$. Assume that the reactor is in state $(\mathbf{n}, \mathbf{m})$ at time t. Then, the system

(i) has a transition $\{\mathbf{n}, \mathbf{m}\} \to \{a_k \mathbf{n}, \mathbf{m}\}$ with rate $\gamma_k n$,

(ii) has a transition $\{\mathbf{n}, \mathbf{m}\} \to \{(a_k^\dagger)^i a_k \mathbf{n}, (b_k^\dagger)^j \mathbf{m}\}$ with rate $\beta_{i,j} n = \beta P_{i,j} n_k$,

(iii) has a transition $\{\mathbf{n}, \mathbf{m}\} \to \{a_k^\dagger \mathbf{n}, b_k \mathbf{m}\}$ with rate λm_k,

(iv) has a transition $\{\mathbf{n}, \mathbf{m}\} \to \{a_{k\pm1}^\dagger \mathbf{n}, \mathbf{m}\}$ with rate ηn_k,

where η is the diffusion rate of neutrons from neighbouring cells $k \pm 1$. Following these definitions, the forward master equation for the probability $\mathcal{P}_t(\mathbf{n}, \mathbf{m})$ that at time t the system is in state $(\mathbf{n}, \mathbf{m})$ obeys

$$\begin{aligned}
\frac{\partial}{\partial t}\mathcal{P}_t(\mathbf{n}, \mathbf{m}) = \sum_k \Big[&- \sum_{i,j} \beta_{i,j} n_k \mathcal{P}_t(\mathbf{n}, \mathbf{m}) + \sum_{i,j} \beta_{i,j}(n_k + 1 - i)\mathcal{P}_t((a_k^\dagger)^i a_k \mathbf{n}, (b_k^\dagger)^j \mathbf{m}) \\
&- \gamma n_k \mathcal{P}_t(\mathbf{n}, \mathbf{m}) + \gamma(n_k + 1)\mathcal{P}_t(a_k^\dagger \mathbf{n}, \mathbf{m}) - \lambda m_k \mathcal{P}_t(\mathbf{n}, \mathbf{m}) + \lambda(m_k + 1)\mathcal{P}_t(a_k \mathbf{n}, b_k^\dagger \mathbf{m}) \\
&- 2\eta n_k \mathcal{P}_t(\mathbf{n}, \mathbf{m}) + \eta(n_{k+1} + 1)\mathcal{P}_t(a_k a_{k+1}^\dagger \mathbf{n}, \mathbf{m}) + \eta(n_{k-1} + 1)\mathcal{P}_t(a_k a_{k-1}^\dagger \mathbf{n}, \mathbf{m}) \Big].
\end{aligned} \tag{8.58}$$

Generally speaking, the solutions of Eq. (8.58) could be sought by resorting to a field-theoretical approach [250]. However, thanks to the master equation being linear, the equations for the spatial moments of the population can again be obtained by simpler algebraic manipulations of Eq. (8.58) (see Appendix A.4.1).

8.7.1 Average particle densities

For the average number of particles in a cell k, namely, $\langle n_k(t)\rangle = \sum_{\mathbf{n},\mathbf{m}} n_k \mathcal{P}_t(\mathbf{n},\mathbf{m})$ and $\langle m_k(t)\rangle = \sum_{\mathbf{n},\mathbf{m}} m_k \mathcal{P}_t(\mathbf{n},\mathbf{m})$, we get in particular the system

$$\begin{aligned}\frac{\partial}{\partial t}\langle n_k(t)\rangle &= (\eta\Delta + \rho - \beta\nu_m)\langle n_k(t)\rangle + \lambda\langle m_k(t)\rangle,\\ \frac{\partial}{\partial t}\langle m_k(t)\rangle &= \beta\nu_m\langle n_k(t)\rangle - \lambda\langle m_k(t)\rangle,\end{aligned} \tag{8.59}$$

where we have used the shorthand notation $\Delta f_k = f_{k+1} - 2f_k + f_{k-1}$ for the discrete Laplacian operator. We can then define the average densities of neutrons and precursors by taking the continuum limit

$$\mathcal{N}(x,t) = \lim_{\ell\to 0}\frac{\langle n_k(t)\rangle}{\ell} \quad \mathcal{M}(x,t) = \lim_{\ell\to 0}\frac{\langle m_k(t)\rangle}{\ell}, \tag{8.60}$$

where $x = k\ell$. By replacing these definitions in the previous equations, the average densities satisfy

$$\begin{aligned}\frac{\partial}{\partial t}\mathcal{N}(x,t) &= (D\nabla^2 + \rho - \beta\nu_m)\mathcal{N}(x,t) + \lambda\mathcal{M}(x,t),\\ \frac{\partial}{\partial t}\mathcal{M}(x,t) &= \beta\nu_m\mathcal{N}(x,t) - \lambda\mathcal{M}(x,t),\end{aligned} \tag{8.61}$$

where we have used the Taylor expansion $\langle\Delta n_k(t)\rangle \simeq \ell^2\nabla^2\mathcal{N}(x,t)$, and $D = \lim_{\ell\to 0}\eta\ell^2$ is the diffusion coefficient of the neutrons.

Imposing as above the zero-reactivity equilibrium initial conditions leads to $\mathcal{N}_0 = \mathcal{N}(x,0) = \vartheta\mathcal{M}(x,0)$, which means that the spatial profile of the neutron and precursor concentrations will be flat. By inspection of Eq. (8.61), it is apparent that starting from this initial condition the concentrations will stay flat, and that their amplitude will follow the same time behaviour as the average total populations $\langle n(t)\rangle$ and $\langle m(t)\rangle$ in Eq. (A.78). In particular, for weak reactivities at long times we have

$$\mathcal{N}(x,t) = \mathcal{N}(t) \simeq \mathcal{N}_0\frac{1+\vartheta+\epsilon}{1+\vartheta}e^{\omega t} \tag{8.62}$$

and the ratio $\mathcal{N}(x,t)/\mathcal{M}(x,t)$ asymptotically converges again to the constant $\vartheta(1+\epsilon)$. Observe that the only dimension-dependent term in Eq. (8.61) is the spatial derivative ∇^2, so that the evolution equations for the concentration would be left almost unchanged in a d-dimensional infinite space $\mathbb{R}^d$, provided that we replace x with $\mathbf{r}$ and ∇^2 with the d-dimensional Laplacian ∇_d^2.

Finally, by analogy with the case of the average neutron population, in the weak reactivity regime we have $\mathcal{N}(t) \simeq \mathcal{N}_p(\vartheta t)$, where $\mathcal{N}_p(\vartheta t)$ is the average neutron density for a reactor that were to be run based on prompt neutrons alone.

8.7.2 Spatial correlation functions

We will define the spatial correlation functions $\langle n_k n_{k+j}\rangle = \sum_{\mathbf{n},\mathbf{m}} n_k n_{k+j}\mathcal{P}_t(\mathbf{n},\mathbf{m})$ and $\langle m_k m_{k+j}\rangle = \sum_{\mathbf{n},\mathbf{m}} m_k m_{k+j}\mathcal{P}_t(\mathbf{n},\mathbf{m})$ and the cross-correlations $\langle n_{k+j}m_k\rangle = \sum_{\mathbf{n},\mathbf{m}} n_{k+j}m_k\mathcal{P}_t(\mathbf{n},\mathbf{m})$. We have dropped the explicit time dependence for the sake of conciseness. Assuming that the initial particle concentrations are spatially flat allows applying a translational symmetry to the system (in particular, for the averages we have $\langle n_k\rangle = \langle n_{k+j}\rangle$ and $\langle m_k\rangle = \langle m_{k+j}\rangle$ $\forall k,j$). It is then convenient

to introduce the normalized and centered moments

$$u_j(t) = \frac{\langle n_k n_{k+j}\rangle}{\langle n_k\rangle^2} - 1 - \frac{\delta_{j,0}}{\langle n_k\rangle}$$
$$v_j(t) = \frac{\langle n_{k+j} m_k\rangle}{\langle n_k\rangle\langle m_k\rangle} - 1$$
$$w_j(t) = \frac{\langle m_k m_{k+j}\rangle}{\langle m_k\rangle^2} - 1 - \frac{\delta_{j,0}}{\langle m_k\rangle}, \tag{8.63}$$

which only depend on the relative distance $|j|$ between site k and $k+j$ [51]. The Kronecker delta term $\delta_{i,j}$ expresses the contribution of self-correlations. The evolution equations for the spatial correlations are provided in Appendix A.4.5, and read

$$\frac{\partial}{\partial t} u_j = 2\left(\eta\Delta - \frac{\lambda}{\chi_t}\right) u_j + 2\frac{\lambda}{\chi_t} v_j + \beta\nu_n^{(2)} \frac{\delta_{j,0}}{\langle n_k\rangle}, \tag{8.64}$$

$$\frac{\partial}{\partial t} v_j = \beta\nu_m u_j + \left(\eta\Delta - \beta\nu_m\chi_t - \frac{\lambda}{\chi_t}\right) v_j + \frac{\lambda}{\chi_t} w_j + \beta\nu_{nm}\chi_t \frac{\delta_{j,0}}{\langle n_k\rangle}, \tag{8.65}$$

$$\frac{\partial}{\partial t} w_j = 2\beta\nu_m\chi_t v_j - 2\beta\nu_m\chi_t w_j + \beta\nu_m^{(2)}\chi_t^2 \frac{\delta_{j,0}}{\langle n_k\rangle}, \tag{8.66}$$

where we have used $\langle n_k\rangle/\langle m_k\rangle = \chi_t$. By taking again the continuum limit $\ell \to 0$, with $r = \ell|j|$ and $\eta\Delta f_j \simeq D\nabla^2 f(r)$, we finally obtain the evolution equations for the correlations $u(r,t) = \lim_{\ell\to 0} u_j(t)$, $v(r,t) = \lim_{\ell\to 0} v_j(t)$, and $w(r,t) = \lim_{\ell\to 0} w_j(t)$, namely

$$\frac{\partial}{\partial t} u(r,t) = 2\left(D\nabla^2 - \frac{\lambda}{\chi_t}\right) u(r,t) + 2\frac{\lambda}{\chi_t} v(r,t) + \beta\nu_n^{(2)} \frac{\delta(r)}{\mathcal{N}(t)}, \tag{8.67}$$

$$\frac{\partial}{\partial t} v(r,t) = \left(D\nabla^2 - \frac{\lambda}{\chi_t} - \beta\nu_m\chi_t\right) v(r,t) + \beta\nu_m\chi_t u(r,t) + \frac{\lambda}{\chi_t} w(r,t) + \beta\nu_{nm}\chi_t \frac{\delta(r)}{\mathcal{N}(t)}, \tag{8.68}$$

$$\frac{\partial}{\partial t} w(r,t) = 2\beta\nu_m\chi_t v(r,t) - 2\beta\nu_m\chi_t w(r,t) + \beta\nu_m^{(2)}\chi_t^2 \frac{\delta(r)}{\mathcal{N}(t)}. \tag{8.69}$$

These equations hold true in any dimension d, provided that ∇^2 is replaced by the d-dimensional Laplacian ∇_d^2.

The long time and long distance expansion of the previous equations for small $|\rho|$ and small ϑ is discussed in Appendix A.4.6 for a d-dimensional domain. By retaining the leading order terms, in this regime we obtain

$$u(r,t) \simeq \frac{\beta\nu_m A'(1-\epsilon)}{2\mathcal{N}_0(1+\vartheta)(1+\vartheta-\epsilon)} H(r,t) + \frac{\beta\nu_m}{\mathcal{N}_0}\frac{\vartheta^2(A'+2B'+C')}{(1+\vartheta)(1+\vartheta-\epsilon)} F(r,t), \tag{8.70}$$

$$v(r,t) \simeq \frac{\beta\nu_m\vartheta(A'+2B')}{2\mathcal{N}_0(1+\vartheta)(1+\vartheta-\epsilon)} H(r,t) + \frac{\beta\nu_m}{\mathcal{N}_0}\frac{\vartheta^2(A'+2B'+C')}{(1+\vartheta)(1+\vartheta-\epsilon)} F(r,t), \tag{8.71}$$

$$w(r,t) \simeq \frac{\beta\nu_m}{\mathcal{N}_0}\frac{\vartheta^2(A'+2B'+C')}{(1+\vartheta)(1+\vartheta-\epsilon)} F(r,t), \tag{8.72}$$

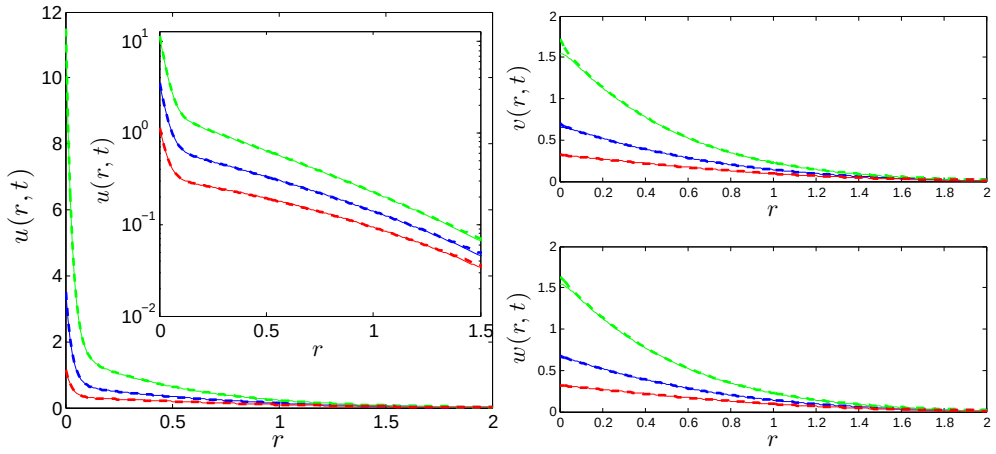

Figure 8.11: Left. Evolution of the normalized and centered pair correlation function $u(r,t)$ for a one-dimensional domain, starting from a zero-reactivity equilibrium condition. Solid lines are the numerical solutions of the exact Eq. (8.67), and dashed lines are the asymptotic solutions provided in Eqs. (8.46) and (8.51). The presence of a peak close to the origin is the signature of spatial clustering. Right. Evolution of the normalized and centered pair correlation function $v(r,t)$ (top) and $w(r,t)$ (bottom) for a one-dimensional domain, starting from a zero-reactivity equilibrium condition. Solid lines are the numerical solutions of the exact Eqs. (8.68) and (8.69), respectively, and dashed lines are the asymptotic solutions provided in Eqs. (8.47) (Eq. (8.52) for the critical case) and (8.48) (Eq. (8.53) for the critical case), respectively. The pair correlation functions are displayed at time $t = 3 \times 10^4$, with the following parameters: $\mathcal{N}_0 = 10^3$, $\vartheta = 8.333 \times 10^{-3}$, $\beta\nu_m = 1.2$, $\lambda = 10^{-2}$, $\nu_n^{(2)} = 2$, $\nu_{nm} = 2.4 \times 10^{-2}$ and $\nu_m^{(2)} = 4 \times 10^{-3}$. Red curves correspond to a supercritical reactor with $\rho = 5 \times 10^{-3}$, green curves correspond to a subcritical reactor with $\rho = -5 \times 10^{-3}$, and blue curves correspond to an exactly critical reactor with $\rho = 0$. For $u(r,t)$, an inset displays the same curves with a logarithmic scale on the ordinate axis.

where we have defined the quantities

$$F(r,t) = e^{-\omega t} \int_0^t dt' e^{\omega t'} G(r,t'), \tag{8.73}$$

where $G(r,t)$ is the Gaussian function

$$G(r,t) = \frac{\exp\left(-\frac{r^2}{8\vartheta\mathcal{D}t}\right)}{(8\pi\vartheta\mathcal{D}t)^{d/2}}, \tag{8.74}$$

and

$$H(r,t) = \frac{e^{-\omega t}}{\beta\nu_m} \left(\frac{\beta\nu_m}{\mathcal{D}}\right)^{\frac{d+2}{4}} \frac{K_{d/2-1}\left(r\sqrt{\beta\nu_m/\mathcal{D}}\right)}{(2\pi)^{d/2} r^{d/2-1}}, \tag{8.75}$$

$K_a(z)$ being the modified Bessel function of the second kind [224]. The parameters read A' $= \nu_n^{(2)}/\nu_m$, $B' = \nu_{nm}/\nu_m$ and $C' = \nu_m^{(2)}/\nu_m$.

The asymptotic expressions in Eqs. (8.70), (8.71) and (8.72) are compared to the numerical solutions of the exact Eqs. (8.67), (8.68) and (8.69) in Figs. 8.11 left and right. In the weak reactivity regime, the asymptotic solutions provide a remarkable approximation of the exact correlation function (small discrepancies are nonetheless visible for short times and distances, as expected). For long times, $u(r,t)$, $v(r,t)$ and $w(r,t)$ have the same asymptotic behaviour. When the reactor is subcritical, the average neutron and precursor densities decrease exponentially fast, and the spatial correlations diverge exponentially fast. On the contrary, when the reactor is supercritical the average neutron and precursor densities grow unbounded exponentially fast, and $u(r,t) \simeq (r,t) \simeq w(r,t)$ asymptotically flatten out as

$$u_\infty(r,t) \simeq \frac{\beta\nu_m}{\mathcal{N}_0} \frac{\vartheta^2(A+2B+C)}{\omega(1+\vartheta)(1+\vartheta-\epsilon)} G(r,t), \tag{8.76}$$

where we have used $F(r,t) \simeq G(r,t)/\omega$ for large times and $\omega > 0$. The case of an exactly critical system leads to some simplifications: by taking the limit $\omega \to 0$ with $\epsilon = 0$ and $\mathcal{D} = D/(1+\vartheta)$ we get

$$\begin{aligned}
u(r,t) &\simeq \frac{A' \left(\frac{\beta\nu_m}{\mathcal{D}}\right)^{\frac{d+2}{4}}}{2\mathcal{N}_0(1+\vartheta)^2} \frac{K_{d/2-1}\left(r\sqrt{\frac{\beta\nu_m}{\mathcal{D}}}\right)}{(2\pi)^{d/2} r^{d/2-1}} + \frac{\beta\nu_m}{\mathcal{N}_0} \frac{\vartheta(A'+2B'+C')}{(1+\vartheta)^2} \frac{\Gamma_{d/2-1}\left(\frac{r^2}{8\vartheta\mathcal{D}t}\right)}{8\pi^{d/2}\mathcal{D}r^{d-2}}, \\
v(r,t) &\simeq \frac{\vartheta(A'+2B') \left(\frac{\beta\nu_m}{\mathcal{D}}\right)^{\frac{d+2}{4}}}{2\mathcal{N}_0(1+\vartheta)^2} \frac{K_{d/2-1}\left(r\sqrt{\frac{\beta\nu_m}{\mathcal{D}}}\right)}{(2\pi)^{d/2} r^{d/2-1}} + \frac{\beta\nu_m}{\mathcal{N}_0} \frac{\vartheta(A'+2B'+C')}{(1+\vartheta)^2} \frac{\Gamma_{d/2-1}\left(\frac{r^2}{8\vartheta\mathcal{D}t}\right)}{8\pi^{d/2}\mathcal{D}r^{d-2}}, \\
w(r,t) &\simeq \frac{\beta\nu_m}{\mathcal{N}_0} \frac{\vartheta(A'+2B'+C')}{(1+\vartheta)^2} \frac{\Gamma_{d/2-1}\left(\frac{r^2}{8\vartheta\mathcal{D}t}\right)}{8\pi^{d/2}\mathcal{D}r^{d-2}},
\end{aligned} \tag{8.77}$$

$\Gamma_a(z)$ being the incomplete Gamma function [224].

The expression of the neutron spatial correlation function $u(r,t)$ is to be compared with that of a reactor without precursors, for which we would have

$$u_p(r,t) = \frac{\beta\nu_n^{(2)}}{\mathcal{N}_0} e^{-\omega_p t} \int_0^t dt' e^{\omega_p t'} \frac{\exp\left(-\frac{r^2}{8Dt'}\right)}{(8\pi D t')^{d/2}} \tag{8.78}$$

for $\epsilon \neq 0$, and

$$u_p(r,t) = \frac{\beta\nu_n^{(2)}}{\mathcal{N}_0} \frac{\Gamma_{d/2-1}\left(\frac{r^2}{8Dt}\right)}{8\pi^{d/2} D r^{d-2}} \tag{8.79}$$

for an exactly critical system [53]. By inspection, observing that the term $\nu_m(A'+2B'+C')$ is dominated by $\nu_n^{(2)}$ and that $\mathcal{D} \simeq D$, we finally have

$$u(r,t) \simeq \vartheta u_p(r,\vartheta t), \tag{8.80}$$

in close analogy with the result for $u(t)$. Precursors are therefore extremely effective also in *quenching the spatial clustering* of the neutrons: in the presence of delayed neutrons, the spatial correlation function of the neutron population has a much slower evolution in time ($t \to \vartheta t$, similarly as for the case of the average density), and its amplitude is further rescaled by a factor ϑ.

Appendix A

Technical notes

Would you tell me, please, which way I ought to go from here?
That depends a good deal on where you want to get to.
I don't much care where –
Then it doesn't matter which way you go.

L. Carroll, Alice in Wonderland (1865).

A.1 Closing the BBGKY hierarchy

The 1−particle distribution f_1 obeys

$$\frac{\partial}{\partial t} f_1 + \mathbf{v}_1 \cdot \nabla_{\mathbf{r}_1} f_s = -\nabla_{\mathbf{v}_1} \cdot \int \mathbf{F}_{2,1} f_2 d\mathbf{r}_2 d\mathbf{v}_2. \tag{A.1}$$

Now, from postulate (i) of Sec. 2.3.2,

$$f_2(\mathbf{r}_1, \mathbf{v}_1, \mathbf{r}_2, \mathbf{v}_2, t) \simeq f_1(\mathbf{r}_1, \mathbf{v}_1, t) f_1(\mathbf{r}_2, \mathbf{v}_2, t) \tag{A.2}$$

so that the function f_2 obeys the two-body Liouville equation

$$\frac{\partial}{\partial t} f_2 + \mathbf{v}_1 \cdot \nabla_{\mathbf{r}_1} f_2 + \mathbf{v}_2 \cdot \nabla_{\mathbf{r}_2} f_2 + \mathbf{F}_{2,1} \cdot \nabla_{\mathbf{v}_1} f_2 + \mathbf{F}_{1,2} \cdot \nabla_{\mathbf{v}_2} f_2 = 0. \tag{A.3}$$

Define τ a time that is long compared to the duration of a collision, and short compared to the duration of a free flight. Let us take the averages

$$\bar{f}_1(\mathbf{r}_1, \mathbf{v}_1, t) = \frac{1}{\tau} \int_0^\tau dt' f_1(\mathbf{r}_1, \mathbf{v}_1, t + t') \tag{A.4}$$

and

$$\bar{f}_2(\mathbf{r}_1, \mathbf{v}_1, \mathbf{r}_2, \mathbf{v}_2, t) = \frac{1}{\tau} \int_0^\tau dt' f_2(\mathbf{r}_1, \mathbf{v}_1, \mathbf{r}_2, \mathbf{v}_2, t + t'). \tag{A.5}$$

As shown by Kirkwood, taking the time average of f_1 and f_2 is expected to flatten the correlations [3, 115]. Applying the time average to Eq. (2.29) yields

$$\frac{\partial}{\partial t} \bar{f}_1 + \mathbf{v}_1 \cdot \nabla_{\mathbf{r}_1} \bar{f}_1 = -\frac{1}{\tau} \nabla_{\mathbf{v}_1} \cdot \int_0^\tau dt' \int \mathbf{F}_{2,1} f_2(t + t') d\mathbf{r}_2 d\mathbf{v}_2, \tag{A.6}$$

where $f_2(t+t')$ can be explicitly solved:

$$f_2(\mathbf{r}_1,\mathbf{v}_1,\mathbf{r}_2,\mathbf{v}_2,t+t') = f_2(\mathbf{r}_1-\Delta_{\mathbf{r}_1}(t'),\mathbf{v}_1-\Delta_{\mathbf{v}_1}(t'),\mathbf{r}_2-\Delta_{\mathbf{r}_2}(t'),\mathbf{v}-\Delta_{\mathbf{v}_2}(t'),t). \tag{A.7}$$

From the binary collision assumptions, the increments are given by

$$\Delta_{\mathbf{r}_i}(t') = \int_0^{t'} dt''\mathbf{v}_i(t'') \tag{A.8}$$

and

$$\Delta_{\mathbf{v}_i}(t') = \int_0^{t'} dt''\mathbf{F}_{j,i}(t''). \tag{A.9}$$

If the mutual interactions are negligible at time $t'=0$ (particles are sufficiently far apart), by applying the postulate (ii) we have

$$f_2(\mathbf{r}_1,\mathbf{v}_1,\mathbf{r}_2,\mathbf{v}_2,t+t') \simeq f_1(\mathbf{r}_1-\Delta_{\mathbf{r}_1}(t'),\mathbf{v}_1-\Delta_{\mathbf{v}_1}(t'),t)f_1(\mathbf{r}_2-\Delta_{\mathbf{r}_2}(t'),\mathbf{v}_2-\Delta_{\mathbf{v}_2}(t'),t). \tag{A.10}$$

Using postulate (iv), we can neglect $\Delta_{\mathbf{r}_1}$ and $\Delta_{\mathbf{r}_1}$ with respect to $\mathbf{r}_1$ and $\mathbf{r}_2$, respectively. Moreover, $\nabla_{\mathbf{v}_1} = -\nabla_{\Delta_{\mathbf{v}_1}}$. Then, the right hand side of Eq. (A.6) can be reduced to

$$\frac{1}{\tau}\int d\mathbf{r}_2 d\mathbf{v}_2\Big[f_1(\mathbf{r}_1,\mathbf{v}_1-\Delta_{\mathbf{v}_1}(\tau),t)f_1(\mathbf{r}_2,\mathbf{v}_2-\Delta_{\mathbf{v}_2}(\tau),t) - f_1(\mathbf{r}_1,\mathbf{v}_1,t)f_1(\mathbf{r}_2,\mathbf{v}_2,t)\Big]. \tag{A.11}$$

Because of the choice of τ as being longer than collision times and shorter than flight times, the position arguments $\mathbf{r}_1$ and $\mathbf{r}_2$ before and after the collisions are left unchanged. Thus, we can set $\mathbf{r}_1=\mathbf{r}_2$ in f_1. Moreover, the integral over $\mathbf{r}_2$ can be replaced by an integral over the relative distance $\mathbf{R}=\mathbf{r}_1-\mathbf{r}_2$. By introducing the cross section Σ, we can write

$$d\mathbf{R} = \tau|\mathbf{v}_1-\mathbf{v}_2|\Sigma(|\mathbf{v}_1-\mathbf{v}_2|,\vartheta)d\Omega, \tag{A.12}$$

where $|\mathbf{v}_1-\mathbf{v}_2|\Sigma(|\mathbf{v}_1-\mathbf{v}_2|,\vartheta)d\Omega$ represents the number of particles of velocity $|\mathbf{v}_1-\mathbf{v}_2|$ scattered into the solid angle $d\Omega$ per unit time and per unit incident flux [3, 14, 115]. The quantity ϑ is the angle in the center of mass frame through which the line joining the particle centers is turned at each collision. By using $\mathbf{v}_1' = \mathbf{v}_1 - \Delta_{\mathbf{v}_1}(\tau)$, Eq. (A.11) yields

$$\int d\mathbf{v}_2 d\Omega|\mathbf{v}_1-\mathbf{v}_2|\Sigma(|\mathbf{v}_1-\mathbf{v}_2|,\vartheta)\Big[f_1(\mathbf{r}_1,\mathbf{v}_1',t)f_1(\mathbf{r}_1,\mathbf{v}_2',t) - f_1(\mathbf{r}_1,\mathbf{v}_1,t)f_1(\mathbf{r}_1,\mathbf{v}_2,t)\Big]. \tag{A.13}$$

By averaging over τ the complete equation, we finally obtain

$$\frac{\partial}{\partial t}\bar{f}_1 + \mathbf{v}_1\cdot\nabla_{\mathbf{r}_1}\bar{f}_1 = \\ \int d\mathbf{v}_2 d\Omega|\mathbf{v}_1-\mathbf{v}_2|\Sigma(|\mathbf{v}_1-\mathbf{v}_2|,\vartheta)\Big[\overline{f_1(\mathbf{r}_1,\mathbf{v}_1',t)f_1(\mathbf{r}_1,\mathbf{v}_2',t)} - \overline{f_1(\mathbf{r}_1,\mathbf{v}_1,t)f_1(\mathbf{r}_1,\mathbf{v}_2,t)}\Big]. \tag{A.14}$$

We make now the hypothesis that $\overline{f_1 f_1} = \bar{f}_1\bar{f}_1$, which would correspond to neglecting correlations over times of the order of τ [3,115]. Under this assumption, we get the following non-linear equation for the quantity $\bar{f}_1$, namely,

$$\frac{\partial}{\partial t}\bar{f}_1 + \mathbf{v}_1\cdot\nabla_{\mathbf{r}_1}\bar{f}_1 = \left(\bar{f}_1,\bar{f}_1\right)_{coll}, \tag{A.15}$$

where the term

$$\left(\bar{f}_1,\bar{f}_1\right)_{coll} = \int d\mathbf{v}_2 d\Omega|\mathbf{v}_1-\mathbf{v}_2|\Sigma(|\mathbf{v}_1-\mathbf{v}_2|,\vartheta)\Big[\bar{f}_1(\mathbf{r}_1,\mathbf{v}_1',t)\bar{f}_1(\mathbf{r}_1,\mathbf{v}_2',t) - \bar{f}_1(\mathbf{r}_1,\mathbf{v}_1,t)\bar{f}_1(\mathbf{r}_1,\mathbf{v}_2,t)\Big]$$

represents the contributions to the phase space balance due to the scattering collisions.

A.2 Feynman-Kac equations

A.2.1 Brownian motion

Consider a regular Brownian motion whose trajectory starts at $\mathbf{x}_0$ at time $t = 0$ and is observed up to a time $t + dt$. From the Brownian particle being Markovian, the trajectory can be decomposed in a first random displacement from $\mathbf{x}_0$ to $\mathbf{x}_0 + \Delta\mathbf{x}$, during a time dt, and then a random path from $\mathbf{x}_0 + \Delta\mathbf{x}$ to the position $\mathbf{x}_{t+dt}$ taken at the final observation time [180, 182]. Correspondingly, the generating function can be written as

$$Q_{t+dt}(s|\mathbf{x}_0) = \mathbb{E}[e^{-s\int_0^{dt}\mathbb{1}_V(\mathbf{x}_{t'})dt' - s\int_{dt}^{t+dt}\mathbb{1}_V(\mathbf{x}_{t'})dt'}]. \tag{A.16}$$

When dt is small, Eq. (A.16) yields

$$Q_{t+dt}(s|\mathbf{x}_0) = e^{-s\mathbb{1}_V(\mathbf{x}_0)dt}\mathbb{E}[e^{-s\int_{dt}^{t+dt}\mathbb{1}_V(\mathbf{x}_{t'})dt'}] = e^{-sV(\mathbf{x}_0)dt}\mathbb{E}_t[Q_t(s|\mathbf{x}_0 + \Delta\mathbf{x})], \tag{A.17}$$

where the former term can be singled out from the expectation sign as being non-random, and in the latter term expectation is taken with respect to the starting point, which is random [180, 182]. In the limit $dt \to 0$, $\Delta\mathbf{x} \to 0$, and we have the Taylor expansion

$$Q_t(s|\mathbf{x}_0 + \Delta\mathbf{x}) \simeq Q_t(s|\mathbf{x}_0) + \Delta\mathbf{x}\cdot\nabla_{\mathbf{x}_0}Q_t(s|\mathbf{x}_0) + \frac{1}{2}(\Delta\mathbf{x})^2\nabla^2_{\mathbf{x}_0}Q_t(s|\mathbf{x}_0) + \cdots. \tag{A.18}$$

By taking expectation, and recalling that for a regular Brownian motion we have $\mathbb{E}[\Delta\mathbf{x}] = 0$ and $\mathbb{E}[(\Delta\mathbf{x})^2] = 2Ddt$ [2, 180], from Eq. (A.18) we get

$$Q_{t+dt}(s|\mathbf{x}_0) \simeq e^{-s\mathbb{1}_V(\mathbf{x}_0)dt}\left[Q_t(s|\mathbf{x}_0) + Ddt\nabla^2_{\mathbf{x}_0}Q_t(s|\mathbf{x}_0)\right], \tag{A.19}$$

which finally yields

$$Q_{t+dt}(s|\mathbf{x}_0) \simeq Q_t(s|\mathbf{x}_0) + Ddt\nabla^2_{\mathbf{x}_0}Q_t(s|\mathbf{x}_0) - s\mathbb{1}_V(\mathbf{x}_0)dtQ_t(s|\mathbf{x}_0), \tag{A.20}$$

when developing at the leading order for vanishing dt. Then, dividing by dt and rearranging terms, we obtain

$$\frac{\partial}{\partial t}Q_t(s|\mathbf{x}_0) = D\nabla^2_{\mathbf{x}_0}Q_t(s|\mathbf{x}_0) - s\mathbb{1}_V(\mathbf{x}_0)Q_t(s|\mathbf{x}_0). \tag{A.21}$$

Suppose now that the Brownian motion undergoes absorption at a rate γ: from the Markovian nature of the process, the probability that the particle having diffused for a time t is absorbed in the interval between t and $t + dt$ is γdt. Consider again a particle starting at $\mathbf{x}_0$ at time $t = 0$: after a dt, by decomposing in elementary mutually exclusive events [2], the particle can either be absorbed in dt (in which case the trajectory terminates), or undergo diffusion and be displaced by $\Delta\mathbf{x}$. Therefore, Eq. (A.17) becomes

$$Q_{t+dt}(s|\mathbf{x}_0) = \gamma dte^{-s\mathbb{1}_V(\mathbf{x}_0)dt} + (1-\gamma dt)e^{-s\mathbb{1}_V(\mathbf{x}_0)dt}\mathbb{E}_t[Q_t(s|\mathbf{x}_0 + \Delta\mathbf{x})], \tag{A.22}$$

where the former term comes from the fact that if the particle is absorbed after a time dt its only contribution to the residence time t_V is $e^{-s\mathbb{1}_V(\mathbf{x}_0)dt}$. By following the same arguments as above, and developing Eq. (A.22) for small dt, we get

$$\frac{\partial}{\partial t}Q_t(s|\mathbf{x}_0) = D\nabla^2_{\mathbf{x}_0}Q_t(s|\mathbf{x}_0) - \gamma Q_t(s|\mathbf{x}_0) - s\mathbb{1}_V(\mathbf{x}_0)Q_t(s|\mathbf{x}_0) + \gamma, \tag{A.23}$$

A.2.2 Exponential flights

Consider the moment generating function $Q_t = \mathbb{E}[e^{-s\ell_V(t)}]$ for exponential flights. Assume an observation time $t + dt$: this can be split into a first interval, from 0 to dt, and then a second interval from dt to $t+dt$. The only requirement is that the process is Markovian: after dt the particle continues its path without memory of the past. We start by observing that in a vanishing small time interval dt, from the definition of the underlying process, the following mutually exclusive events are possible: with probability $1-\Sigma(\mathbf{r}_0)v_0dt$ the particle does not interact with the medium, in which case the walker keeps going in the same direction $\boldsymbol{\omega}_0$ by a space interval $d\mathbf{r}_0 = v_0\boldsymbol{\omega}_0 dt$; with probability $\Sigma_s(\mathbf{r}_0)v_0dt$ the particle has a scattering collision, in which case the particle is isotropically diffused to a random direction $\boldsymbol{\omega}'$ obeying the probability density $1/\Omega_d$; finally, with probability $\Sigma_a(\mathbf{r}_0)v_0dt$ the particle has an absorbing collision, in which case the trajectory is terminated, and no further contribution is added to ℓ_V. This argument leads to the equation

$$\begin{aligned} Q_{t+dt}(s|\mathbf{r}_0,\boldsymbol{\omega}_0) = (1-\Sigma(\mathbf{r}_0)v_0dt)e^{-sv_0\mathbb{1}_V(\mathbf{r}_0)dt}Q_t(s|\mathbf{r}_0+d\mathbf{r}_0,\boldsymbol{\omega}_0) \\ + \Sigma_a(\mathbf{r}_0)v_0dt + \Sigma_s(\mathbf{r}_0)v_0dt\mathbb{E}[Q_t(s|\mathbf{r}_0,\boldsymbol{\omega}')]. \end{aligned} \tag{A.24}$$

The Dynkin's formula [251] allows expressing the average over the random directions as

$$\mathbb{E}[Q_t(s|\mathbf{r}_0,\boldsymbol{\omega}_0')] = \int \frac{d\boldsymbol{\omega}_0'}{\Omega_d} Q_t(s|\mathbf{r}_0,\boldsymbol{\omega}_0'). \tag{A.25}$$

Now, when dt is small, at the leading order we have the Taylor expansion

$$Q_t(s|\mathbf{r}_0+d\mathbf{r}_0,\boldsymbol{\omega}_0) = Q_t(s|\mathbf{r}_0,\boldsymbol{\omega}_0) + v_0\boldsymbol{\omega}_0\cdot\nabla_{\mathbf{r}_0}Q_t dt + \cdots, \tag{A.26}$$

along the direction of $\boldsymbol{\omega}_0$. By recollecting all terms we then get

$$Q_{t+dt} = Q_t + v_0\boldsymbol{\omega}_0\cdot\nabla_{\mathbf{r}_0}Q_t dt - v_0\Sigma Q_t dt - sv\mathbb{1}_V dt + \Sigma_a v_0 dt + \Sigma_s v_0 dt\int\frac{d\boldsymbol{\omega}_0'}{\Omega_d}Q_t(s|\mathbf{r}_0,\boldsymbol{\omega}_0'). \tag{A.27}$$

By dividing by v_0dt and taking the limit $dt\to 0$, we finally obtain the backward Feynman-Kac equation for the moment generating function Q_t, namely

$$\frac{1}{v_0}\frac{\partial}{\partial t}Q_t = \mathcal{L}^\dagger Q_t - s\mathbb{1}_V(\mathbf{r}_0)Q_t + \Sigma_a(\mathbf{r}_0), \tag{A.28}$$

where we have set

$$\mathcal{L}^\dagger = \boldsymbol{\omega}_0\cdot\nabla_{\mathbf{r}_0} - \Sigma(\mathbf{r}_0) + \Sigma_s(\mathbf{r}_0)\int\frac{d\boldsymbol{\omega}_0'}{\Omega_d}. \tag{A.29}$$

A.2.3 Discrete Feynman-Kac equation

Consider a single walker emitted at $\mathbf{r}_0,\boldsymbol{\omega}_0$ and entering its first collision with coordinates $\mathbf{r}_1,\boldsymbol{\omega}_0$. Denote by

$$\tilde{Q}_g(u|\mathbf{r}_1,\boldsymbol{\omega}_0) = \mathbb{E}[e^{-un_V(g)}](\mathbf{r}_1,\boldsymbol{\omega}_0) \tag{A.30}$$

the corresponding moment generating function. The generating functions Q_g and $\tilde{Q}_g$ are related by

$$Q_g(u|\mathbf{r}_0,\boldsymbol{\omega}) = \int d\mathbf{r}_1\tilde{Q}_g(u|\mathbf{r}_1,\boldsymbol{\omega})T^\dagger(\mathbf{r}_1\to\mathbf{r}_0|\boldsymbol{\omega}). \tag{A.31}$$

The separation between $\mathbf{r}_1$ and $\mathbf{r}_0$, at a first glance somewhat artificial, is actually due to the special role of the source: a particle emitted from the source is just transported to the first collision point, and can not be absorbed at $\mathbf{r}_0$ [252, 253].

When entering the collision at $\mathbf{r}_1$, the particle is either absorbed with probability $p_a(\mathbf{r}_1)$, or scattered to a random direction $\boldsymbol{\omega}'$, with probability $p_s(\mathbf{r}_1)$. Exponential flights are Markovian at collision points, which allows splitting the subsequent trajectory into a first jump, from $\mathbf{r}_1$ to $\mathbf{r}'$ in direction $\boldsymbol{\omega}'$, and a path from $\mathbf{r}'$ to the position held at the $(g+1)$-th generation. The displacement $\mathbf{r}' - \mathbf{r}_1$ obeys the jump length density T, and the direction $\boldsymbol{\omega}'$ the density $1/\Omega_d$. Hence, we have

$$\tilde{Q}_{g+1}(u|\mathbf{r}_1, \boldsymbol{\omega}_0) = p_a(\mathbf{r}_1)e^{-u\mathbb{1}_V(\mathbf{r}_1)} + p_s(\mathbf{r}_1)e^{-u\mathbb{1}_V(\mathbf{r}_1)}\mathbb{E}[\tilde{Q}_g(u|\mathbf{r}'_1, \boldsymbol{\omega}'_1)], \tag{A.32}$$

where expectation is taken with respect to the random displacements and directions, and the term $e^{-u\mathbb{1}_V(\mathbf{r}_1)}$ can be singled out because it is not stochastic. Now, the discrete Dynkin's formula [254,255] allows the average over displacements and directions to be expressed as

$$\mathbb{E}[\tilde{Q}_g(u|\mathbf{r}', \boldsymbol{\omega}')] = \int \frac{d\boldsymbol{\omega}'_0}{\Omega_d} \int T^\dagger(\mathbf{r}'_1 \to \mathbf{r}_1|\boldsymbol{\omega}'_0)\tilde{Q}_g(u|\mathbf{r}'_1, \boldsymbol{\omega}'_0)d\mathbf{r}'_1, \tag{A.33}$$

where $T^\dagger$ is the adjoint density associated to T [113, 157]. Intuitively, $T^\dagger$ displaces the walker backward by one generation. Therefore, we obtain the discrete Feynman-Kac equation in integral form, namely

$$\tilde{Q}_{g+1}(u|\mathbf{r}_1, \boldsymbol{\omega}_0) = e^{-u\mathbb{1}_V(\mathbf{r}_1)}\left(p_a(\mathbf{r}_1) + p_s(\mathbf{r}_1)\int \frac{d\boldsymbol{\omega}'_0}{\Omega_d} Q_g(u|\mathbf{r}_1, \boldsymbol{\omega}'_0)\right). \tag{A.34}$$

Finally, by integrating over $T^\dagger$ both sides of Eq. (A.34) we get

$$Q_{g+1}(u|\mathbf{r}_0, \boldsymbol{\omega}_0) = \int d\mathbf{r}_1 T^\dagger(\mathbf{r}_1 \to \mathbf{r}_0|\boldsymbol{\omega}_0)e^{-u\mathbb{1}_V(\mathbf{r}_1)}\left(p_a + p_s\int \frac{d\boldsymbol{\omega}'_0}{\Omega_d} Q_g(u|\mathbf{r}_1, \boldsymbol{\omega}'_0)\right). \tag{A.35}$$

It can be shown [30, 113] that integral equations in the form

$$f(\mathbf{r}_0, \boldsymbol{\omega}_0) = \int d\mathbf{r}_1 T^\dagger(\mathbf{r}_1 \to \mathbf{r}_0|\boldsymbol{\omega}_0)g(\mathbf{r}_1, \boldsymbol{\omega}_0), \tag{A.36}$$

where $T^\dagger$ is the adjoint exponential kernel with cross section Σ, can be equivalently recast into

$$\boldsymbol{\omega}_0 \cdot \nabla_{\mathbf{r}_0} f(\mathbf{r}_0, \boldsymbol{\omega}_0) - \Sigma(\mathbf{r}_0)f(\mathbf{r}_0, \boldsymbol{\omega}_0) + \Sigma(\mathbf{r}_0)g(\mathbf{r}_0, \boldsymbol{\omega}_0) = 0. \tag{A.37}$$

Therefore, Eq. (A.34) gives the *discrete Feynman-Kac equation* in integral-differential form

$$-\boldsymbol{\omega}_0 \cdot \nabla_{\mathbf{r}_0} Q_{g+1}(u|\mathbf{r}_0, \boldsymbol{\omega}_0) + \Sigma Q_{g+1}(u|\mathbf{r}_0, \boldsymbol{\omega}_0) = e^{-u\mathbb{1}_V(\mathbf{r}_0)}\left(\Sigma_a + \Sigma_s\int \frac{d\boldsymbol{\omega}'_0}{\Omega_d} Q_g(u|\mathbf{r}_1, \boldsymbol{\omega}'_0)\right). \tag{A.38}$$

A.2.4 Branching Brownian motion

Consider a branching Brownian motion whose trajectory starts at $\mathbf{x}_0$ at time $t = 0$ and is observed up to a time $t + dt$: from the branching Brownian particle being Markovian, the trajectory can be decomposed in a first random displacement from $\mathbf{x}_0$ to $\mathbf{x}_0 + \Delta\mathbf{x}$, during a time dt, and then a random path from $\mathbf{x}_0 + \Delta\mathbf{x}$ to the position $\mathbf{x}_{t+dt}$ taken at the final observation time. The probability that the particle has an absorption event in the interval between t and $t + dt$ is γdt, and the probability of a reproduction event is βdt. With complementary probability $1 - (\gamma + \beta)dt$, the particle keeps diffusing. By decomposing in mutually exclusive elementary events, Eq. (4.3) yields

$$\begin{aligned} Q_{t+dt}(s|\mathbf{x}_0) = {} & \beta dt e^{-s\mathbb{1}_V(\mathbf{x}_0)dt}\Big[p_0 + p_1 Q_t(s|\mathbf{x}_0) + p_2 Q_t^2(s|\mathbf{x}_0) + \cdots\Big] \\ & + \gamma dt e^{-s\mathbb{1}_V(\mathbf{x}_0)dt} + [1 - (\gamma + \beta)dt]e^{-s\mathbb{1}_V(\mathbf{x}_0)dt}\mathbb{E}[Q_t(s|\mathbf{x}_0 + \Delta\mathbf{x})]. \end{aligned} \tag{A.39}$$

The terms due to branching can be explained as follows. If no particle is re-emitted, which happens with probability p_0, the only contribution to the residence time t_V is $e^{-s\mathbb{1}_V(\mathbf{x}_0)dt}$. If a single particle is re-emitted (with probability p_1), then the moment generating function is simply $Q_t(s|\mathbf{x}_0)$, the position of the walker being unchanged in dt.

If two particles emerge from the reproduction event (with probability p_2), then the probability density for the residence time in V due to the sum of the contributions of each particle would be given by the *convolution* of the respective probability densities of residence times. Since particles supposedly evolve (and are generated) independently of each other, the associated generating function will be simply given by the *product* of the respective generating functions. This rule applies to higher order contributions due to 3 and more particles born during the time interval dt, each weighted by the appropriate probability p_i.

By introducing the probability generating function

$$G[z] = p_0 + p_1 z + p_2 z^2 + \cdots = \sum_i p_i z^i, \tag{A.40}$$

and developing for small dt, equation Eq. (A.39) yields the moment generating function of the residence time of a branching Brownian motion, namely,

$$\frac{\partial}{\partial t} Q_t(s|\mathbf{x}_0) = D\nabla^2_{\mathbf{x}_0} Q_t(s|\mathbf{x}_0) - (\gamma+\beta) Q_t(s|\mathbf{x}_0) - s\mathbb{1}_V(\mathbf{x}_0) Q_t(s|\mathbf{x}_0) + \gamma + \beta G[Q_t(s|\mathbf{x}_0)], \tag{A.41}$$

which relates the moment generating function $Q_t(s|\mathbf{x}_0)$ to the probability generating function G.

A.2.5 Branching exponential flights

Consider the associated moment generating function

$$Q_t(s|\mathbf{r}_0, \boldsymbol{\omega}_0) = \mathbb{E}[e^{-s\ell_V(t)}](\mathbf{r}_0, \boldsymbol{\omega}_0) \tag{A.42}$$

for a single branching exponential flight initially at $\mathbf{r}_0, \boldsymbol{\omega}_0$ at observation time $t = 0$. Assume an observation time $t+dt$: this can be split into a first interval, from 0 to dt, and then a second interval from dt to $t+dt$ (this stems from the underlying branching process being Markovian). In a vanishing small time interval dt, the following mutually exclusive events are possible: the particle does not interact with the medium (with probability $1 - \Sigma v_0 dt$), in which case the walker keeps going in the same direction by a space interval $d\mathbf{r}_0 = v_0 \boldsymbol{\omega}_0 dt$; the particle is scattered with probability $\Sigma_s v_0 dt$; the particle is absorbed with probability $\Sigma_a v_0 dt$; the particle gives rise to a fission with probabilty $\Sigma_f v_0 dt$.

In the case of a fission, the walker disappears and gives rise to i descendants at the same position, with isotropically distributed random directions $\boldsymbol{\omega}'_k$. When $i \geq 1$ (identical) particles are generated, the probability that the contribution to the total travelled length coming from each walker adds up precisely to ℓ_V is given by the convolution of the probability that the first particle spends a length ℓ_1, the second ℓ_2, and the k-th a length $\ell_V - \ell_1 - \ell_2 - \cdots$. In the transformed space, the convolution products amount to a simple product of generating functions.

This argument leads to the equation

$$\begin{aligned} Q_{t+dt}(s|\mathbf{r}_0, \boldsymbol{\omega}_0) = {} & (1 - \Sigma v_0 dt) e^{-sv\mathbb{1}_V(\mathbf{r}_0)dt} Q_t(s|\mathbf{r}_0 + d\mathbf{r}_0, \boldsymbol{\omega}_0) \\ & + \Sigma_s v_0 dt \mathbb{E}[Q_t(s|\mathbf{r}_0, \boldsymbol{\omega}')] + \Sigma_a v_0 dt \\ & + \Sigma_f v_0 dt \left[p_0 + p_1 \mathbb{E}[Q_t(s|\mathbf{r}_0, \boldsymbol{\omega}'_1)] + p_2 \mathbb{E}[Q_t(s|\mathbf{r}_0, \boldsymbol{\omega}'_{21}) Q_t(s|\mathbf{r}_0, \boldsymbol{\omega}'_{22})] + \cdots \right], \end{aligned} \tag{A.43}$$

where expectations are taken with respect to the random directions $\boldsymbol{\omega}'_i$. Now, if we suppose that the descendant directions are independent, the expectation of a product of random variables becomes the product of expectations, so that

$$p_0 + p_1\mathbb{E}[Q_t(s|\mathbf{r}_0,\boldsymbol{\omega}'_1)] + p_2\mathbb{E}[Q_t(s|\mathbf{r}_0,\boldsymbol{\omega}'_{21})Q_t(s|\mathbf{r}_0,\boldsymbol{\omega}'_{22})] + \cdots = G\left[\langle Q_t(s|\mathbf{r}_0,\boldsymbol{\omega}'_0)\rangle_\Omega\right], \tag{A.44}$$

where

$$G[z] = p_0 + p_1 z + p_2 z^2 + \cdots \tag{A.45}$$

is the probability generating function associated to p_i, and $\langle\cdots\rangle_\Omega$ denotes the average over the random directions. By developing the resulting equation for small $dt \to 0$ and keeping only leading order terms, we finally obtain the *backward Feynman-Kac equation* for the moment generating function Q_t of *branching exponential flights*, namely

$$\frac{1}{v_0}\frac{\partial}{\partial t}Q_t = \boldsymbol{\omega}_0\cdot\nabla_{\mathbf{r}_0}Q_t - \Sigma Q_t - s\mathbb{1}_V(\mathbf{r}_0)Q_t + \Sigma_a + \Sigma_s\langle Q_t\rangle_\Omega + \Sigma_f G[\langle Q_t\rangle_\Omega], \tag{A.46}$$

which relates the generating function Q_t of the travelled length ℓ_V to the generating function $G[z]$ of the offspring number i.

A.2.6 Discrete Feynman-Kac equations

Let us begin with a single branching exponential flight entering its *first collision* with coordinates $\mathbf{r}_1, \boldsymbol{\omega}_0$, and denote by

$$\tilde{Q}_g(u|\mathbf{r}_1,\boldsymbol{\omega}_0) = \mathbb{E}[e^{-un_V(g)}](\mathbf{r}_1,\boldsymbol{\omega}_0) \tag{A.47}$$

the corresponding moment generating function. A particle emitted from the source is just transported to the first collision point, and can not be absorbed nor multiplied at $\mathbf{r}_0$. Exponential flights are Markovian at collision points, which allows splitting each subsequent trajectory into a first jump, from $\mathbf{r}_1$ to $\mathbf{r}'$ in direction $\boldsymbol{\omega}'$, and a branching path from $\mathbf{r}'$ to the positions held at the $(g+1)$-th generation. The displacement $\mathbf{r}' - \mathbf{r}_1$ obeys the jump length density T, and the direction $\boldsymbol{\omega}'$ is isotropic. If the trajectory is absorbed at $\mathbf{r}_1$, there will be no further events contributing to n_V. Hence, we have

$$\begin{aligned}\tilde{Q}_{g+1}(u|\mathbf{r}_1,\boldsymbol{\omega}_0) &= p_a e^{-u\mathbb{1}_V(\mathbf{r}_1)} + p_s e^{-u\mathbb{1}_V(\mathbf{r}_1)}\mathbb{E}[\tilde{Q}_g(u|\mathbf{r}'_1,\boldsymbol{\omega}'_1)] \\ &+ p_f e^{-u\mathbb{1}_V(\mathbf{r}_1)}\Big[p_0 + p_1\mathbb{E}[\tilde{Q}_g(u|\mathbf{r}'_1,\boldsymbol{\omega}'_1)] + p_2\mathbb{E}[\tilde{Q}_g(u|\mathbf{r}'_{21},\boldsymbol{\omega}'_{21})\tilde{Q}_g(u|\mathbf{r}'_{22},\boldsymbol{\omega}'_{22})] + \cdots\Big],\end{aligned} \tag{A.48}$$

where expectation is taken with respect to the random displacements and directions, and the term $e^{-u\mathbb{1}_V(\mathbf{r}_1)}$ can be singled out because it is not stochastic. The terms at the right hand side in Eq. (A.48) can be understood as follows: the probability that i identical and indistinguishable particles (born at $\mathbf{r}_1$) give rise to n_V collisions in V is given by the convolution product that the first makes n_1 collisions, the second n_2, ..., and the i-th $n_V - n_1 - n_2 - \cdots$. In the transformed space, this convolution becomes a simple product of generating functions. If we assume that the descendant particles are independent, the expectation of the products in Eq. (A.48) becomes the product of the expectations. Now, the discrete Dynkin's formula [254] allows the average over displacements and directions to be expressed as

$$\mathbb{E}[\tilde{Q}_g(u|\mathbf{r}',\boldsymbol{\omega}')] = \int\frac{d\boldsymbol{\omega}'_0}{\Omega_d}\int T^\dagger(\mathbf{r}'_1\to\mathbf{r}_1|\boldsymbol{\omega}'_0)\tilde{Q}_g(u|\mathbf{r}'_1,\boldsymbol{\omega}'_0)d\mathbf{r}'_1 d\boldsymbol{\omega}'_0. \tag{A.49}$$

We therefore obtain

$$\tilde{Q}_{g+1}(u|\mathbf{r}_1,\boldsymbol{\omega}_0) = e^{-u\mathbb{1}_V(\mathbf{r}_1)}\Big[p_a + p_s\langle Q_g\rangle_\Omega + p_f G\left[\langle Q_g\rangle_\Omega\right]\Big]. \tag{A.50}$$

Finally, by integrating over $T^\dagger$ both sides of Eq. (A.50) we get

$$Q_{g+1}(u|\mathbf{r}_0,\boldsymbol{\omega}_0) = \int d\mathbf{r}_1 T^\dagger(\mathbf{r}_1\to\mathbf{r}_0|\boldsymbol{\omega}_0) e^{-u\mathbb{1}_V(\mathbf{r}_1)}\Big[p_a + p_s\langle Q_g\rangle_\Omega + p_f G\left[\langle Q_g\rangle_\Omega\right]\Big]. \tag{A.51}$$

By using the same transformation of exponential kernels as in A.2.3, Eq. (A.50) yields the discrete Feynman-Kac equation in integro-differential form

$$-\boldsymbol{\omega}_0\cdot\nabla_{\mathbf{r}_0}Q_{g+1}(u|\mathbf{r}_0,\boldsymbol{\omega}_0) + \Sigma Q_{g+1}(u|\mathbf{r}_0,\boldsymbol{\omega}_0) = e^{-u\mathbb{1}_V(\mathbf{r}_0)}\Big[\Sigma_a + \Sigma_s\langle Q_g\rangle_\Omega + \Sigma_f G\left[\langle Q_g\rangle_\Omega\right]\Big], \tag{A.52}$$

which relates the generating function Q_g of the number of visits n_V to the generating function G of the offspring number i.

A.3 Spatial correlations in one-dimensional domains

Consider a box of half-size L, i.e., a segment $[-L, L]$ with $V = 2L$. At the boundaries $x = \pm L$, we impose reflecting (Neumann) conditions. At criticality, the Green's function for this system reads [191]

$$\mathcal{G}_t(x,x_0) = \frac{1}{2L} + \frac{1}{L}\sum_{k=1}^{\infty}\varphi_k(x)\varphi_k(x_0)e^{-\alpha_k t}, \tag{A.53}$$

where we have set

$$\varphi_k(x) = \cos\left(\frac{k\pi(L-x)}{2L}\right) \tag{A.54}$$

and

$$\alpha_k = \left(\frac{\pi}{2}\right)^2\frac{D}{L^2}k^2. \tag{A.55}$$

We can identify the mixing time with $\tau_D = (2/\pi)^2(L^2/D)$. If we choose the uniform spatial distribution $q(x_0) = 1/2L$ at time $t = 0$, the average density simply reads

$$c_t(x_i) = \frac{N}{2L}. \tag{A.56}$$

As for the pair correlation function, the case of the free system is obtained by resorting to Eq. 8.7, which yields

$$h_t^f(x_i,x_j) = \frac{N(N-1)}{(2L)^2} + \frac{\beta\nu_2 N}{(2L)^2}\left[t + \sum_{k=1}^{\infty}\varphi_k(x_i)\varphi_k(x_j)\frac{1-e^{-2\alpha_k t}}{\alpha_k}\right], \tag{A.57}$$

For times $t \gg \tau_D$, the exponential term in Eq. A.57 vanishes, and the spatial shape of $h_t^f(x_i,x_j)$ is frozen. In particular, the series appearing at the right-hand side is bounded, namely,

$$\sum_{k=1}^{\infty}\frac{\varphi_k(x_i)\varphi_k(x_j)}{\alpha_k} \le \frac{2}{3}\frac{L^2}{D}. \tag{A.58}$$

Then, for $N \gg 1$ the amplitude of the normalized and centered pair correlation function asymptotically grows as

$$g_t^f(x_i, x_j) = \frac{h_t^f(x_i, x_j) - c_t(x_i)c_t(x_j)}{c_t(x_i)c_t(x_j)} \simeq \frac{\beta\nu_2}{N}t. \tag{A.59}$$

Therefore, for times $t \gg N/(\beta\nu_2)$, $g_f(x_i, x_j, t) \gg 1$, which allows identifying the extinction time $\tau_E = N/(\beta\nu_2)$. Observe that, for $N \gg 1$, $g_f(x_i, x_j, t)$ can be expressed in terms of the two characteristic time scales, namely,

$$g_t^f(x_i, x_j) = \frac{t}{\tau_E} + \frac{\tau_D}{\tau_E}\sum_{k=1}^{\infty}\varphi_k(x_i)\varphi_k(x_j)\frac{1 - e^{-2k^2\frac{t}{\tau_D}}}{k^2}. \tag{A.60}$$

The average square distance between particles

$$\langle r^2\rangle_f(t) = \frac{\int dx_i \int dx_j (x_i - x_j)^2 h_t^f(x_i, x_j)}{\int dx_i \int dx_j h_t^f(x_i, x_j)} \tag{A.61}$$

can be obtained by integration. At time $t = 0$,

$$\langle r^2\rangle_f(0) = \frac{2}{3}L^2 = \langle r^2\rangle_{id}. \tag{A.62}$$

At times $t \gg \tau_E$, $h_t^f(x_i, x_j)$ becomes spatially flat, and $\langle r^2\rangle_f(t)$ converges again to the ideal average square distance, namely, $\lim_{t\to\infty}\langle r^2\rangle_f(t) = \langle r^2\rangle_{id}$.

For the case of population control, from Eq. 8.10 we get

$$h_t^c(x_i, x_j) = \frac{N(N-1)}{(2L)^2} + \frac{\beta\nu_2 N}{(2L)^2}\sum_{k=1}^{\infty}\varphi_k(x_i)\varphi_k(x_j)\frac{1 - e^{-(2\alpha_k + \beta_p)t}}{\alpha_k + \frac{\beta_p}{2}}, \tag{A.63}$$

where $\beta_p = \beta/(N-1)$. Assuming that $\tau_E \gg \tau_D$, for times $t \gg \tau_D$ the series appearing at the right-hand side is bounded, namely,

$$\sum_{k=1}^{\infty}\frac{\varphi_k(x_i)\varphi_k(x_j)}{\alpha_k + \frac{\beta_p}{2}} \leq \frac{\sqrt{\frac{2\beta_p L^2}{D}}\coth\left(\sqrt{\frac{2\beta_p L^2}{D}}\right) - 1}{\beta_p}. \tag{A.64}$$

For $N \gg 1$ the normalized and centered pair correlation function at long times converges to

$$g_\infty^c(x_i, x_j) = \frac{\tau_D}{\tau_E}\sum_{k=1}^{\infty}\frac{\varphi_k(x_i)\varphi_k(x_j)}{k^2 + \frac{\tau_D}{2\tau_E}}. \tag{A.65}$$

In particular, its amplitude is asymptotically bounded by

$$|g_t^c(x_i, x_j)| \leq \frac{\beta\nu_2}{N}\frac{2}{3}\frac{L^2}{D}, \tag{A.66}$$

where the absolute value is taken because $g_t^c(x_i, x_j)$ can be negative.

As for the average square distance, at time $t = 0$ we have again $\langle r^2\rangle_c(0) = \langle r^2\rangle_{id}$, as expected. The asymptotic behaviour of $\langle r^2\rangle_c(t)$ at times $t \gg \tau_D$ can be computed exactly, and reads

$$\langle r^2\rangle_c^\infty = \lim_{t\to\infty}\langle r^2\rangle_c(t) = 4\frac{D}{\beta_p}\left[1 - \sqrt{\frac{2D}{\beta_p L^2}}\tanh\left(\sqrt{\frac{\beta_p L^2}{2D}}\right)\right]. \tag{A.67}$$

In the limit of extremely large populations, we have $\lim_{N\to\infty}\langle r^2\rangle_c = (2/3)L^2$ and we recover the ideal case.

A.4 Delayed neutrons

A.4.1 Obtaining the moments from the master equation

We sketch here the derivation of the moment equations from the master equation. A more thorough discussion can be found in [51, 53]. Consider for instance a master equation in the form

$$\frac{\partial}{\partial t}\mathcal{P}_t(n) = W(n-1)\mathcal{P}_t(n-1) - Wn\mathcal{P}_t(n), \tag{A.68}$$

where W is a rate. Upon multiplying each term by a factor n^m and summing over n, the left-hand-side immediately yields $\partial_t\langle n^m\rangle$. At the right-hand-side, a change of index $n \to n+1$ transforms the term $W\sum_n n^m(n-1)\mathcal{P}_t(n-1)$ into $W\sum_n(n+1)^m n\mathcal{P}_t(n)$. Then, we get

$$\frac{\partial}{\partial t}\langle n^m\rangle = W\langle n(n+1)^m\rangle - W\langle n^{m+1}\rangle. \tag{A.69}$$

Observe that $n(n+1)^m - n^{m+1}$ is a polynomial of order m. For instance, for the average we have $m = 1$ and

$$\frac{\partial}{\partial t}\langle n\rangle = W\langle n\rangle, \tag{A.70}$$

whereas for the second moment $m = 2$ and

$$\frac{\partial}{\partial t}\langle n^2\rangle = 2W\langle n^2\rangle + W\langle n\rangle. \tag{A.71}$$

The spatial behaviour can be obtained by following the same strategy. Observe that the creation and annihilation operators commute, i.e., $a_k a_k^\dagger \mathbf{n} = a_k^\dagger a_k \mathbf{n}$. Consider, e.g., a master equation in the form

$$\frac{\partial}{\partial t}\mathcal{P}_t(\mathbf{n}) = \sum_i [W(n_i-1)\mathcal{P}_t(a_i\mathbf{n}) - Wn_i\mathcal{P}_t(\mathbf{n})]. \tag{A.72}$$

Upon multiplication of each term by n_k^m and summation over $\mathbf{n}$, the left-hand-side yields $\partial_t\langle n_k^m\rangle$. At the right-hand-side, the term $\sum_{\mathbf{n}}\sum_i n_k^m W(n_i-1)\mathcal{P}_t(a_i\mathbf{n})$ can be grouped with $-\sum_{\mathbf{n}}\sum_i n_k^m W n_i\mathcal{P}_t(\mathbf{n})$ by changing the summation variable $\mathbf{n} \to a_i^\dagger\mathbf{n}$. This gives

$$W\sum_{\mathbf{n}}\sum_i [(n_k+\delta_{k,i})^m n_i - n_k^m n_i]\mathcal{P}_t(\mathbf{n}). \tag{A.73}$$

The only non-vanishing term of the sum over i is then for $i = k$, which finally yields

$$\frac{\partial}{\partial t}\langle n_k^m\rangle = W\langle(n_k+1)^m n_k\rangle - W\langle n_k^{m+1}\rangle. \tag{A.74}$$

For instance, for the average we have

$$\frac{\partial}{\partial t}\langle n_k\rangle = W\langle n_k\rangle, \tag{A.75}$$

whereas for the second moment

$$\frac{\partial}{\partial t}\langle n_k^2\rangle = 2W\langle n_k^2\rangle + W\langle n_k\rangle. \tag{A.76}$$

A.4.2 Asymptotic analysis of the average total populations

Equations (8.27) can be solved exactly, and yield

$$\langle n(t)\rangle = n_0 \frac{(\rho-\Omega_2)e^{\Omega_1 t} + (\Omega_1-\rho)e^{\Omega_2 t}}{\Omega_1-\Omega_2} \tag{A.77}$$

$$\langle m(t)\rangle = m_0 \frac{\Omega_2 e^{\Omega_1 t} - \Omega_1 e^{\Omega_2 t}}{\Omega_2-\Omega_1}, \tag{A.78}$$

where the eigen-frequencies $\Omega_{1,2}$ are determined by the roots of the characteristic polynomial associated to (8.27), namely,

$$\Omega_{1,2} = \frac{-\lambda+\rho-\beta\nu_m \pm \sqrt{4\lambda\rho + (\lambda-\rho+\beta\nu_m)^2}}{2}. \tag{A.79}$$

Then, since $\Omega_1 \geq \Omega_2$ and $\Omega_2 < 0$, for long times $t \gg 1/(\Omega_1-\Omega_2)$ the moments asymptotically behave as

$$\langle n(t)\rangle \simeq n_0 \frac{\rho-\Omega_2}{\Omega_1-\Omega_2} e^{\Omega_1 t} \tag{A.80}$$

$$\langle m(t)\rangle \simeq m_0 \frac{\Omega_2}{\Omega_2-\Omega_1} e^{\Omega_1 t}. \tag{A.81}$$

The sign of Ω_1 depends on the reactivity ρ. The ratio between the two average populations asymptotically converges to a constant, namely,

$$\frac{\langle n(t)\rangle}{\langle m(t)\rangle} \simeq \vartheta \frac{\Omega_2-\rho}{\Omega_2}. \tag{A.82}$$

If the net reactivity is weak, expanding in small powers of $|\rho|$ yields the characteristic roots

$$\Omega_1 \simeq \frac{\vartheta}{1+\vartheta}\rho \tag{A.83}$$

$$\Omega_2 \simeq -\beta\nu_m(1+\vartheta-\epsilon), \tag{A.84}$$

where we have introduced

$$\epsilon = \frac{\rho}{\beta\nu_m}\frac{1}{1+\vartheta}. \tag{A.85}$$

For long times, the average densities will then exponentially grow or shrink with an asymptotic period

$$\omega = \frac{\vartheta}{1+\vartheta}\rho. \tag{A.86}$$

A.4.3 Equations for the second moments

The equations for the second moments

$$\langle n^2(t)\rangle = \sum_{n,m} n^2 \mathcal{P}_t(n,m), \quad \langle m^2(t)\rangle = \sum_{n,m} m^2 \mathcal{P}_t(n,m) \tag{A.87}$$

and for the cross-moment

$$\langle n(t)m(t)\rangle = \sum_{n,m} nm\mathcal{P}_t(n,m) \tag{A.88}$$

are slightly cumbersome. After some manipulations (see Appendix A.4.1), we get

$$\frac{\partial}{\partial t}\langle n^2(t)\rangle = 2(\rho-\beta\nu_m)\langle n^2(t)\rangle + 2\lambda\langle n(t)m(t)\rangle + (\beta\nu_n^{(2)}+\beta\nu_m-\rho)\langle n(t)\rangle + \lambda\langle m(t)\rangle, \tag{A.89}$$

$$\begin{aligned}\frac{\partial}{\partial t}\langle n(t)m(t)\rangle = {} & (\rho-\beta\nu_m-\lambda)\langle n(t)m(t)\rangle + \beta\nu_m\langle n^2(t)\rangle \\ & + \lambda\langle m^2(t)\rangle + \beta\nu_{nm}\langle n(t)\rangle - \beta\nu_m\langle n(t)\rangle - \lambda\langle m(t)\rangle,\end{aligned} \tag{A.90}$$

$$\frac{\partial}{\partial t}\langle m^2(t)\rangle = -2\lambda\langle m^2(t)\rangle + 2\beta\nu_m\langle n(t)m(t)\rangle + (\beta\nu_m^{(2)}+\beta\nu_m)\langle n(t)\rangle + \lambda\langle m(t)\rangle, \tag{A.91}$$

where we have defined the factorial moments $\nu_n^{(2)} = \sum_{i,j} i(i-1)P_{i,j}$ and $\nu_m^{(2)} = \sum_{i,j} j(j-1)P_{i,j}$ and the cross-moment $\nu_{nm} = \sum_{i,j} ijP_{i,j}$. These equations are to be solved together with the initial conditions $\langle n^2(0)\rangle = n_0^2$, $\langle n(0)m(0)\rangle = n_0m_0$ and $\langle m^2(0)\rangle = m_0^2$. Similar results for the second moments have been previously obtained by several authors by following different strategies [4, 27, 32, 116].

A.4.4 Second moments of the total populations: asymptotic analysis

The system of differential equations (8.41), (8.42) and (8.43) can be written in the compact form

$$\frac{1}{\beta\nu_m}\frac{\partial}{\partial t}\mathbf{U}(t) = \mathbf{M}\mathbf{U}(t) + \mathbf{Q}\frac{e^{-\omega t}}{n_0}, \tag{A.92}$$

by setting $\mathbf{U}(t) = [u(t), v(t), w(t)]^T$,

$$\mathbf{M} = \begin{pmatrix} -2(1-\epsilon) & 2(1-\epsilon) & 0 \\ \vartheta & -1-\vartheta+\epsilon & 1-\epsilon \\ 0 & 2\vartheta & -2\vartheta \end{pmatrix} \tag{A.93}$$

and $\mathbf{Q} = \left[A, \vartheta B, \vartheta^2 C\right]^T$, with

$$A = \frac{\nu_n^{(2)}}{\nu_m}\left(1-\frac{\epsilon}{1+\vartheta}\right) + 2\left(1-2\frac{\epsilon}{1+\vartheta}\right) \tag{A.94}$$

$$B = \frac{\nu_{nm}}{\nu_m} - 2 \tag{A.95}$$

$$C = \frac{\nu_m^{(2)}}{\nu_m} + 2. \tag{A.96}$$

Then, by taking the Laplace transform of each term, we get the algebraic system

$$\left(\mathbf{M} - \frac{s}{\beta\nu_m}\mathbf{I}\right)\tilde{\mathbf{U}}(s) = -\frac{1}{n_0}\frac{1}{\omega+s}\mathbf{Q}, \tag{A.97}$$

where s denotes the Laplace variable and $\mathbf{I}$ the identity matrix. The asymptotic behaviour of the variances can be determined by solving the system (A.97) and expanding the transformed solutions $\tilde{\mathbf{U}}(s) = [\tilde{u}(s), \tilde{v}(s), \tilde{w}(s)]^T$ in dominant powers for small s. By retaining the leading order terms we get

$$\tilde{u}(s) \simeq \frac{\beta\nu_m}{n_0}\frac{\vartheta^2(A+2B+C)}{(1+\vartheta)(1+\vartheta-\epsilon)}\tilde{F}(s) + \frac{A(1-\epsilon)+\vartheta(3A+2B)}{2n_0(1+\vartheta)(1+\vartheta-\epsilon)}s\tilde{F}(s), \tag{A.98}$$

$$\tilde{v}(s) \simeq \frac{\beta\nu_m}{n_0}\frac{\vartheta^2(A+2B+C)}{(1+\vartheta)(1+\vartheta-\epsilon)}\tilde{F}(s) + \frac{\vartheta(A+2B)}{2n_0(1+\vartheta)(1+\vartheta-\epsilon)}s\tilde{F}(s), \tag{A.99}$$

$$\tilde{w}(s) \simeq \frac{\beta\nu_m}{n_0}\frac{\vartheta^2(A+2B+C)}{(1+\vartheta)(1+\vartheta-\epsilon)}\tilde{F}(s), \tag{A.100}$$

where we have defined

$$\tilde{F}(s) = \frac{1}{s(\omega+s)}. \tag{A.101}$$

Then, by reverting to the real space we obtain

$$u(t) \simeq \frac{A(1-\epsilon)+\vartheta(3A+2B)}{2n_0(1+\vartheta)(1+\vartheta-\epsilon)}e^{-\omega t} + \frac{\beta\nu_m}{n_0}\frac{\vartheta^2(A+2B+C)}{(1+\vartheta)(1+\vartheta-\epsilon)}\frac{1-e^{-\omega t}}{\omega}, \tag{A.102}$$

$$v(t) \simeq \frac{\vartheta(A+2B)}{2n_0(1+\vartheta)(1+\vartheta-\epsilon)}e^{-\omega t} + \frac{\beta\nu_m}{n_0}\frac{\vartheta^2(A+2B+C)}{(1+\vartheta)(1+\vartheta-\epsilon)}\frac{1-e^{-\omega t}}{\omega}, \tag{A.103}$$

$$w(t) \simeq \frac{\beta\nu_m}{n_0}\frac{\vartheta^2(A+2B+C)}{(1+\vartheta)(1+\vartheta-\epsilon)}\frac{1-e^{-\omega t}}{\omega}. \tag{A.104}$$

A.4.5 Equations for the spatial correlations

By manipulating the master equation (8.58) (see Appendix A.4.1), we obtain the evolution equations

$$\begin{aligned}\frac{\partial}{\partial t}\langle n_k n_{k+j}\rangle &= 2(\rho-\beta\nu_m)\langle n_k n_{k+j}\rangle + \eta\langle n_k\Delta n_{k+j}\rangle + \eta\langle n_{k+j}\Delta n_k\rangle + \lambda(\langle n_{k+j}m_k\rangle + \langle n_k m_{k+j}\rangle)\\ &+ \delta_{j,0}((\beta\nu_n^{(2)}+\beta\nu_m-\rho)\langle n_k\rangle + \lambda\langle m_k\rangle) + \delta_{j,0}\eta(\langle n_{k+1}\rangle\\ &+ \langle n_{k-1}\rangle + 2\langle n_k\rangle) - \delta_{j,1}\eta(\langle n_{k+1}\rangle + \langle n_k\rangle) - \delta_{j,-1}\eta(\langle n_k\rangle + \langle n_{k-1}\rangle),\end{aligned} \tag{A.105}$$

$$\begin{aligned}\frac{\partial}{\partial t}\langle n_{k+j}m_k\rangle &= (\rho-\beta\nu_m-\lambda)\langle n_{k+j}m_k\rangle + \eta\langle m_k\Delta n_{k+j}\rangle + \beta\nu_m\langle n_k n_{k+j}\rangle + \lambda\langle m_k m_{k+j}\rangle\\ &+ \delta_{j,0}((\beta\nu_{nm}+\beta\nu_m-\beta\nu_m)\langle n_k\rangle - \lambda\langle m_k\rangle),\end{aligned} \tag{A.106}$$

$$\begin{aligned}\frac{\partial}{\partial t}\langle m_k m_{k+j}\rangle &= -\lambda\langle m_k m_{k+j}\rangle + \beta\nu_m(\langle n_{k+j}m_k\rangle + \langle n_k m_{k+j}\rangle)\\ &+ \delta_{j,0}((\beta\nu_m^{(2)}+\beta\nu_m)\langle n_k\rangle + \lambda\langle m_k\rangle).\end{aligned} \tag{A.107}$$

A.4.6 Asymptotic analysis of the spatial correlations

In the long time limit, $\mathcal{N}(t) \simeq \mathcal{N}_0 e^{\omega t}$ and $\chi_t \simeq \vartheta(1+\epsilon)$, so that we can rewrite Eqs. (8.67), (8.68) and (8.69) as

$$\frac{1}{\beta\nu_m}\frac{\partial}{\partial t}\mathbf{U}(r,t) = (\mathbf{M} + \mathbf{D}\nabla^2)\mathbf{U}(r,t) + \mathbf{Q}'\frac{e^{-\omega t}}{\mathcal{N}_0}\delta(r), \tag{A.108}$$

where we have defined the correlation vector $\mathbf{U}(r,t) = [u(r,t), v(r,t), w(r,t)]^T$, the rescaled diffusion matrix

$$\mathbf{D} = \frac{D}{\beta\nu_m}\begin{pmatrix} 2 & 0 & 0 \\ 0 & 1 & 0 \\ 0 & 0 & 0 \end{pmatrix}. \tag{A.109}$$

and $\mathbf{Q}' = \left[A', \vartheta B', \vartheta^2 C'\right]^T$, with $A' = \nu_n^{(2)}/\nu_m$, $B' = \nu_{nm}/\nu_m$ and $C' = \nu_m^{(2)}/\nu_m$. The matrix $\mathbf{M}$ has been defined in Eq. (A.93). Observe that $\mathbf{M}$ and $\mathbf{D}$ do not commute.

By taking the Laplace and Fourier transforms, this system of partial differential equations reduces to an algebraic system for the transformed vector $\tilde{\mathbf{U}}(k,s) = [\tilde{u}(k,s), \tilde{v}(k,s), \tilde{w}(k,s)]^T$, namely,

$$\left(\mathbf{M} - k^2\mathbf{D} - \frac{s}{\beta\nu_m}\mathbf{I}\right)\tilde{\mathbf{U}}(k,s) = -\frac{1}{\mathcal{N}_0}\frac{1}{\omega+s}\mathbf{Q}', \tag{A.110}$$

where k denotes the Fourier variable. The asymptotic solution in time and space for the system is obtained by taking $s \to 0$ and $|k| \to 0$, respectively. By retaining the leading order terms for small ϵ and small ϑ we get

$$\begin{aligned}
\tilde{u}(k,s) &\simeq \frac{\beta\nu_m}{\mathcal{N}_0}\frac{\vartheta^2(A'+2B'+C')}{(1+\vartheta)(1+\vartheta-\epsilon)}\tilde{F}(k,s) + \frac{\beta\nu_m A'(1-\epsilon)}{2\mathcal{N}_0(1+\vartheta)(1+\vartheta-\epsilon)}\tilde{H}(k,s), \\
\tilde{v}(k,s) &\simeq \frac{\beta\nu_m}{\mathcal{N}_0}\frac{\vartheta^2(A'+2B'+C')}{(1+\vartheta)(1+\vartheta-\epsilon)}\tilde{F}(k,s) + \frac{\beta\nu_m\vartheta(A'+2B')}{2\mathcal{N}_0(1+\vartheta)(1+\vartheta-\epsilon)}\tilde{H}(k,s), \\
\tilde{w}(k,s) &\simeq \frac{\beta\nu_m}{\mathcal{N}_0}\frac{\vartheta^2(A'+2B'+C')}{(1+\vartheta)(1+\vartheta-\epsilon)}\tilde{F}(k,s),
\end{aligned} \tag{A.111}$$

where we have set

$$\tilde{F}(k,s) = \frac{1}{(\omega+s)\,(2\vartheta\mathcal{D}k^2+s)}, \tag{A.112}$$

with $\mathcal{D} = D/(1+\vartheta-\epsilon)$, and

$$\tilde{H}(k,s) = \frac{1}{(\omega+s)\,(\mathcal{D}k^2+\beta\nu_m)}. \tag{A.113}$$

For domains where spherical symmetry applies, the d-dimensional inverse Fourier transform may be expressed as

$$f(r) = \mathcal{F}^{-1}[\tilde{f}(k)] = \frac{r^{1-d/2}}{(2\pi)^{d/2}}\int_0^\infty k^{d/2} J_{d/2-1}(kr)\tilde{f}(k)dk, \tag{A.114}$$

where $J_a(z)$ is the modified Bessel function of the first kind [224]. Now, observe that

$$F(r,t) = \mathcal{F}^{-1}[\mathcal{L}^{-1}[\tilde{F}(k,s)]] = e^{-\omega t}\int_0^t dt' e^{\omega t'} G(r,t'), \tag{A.115}$$

where $G(r,t)$ is the Gaussian function

$$G(r,t) = \frac{\exp\left(-\frac{r^2}{8\vartheta\mathcal{D}t}\right)}{(8\pi\vartheta\mathcal{D}t)^{d/2}}, \tag{A.116}$$

and

$$H(r,t) = \mathcal{F}^{-1}[\mathcal{L}^{-1}[\tilde{H}(k,s)]] = \frac{e^{-\omega t}}{\beta\nu_m}\left(\frac{\beta\nu_m}{\mathcal{D}}\right)^{\frac{d+2}{4}} \frac{K_{d/2-1}\left(r\sqrt{\beta\nu_m/\mathcal{D}}\right)}{(2\pi)^{d/2}r^{d/2-1}}, \tag{A.117}$$

$K_a(z)$ being the modified Bessel function of the second kind [224]. The solution $\mathbf{U}(r,t)$ in real space can be therefore expressed as:

$$\begin{aligned}
u(r,t) &\simeq \frac{\beta\nu_m A'(1-\epsilon)}{2\mathcal{N}_0(1+\vartheta)(1+\vartheta-\epsilon)}H(r,t) + \frac{\beta\nu_m}{\mathcal{N}_0}\frac{\vartheta^2(A'+2B'+C')}{(1+\vartheta)(1+\vartheta-\epsilon)}F(r,t),\\
v(r,t) &\simeq \frac{\beta\nu_m \vartheta(A'+2B')}{2\mathcal{N}_0(1+\vartheta)(1+\vartheta-\epsilon)}H(r,t) + \frac{\beta\nu_m}{\mathcal{N}_0}\frac{\vartheta^2(A'+2B'+C')}{(1+\vartheta)(1+\vartheta-\epsilon)}F(r,t),\\
w(r,t) &\simeq \frac{\beta\nu_m}{\mathcal{N}_0}\frac{\vartheta^2(A'+2B'+C')}{(1+\vartheta)(1+\vartheta-\epsilon)}F(r,t).
\end{aligned} \tag{A.118}$$

Bibliography

[1] A. T. Bharucha-Reid, *Elements of the theory of Markov processes and their applications* (Academic Press, NY, 1968).

[2] W. Feller, *An introduction to probability theory and its applications* (Wiley, NY, 1970).

[3] M. M. R. Williams, *Mathematical Methods in Particle Transport Theory* (Butterworth, 1971).

[4] M. M. R. Williams, *Random processes in nuclear reactors* (Pergamon Press, Oxford, 1974).

[5] J. J. Duderstadt and W. R. Martin, *Transport theory* (Wiley, NY, 1979).

[6] H. Berg, *Random Walks in Biology* (Princeton University Press, 1993).

[7] G. H. Weiss, *Aspects and applications of the random walk* (North Holland Press, Amsterdam, 1994).

[8] B. D. Hughes, *Random walks and random environments* (Clarendon Press, Oxford, 1995).

[9] J. Ph. Bouchaud and M. Potters, *The theory of financial risk and derivative pricing* (CUP, 2003).

[10] P. I. Sheng, *Introduction to wave scattering, localization and mesoscopic phenomena* (Springer series in materials science, 2006).

[11] E. Akkermans and G. Montambaux, *Mesoscopic physics of electrons and photons* (Cambridge University Press, 2007).

[12] E. Cussler, *Diffusion: Mass Transfer in Fluid Systems* (CUP, 2009).

[13] L. Boltzmann, *Lectures on gas theory* (1872). Translated from German by G. Brush in (University of California Press, 1964).

[14] C. Cercignani, *The Boltzmann equation and its applications* (Springer, 1988).

[15] R. Brown, Phil. Mag. **4**, 161 (1828).

[16] A. Einstein, *Investigations on the theory of the Brownian movement* (Dover, 1956).

[17] M. Von Smoluchowski, Ann. Phys. **21**, 756 (1906).

[18] R. Metzler, J. Klafter, Phys. Rep. **339**, 1 (2000).

[19] R. Metzler, J. Klafter, J. Phys. A: Math. Gen. **37**, R161 (2004).

[20] J. B. Perrin, Ann. Chem. Phys. **18**, 1 (1909).

[21] P. Langevin, C. R. Acad. Sci. Paris **146**, 530 (1908).

[22] A. N. Kolmogorov and N. A. Dmitriev, C. R. Acad. Sci. URSS **56**, 1 (1947).

[23] A. N. Kolmogorov and B. A. Sevast'yanov, C. R. Acad. Sci. URSS **56**, 783 (1947).

[24] A. N. Kolmogorov, I. G. Petrovskii and N. Piskunov, Bull. Moscow Univ. Ser. Math. **1**, 1 (1937).

[25] L. Pál, Il Nuovo Cimento, Suppl. VII **25** (1958).

[26] G. I. Bell, Nucl. Sci. Eng. **21**, 390 (1965).

[27] R. Sanchez, Transp. Theor. Stat. Phys. **26**, 469 (1997).

[28] K. B. Athreya and P. Ney, *Branching processes* (Grundlehren Series, Springer-Verlag, New York, 1972).

[29] T. E. Harris, *The theory of branching processes* (Springer, Berlin, 1963).

[30] G. I. Bell and S. Glasstone, *Nuclear reactor theory* (Van Nostrand Reinhold Company, New York, 1970).

[31] M. Weinberg and E. P. Wigner, *The physical theory of neutron chain reactors* (UCP, Chicago, 1958).

[32] I. Pázsit and L. Pál, *Neutron Fluctuations: A Treatise on the Physics of Branching Processes* (Elsevier, Oxford, 2008).

[33] J.-F. Le Gall, *Spatial branching processes, random snakes and partial differential equations* (Birkhäuser, Zurich, 2012).

[34] I. Pázsit and C. Demazière, *Noise techniques in nuclear systems*, in Handbook of Nuclear Engineering, 1629-1737 (2010).

[35] I. Pázsit and Y. Yamane, Nucl. Instrum. Meth. Phys. Res. Section A **403**, 431 (1998).

[36] S. B. Degweker, Ann. Nucl. Energy **21**, 531-539 (1994).

[37] I. Pázsit, J. Phys. D: Appl. Phys. *20*, 151 (1987).

[38] M. S. Bartlett, *Stochastic Population Models in Ecology and Epidemiology* (1960).

[39] P. Jagers, *Branching Processes with Biological Applications* (Wiley Series in Probability and Mathematical Statistics, London, 1975).

[40] J. D. Murray, *Mathematical Biology* (Berlin, Springer Verlag, 1989).

[41] D. Tilman and P. Kareiva, *Spatial Ecology* (Princeton University Press, Princeton, 1997).

[42] W. R. Young, A. J. Roberts, G. Stuhne, Nature **412**, 328 (2001).

[43] D. A. Dawson, Z. Wahrsch. Verw. Gebiete **40**, 125 (1972).

[44] J. T. Cox and D. Griffeath, Annals Prob. **13**, 1108 (1985).

[45] I. Iscoe, Prob. Th. Rel. Fields **71**, 85 (1986).

[46] J. Bertoin, Stoch. Proc. and Appl. **120**, 678 (2010).

[47] D. J. Lawson and H. J. Jensen, Phys. Rev. Lett. **98**, 098102 (2007).

[48] S. Sawyer and J. Fleischman, Proceedings of the National Academy of Sciences USA **76**, 872 (1979).

[49] I. Golding, Y. Kozlovsky, I. Cohen, and E. Ben-Jacob, Physica A **260**, 510 (1998).

[50] H. T. Hillen and G. Othmer, Siam J. Appl. Math **61**, 751 (2000).

[51] B. Houchmandzadeh, Phys. Rev. E **66**, 052902 (2002).

[52] B. Houchmandzadeh, Phys. Rev. Lett. **101**, 078103 (2008).

[53] B. Houchmandzadeh, Phys. Rev. E **80**, 051920 (2009).

[54] F. Bartumeus et al., J. Theor. Bio. **252**, 43 (2008).

[55] G. Le Caër, J. Stat. Phys. **140**, 728 (2010).

[56] G. Le Caër, J. Stat. Phys. **144**, 23 (2011).

[57] E. Orsingher and A. De Gregorio, J. Theor. Probab. **20**, 769 (2007).

[58] H. G. Othmer, S. R. Dunbar, and W. Alt, J. Math. Biol. **26**, 263 (1988).

[59] A. M. Edwards, et al., Nature **449**, 1044 (2007).

[60] A. D. Kolesnik, J. Stat. Phys. **131**, 1039 (2008).

[61] N. T. J. Bailey *The Mathematical Theory of Infectious Diseases and its Applications* (Griffin, London, 1957).

[62] E. Dumonteil, S. N. Majumdar, A. Rosso, and A. Zoia, Proc. Natl. Acad. Sci. USA **110**, 4239 (2013).

[63] D. Brockmann, L. Hufnagel, and T. Geisel, Nature **439**, 462 (2006).

[64] V. Colizza, A. Barrat, M. Barthélemy, and A. Vespignani, Proc. Natl. Acad. Sci. USA, **103** 2015 (2006).

[65] H. Andersson and T. Britton, *Stochastic Epidemic Models and their Statistical Analysis* (Lecture Notes in Statistics **151**, Springer-Verlag, New York, 2000).

[66] S. Chandrasekhar, Rev. Mod. Physics **15**, 1 (1943).

[67] M. Modest, *Radiative heat transfer* (Academic Press, NY, 2003).

[68] B. J. Berne and R. Pecora, *Dynamic Light Scattering With Applications to Chemistry, Biology, and Physics* (Dover Publications, 2000).

[69] M. C. W. van Rossum and T. M. Nieuwenhuizen, Rev. Mod. Phys. **71**, 313 (1999).

[70] P. Barthelemy, J. Bertolotti, and D. S. Wiersma, Nature **453**, 495 (2009).

[71] T. Svensson, K. Vynck, M. Grisi, R. Savo, M. Burresi, and D. S. Wiersma, Phys. Rev. E **87**, 022120 (2013).

[72] T. Svensson, K. Vynck, E. Adolfsson, A. Farina, A. Pifferi, and D. S. Wiersma, Phys. Rev. E **89**, 022141 (2014).

[73] A. B. Davis and A. Marshak, J. Quant. Spectrosc. Radiat. Transfer **84**, 3 (2004).

[74] A. B. Davis, *Computational Methods in Transport, Lecture Notes in Comput. Sci. Eng.* **48**, 85 (2006).

[75] A. B. Kostinski and R. A. Shaw, J. Fluid Mech. **434**, 389 (2001).

[76] E. W. Larsen and R. Vasques, J. Quant. Spectrosc. Radiat. Transfer **112**, 619 (2011).

[77] V. Tuchin, *Tissue Optics: Light Scattering Methods and Instruments for Medical Diagnosis* (SPIE Press, 2007).

[78] A. Welch and M. J. C. Gemert, *Optical-Thermal Response of Laser-Irradiated Tissue* (Springer, 2010).

[79] N. Mercadier, W. Guerin, M. Chevrollier, and R. Kaiser, Nature Physics **5**, 602 (2008).

[80] C. Jacoboni and L. Reggiani, Rev. Mod. Phys. **55**, 645 (1983).

[81] P. J. Price, Semicond. Semimet. **14**, 249 (1979).

[82] C. Jacoboni and P. Lugli, *The Monte Carlo method for semiconductor device simulation* (Springer, 1989).

[83] M. V. Fischetti and S. E. Laux, Phys. Rev. B **38**, 9721 (1988).

[84] M. V. Fischetti and S. E. Laux, Phys. Rev. B **48**, 2244 (1993).

[85] H. Scher and M. Lax, Phys. Rev. B **7**, 4491 (1973).

[86] H. Scher and M. Lax, Phys. Rev. B **7**, 4502 (1973).

[87] T. Kurosawa, Proceedings of the 3^{rd} International Conference on Hot Carriers in Semiconductors (1964).

[88] E. W. Montroll, G. H. Weiss, J. Math. Phys. **6**, 167 (1965).

[89] D. ben Avraham and S. Havlin, *Diffusion and reactions in fractals and disordered systems* (CUP, UK, 2000).

[90] P. L. Krapivsky, S. Redner, and E. Ben-Naim, *A kinetic view of Statistical Physics* (CUP, UK, 2010).

[91] C. Le Bris, T. Lelièvre, M. Luskin and D. Perez, Monte Carlo Methods and Applications **18**, 119-146 (2012).

[92] C. Le Bris and Ph. G. Ciarlet Eds., *Computational Chemistry, Handbook of Numerical Analysis*, vol. X (North-Holland, 2003).

[93] C. Chatelain, Y. Kantor, M. Kardar, Phys. Rev. E **78**, 021129 (2008).

[94] J. Chuang, Y. Kantor, M. Kardar, Phys. Rev. E **65**, 011802 (2001).

[95] Y. Kantor, M. Kardar, Phys. Rev. E **69**, 021806 (2004).

[96] A. Zoia, A. Rosso, and S. N. Majumdar, Phys. Rev. Lett. **102**, 120602 (2009).

[97] N. Agmon, Chem. Phys. Lett. **497**, 184 (2010).

[98] N. Agmon, J. Phys. Chem. A **115**, 5838 (2011).

[99] N. Agmon, J. Chem. Phys. **81**, 3644 (1984).

[100] C. Le Bris and T. Lelièvre, in *Multiscale modeling and simulation in science*, Lecture Notes in Computational Science and Engineering **66**, 49-137 (2009).

[101] J. Ph. Bouchaud and A. Georges, Phys. Rep. **195**, 127 (1990).

[102] S. Condamin et al., Nature **450**, 40 (2007).

[103] E. Majorana, Scientia **36**, 58 (1942).

[104] G. Viswanathan, *The Physics of Foraging: An Introduction to Random Searches and Biological Encounters* (Cambridge University Press, 2011).

[105] O. Bénichou, C. Loverdo, M. Moreau, and R. Voituriez, Rev. Mod. Physics **83**, 81 (2011).

[106] S. Blanco and R. Fournier, Europhys. Lett. **61**, 168 (2003).

[107] S. Blanco and R. Fournier, Phys. Rev. Lett. **97**, 230604 (2006).

[108] S. Condamin, O. Bénichou, and M. Moreau, Phys. Rev. Lett. **95**, 260601 (2005).

[109] O. Bénichou, M. Coppey, M. Moreau, P. H. Suet, and R. Voituriez, Europhys. Lett. **70**, 42 (2005).

[110] G.F. Newell, *A simplified car-following theory: a lower order model* (Institute of Transportation Studies, University of California, Berkeley, 2002).

[111] G.F. Newell, Quart. J. Appl. Math. **13**, 353 (1956).

[112] R. K. Osborn and S. Yip, *The foundations of neutron transport theory* (Gordon and Breach, New York, 1966).

[113] K. M. Case and P. F. Zweifel, *Linear transport theory* (Addison-Wesley, Reading, 1967).

[114] G. Milton Wing, *An introduction to transport theory* (Wiley, NY, 1962).

[115] R. L. Liboff *Kinetic Theory: Classical, Quantum and Relativistic Descriptions* (Springer, 2003).

[116] R. K. Osborn and M. Natelson, J. Nuc. Energy Parts A/B **19**, 619 (1966).

[117] M. Natelson, R. K. Osborn and F. Shure, J. Nuc. Energy Parts A/B **20**, 557 (1966).

[118] A. Zoia, C. Latrille, and A. Cartalade, Phys. Rev. E 79, 041125 (2009).

[119] A. Zoia, C. Latrille, A. Beccantini, and A. Cartalade, J. Contam. Hydrol. 109, 14-26 (2009).

[120] J. A. Wesson, *Tokamaks*, 3^{rd} Ed. (Clarendon Press, 2003).

[121] I. I. Pázsit, Ann. Nucl. Energy **14**, 25 (1987).

[122] B.R. Betzler et al., LA-UR-12-24472 (2012).

[123] W. Pfeiffer, J.R. Brown, and A.C. Marshall, GA-A13079, General Atomic (1974).

[124] C.M. Persson et al., Ann. Nucl. Energy. **35**, 2357 (2008).

[125] R. Sanchez and P. Jaegers, LA-UR-98-336 (1998).

[126] Y. Cao and J.C. Lee, Nucl. Sci. Eng. **165**, 270-282 (2008).

[127] W. Greenberg, C. van der Mee, and V. Protopopescu, V., *Boundary value problems in abstract kinetic theory* (Birkhäuser, Basel 1987).

[128] J. Lehner and G.M Wing, G.M., Commun. Pure Appl. Math. **8**, 217-234 (1955).

[129] J. Lehner and G.M. Wing, G.M., Duke Math. J. **23**, 125-142 (1956).

[130] G. Pimbley, J. Math. Mech. **8**, 837-866 (1959).

[131] M. Nelkin, Physica **29**, 261 (1963).

[132] N. Corngold, Nucl. Sci. Eng. **19**, 30 (1964).

[133] K. Jörgens, Commun. Pure Appl. Math. **11**, 219-242 (1958).

[134] R. Van Norton, NYO Report 9085, New York University (1960).

[135] D.C. Sahni and N.G. Sjöstrand, Progr. Nucl. En. **23**, 241-289 (1990).

[136] D.C. Sahni, Progr. Nucl. En. **30**, 305-320 (1996).

[137] S. Albertoni and B. Montagnini, J. Math. Anal. and Appl. **13**, 19-48 (1966).

[138] E.W. Larsen and P.F. Zweifel, J. Math. Phys. **15**, 1987-1997 (1974).

[139] E.W. Larsen, J. Math. Phys. **20**, 1776-1782 (1979).

[140] E.R. Cohen, in *Proceedings of the 2nd UN conference of the peaceful uses of atomic energy*, P/629, Geneva, Switzerland (1958).

[141] A.F. Henry, Nucl. Sci. Eng. **20**, 338-351 (1964).

[142] J. C. J. Paasschens, Phys. Rev. E **56**, 1135 (1997).

[143] G. H. Weiss, Physica A **311**, 381 (2002).

[144] E. Jakeman and R. J. A. Tough, J. Opt. Soc. Am. A **4**, 1764 (1987).

[145] A. Zoia, E. Dumonteil, and A. Mazzolo, Phys. Rev. E **83**, 041137 (2011).

[146] M. Iosifescu, *Finite Markov processes and their applications*, (Wiley series in probability and mathematical statistics, Wiley, 1980).

[147] J. Dutka, Arch. Hist. Exact Sci. **32**, 351 (1985).

[148] C. C. Grosjean, Physica **19**, 29 (1953).

[149] W. Stadje, J. Stat. Phys. **46**, 207 (1987).

[150] B. Conolly and D. Roberts, Eur. J. Op. Res. **28**, 308 (1987).

[151] K. Pearson, Nature **27**, 294 (1905).

[152] J. C. Kluyver, Proc. Koninklijke Akademie van Wetenschappen te Amsterdam **8**, 341 (1906).

[153] J. W. Strutt (Lord Rayleigh), Phil. Mag. **6**, 321 (1919).

[154] J. W. Gibbs, *Elementary principles in statistical mechanics* (Arnold, London, 1902).

[155] G. Placzek and W. Seidel, Phys. Rev. **72**, 550 (1947).

[156] I. Freund, Phys. Rev. A **45**, 8854 (1992).

[157] J. Spanier and E. M. Gelbard, *Monte Carlo principles and neutron transport problems* (Addison-Wesley, Reading, 1969).

[158] I. Lux and L. Koblinger, *Monte Carlo particle transport methods: neutron and photon calculations* (CRC Press, Boca Raton, 1991).

[159] F. Brown, *Fundamentals of Monte Carlo Particle Transport*, LA-UR-05-4983 (2005).

[160] R. Y. Rubinstein and D. P. Kroese, *Simulation and the Monte Carlo Method* (Wiley, NY, 2007).

[161] N. Metropolis, Los Alamos Science, special issue **15**, 125 (1987).

[162] N. Metropolis and S. Ulam, J. Am. Stat. Assoc. **44**, 335 (1949).

[163] R. Eckhardt, Los Alamos Science, special issue **15**, 131 (1987).

[164] N. Metropolis, A. Rosenbluth, M. N. Rosenbluth, A. H. Teller, and E. Teller, J. Chem. Phys. **21**, 1087 (1953).

[165] T. E. Booth, Appl. Radiat. Isot. **70**, 1042 (2012).

[166] S. Redner, *A guide to first-passage processes* (CUP, UK, 2001).

[167] O. Bénichou et al., J. Stat. Phys. **142**, 657 (2011).

[168] A. M. Berezhkovskii, V. Zaloj, and N. Agmon, Phys. Rev. E **57**, 3937 (1998).

[169] D. S. Grebenkov, Phys. Rev. E **76**, 041139 (2007).

[170] D. S. Grebenkov, J. Stat. Phys. **141**, 532 (2010).

[171] A. Bar-Haim and J. Klafter, J. Chem. Phys. **109**, 5187 (1998).

[172] S. N. Majumdar and A. Comtet, Phys. Rev. Lett. **89**, 060601 (2002).

[173] S. N. Majumdar, Physica A **389**, 4299 (2010).

[174] E. Barkai, J. Stat. Phys. **123**, 883 (2006).

[175] A. Mazzolo, Europhys. Lett. **68**, 350 (2004).

[176] A. Zoia, E. Dumonteil, and A. Mazzolo, Phys. Rev. Lett. **106**, 220602 (2011).

[177] A. Zoia, E. Dumonteil, and A. Mazzolo, Phys. Rev. E **84**, 021139 (2011).

[178] P. Del Moral, *Feynman-Kac formulae. Genealogical and interacting particle systems with applications*, (Springer, NY, 2004).

[179] P. J. Fitzsimmons and J. Pitman, Stoch. Proc. Appl. **79**, 117 (1999).

[180] S. N. Majumdar, Curr. Sci. **89**, 2076 (2005).

[181] R. P. Feynman, Rev. Mod. Phys. **20**, 367 (1948).

[182] D. A. Darling and M. Kac, Trans. Amer. Math. Soc. **84**, 444 (1957).

[183] M. Kac, Trans. Amer. Math. Soc. **65**, 1 (1949).

[184] M. Kac, in Proc. Second Berkeley Symp. on Math. Statist. and Prob. (UCP, 1951), pp. 189-215.

[185] M. Kac, *Probability and related topics in physical sciences* (Lectures in applied mathematics, Wiley, 1957).

[186] Kac, M., Rocky Mountain Journal of Mathematics **4**, 497 (1974)

[187] M. Kac, *Some stochastic problems in Physics and Mechanics*, Colloquium lectures in the pure and applied sciences, Field research laboratory, Socony Mobil Oil Company, Inc. (1956).

[188] L. Turgeman, S. Carmi, and E. Barkai, Phys. Rev. Lett. **103**, 190201 (2009).

[189] S. Carmi and E. Barkai, Phys. Rev. E **84**, 061104 (2011).

[190] S. Carmi, L. Turgeman, and E. Barkai, J. Stat. Phys. **141**, 1071 (2010).

[191] D. S. Grebenkov and B. -T. Nguyen, SIAM Review **55**, 601 (2013).

[192] J. Pitman, *Combinatorial Stochastic Processes* (Springer, Berlin, 2006)

[193] J. Riordan, *Introduction to combinatorial analysis* (PUP, 1980).

[194] J. Lamperti, Trans. Am. Math. Soc. **88**, 380 (1958).

[195] S. Sabhapandit, S. N. Majumdar, and A. Comtet, Phys. Rev. E **73**, 051102 (2006).

[196] C. Godrèche and J. M. Luck, J. Stat. Phys. **104**, 489 (2001).

[197] A. Baldassarri et al., Phys. Rev. E **59**, 20 (1999).

[198] E. Sparre Andersen, Math. Scand. **2**, 195 (1954).

[199] Yi-C. Zhang, M. Serva, and M. Polikarpov, J. Stat. Phys. **58**, 849 (1990).

[200] M. Meyer, S. Havlin, and A. Bunde, Phys. Rev. E **54**, 5567 (1996).

[201] H. W. Watson and F. Galton, J. Anthropol. Inst. Great Britain **4**, 138 (1875).

[202] B. Derrida and H. Spohn, J. Stat. Phys. **51**, 817 (1988).

[203] E. Brunet and B. Derrida, EPL **87**, 60010 (2009).

[204] B. Derrida and D. Simon, EPL **78**, 60006 (2007).

[205] van Saarloos, W., Phys. Rep. **386**, 29 (2003).

[206] J. Berestycki, J. Stat. Phys. **113**, 411 (2003).

[207] J. Berestycki, S. Harris, and A. Kyprianou, Ann. Appl. Prob. **21**, 1749 (2011).

[208] E. Aïdékon, J. Berestycki, E. Brunet, and Z. Shi, Prob. Theory Rel. Fields **157**, 405 (2013).

[209] S. Watanabe, Proc. Symp. Pure Math. **57**, 157 (1995).

[210] A. Zoia, E. Dumonteil, A. Mazzolo, and S. Mohamed, J. Phys. A: Math. Theor. **45**, 425002 (2012).

[211] A. Zoia, E. Dumonteil, and A. Mazzolo, Europhys. Lett. **98**, 40012 (2012).

[212] J.E. Hoogenboom, in *Proceedings of the PHYSOR conference*, Seoul, Korea (2002).

[213] K.P. Singh, R.S. Modak, S.B. Degweker, and K. Singh, Ann. Nucl. Energy **38**, 1996-2004 (2011).

[214] Y. Nauchi, in *Proceedings of the SNA+MC 2013 conference*, Paris, France (2014).

[215] A. Zoia, E., Brun, F. Damian, and F. Malvagi, Ann. Nucl. Energy **75**, 627 (2015).

[216] T. Yamamoto, Progr. Nuc. Sci. Tech. **2**, 826-835 (2011).

[217] T.R. Hill, LA-9602-MS (UC-32) (1983).

[218] D. Brockway, P. Soran, and P. Whalen, LA-UR-85-1224 (1985).

[219] D.E. Cullen, et al., UCRL-TR-201506 (2003).

[220] A. Zoia, E. Brun, and F. Malvagi, Ann. Nucl. Energy **63**, 276-284 (2014).

[221] B. Montagnini and V. Pierpaoli, Transp. Theory and Stat. Phys. **1**, 59-75 (1971).

[222] D. R. Cox and P. A. W. Lewis, *The Statistical Analysis of Series of Events* (Methuen, London, 1966).

[223] R. P. Feynman F. de Hoffmann, and R. Serber, J. Nuc. Energy **3**, 64 (1956).

[224] A. Erdélyi et al., *Higher transcendental functions* (Krieger, NY, 1981).

[225] C. de Mulatier, A. Mazzolo, and A. Zoia, EPL **107**, 30001 (2014).

[226] A. Mazzolo, J. Phys. A: Math. Theor. **42**, 105002 (2009).

[227] A. Zoia, E. Dumonteil, and A. Mazzolo, EPL **100**, 40002 (2012).

[228] A. Mazzolo, J. Phys. A: Math. Theor. **37**, 7095 (2004).

[229] L. A. Santaló, *Integral Geometry and Geometric Probability* (Addison-Wesley, Reading, MA, 1976).

[230] J.N. Bardsley and A. Dubi, SIAM J. Appl. Math. **40**, 71 (1981).

[231] M. J. Dixmier, Physique **39**, 873 (1978).

[232] A. Mazzolo, Ann. Nuc. Energy **32**, 549 (2005).

[233] A. Zoia, A. Rosso, and M. Kardar, Phys. Rev. E **76**, 021116 (2007).

[234] G. Zumofen, J. Klafter, Phys. Rev. E **51**, 2805 (1995).

[235] A. Mazzolo, B. Roesslinger, and W. Gille, J. Math. Phys. **44**, 6195 (2003).

[236] P. Whittle, Biometrika **42**, 116-122 (1955).

[237] D. G. Kendall, in Proc. 3rd Berkeley Symp. Math. Statist. Prob. **4**, 149-165 (1956).

[238] P. Elliott, J. C. Wakefield, N. G. Best, and D. J. Briggs, *Spatial Epidemiology: Methods and Applications* (Oxford University Press 2000).

[239] J. Radcliffe, J. Appl. Prob. **13**, 338-344 (1976).

[240] J. S. Wang, J. Appl. Prob. **17**, 301-312 (1980).

[241] J. Randon-Furling, S. N. Majumdar, and A. Comtet, Phys. Rev. Lett. **103**, 140602 (2009).

[242] S. N. Majumdar, A. Comtet, J. Randon-Furling, J. Stat. Phys. **138**, 955 (2010).

[243] A. Reymbaut, S. N. Majumdar, and A. Rosso, J. Phys. A-Math. & Theor. **44**, 415001 (2011).

[244] A. Cauchy, Mem. Acad. Sci. Inst. Fr. **22**, 3 (1850).

[245] S. N. Majumdar and P. L. Krapivsky, Physica A **318**, 161-170 (2003).

[246] E. Dumonteil, F. Malvagi, A. Zoia, A. Mazzolo, D. Artusio, C. Dieudonné, C. de Mulatier, Ann. Nuc. Energy **63**, 612 (2014).

[247] H. S. Carslaw and J. C. Jaeger, *Conduction of Heat in Solids* (Clarendon Press, Oxford, 1984).

[248] M. Paessens and G. M. Schütz, J. Phys. A: Math. Gen. **37**, 4709 (2004).

[249] X. Durang and M. Henkel, J. Phys. A: Math. Theor. **42**, 395004 (2009).

[250] U. C. Täuber, M. Howard, and B. P. Vollmayr-Lee, J. Phys. A: Math. Gen. **38**, R79 (2005).

[251] E. B. Dynkin, Theory of Markov processes (Dover, 2006).

[252] A. Zoia, E. Dumonteil, and A. Mazzolo, Phys. Rev. E **84**, 061130 (2011).

[253] A. Zoia, E. Dumonteil, and A. Mazzolo, Phys. Rev. E **85**, 011132 (2012).

[254] S. P. Meyn and R. L. Tweedie, Adv. Appl. Prob. **24**, 542 (1992).

[255] E. Csàki, J. Stat. Plann. Inference **34**, 63 (1993).